

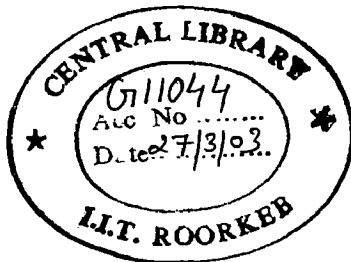
**STRESS ANALYSIS IN CONCRETE OVER THE DRAFT TUBE
IN
A POWER HOUSE BY FINITE ELEMENT METHOD**

A DISSERTATION

*Submitted in partial fulfillment of the
requirements for the award of the degree*
of
MASTER OF TECHNOLOGY
in
WATER RESOURCES DEVELOPMENT

By

GOURANGA MANDAL



**WATER RESOURCES DEVELOPMENT TRAINING CENTRE
INDIAN INSTITUTE OF TECHNOLOGY ROORKEE
ROORKEE -247 667 (INDIA)**

January, 2003

12

CANDIDATE'S DECLARATION

I do hereby declare that the work, which is being presented in this dissertation entitled "**STRESS ANALYSIS IN CONCRETE OVER THE DRAFT TUBE IN A POWER HOUSE BY FINITE ELEMENT METHOD**" in partial fulfilment of the requirement for the award of the Degree of **Master of Technology** in **WATER RESOURCES DEVELOPMENT (CIVIL)**, and submitted in the department of Water Resources Development Training Centre, Indian Institute of Technology, Roorkee, is an authentic record of my own work carried out during the period from July, 2002 to January, 2003 under the guidance of **Dr. B.N. Asthana**, Emeritus Fellow, **Prof. Gopal Chauhan** and **Dr. Rampal Singh**, Professors, Water Resources Development Training Centre, Indian Institute of Technology, Roorkee, Roorkee.

The matter embodied in this dissertation has not been submitted by me for the award of any other degree.

Dated: ^{8th} January, 2003,

Place: Roorkee.


(GOURANGA MANDAL)

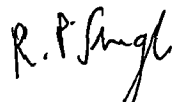
This is to certify that the above statement made by the candidate is correct to the best of our knowledge.



(Dr. B.N. Asthana)

Emeritus Fellow,

WRDTC, IIT Roorkee.



(Dr. Rampal Singh)

Professor,

WRDTC, IIT Roorkee.



(Prof. Gopal Chauhan)

Professor,

WRDTC, IIT Roorkee.

ACKNOWLEDGEMENT

I take this as a great pleasure and proud privilege to express my deep sense of respect and gratitude to **Dr. B.N. Asthana**, Emeritus Fellow, **Prof. Gopal Chauhan** and **Dr. Rampal Singh**, Professors, Water Resources Development Training Centre, Indian Institute of Technology, Roorkee for their valuable, inspiring and painstaking guidance in bringing out this work.

I would like to extend hearty thanks to **Dr. U.C. Chaube**, Prof and Head of Department, all the faculty members and staff of the WRDTC for their kind cooperation.

I am also indebted to the Department of Water Resources, Government of Orissa for sponsoring me to undertake this course. I thank my Engineer-in-Chief and all my colleagues for their cooperation and constant encouragement. My thanks are due to my colleagues Mr. M. Arul Selvam, Mr. Arun Paul, Mr. J.Deva Sundar, Dr. S. Bala Prasad and Mr. M.D. Patil for their cooperation.

I am also thankful to all my fellow trainee officers of WRDTC for their cooperation and encouragement.

Last but not the least I would like to express my greatest appreciation to my beloved brothers and my wife Smt. Pravasini and daughters Shailaja and Shameeksha for their prayers, encouragement and patience with out which it was very difficult to complete this course.

Gouranga Mandal
(GOURANGA MANDAL)

CONTENTS

	Page No.
CANDIDATE'S DECLARATION	(i)
ACKNOWLEDGEMENT	(ii)
CONTENTS	(iii)
LIST OF TABLES	(vii)
LIST OF FIGURES	(x)
SYNOPSIS	(xvi)
 CHAPTERS	
1 INTRODUCTION	1
1.1 General	1
1.2 Loads And Forces On The Substructure	1
1.3 Design Practices	4
1.4 Scope Of The Study	6
1.5 Organisation Of The Study	7
2 LITERATURE REVIEW	8
2.1 General	8
2.2 Stress Analysis Under Photo-elasticity Technique	8
2.2.1 Description of the Method	8
2.2.2 Basic Photo elastic equation	9
2.3 Stress Analysis Under Finite Element Method	10
2.3.1 2-D Finite Element Method	10
2.3.2 3-D Finite Element Method	11
3 THE FINITE ELEMENT MEHTOD	12
3.1 General	12
3.2 Description Of The Method	12
3.2.1 Discretisation of the continuum	12
3.2.2 Selection of proper interpolation or displacement model	13

3.2.3	Convergence requirements	13
3.2.4	Nodal Degree of Freedom	14
3.2.5	Element stiffness matrix	14
3.2.6	Nodal forces and loads	15
3.2.7	Assembly of algebraic equations for the overall discretised continuum	15
3.2.8	Boundary conditions	16
3.2.9	Solution for the unknown displacements	17
3.3	Summary of Procedure	17
3.4	Mathematical Model	18
3.4.1	General	18
3.4.2	Interpolation function	18
3.4.3	Displacement function	19
3.4.4	Shape functions	20
3.4.5	Strains	21
3.4.6	Stresses	23
3.4.7	Stiffness matrix	24
3.5	Sign Convention	25
3.6	Processes In ANSYS	26
3.7	ANSYS Inputs	26
4	SUBSTRUCTURE MODEL	27
4.1	General	27
4.2	Assumptions In The Model	27
4.3	Dimensions Of The Model	27
4.4	Loading Conditions	28
4.4.1	Load condition 1	28
4.4.2	Load condition 2	28
4.4.3	Load condition 3	28
4.4.4	Load condition 4	29
4.5	Steps In Modeling	29
4.5.1	Modeling	29

4.5.2	Define element type	31
4.5.3	Define material property	32
4.5.4	Meshing of model	32
4.5.5	Solution part	32
5	RESULTS OF ANALYSIS	40
5.1	Nature Of Stress Component σ_x in X-Direction	40
5.1.1	Load condition 1	40
5.1.2	Load condition 2	41
5.1.3	Load condition 3	42
5.1.4	Load condition 4	42
5.2	Nature Of Stress Component σ_z in Z-Direction	43
5.2.1	Load condition 1	43
5.2.2	Load condition 2	44
5.2.3	Load condition 3	45
5.2.4	Load condition 4	45
5.3	Nature Of Stress Component σ_y in Y-Direction	46
5.3.1	Load condition 1	46
5.3.2	Load condition 2	47
5.3.3	Load condition 3	48
5.3.4	Load condition 4	48
5.4	Summary Of Results	49
(a)	FEM Analysis	
Stress Contours Plotted For SX Under Load Condition 1		51
Stress Contours Plotted For SX Under Load Condition 2		57
Stress Contours Plotted For SX Under Load Condition 3		63
Stress Contours Plotted For SX Under Load Condition 4		69
Stress Contours Plotted For SZ Under Load Condition 1		75
Stress Contours Plotted For SZ Under Load Condition 2		81
Stress Contours Plotted For SZ Under Load Condition 3		87
Stress Contours Plotted For SZ Under Load Condition 4		93

Stress Contours Plotted For SY Under Load Condition 1	99
Stress Contours Plotted For SY Under Load Condition 2	107
Stress Contours Plotted For SY Under Load Condition 3	115
Stress Contours Plotted For SY Under Load Condition 4	123
(b) By Photo-elasticity Method	
Stress Contours Plotted For SX ⁽¹⁰⁾	131
Stress Contours Plotted For SZ ⁽¹⁰⁾	133
Stress Contours Plotted For SY ⁽¹⁰⁾	135
6 CONCLUSIONS AND SUGGESTIONS	139
6.1 Conclusions	139
6.2 Suggestions For Further Study	139
REFERENCES	141
APPENDIX	142
Stress Component SX Under Load Condition 1	142
Stress Component SX Under Load Condition 2	146
Stress Component SX Under Load Condition 3	150
Stress Component SX Under Load Condition 4	154
Stress Component SZ Under Load Condition 1	158
Stress Component SZ Under Load Condition 2	163
Stress Component SZ Under Load Condition 3	168
Stress Component SZ Under Load Condition 4	173
Stress Component SY Under Load Condition 1	178
Stress Component SY Under Load Condition 2	183
Stress Component SY Under Load Condition 3	188
Stress Component SY Under Load Condition 4	193

LIST OF TABLES

Table No.	Title	Page No.
4.1	Location Of Slices	34
4.2	Location Of Points	34
4.3	Location Of Strips	34
5.1	Nodal Stresses At Slice 7 (under concentrated load between Slice 8 & 9)	143
5.2	Nodal Stresses At Slice 8 (under concentrated load between Slice 8 & 9)	143
5.3	Nodal Stresses At Slice 9 (under concentrated load between Slice 8 & 9)	144
5.4	Nodal Stresses At Slice 10 (under concentrated load between Slice 8 & 9)	145
5.5	Nodal Stresses At Slice 11 (under concentrated load between Slice 8 & 9)	145
5.6	Nodal Stresses At Slice 7 (under concentrated load between Slice 9 & 10)	147
5.7	Nodal Stresses At Slice 8 (under concentrated load between Slice 9 & 10)	147
5.8	Nodal Stresses At Slice 9 (under concentrated load between Slice 9 & 10)	148
5.9	Nodal Stresses At Slice 10 (under concentrated load between Slice 9 & 10)	149
5.10	Nodal Stresses At Slice 11 (under concentrated load between Slice 9 & 10)	149
5.11	Nodal Stresses At Slice 7 (under UDL above elbow concrete)	151
5.12	Nodal Stresses At Slice 8 (under UDL above elbow concrete)	151
5.13	Nodal Stresses At Slice 9 (under UDL above elbow concrete)	152
5.14	Nodal Stresses At Slice 10 (under UDL above elbow concrete)	153
5.15	Nodal Stresses At Slice 11 (under UDL above elbow concrete)	153
5.16	Nodal Stresses At Slice 7 (under concentrated load simulating gantry column loads)	155
5.17	Nodal Stresses At Slice 8 (under concentrated load simulating gantry column loads)	155
5.18	Nodal Stresses At Slice 9 (under concentrated load simulating gantry column loads)	156
5.19	Nodal Stresses At Slice 10 (under concentrated load simulating gantry column loads)	157
5.20	Nodal Stresses At Slice 11 (under concentrated load simulating gantry column loads)	157
5.21	Nodal Stresses At Point 3 (under concentrated load between Slice 8 & 9)	159

5.22	Nodal Stresses At Point 6 (under concentrated load between Slice 8 & 9)	160
5.23	Nodal Stresses At Point 8 (under concentrated load between Slice 8 & 9)	161
5.24	Nodal Stresses At Point 10 (under concentrated load between Slice 8 & 9)	162
5.25	Nodal Stresses At Point 12 (under concentrated load between Slice 8 & 9)	162
5.26	Nodal Stresses At Point 3 (under concentrated load between Slice 9 & 10)	164
5.27	Nodal Stresses At Point 6 (under concentrated load between Slice 9 & 10)	165
5.28	Nodal Stresses At Point 8 (under concentrated load between Slice 9 & 10)	166
5.29	Nodal Stresses At Point 10 (under concentrated load between Slice 9 & 10)	167
5.30	Nodal Stresses At Point 12 (under concentrated load between Slice 9 & 10)	167
5.31	Nodal Stresses At Point 3 (under UDL above elbow concrete)	169
5.32	Nodal Stresses At Point 6 (under UDL above elbow concrete)	170
5.33	Nodal Stresses At Point 8 (under UDL above elbow concrete)	171
5.34	Nodal Stresses At Point 10 (under UDL above elbow concrete)	172
5.35	Nodal Stresses At Point 12 (under UDL above elbow concrete)	172
5.36	Nodal Stresses At Point 3 (under concentrated load simulating gantry column loads)	174
5.37	Nodal Stresses At Point 6 (under concentrated load simulating gantry column loads)	175
5.38	Nodal Stresses At Point 8 (under concentrated load simulating gantry column loads)	176
5.39	Nodal Stresses At Point 10 (under concentrated load simulating gantry column loads)	177
5.40	Nodal Stresses At Point 12 (under concentrated load simulating gantry column loads)	177
5.41	Nodal Stresses At Strip 7 (under concentrated load between Slice 8 & 9)	179
5.42	Nodal Stresses At Strip 8 (under concentrated load between Slice 8 & 9)	179
5.43	Nodal Stresses At Strip 9 (under concentrated load between Slice 8 & 9)	180
5.44	Nodal Stresses At Strip 10 (under concentrated load between Slice 8 & 9)	180
5.45	Nodal Stresses At Strip 11 (under concentrated load between Slice 8 & 9)	181

5.46	Nodal Stresses At Strip 12 (under concentrated load between Slice 8 & 9)	182
5.47	Nodal Stresses At Strip 13 (under concentrated load between Slice 8 & 9)	182
5.48	Nodal Stresses At Strip 7 (under concentrated load between Slice 9 & 10)	184
5.49	Nodal Stresses At Strip 8 (under concentrated load between Slice 9 & 10)	184
5.50	Nodal Stresses At Strip 9 (under concentrated load between Slice 9 & 10)	185
5.51	Nodal Stresses At Strip 10 (under concentrated load between Slice 9 & 10)	185
5.52	Nodal Stresses At Strip 11 (under concentrated load between Slice 9 & 10)	186
5.53	Nodal Stresses At Strip 12 (under concentrated load between Slice 9 & 10)	187
5.54	Nodal Stresses At Strip 13 (under concentrated load between Slice 9 & 10)	187
5.55	Nodal Stresses At Strip 7 (under UDL above elbow concrete)	189
5.56	Nodal Stresses At Strip 8 (under UDL above elbow concrete)	189
5.57	Nodal Stresses At Strip 9 (under UDL above elbow concrete)	190
5.58	Nodal Stresses At Strip 10 (under UDL above elbow concrete)	190
5.59	Nodal Stresses At Strip 11 (under UDL above elbow concrete)	191
5.60	Nodal Stresses At Strip 12 (under UDL above elbow concrete)	192
5.61	Nodal Stresses At Strip 13 (under UDL above elbow concrete)	192
5.62	Nodal Stresses At Strip 7 (under concentrated load simulating gantry column loads)	194
5.63	Nodal Stresses At Strip 8 (under concentrated load simulating gantry column loads)	194
5.64	Nodal Stresses At Strip 9 (under concentrated load simulating gantry column loads)	195
5.65	Nodal Stresses At Strip 10 (under concentrated load simulating gantry column loads)	195
5.66	Nodal Stresses At Strip 11 (under concentrated load simulating gantry column loads)	196
5.67	Nodal Stresses At Strip 12 (under concentrated load simulating gantry column loads)	197
5.68	Nodal Stresses At Strip 13 (under concentrated load simulating gantry column loads)	197

LIST OF FIGURES

Fig. No.	Title	Page No.
	Figure showing sub-division of substructure	xvii
1.1.	Forces acting on a power house	2
1.2	Location of different loads in a power house	
	(a) Position of Loads at various levels and concrete in power house (plant and equipment not shown)	3
	(b) Internal plan of machine Hall (Excluding draft tube extension downstream) showing relative position of loads acting at different levels	4
1.3	Sub-division of Zone 1 into Strips for structural supports	6
3.1.	A 20 noded isoparametric solid element	19
3.2	Stress vector definition	25
4.1	Plan of Substructure showing Slices and Points.	35
4.2	Substructure Model	36
4.3	View of Substructure Model with inner passage	36
4.4	View of Substructure Model after meshing	37
4.5.	Substructure Model (Loaded with a concentrated load of 12.5 kg over a square base of 6.35 mm x 6.35 mm between Slice 8 & 9 centrally above elbow concrete)	37
4.6	Substructure Model (Loaded with a concentrated load of 12.5 kg over a square base of 6.35 mm x 6.35 mm between Slice 9 & 10 centrally above elbow concrete)	38
4.7	Substructure Model (Loaded with UDL of 0.2 kg/cm ² above elbow concrete on top of substructure between Z = 69.9 to 100 mm simulating generator barrel load)	38
4.8	Substructure Model (Loaded with concentrated loads of 12.5 kg over square bases of 6.35 mm x 6.35 mm each on either supports on the line of downstream power house wall simulating gantry column loads)	39

4.9	Transverse Section of the Model at Point 12 (X=53.12mm) showing Strips	39
5.1	Stress contours for SX (kg/sq. cm) at Slice 7 under concentrated load between Slice 8 & 9.	52
5.2	Stress contours for SX (kg/sq. cm) at Slice 8 under concentrated load between Slice 8 & 9.	53
5.3	Stress contours for SX (kg/sq. cm) at Slice 9 under concentrated load between Slice 8 & 9.	54
5.4	Stress contours for SX (kg/sq. cm) at Slice 10 under concentrated load between Slice 8 & 9.	55
5.5	Stress contours for SX (kg/sq. cm) at Slice 11 under concentrated load between Slice 8 & 9.	56
5.6	Stress contours for SX (kg/sq. cm) at Slice 7 under concentrated road between Slice 9 & 10	58
5.7	Stress contours for SX (kg/sq. cm) at Slice 8 under concentrated road between Slice 9 & 10	59
5.8	Stress contours for SX (kg/sq. cm) at Slice 9 under concentrated road between Slice 9 & 10	60
5.9	Stress contours for SX (kg/sq. cm) at Slice 10 under concentrated road between Slice 9 & 10	61
5.10	Stress contours for SX (kg/sq. cm) at Slice 11 under concentrated road between Slice 9 & 10	62
5.11	Stress contours for SX (kg/sq. cm) at Slice 7 under UDL above elbow concrete	64
5.12	Stress contours for SX (kg/sq. cm) at Slice 8 under UDL above elbow concrete	65
5.13	Stress contours for SX (kg/sq. cm) at Slice 9 under UDL above elbow concrete	66
5.14	Stress contours for SX (kg/sq. cm) at Slice 10 under UDL above elbow concrete	67
5.15	Stress contours for SX (kg/sq. cm) at Slice 11 under UDL above elbow concrete	68

5.16	Stress contours for SX (kg/sq. cm) at Slice 7 under concentrated load simulating gantry column loads	70
5.17	Stress contours for SX (kg/sq. cm) at Slice 8 under concentrated load simulating gantry column loads	71
5.18	Stress contours for SX (kg/sq. cm) at Slice 9 under concentrated load simulating gantry column loads	72
5.19	Stress contours for SX (kg/sq. cm) at Slice 10 under concentrated load simulating gantry column loads	73
5.20	Stress contours for SX (kg/sq. cm) at Slice 11 under concentrated load simulating gantry column loads	74
5.21	Stress contours for SZ (kg/sq. cm) at Point 3 under concentrated load between Slice 8 & 9	76
5.22	Stress contours for SZ (kg/sq. cm) at Point 6 under concentrated load between Slice 8 & 9	77
5.23	Stress contours for SZ (kg/sq. cm) at Point 8 under concentrated load between Slice 8 & 9	78
5.24	Stress contours for SZ (kg/sq. cm) at Point 10 under concentrated load between Slice 8 & 9	79
5.25	Stress contours for SZ (kg/sq. cm) at Point 12 under concentrated load between Slice 8 & 9	80
5.26	Stress contours for SZ (kg/sq. cm) at Point 3 under concentrated load between Slice 9 & 10	82
5.27	Stress contours for SZ (kg/sq. cm) at Point 6 under concentrated load between Slice 9 & 10	83
5.28	Stress contours for SZ (kg/sq. cm) at Point 8 under concentrated load between Slice 9 & 10	84
5.29	Stress contours for SZ (kg/sq. cm) at Point 10 under concentrated load between Slice 9 & 10	85
5.30	Stress contours for SZ (kg/sq. cm) at Point 12 under concentrated load between Slice 9 & 10	86
5.31	Stress contours for SZ (kg/sq. cm) at Point 3 under UDL above elbow concrete	88

5.32	Stress contours for SZ (kg/sq. cm) at Point 6 under UDL above elbow concrete	89
5.33	Stress contours for SZ (kg/sq. cm) at Point 8 under UDL above elbow concrete	90
5.34	Stress contours for SZ (kg/sq. cm) at Point 10 under UDL above elbow concrete	91
5.35	Stress contours for SZ (kg/sq. cm) at Point 12 under UDL above elbow concrete	92
5.36	Stress contours for SZ (kg/sq. cm) at Point 3 under concentrated load simulating gantry column loads	94
5.37	Stress contours for SZ (kg/sq. cm) at Point 6 under concentrated load simulating gantry column loads	95
5.38	Stress contours for SZ (kg/sq. cm) at Point 8 under concentrated load simulating gantry column loads	96
5.39	Stress contours for SZ (kg/sq. cm) at Point 10 under concentrated load simulating gantry column loads	97
5.40	Stress contours for SZ (kg/sq. cm) at Point 12 under concentrated load simulating gantry column loads	98
5.41	Stress contours for SY (kg/sq. cm) Strip 7 under concentrated load between Slice 8 & 9	100
5.42	Stress contours for SY (kg/sq. cm) Strip 8 under concentrated load between Slice 8 & 9	101
5.43	Stress contours for SY (kg/sq. cm) Strip 9 under concentrated load between Slice 8 & 9	102
5.44	Stress contours for SY (kg/sq. cm) Strip 10 under concentrated load between Slice 8 & 9	103
5.45	Stress contours for SY (kg/sq. cm) Strip 11 under concentrated load between Slice 8 & 9	104
5.46	Stress contours for SY (kg/sq. cm) Strip 12 under concentrated load between Slice 8 & 9	105
5.47	Stress contours for SY (kg/sq. cm) Strip 13 under concentrated load between Slice 8 & 9	106

5.48	Stress contours for SY (kg/sq. cm) at Strip 7 under concentrated load between Slice 9 & 10	108
5.49	Stress contours for SY (kg/sq. cm) at Strip 8 under concentrated load between Slice 9 & 10	109
5.50	Stress contours for SY (kg/sq. cm) at Strip 9 under concentrated load between Slice 9 & 10	110
5.51	Stress contours for SY (kg/sq. cm) at Strip 10 under concentrated load between Slice 9 & 10	111
5.52	Stress contours for SY (kg/sq. cm) at Strip 11 under concentrated load between Slice 9 & 10	112
5.53	Stress contours for SY (kg/sq. cm) at Strip 12 under concentrated load between Slice 9 & 10	113
5.54	Stress contours for SY (kg/sq. cm) at Strip 13 under concentrated load between Slice 9 & 10	114
5.55	Stress contours for SY (kg/sq. cm) at Strip 7 under UDL above elbow concrete	116
5.56	Stress contours for SY (kg/sq. cm) at Strip 8 under UDL above elbow concrete	117
5.57	Stress contours for SY (kg/sq. cm) at Strip 9 under UDL above elbow concrete	118
5.58	Stress contours for SY (kg/sq. cm) at Strip 10 under UDL above elbow concrete	119
5.59	Stress contours for SY (kg/sq. cm) at Strip 11 under UDL above elbow concrete	120
5.60	Stress contours for SY (kg/sq. cm) at Strip 12 under UDL above elbow concrete	121
5.61	Stress contours for SY (kg/sq. cm) at Strip 13 under UDL above elbow concrete	122
5.62	Stress contours for SY (kg/sq. cm) at Strip 7 under concentrated load simulating gantry column loads.	124
5.63	Stress contours for SY (kg/sq. cm) at Strip 8 under concentrated load simulating gantry column loads.	125

5.64	Stress contours for SY (kg/sq. cm) at Strip 9 under concentrated load simulating gantry column loads.	126
5.65	Stress contours for SY (kg/sq. cm) at Strip 10 under concentrated load simulating gantry column loads.	127
5.66	Stress contours for SY (kg/sq. cm) at Strip 11 under concentrated load simulating gantry column loads.	128
5.67	Stress contours for SY (kg/sq. cm) at Strip 12 under concentrated load simulating gantry column loads.	129
5.68	Stress contours for SY (kg/sq. cm) at Strip 13 under concentrated load simulating gantry column loads.	130
5.69	Stress contours plotted for SX ⁽¹⁰⁾	
	(a) Slice 7	131
	(b) Slice 8	131
	(c) Slice 9	131
	(d) Slice 10	132
	(e) Slice 11	132
5.70	Stress contours plotted for SZ ⁽¹⁰⁾	
	(a) Point 3	133
	(b) Point 6	133
	(c) Point 8	133
	(d) Point 10	134
	(e) Point 12	134
5.71	Stress contours plotted for SY ⁽¹⁰⁾	
	(a) Strip 7	135
	(b) Strip 8	135
	(c) Strip 9	136
	(d) Strip 10	136
	(e) Strip 11	137
	(f) Strip 12	137
	(g) Strip 13	138

SYNOPSIS

The hydel power station from structural viewpoint is divided into 3 divisions namely substructure, intermediate structure and superstructure. These parts also have different hydraulic and structural functions. The present study is concerned with substructure only. Substructure is a massive concrete structure containing draft tube cavity. It performs the function of distributing loads to the foundation. It being the lowest part of power house supports all the loads coming from intermediate structure and superstructure lying above it. This study deals with a surface power station with vertical setting reaction turbine having elbow type draft tube.

The substructure, which extends from the top of draft tube roof to the foundation, contains hollow spaces and cavities of complex shapes. The main cavity is called draft tube and functions as water passage for exit of water. Other cavities are for inspection and drainage. In addition to these it may contain galleries for installation of measuring instruments. So the substructure is not a solid structure. Moreover all the loads transferred from intermediate and superstructure act on top of it. These loads are generally of following types.

- i) Loads including plant & equipment
- ii) Forces induced by water
- iii) Uplift forces
- iv) Wind loads
- v) Earth Pressure
- vi) Crane load
- vii) Seismic forces
- viii) Any other load specific to location

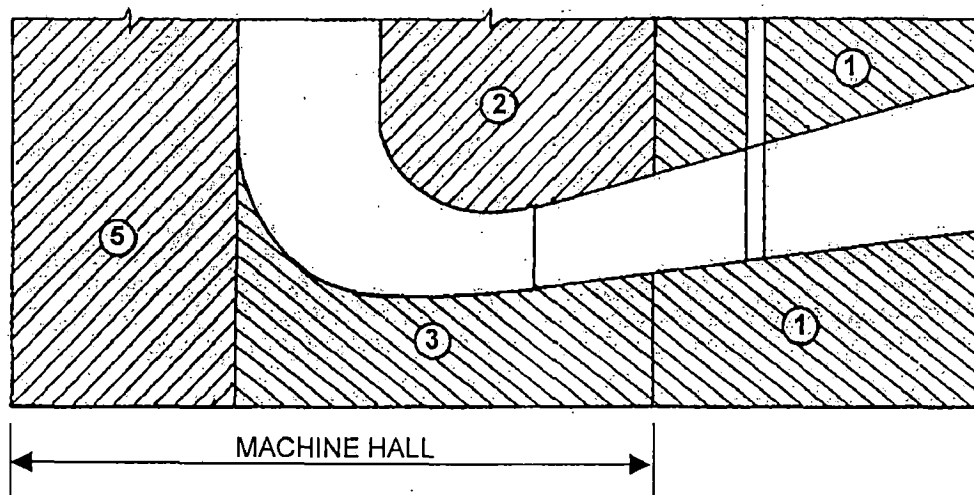
The vertical loads considered are

- i) Weight of the concrete in the substructure
- ii) Weight of the generating part such as turbine, auxiliary equipment, etc.

- iii) Weight of the embedded items such as the draft tube liner, the speed ring, the steel scroll case etc.
- iv) The weight of the superstructure, i.e. the roof, the crane, the walls, the columns etc.

The shape of draft tube and cavities in the substructure are complex and forces acting are many and that too at different levels of power house. Therefore it is difficult to compute stresses in concrete. This structure is generally analysed either as a box structure in two directions or by sub- dividing it into various components as below.

- 1) Cantilever portion out side the power house,
- 2) Elbow portion above the draft tube,
- 3) Bottom slab within the power house,
- 4) The vertical members (not shown in the enclosed figure) and
- 5) Solid mass upstream of draft tube.



REFERENCE

- 1. CANTILEVER PORTION OUTSIDE THE POWER HOUSE WALL
- 2. ELBOW PORTION ABOVE THE DRAFT TUBE
- 3. BOTTOM SLAB WITHIN MACHINE HALL
- 4. VERTICAL MEMBERS NOT SHOWN
- 5. SOLID MASS UPSTREAM OF DRAFT TUBE

FIGURE SHOWING SUB DIVISIONS OF SUBSTRUCTURE

Various design organizations use different design practices based on engineering judgement. The problem of finding stresses in the substructure is essentially three-dimensional. Out of the above five components of substructure the present study is limited to the elbow portion above the draft tube throat. This portion is invariably excessively thick in order to give the required shape to the draft tube. This member has changing curvature and varying thickness. So its exact analysis is not possible.

The substructure can thus be accurately analysed only by a three dimensional analysis. For the three dimensional analysis of such complex shaped structure tools available are three-dimensional Finite Element Method and three-dimensional Photo elasticity method.

The Finite Element Method using ANSYS Package is used to analyse the elbow portion of substructure in this study. The results are compared with that available by using photo elasticity method ⁽¹⁰⁾.

In this study the substructure model is assumed enclosed on all three sides except on the downstream side and acted upon by a concentrated load above elbow portion, simulating pedestal support for spiral case liner which is not embedded in concrete. After comparing and validating the results of this case with photo elasticity results, further stress analysis has been carried out under the following load conditions.

- i) Shifting the point of application of the above concentrated load.
- ii) Applying uniformly distributed load above elbow concrete simulating generator barrel load.
- iii) Applying the above concentrated load on either supports on the line of downstream power house wall simulating gantry column loads.

Stress conditions in elbow concrete for above loading conditions have been presented in this study. These will help the designer to have the insight for the stress pattern in elbow concrete under different loads.

CHAPTER 1

INTRODUCTION

1.1 GENERAL

Substructure of a power house is that portion which contains the draft tube and transfers all loads to foundation. The shape of the substructure and its dimensions depend upon the type of turbine and type of (horizontal or vertical) setting of the shaft. In reaction turbine an elbow type draft tube is required to regain the velocity head of the exit water from the turbine runner as much as possible.

The substructure containing the draft tube structurally has two functions. Firstly it is to safely support the superimposed loads of the plant embedded in intermediate part over cavity (mainly due to draft tube) and secondly to act as a transition foundation member to distribute the heavy loads due to plant, water, superstructure and horizontal forces on account of penstock thrust, wind, tail water, earth pressure etc. on the foundation such that the pressures are within safe limits of bearing capacity of the foundation strata.

1.2 LOADS AND FORCES ON THE SUBSTRUCTURE

Fig.1.1 and 1.2 show a section of power house and forces acting on it. The arrows indicate the center of gravity of the various forces and loads and may not give the exact point of application of these loads. The figures indicate that neither the substructure nor the loads acting over it are symmetrical. Moreover the loads are acting at different levels of the concrete. From the above figures it is evident that the shape of the substructure is quite complex and the loads and forces acting on it are also not symmetrical.

Distribution of generator load, which contributes major load of moving parts, is through concrete in three dimensions. A uniform distribution of loads on top of the substructure through mass concrete is not possible due to its eccentricity and the presence of cavities of spiral case etc. The distribution of column loads is also non-uniform. The loads of spiral case and speed ring are transmitted over top of the substructure through concrete pedestals.

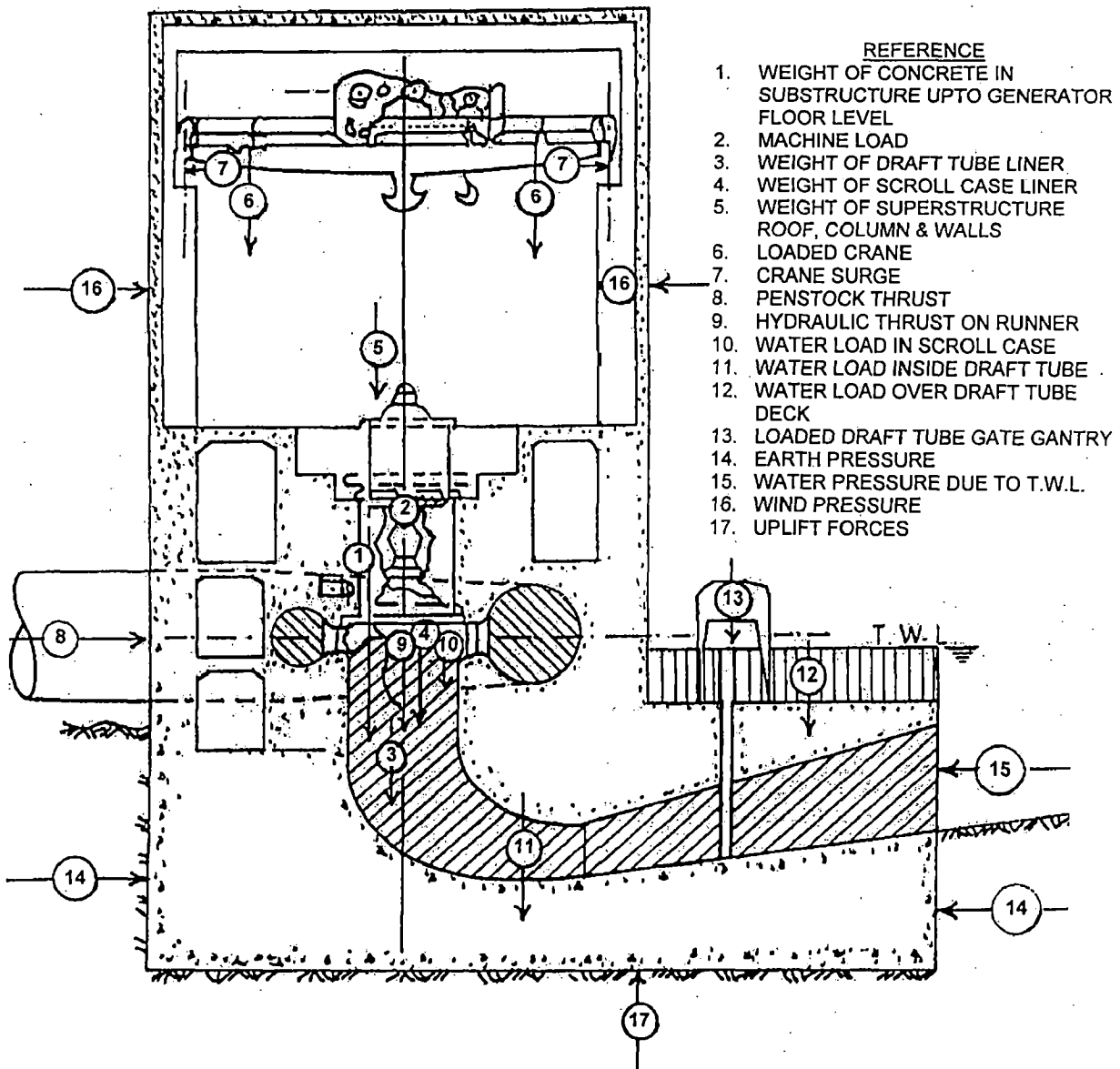
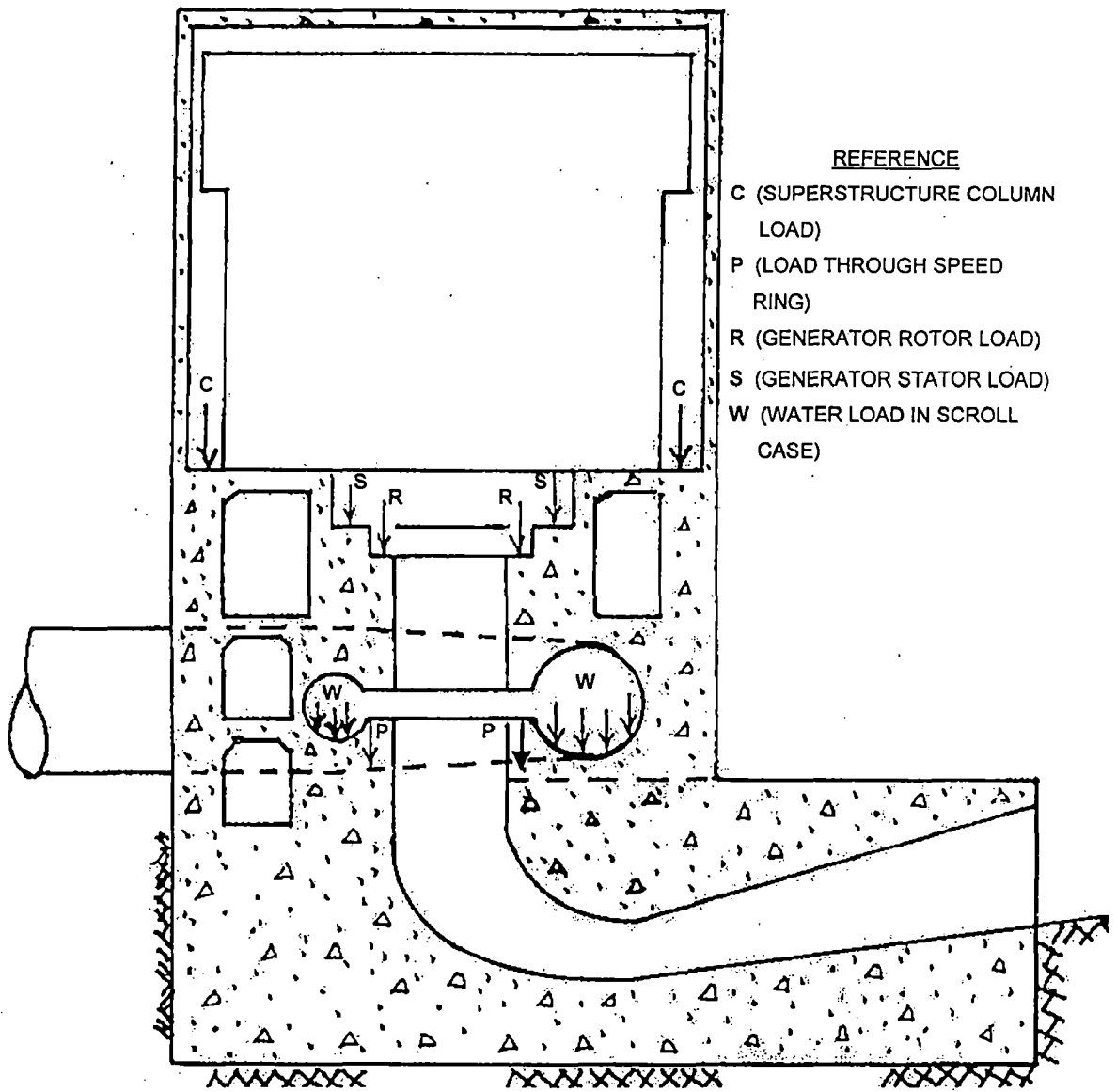


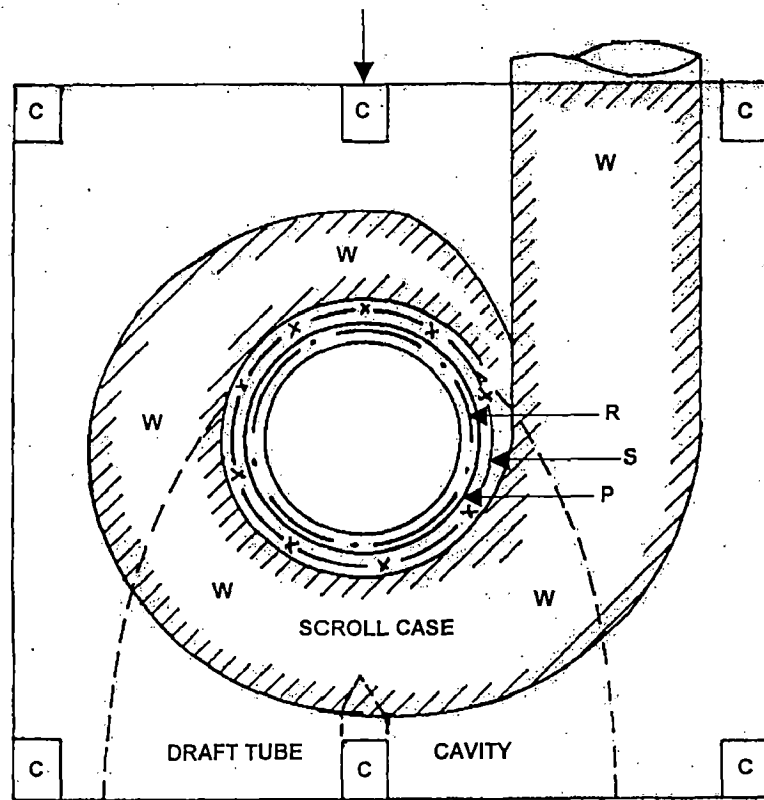
FIG. 1.1: FORCES ACTING ON A POWER HOUSE

The substructure has to support all the loads enumerated above through the elbow concrete over the cavity of draft tube and then to transmit the superimposed loads along with its dead load on to the foundation so that foundation bearing pressures do not exceed the permissible bearing capacity. Further variation in the distribution of foundation pressures occur on account of the horizontal forces due to penstock thrust, wind, tail water and earthquake.



(a) Position Of Loads At Various Levels And Concrete In Power House (Equipment & Plant Not Shown)

FIG. 1.2: LOCATION OF DIFFERENT LOADS IN A POWER HOUSE (Contd.)



(b) Internal Plan Of Machine Hall (Excluding Draft Tube Extension Downstream) Showing Relative Position Of Loads Acting At Different Levels

FIG. 1.2: LOCATION OF DIFFERENT LOADS IN A POWER HOUSE

1.3 DESIGN PRACTICES

Different practices adopted for the design by various design organizations are as follows.

i) T.V.A. Practice

The reinforcement is computed on the basis of bending stresses caused in the first lift of roof when the second lift is placed on top of it. For subsequent lifts the roof slab is supposed to develop arch action with supports on side piers. To this is added the reinforcement computed on shrinkage of the heavy roof slab subjected to restraining reactions from the piers and side walls.

ii) On account of its great depth, this slab is treated as a deep girder.

iii) The superimposed loads are assumed to be transferred by means of parabolic arches within mass concrete, which span over the opening.

These series of arches are suitably reinforced, taking into consideration the vertical and horizontal components of arch action. The mass of concrete lying below the hypothetical arches can be treated as supported on this arch. Another variation of this idea is to treat this portion as a lintel spanning between the opening with a load of concrete lying within the 45° isosceles triangle.

- iv) It is treated as a rigid body in which forces are distributed to both sides of the draft tube along a funicular curve.
- v) This portion as well as the floor and sides are treated as a massive block with tunnel shaped cavity in it.
- vi) This portion is treated as a top member of a frame work, the scroll case concrete above it acting as a medium to distribute the superimposed loads as well as contributing its own dead weight.
- vii) The Central Water and Power Commission recommend the following method for analyzing this portion. It is divided into two zones as shown in Fig.1.3. Zone 2 is directly below the downstream power house wall and is designed as deep girder for superimposed and dead loads. Zone 1 is divided into three strips A, B & C as shown in the figure. Strip A is just downstream of the throat ring of draft tube liner and is supposed to carry one-fourth generator load, one-third weight of liner and dead load of concrete below turbine floor. This is supported on strip B on either side of the throat for draft tube. Strip B is supported on the mass concrete and strip C. Strip B is supposed to carry the live load on floor and concrete dead load besides the reactions of strip A. Strip C which carries the reactions of strip B and the concrete dead load is analyzed by consistent deflections as below.
 - a) Load transmitted by the deep beam is such that the deflection of the beam is equal to the pier shortening.
 - b) The support to C is provided partly as a cantilever beam from zone 2 and partly as a beam supported on pier, it being supposed that the cantilever action is 75% and the beam action is 25%.

There is no acceptable design practice and correct analysis is not possible unless analysed as three-dimensional problem.

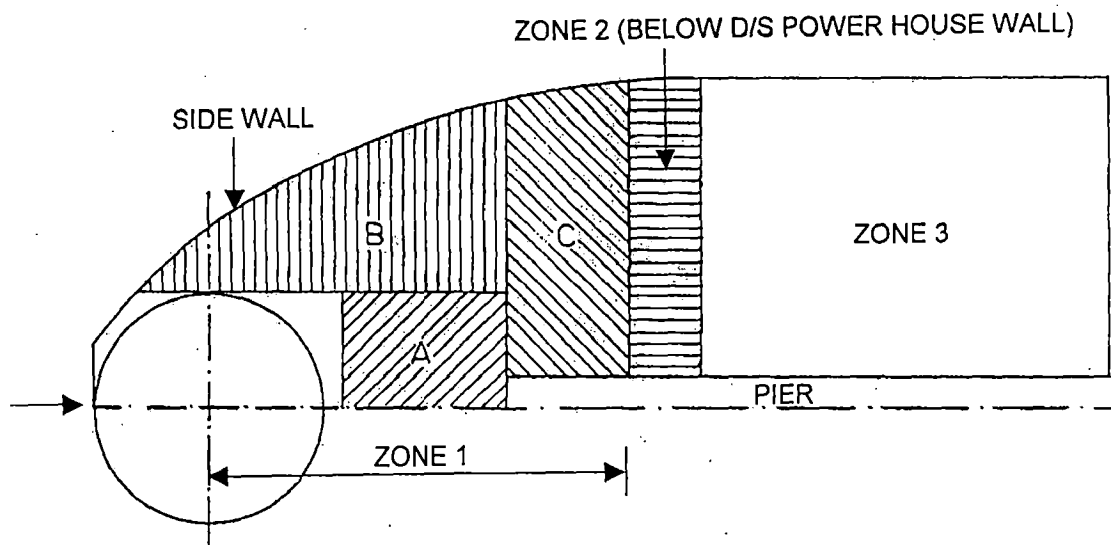


FIG. 1.3: SUBDIVISION OF ZONE 1 INTO STRIPS FOR STRUCTURAL SUPPORTS

The general practice is to analyse the substructure in two directions. In the transverse direction along the flow of water, distribution of vertical loads is nonuniform and prominent horizontal forces exist. In this direction the substructure is designed as a transition foundation member. In the longitudinal direction the substructure is designed to safely carry the superimposed loads of the machine etc. over the draft tube cavity.

Besides loads, temperature and shrinkage stresses are also to be taken into account. Sometimes magnitude of these stresses may exceed the stresses due to the superimposed loads. That is why some organizations do not give importance to stresses due to loads and provide reinforcement only for shrinkage stresses.

1.4 SCOPE OF THE STUDY

From the above, it is clear that the present knowledge about the actual structural behaviour of the substructure is inadequate and the prevalent design practices are only approximate. It is, therefore useful for the designer to know the true behaviour of the structure in order to work out an economic and safe design. A few attempts have been made using Photo elastic experimental technique and 2-D FEM to analyse the substructure for a few loading conditions only.

An attempt has therefore been made in this study to investigate stresses in elbow concrete spanning over draft tube on account of a various loading

conditions by analyzing it as three-dimensional structure using Finite Element Method.

1.5 ORGANISATION OF THE STUDY

This study is presented in this report in the following six chapters. The contents of each chapter are briefly described below:

Chapter 1 Introduction.

Chapter 2 deals with the literature review

Chapter 3 gives the concept of the Finite Element Method (FEM) and basic equations.

Chapter 4 explains the details of substructure model with assumptions, dimensions and steps for preparing the model.

Chapter 5 contains the results of analysis.

Chapter 6 deals with the conclusions and suggestions for further study.

CHAPTER 2

LITERATURE REVIEW

2.1 GENERAL

Methods employed for 3-D analysis are Photo elasticity technique and FEM.

2.2 STRESS ANALYSIS UNDER PHOTO ELASTICITY TECHNIQUE

2.2.1 Description Of The Method

Method employed for finding stress in 3-D model photo elasticity technique is stress freezing method⁽⁴⁾.

It is based on the diaphase behaviour of polymer materials when heated. The polymeric materials are composed of long chain hydrocarbon molecules some of which are well bonded into a 3-D network of primary bonds. However a large number of molecules are less solidly bonded together into shorter secondary chains. At room temperature both primary and secondary molecular bonds act to resist deformation due to applied load. However as the temperature of the polymer is increased the secondary bonds breakdown and the primary bonds in effect carry the entire applied load. Since the secondary bonds constitute a very large portion of the polymer, the deflections which the primary bonds undergo are quite large yet elastic in character.

If the temperature of the polymer is lowered to room temperature while the load is maintained on the model, the secondary bonds will be reformed between the highly elongated primary bonds and serve to lock them into their extended positions.

When the load is removed the primary bonds relax to a very modest degree but the main portion of their deformation is not recovered. The elastic deformation of the primary bonds is permanently locked into the model by the reformed secondary bonds.

As these deformations are locked in on a molecular scale, the accompanying birefringence is maintained in any small section cut from the original model. The cutting or slicing process may relieve the molecular layer on

each face of a slice cut from a model but this relieved layer is so thin relative to the thickness of the slice that the effect is not observed.

Procedure for the stress freezing procedure is described below.

1. Place the model into the stress-freezing oven.
2. Heat the model relatively rapidly until the critical temperature is attained.
3. Apply the required loads.
4. Soak the model at least 2 to 4 hours until a uniform temperature throughout the model is obtained.
5. Cool the model sufficiently slowly that temperature gradients are minimized at the rate of 1^o C per hour.
6. Remove the load and slice the model.

2.2.2 Basic Photo-elastic Equation

The basic photo elastic equation⁽⁴⁾ is

$$\sigma_1 - \sigma_2 = \frac{Nf_\sigma}{h} \quad (2.1)$$

where h = thickness of the slice in inch.

σ_1, σ_2 = principal stresses along two principal axes.

$$N = \frac{\Delta}{2\pi} \quad (2.2)$$

where N = relative retardation in terms of complete cycle of retardation, 2π .

Δ = relative retardation,

$$f_\sigma = \frac{\lambda}{c} = \text{the material stress fringe value in psi-in,} \quad (2.3)$$

where λ = wave length,

$$c = c_1 - c_2 = \text{relative stress optic coefficient,} \quad (2.4)$$

where c_1 and c_2 are stress optic coefficients along the two principal axes.

According to Maxwell:

“The changes in the indices of refraction are linearly proportional to the stresses induced in the model” i.e.

$$\begin{aligned} n_1 - n_0 &= c_1\sigma_1 + c_2\sigma_2 \\ n_2 - n_0 &= c_1\sigma_2 + c_2\sigma_1 \end{aligned} \quad (2.5)$$

where n_0 = index of refraction of the model in the unstressed state,

n_1, n_2 are indices of refraction along the two principal axes associated with σ_1 & σ_2 respectively.

The component stresses computed from the above experimental method are presented in the form of stress contours at different planes. Analysis of substructure of a power house using photo elastic technique has been carried out by Nigam⁽¹⁰⁾ for a point load and stress contours are given in his book "Handbook of Hydro Electric Engineering (1985)".

2.3 STRESS ANALYSIS UNDER FINITE ELEMENT METHOD

2.3.1 2-D Finite Element Method

Finite Element Method is essentially a generation of standard structural analytical procedure, which permits the calculations of stresses and deflections in two and three-dimensional structures. The basic concept of the FEM is discussed in Chapter 3. This method is not the structural approximation of the continuum, but rather the use of 2 or 3 dimensional structural elements assembled together, being interconnected at nodal points, which represent the whole structure. For three-dimensional discretization a large number of elements of different shapes are to be employed to achieve a reasonable physical approximation. So there was a necessity for a very large capacity computer, which is at present available.

Dandekar⁽⁵⁾ has taken up the study of "Design Of Substructure Of Hydropower Stations" with case study of Khodri Power Station of Yamuna Hydel Project in two dimensional FEM. In longitudinal direction he has treated it as a plane strain case by considering number of sections at close intervals and as a plain stress case in transverse direction. If it is to consider plane strain case in longitudinal direction, clear objection will arise as the sectional properties of the substructure change continuously along the transverse direction because of varying shape and size of the draft tube cavity. So the stress pattern obtained from the two dimensional analysis will not be sufficiently valid to the tune of exactness and will introduce discontinuity at boundaries of the sections considered for observation. In the transverse direction also the substructure cannot be treated as a plane strain case because of the shape of the draft tube cavity also changes in this direction at different locations. So in this analysis plane stress case has been assumed. Further he has considered triangular elements and used self weight of structure and machine loads as uniformly

distributed with the boundary condition that displacement and rotation on lower and side boundaries (in X and Y directions) as zero. The main conclusion drawn from his study was that concentration of stresses occurs around the cavities in the structure, with tensile stresses at the top and bottom and compression at the sides of the cavities.

2.3.2 3-D Finite Element Method

The substructure of power house is essentially a 3-dimensional structure with complex shaped cavities having curvature in both direction and loading conditions are also vary both in longitudinal and transverse directions. So the assumptions of two-dimensional model for the substructure will not give the exact picture of nature of stresses developed at different locations. A 3-dimensional model study will give a clear picture sufficiently reliable and correct stress distribution pattern. In 3-dimensional model, number of elements can be increased to get more accurate results. So in the present study, in the FEM analysis, a 3-dimensional model of powerhouse substructure has been adopted with the help of ANSYS Package and results worked out are plotted and presented in the form of stress contours.

CHAPTER 3

THE FINITE ELEMENT METHOD

3.1 GENERAL

The finite element method is a numerical procedure for analysing structures, which permit the calculations of stresses and deflections. The most distinctive feature of finite element method that separates it from others is the division of a given domain into a set of sub-domains, called elements. The finite element procedure produces many simultaneous algebraic equations which are generated and solved on a digital computer. Results are rarely exact. However, errors are minimized by processing more equations, and results accurate enough for engineering purposes are obtainable at reasonable cost.

Using such elements, the structural idealization is obtained merely by dividing the original continuum into segments, all the material properties of the original system being retained in the individual elements. This is known as discretization. Instead of solving the problem for entire body in one operation, the solutions are formulated at each constituent unit and combined to obtain the solution for the original structure.

3.2 DESCRIPTION OF THE METHOD

3.2.1 Discretisation Of The Continuum

Discretisation is the process in which the given body is subdivided into an equivalent system of finite elements. Hence the body of the structure is essentially a piece of the whole. These elements provide natural representation of the properties of the original continuum. It may be noted that the continuum is simply zoned into small regions by imaginary planes in 3-D bodies and by imaginary lines in 2-D bodies. The first decision is to make the choice of the elements type. The boundaries of finite element may be straight or curvilinear.

The size of the element and the number into which the continuum is to be discretized depends upon the choice of the designer. As a general guideline it can be said that where the stress or strain gradients are expected to be comparatively flat i.e. variation is not rapid; the mesh can be coarse to reduce computations. Whereas in the zones in which stress or strain gradients are

expected to be steep i.e. pronounce variation occurs a finer mesh is indicated to get more accurate results. Theoretically speaking to get an exact solution the number of nodal points is infinite. So a trade off has to be made between computation effort and corresponding accuracy.

3.2.2 Selection Of Proper Interpolation Or Displacement Model

In finite element method we approximate a solution to a complicated problem by subdividing the region of interest into finite number of elements and representing the solution within each element by a relatively simple function of polynomials for ease of computation.

For the triangular element the linear polynomial

$$\phi = a_1 + a_2x + a_3y \quad (3.1)$$

is appropriate

where a_1, a_2, a_3 are constants which can be expressed in terms of ϕ_1, ϕ_2 and ϕ_3 which are values of ϕ at these nodes.

For the four noded quadrilateral the bilinear function.

$$\phi = a_1 + a_2x + a_3y + a_4xy \quad (3.2)$$

is appropriate

Eight node quadrilateral has eight a_i in its polynomial expansion and can represent a parabolic function.

Equation (3.1) & (3.2) are interpolations of function ϕ in terms of the position (x, y) within an element. If mesh of element is not too coarse and if ϕ_i happened to be exact, then ϕ away from nodes would be a good approximation.

3.2.3 Convergence Requirements

In any acceptable numerical formulation the numerical solution must converge or tend to the exact solution of the problem. For this the criteria is

- a) Displacement model must be continuous within the element and the displacements must be compatible within the adjacent elements.

The first part is automatically satisfied if displacement functions are polynomials. The second part implies that the adjacent elements must deform without causing openings, overlaps or discontinuities between them. This can be satisfied if displacements along the side of an element depend only upon

displacements of the nodes occurring on that side. Since the displacements of nodes on common boundary will be same, displacement for boundary line for both elements will be identical.

b) The displacement model must include rigid body displacement of the element.

Basically this condition states that there should exist such combinations of values of coefficients in displacement function that cause all points in the elements to experience the same displacement.

c) The displacement model must include the constant strain states of elements.

This means that there should exist such combinations of values of the coefficients in the displacement function that cause all points on the element to experience the same strain. The necessity of this requirement can be understood if we imagine that the continuum is divided into infinitesimally small elements. In such a case the strains in each element approach constant values all over the element. The terms α_3 and α_6 in the following equations

$$\begin{aligned}u(x) &= \alpha_1 + \alpha_2x + \alpha_3y \\v(y) &= \alpha_4 + \alpha_5x + \alpha_6y\end{aligned}\tag{3.3}$$

provide for uniform strain in x and y directions. The elements, which meet first criterion, are called compatible or conforming. The elements, which meet second and third criteria, are called complete. For plain strain and plain stress and 3-D elasticity the three conditions mentioned above are easily satisfied by linear polynomials.

3.2.4 Nodal Degree Of Freedom

The nodal displacements, rotations and/or strains necessary to specify completely the deformation of finite elements are called degrees of freedom (DOF) of elements.

3.2.5 Element Stiffness Matrix

The equilibrium equation derived from principle of minimum potential energy between nodal loads and nodal displacements is expressed as

$$\{F\}^e = [K]^e \{\delta\}^e$$

where $\{F\}^e$ = nodal force vector

$\{\delta\}^e$ = nodal displacement vector

$[K]^e$ = element stiffness matrix.

The stiffness matrix consists of the coefficients of equilibrium equations derived from material and geometric properties of the element. The elements of stiffness matrix are the influence coefficients. Stiffness of a structure is an influence coefficient that gives the force at one point on a structure associated with a unit displacement at the same or a different point⁽⁷⁾.

Local material properties as stated above are one of the factors, which, determine stiffness matrix. For an elastic isotropic body, Modulus of Elasticity (E) and Poisson's Ratio (ν) define the local material properties. The stiffness matrix is essentially a symmetric matrix, which follows from the principle of stationary potential energy, that "In an elastic structure work done by internal forces is equal in magnitude to the change in strain energy". And also from Maxwell Betti reciprocal theorem which states that: "If two sets of loads $\{F\}_1$ and $\{F\}_2$ act on a structure, work done by the first set in acting through displacements caused by the second set is equal to the work done by second set in acting through displacements caused by first set"⁽⁶⁾.

3.2.6 Nodal Forces And Loads

Generally when subdividing a structure we select nodal locations that coincide with the locations of the concentrated external forces. In case of distributed loading over the body such as water pressure on dam or the gravity forces the loads acting over an element are distributed to the nodes of that element by principle of minimum potential energy. If the body forces are due to gravity only then they are equally distributed among the three nodes of a triangular element.

3.2.7 Assembly Of Algebraic Equations For The Overall Discretized Continuum

This process includes the assembly of overall or global stiffness matrix for the entire body from individual stiffness matrices of the elements and the overall or global force or load vectors. In general the basis for an assembly method is

that the nodal interconnections require the displacement at a node to be the same for all elements adjacent to that node. The overall equilibrium relations between global stiffness matrix $[K]$, the total load vector $\{F\}$ and the nodal displacement vector for entire body $\{\delta\}$ is expressed by a set of simultaneous equations.

$$[K] \{\delta\} = \{F\}$$

The global stiffness matrix $[K]$ will be banded and also symmetric of size of $n \times n$ where, n = total number of nodal points in the entire body. The steps involved in generation of global stiffness matrix are:

- i) All elements of global stiffness matrix $[K]$ are assumed to be equal to zero.
- ii) Individual element stiffness matrices $[K]$ are determined successively.
- iii) The element k_{ij} of element stiffness matrix are directed to the address of element K_{ij} of global stiffness matrix which means

$$K_{ij} = \sum k_{ij}$$

Similarly nodal load $\{F_i\}^e$ at a node 'i' of an element 'e' is directed to the address of $\{F_i\}$ of total load vector i.e.

$$\{F_i\} = \sum \{F_i\}^e$$

3.2.8 Boundary Conditions

A problem in solid mechanics is not completely specified unless boundary conditions are prescribed. Boundary conditions arise from the fact that at certain points or near the edges the displacements are prescribed. The physical significance of this is that a loaded body or a structure is free to experience unlimited rigid body motion unless some supports or kinematic constraints are imposed that will ensure the equilibrium of the loads. These constraints are called boundary conditions. There are two basic types of boundary conditions, geometric and natural. One of the principal advantages of Finite Element Method is, we need to specify only geometric boundary conditions, and the natural boundary conditions are implicitly satisfied in the solution procedure as long as we employ a suitable valid variational principle. In other numerical methods, solutions are to be obtained by trial and error method to satisfy boundary conditions whereas in Finite Element Method boundary conditions are inserted

prior to solving algebraic equations and the solution is obtained directly without requiring any trial.

3.2.9 Solution For The Unknown Displacements

The algebraic equations $[K]\{\delta\}=\{F\}$ formed are solved for unknown displacements $\{\delta\}$ wherein $[K]$ and $\{F\}$ are already determined. The equations can be solved either by iterative or elimination procedure. Once the nodal displacements are found, then element strains or stresses can be easily found from generalized Hooke's law for a linear isotropic material.

The assumption in displacement function, the stresses or strains are constant at all points over the element, may cause discontinuities at the boundaries of adjacent elements. To avoid this sometimes it is assumed the values of stresses and strains obtained are for the centers of gravity of the elements and linear variation is assumed to calculate them at other points in the body.

3.3 SUMMARY OF PROCEDURE

The principal computational steps of linear static stress analysis by Finite Element Method are now listed⁽³⁾.

- i) **Input And Initialization:** Input the number of nodes and elements, nodal co-ordinates, structure node numbers of each element, material properties, temperature changes, mechanical loads and boundary conditions. Reserve storage space for structure arrays $[K]$ and $\{F\}$. Initialize $[K]$ and $\{F\}$ to null arrays. If array ID is used to manage boundary conditions, initialize ID and then convert it to a table of equation numbers.
- ii) **Compute Element Properties:** For each element compute element property matrix $[k]$ and element load vector $\{f\}$.
- iii) **Assemble The Structure:** Add $[k]$ into $[K]$ and $\{f\}$ into $\{F\}$. Go back to step 2, repeat steps 2 and 3 until all elements are assembled. Add external loads $\{P\}$ to $\{F\}$. Impose displacement boundary conditions (if not imposed implicitly during assembly by use of array ID).
- iv) **Solve the Equations:** $[K]\{\delta\} = \{F\}$ for $\{\delta\}$

- v) **Stress Calculation:** For each element extract nodal D.O.F. of element $\{\delta\}^e$ from nodal D.O.F. of structure $\{\delta\}$. Compute mechanical strains, if any and convert resultant strains to stresses.

3.4 MATHEMATICAL MODEL

3.4.1 General

Most Engineers and Scientists studying physical phenomena are involved with two major tasks:

1. Mathematical formulation of the physical process.
2. Numerical analysis of the mathematical model.

Development of the mathematical model of a process is achieved through assumptions concerning how the process works. In a numerical simulation, we use a numerical method and a computer to evaluate the mathematical model. While the derivation of the governing equations for most problems is not unduly difficult, their solution by exact methods of analysis is a formidable task. In such cases, approximate methods of analysis provide alternative means of finding solution. Among these finite element method is most frequently used.

Finite element method is endowed with three basic features.

1. A geometrically complex domain of the problem is represented as a collection of geometrically simple sub domains called finite elements.
2. Over each element, the approximation functions are derived using the basic idea that any continuous function can be represented by a linear combination of algebraic polynomials.
3. Algebraic relations among the undetermined coefficients (i.e. nodal values) are obtained by satisfying the governing equations over each element.

The approximation functions are derived using concepts from interpolation theory and are called interpolation functions. The degree of interpolation functions depends on the number of nodes in the element and the order of differential equation being solved.

3.4.2 Interpolation Function

The finite element approximation $U^e(x, y)$ of $u(x, y)$ over an element Ω^e must satisfy the following conditions in order for the approximate solution to be convergent to the true one⁽¹²⁾.

1. U^e must be differentiable.
2. The polynomials used to represent U^e must be complete (i.e. all terms beginning with a constant term up to the highest order used in the polynomial, should be included in U^e).
3. All terms in the polynomial should be linearly independent.

The number of linearly independent terms in the representation of U^e dictates the shape and number of DOF of the element.

3.4.3 Displacement Function

A 20 noded isoparametric finite element is shown in Fig. 3.1. For a typical finite element 'e' defined by nodes i, j, k etc. the displacements $\{f\}$ within the element are expressed as:

$$\{f\} = [N] \{\delta\}^e \quad (3.4)$$

where $[N] = [N_i \ N_j \ N_m \ \dots]$

and $\{\delta\}^e = \{\delta_i \ \delta_j \ \delta_m \ \dots\}$ (3.5)

The components of $[N]$ are in general functions of position and $\{\delta\}^e$ represents a listing of nodal displacements for a particular element.

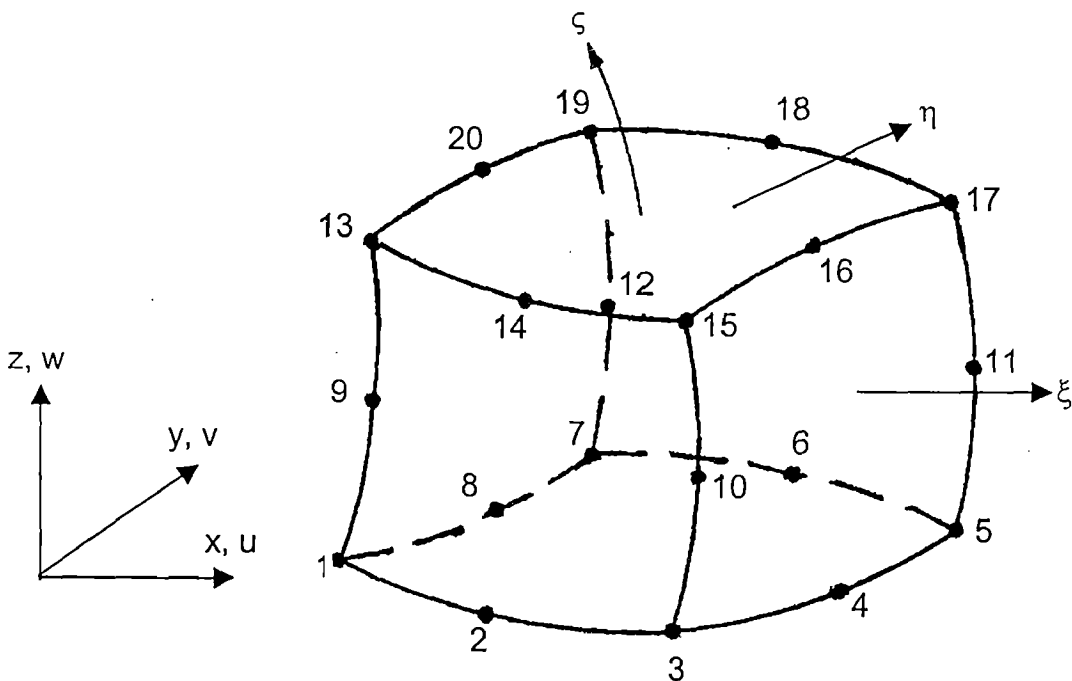


FIG. 3.1: A 20 NODED ISOPARAMETRIC SOLID ELEMENT

For the three dimensional element

$$\{f\} = \begin{Bmatrix} u \\ v \\ w \end{Bmatrix} \quad (3.6)$$

represents the displacements in x, y and z directions at a point within the element and

$$\{\delta_i\} = \begin{Bmatrix} u_i \\ v_i \\ w_i \end{Bmatrix} \quad (3.7)$$

are the corresponding displacements of node i.

$[N_i]$ is equal to $[N_i I]$ where N_i is the shape function of node i and I is an identity matrix.

3.4.4 Shape Functions

The shape function for a 20 noded isoparametric hexahedral element⁽⁹⁾ used in this study (shown in Fig. 3.1) are given by the following.

At corner nodes (node numbers 1, 3, 5, 7, 13, 15, 17, 19)

$$N_i = 1/8 (1 + \xi_0) (1 + \eta_0) (1 + \zeta_0) (-2 + \xi_0 + \eta_0 + \zeta_0) \quad (3.8a)$$

For mid side nodes:

i) $\xi_i = 0, \eta_i = \pm 1, \zeta_i = \pm 1$

(node numbers 2, 6, 14, 18)

$$N_i = 1/4 (1 - \xi^2) (1 + \eta_0) (1 + \zeta_0) \quad (3.8b)$$

ii) $\eta_i = 0; \xi_i = \pm 1; \zeta_i = \pm 1$

(node numbers 4, 8, 16, 20)

$$N_i = 1/4 (1 - \eta^2) (1 + \xi_0) (1 + \zeta_0) \quad (3.8c)$$

iii) $\zeta_i = 0; \xi_i = \pm 1; \eta_i = \pm 1$

(node numbers 9, 10, 11, 12)

$$N_i = 1/4 (1 - \zeta^2) (1 + \xi_0) (1 + \eta_0) \quad (3.8d)$$

where

$$\left. \begin{aligned} \xi_0 &= \xi \xi_i \\ \eta_0 &= \eta \eta_i \\ \zeta_0 &= \zeta \zeta_i \end{aligned} \right\} \quad (3.9)$$

ξ_i, η_i, ζ_i are the local coordinates of the i^{th} node and ξ, η and ζ are the local coordinates of the point concerned.

3.4.5 Strains

With displacements known at all points within the element the strains at any point can be determined. Six strain components are relevant in three-dimensional analysis and the strain vector can be expressed as:

$$\{\epsilon\} = \begin{Bmatrix} \epsilon_x \\ \epsilon_y \\ \epsilon_z \\ \epsilon_{xy} \\ \epsilon_{yz} \\ \epsilon_{zx} \end{Bmatrix} = \begin{Bmatrix} \frac{\partial u}{\partial x} \\ \frac{\partial v}{\partial y} \\ \frac{\partial w}{\partial z} \\ \frac{\partial u}{\partial y} + \frac{\partial v}{\partial x} \\ \frac{\partial v}{\partial z} + \frac{\partial w}{\partial y} \\ \frac{\partial w}{\partial x} + \frac{\partial u}{\partial z} \end{Bmatrix} \quad (3.10)$$

which can be further written as :

$$\{\epsilon\} = [B] \{\delta\}^e = [B_i \ B_j \ B_k \ \dots] \{\delta\}^e \quad (3.11)$$

in which $[B_i]$ is the strain displacement matrix.

$[B_i]$ is given by

$$[B_i] = \begin{bmatrix} \frac{\partial N_i}{\partial x} & 0 & 0 \\ 0 & \frac{\partial N_i}{\partial y} & 0 \\ 0 & 0 & \frac{\partial N_i}{\partial z} \\ \frac{\partial N_i}{\partial y} & \frac{\partial N_i}{\partial x} & 0 \\ 0 & \frac{\partial N_i}{\partial z} & \frac{\partial N_i}{\partial y} \\ \frac{\partial N_i}{\partial z} & 0 & \frac{\partial N_i}{\partial x} \end{bmatrix} \quad (3.12)$$

with other sub matrices obtained in a similar manner simply by interchange of subscripts.

For isoparametric elements

$$\begin{aligned} x &= \sum_{i=1}^n N_i x_i, \quad y = \sum_{i=1}^n N_i y_i, \quad z = \sum_{i=1}^n N_i z_i \\ u &= \sum_{i=1}^n N_i u_i, \quad v = \sum_{i=1}^n N_i v_i, \quad w = \sum_{i=1}^n N_i w_i \end{aligned} \quad (3.13)$$

the summation being over total number of nodes in an element.

Because the displacement model is formulated in terms of the natural coordinates ξ , η and ζ and it is necessary to relate Eq. (3.12) to the derivatives with respect to these local coordinates.

The natural coordinates ξ , η and ζ are functions of global coordinates x , y , z . Using the chain rule of partial differentiation we can write:

$$\frac{\partial N_i}{\partial \xi} = \frac{\partial N_i}{\partial x} \frac{\partial x}{\partial \xi} + \frac{\partial N_i}{\partial y} \frac{\partial y}{\partial \xi} + \frac{\partial N_i}{\partial z} \frac{\partial z}{\partial \xi} \quad (3.14)$$

Performing the same differentiation with respect to the other two coordinates and writing in matrix form

$$\begin{Bmatrix} \frac{\partial N_i}{\partial \xi} \\ \frac{\partial N_i}{\partial \eta} \\ \frac{\partial N_i}{\partial \zeta} \end{Bmatrix} = \begin{bmatrix} \frac{\partial x}{\partial \xi} & \frac{\partial y}{\partial \xi} & \frac{\partial z}{\partial \xi} \\ \frac{\partial x}{\partial \eta} & \frac{\partial y}{\partial \eta} & \frac{\partial z}{\partial \eta} \\ \frac{\partial x}{\partial \zeta} & \frac{\partial y}{\partial \zeta} & \frac{\partial z}{\partial \zeta} \end{bmatrix} \begin{Bmatrix} \frac{\partial N_i}{\partial x} \\ \frac{\partial N_i}{\partial y} \\ \frac{\partial N_i}{\partial z} \end{Bmatrix} = [J] \begin{Bmatrix} \frac{\partial N_i}{\partial x} \\ \frac{\partial N_i}{\partial y} \\ \frac{\partial N_i}{\partial z} \end{Bmatrix} \quad (3.15)$$

where $[J]$ is given by:

$$[J] = \begin{bmatrix} \frac{\partial x}{\partial \xi} & \frac{\partial y}{\partial \xi} & \frac{\partial z}{\partial \xi} \\ \frac{\partial x}{\partial \eta} & \frac{\partial y}{\partial \eta} & \frac{\partial z}{\partial \eta} \\ \frac{\partial x}{\partial \zeta} & \frac{\partial y}{\partial \zeta} & \frac{\partial z}{\partial \zeta} \end{bmatrix} \quad (3.16)$$

The matrix $[J]$ is called the Jacobian matrix. The global derivatives can be found by inverting $[J]$ as follows:

$$\begin{Bmatrix} \frac{\partial N_i}{\partial x} \\ \frac{\partial N_i}{\partial y} \\ \frac{\partial N_i}{\partial z} \end{Bmatrix} = [J]^{-1} \begin{Bmatrix} \frac{\partial N_i}{\partial \xi} \\ \frac{\partial N_i}{\partial \eta} \\ \frac{\partial N_i}{\partial \zeta} \end{Bmatrix} \quad (3.17)$$

Substituting Eq. (3.13) into Eq. (3.16) the Jacobian matrix is given by

$$[J] = \begin{bmatrix} \sum \frac{\partial N_i}{\partial \xi} x_i & \sum \frac{\partial N_i}{\partial \xi} y_i & \sum \frac{\partial N_i}{\partial \xi} z_i \\ \sum \frac{\partial N_i}{\partial \eta} x_i & \sum \frac{\partial N_i}{\partial \eta} y_i & \sum \frac{\partial N_i}{\partial \eta} z_i \\ \sum \frac{\partial N_i}{\partial \zeta} x_i & \sum \frac{\partial N_i}{\partial \zeta} y_i & \sum \frac{\partial N_i}{\partial \zeta} z_i \end{bmatrix} \quad (3.18a)$$

$$[J] = \begin{bmatrix} \frac{\partial N_1}{\partial \xi} & \frac{\partial N_2}{\partial \xi} & \dots \\ \frac{\partial N_1}{\partial \eta} & \frac{\partial N_2}{\partial \eta} & \dots \\ \frac{\partial N_1}{\partial \zeta} & \frac{\partial N_2}{\partial \zeta} & \dots \end{bmatrix} \begin{bmatrix} x_1 & y_1 & z_1 \\ x_2 & y_2 & z_2 \\ x_3 & y_3 & z_3 \\ \cdot & \cdot & \cdot \\ \cdot & \cdot & \cdot \\ \cdot & \cdot & \cdot \end{bmatrix} \quad (3.18b)$$

3.4.6 Stresses

The stresses are related to the strains as:

$$\{\sigma\} = [D] (\{\epsilon\} - \{\epsilon_0\}) + \{\sigma_0\} \quad (3.19)$$

where $[D]$ is an elasticity matrix containing the appropriate material properties.

$\{\epsilon_0\}$ is the initial strain vector.

$\{\sigma\}$ is the stress vector given by

$$\{\sigma\} = \{\sigma_x, \sigma_y, \sigma_z, \sigma_{xy}, \sigma_{yz}, \sigma_{zx}\}^T \text{ and}$$

$\{\sigma_0\}$ is the initial stress vector.

For elastic, isotropic material the elasticity matrix is given by:

$$[D] = \frac{E}{(1+\nu)(1-2\nu)} \begin{bmatrix} 1-\nu & \nu & \nu & 0 & 0 & 0 \\ \nu & 1-\nu & \nu & 0 & 0 & 0 \\ \nu & \nu & 1-\nu & 0 & 0 & 0 \\ 0 & 0 & 0 & \frac{1-2\nu}{2} & 0 & 0 \\ 0 & 0 & 0 & 0 & \frac{1-2\nu}{2} & 0 \\ 0 & 0 & 0 & 0 & 0 & \frac{1-2\nu}{2} \end{bmatrix} \quad (3.20)$$

where E is the Young's modulus of elasticity and ν the Poisson's ratio of the material of the element.

3.4.7 Stiffness Matrix

The stiffness matrix of the element is given by the following relation

$$\{F\}^e = [K]^e \{\delta\}^e \quad (3.21)$$

where $\{F\}^e$ is the element nodal load vector, $\{\delta\}^e =$ nodal displacement vector and $[K]^e$ the element stiffness matrix given by :

$$[K]^e = \int [B]^T [D][B] dV = [B]^T [D][B] \int dV = [B]^T [D][B] V \quad (3.22)$$

where V refers to the volume of the element.

The equivalent nodal forces are obtained as

i) Forces due to body forces $\{\phi_x, \phi_y, \phi_z\}^T$ per unit volume are given by

$$\{F\}_b = \int_v [N]^T \{\phi\} dV \quad (3.23a)$$

ii) Forces due to pressure distribution $\{p_x, p_y, p_z\}^T$ per unit area are given by :

$$\{F\}_p = \int_v [N]^T \{p\} dA \quad (3.23b)$$

For the complete structure relation of the form given below is obtained

$$[K] \{\delta\} = \{F\} \quad (3.24)$$

Where $\{\delta\}$ is the vector of global displacements, $\{F\}$ the load vector and $[K]$ the stiffness matrix.

The global stiffness matrix $[K]$ is obtained by directly adding the individual stiffness coefficients in the global stiffness matrix. Similarly the global load vector for the system is also obtained by adding individual element loads at the appropriate locations in the global vector.

The mathematical statement of the assembly procedure is:

$$\begin{aligned} [K] &= \sum_{e=1}^E [K]^e \\ \{F\} &= \sum_{e=1}^E \{F\}^e \end{aligned} \quad (3.25)$$

where E is the total number of elements.

To transform the variable and the region with respect to which the integration is made the relationship

$$dV = dx \, dy \, dz = \det[J] \, d\xi \, d\eta \, d\zeta \quad (3.26)$$

is used.

Writing explicitly

$$\int_{-1}^{+1} \int_{-1}^{+1} \int_{-1}^{+1} \det[J] \, d\xi \, d\eta \, d\zeta \quad (3.27)$$

and the characteristic element stiffness matrix can be expressed as

$$[K]^e = [B]^T [D] [B] \int_{-1}^{+1} \int_{-1}^{+1} \int_{-1}^{+1} \det[J] \, d\xi \, d\eta \, d\zeta \quad (3.28)$$

A 2 x 2 x 2 integration has been used for the three dimensional analysis.

3.5 SIGN CONVENTION

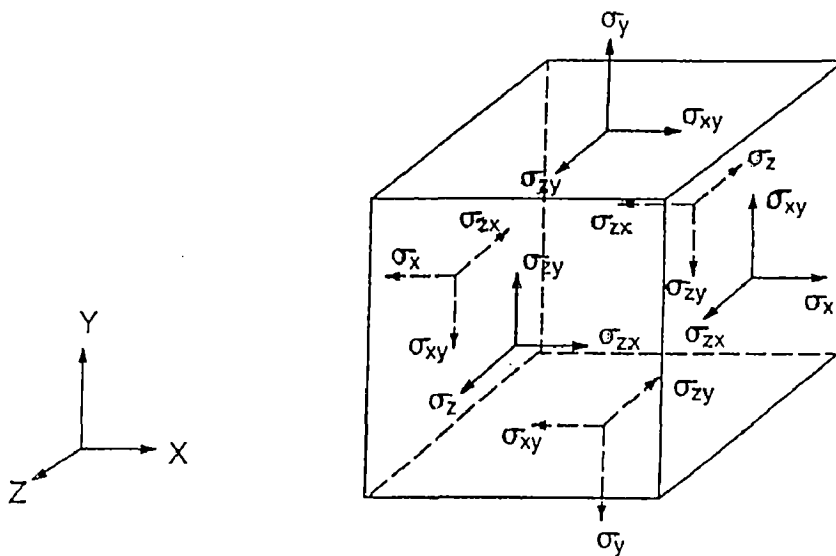


FIG. 3.2: STRESS VECTOR DEFINITION

The stress vectors are shown in Fig.3.2. The sign convention for ANSYS programme is that tension is positive and compression is negative. Shear is positive when the two applicable positive axes rotate towards each other.

3.6 PROCESSES IN ANSYS

ANSYS programme has many finite element analysis capabilities, ranging from a simple linear, static analysis to a complex, non-linear, transient dynamic analysis.

The distinct steps in ANSYS are as follow.

- i) Building the model.
- ii) Define an element type.
- iii) Define material properties.
- iv) Meshing the model into elements and nodes.
- v) Apply boundary conditions and loads.
- vi) Obtain the solution.

ANSYS process status consists of

- Form element matrices.
- Prepares elements for solver.
- Solves equations.
- Calculates element results.

vii) Review of results in general post processor.

3.7 ANSYS INPUTS

E_x = Young's Modulus in X direction (input as EX)

ν_{xy} = Poisson's ratio (input as NUXY)

CHAPTER 4

SUBSTRUCTURE MODEL

4.1 GENERAL

A 3-D model of the substructure has been prepared having same dimension as the power house analysed by photo elasticity method⁽¹⁰⁾ to determine the stresses. It is subjected to same concentrated load over elbow portion. It is done to validate the FEM programme by comparing the stresses of the FEM model with those obtained by photo elasticity method. FEM analysis of the same model is, thereafter, carried out under other loading conditions to get an insight to the structural behaviour of the substructure especially the elbow portion. The shape of the draft tube adopted is without pier and the dimensions are as per U.S.B.R. criterion.

4.2 ASSUMPTIONS IN THE MODEL

The various simplified assumptions made are given below:

- i) The material is within its elastic limit.
- ii) The material is isotropic.
- iii) Concrete around the draft tube is homogeneous.
- iv) Foundation of substructures is rigid.
- v) The power house model represents a structure, which is usually adopted for a reaction turbine (Francis or Kaplan) with vertical setting of shaft.
- vi) The substructure model is enclosed on all sides except on the downstream side.
- vii) Shape of draft tube is as per U.S.B.R. design.
- viii) Model does not provide any gallery for approaching the draft tube.
- ix) Young's Modulus of Elasticity of concrete (E_{xx}) = 2.05×10^5 kg/cm².
- x) Poisson's Ratio of concrete (ν) = 0.2

4.3 DIMENSIONS OF THE MODEL

- i) Discharge diameter (D) is 25.4 mm.
- ii) Base of model is 157.45 mm (long) x 109 mm (wide).
- iii) Minimum vertical dimension of the draft tube is 0.69 D while at exit

it is $0.91D$. Width of opening at its extremity is 79.55 mm.

- iv) Invert of draft tube is $0.59 D$ above base.
- v) Projection of power house from main machine hall is 57.45 mm.
- vi) The minimum dimension above draft tube is $1.23 D$ in projected space.
- vii) Width of wall on penstock side is 16 mm and other side is 13.45 mm as the penstock profile goes beyond the draft tube profile in direction of flow.
- viii) A space of 44.5 mm is kept upstream of turbine pit.
- ix) Total height of model is 69 mm.
- x) Inner radius = $R_i = 0.59D = 15$ mm.
- xi) Outer radius = $R_o = 1.32 D = 32.52$ mm.

4.4 LOADING CONDITIONS

The model is analysed under the following four loading conditions as listed below.

4.4.1 Load Condition 1

A concentrated load of 12.5 kg over a square base of 6.35 mm x 6.35 mm was applied centrally above elbow concrete between Slice 8($Z=74.476$ mm) and Slice 9($Z=83.973$ mm).

Coordinate location of load: $X = 49.225$ to 58.267 mm.

$Y = 69.0$ mm.

$Z = 74.476$ to 83.973 mm.

4.4.2 Load Condition 2

The same concentrated load of 12.5 kg over a square base of 6.35 mm x 6.35 mm was applied centrally above elbow concrete between Slice 9($Z=83.973$ mm) and Slice 10($Z=92.476$ mm).

Coordinate location of load: $X = 49.225$ to 58.267 mm.

$Y = 69.0$ mm.

$Z = 83.973$ mm to 92.476 mm.

4.4.3 Load Condition 3

Uniformly distributed load of 0.2 kg/cm^2 was applied above elbow concrete on top of substructure simulating generator barrel load (between $Z=69.9$ to 100 mm).

Coordinate location of load: X = 0 to 109 mm.
Y = 69.0 mm.
Z = 69.9 to 100.0 mm.

4.4.4 Load Condition 4

The same concentrated load of 12.5 kg over square bases of 6.35 mm x 6.35 mm each were applied on either supports on the line of downstream power house wall simulating gantry column loads between Slice 10 and 11.

Coordinate location of loads:

Left location	X = 0 to 6.35 mm. Y = 69.0 mm. Z = 93.65 to 100.0 mm.
Right location	X = 102.65 to 109 mm. Y = 69.0 mm. Z = 93.65 to 100.0 mm.

In order to solve the problem for power house substructure design it is necessary to find the true nature of stresses in concrete with finite dimension and containing cavities and hollows. Some results of photo elasticity study of the 3-D model⁽¹⁰⁾ are available. But photo elasticity study for a substructure is cumbersome and found not to be feasible on account of cost and time involved. The method of numerical stress analysis by finite element method using ANSYS is less time consuming and is adopted in this case.

4.5 STEPS IN MODELING

4.5.1 Modeling

File Name: Substructure

File Change Title: Stress Analysis of Elbow concrete.

Preference: Structural O.K.

Create KPs in Active C.S.

<u>KP No.</u>	<u>X in mm</u>	<u>Y in mm</u>	<u>Z in mm</u>
1	0	0	0
2	109	0	0
3	109	0	157.45
4	0	0	157.45
5	0	69	0
6	109	69	0
7	109	69	157.45
8	0	69	157.45

Plot Control, Pan Zoom Rotate

Create 12 lines

1-2-3-4-1

5-6-7-8-5

1-5,2-6, 3-7, 4-8

Create KPs	<u>KP No.</u>	<u>X in mm</u>	<u>Y in mm</u>	<u>Z in mm</u>
	9	40.6	69	44.5
	10	66.0	69	44.5

Create line 9-10 (Line No. 13)

Copy line No. 13 by Z offset 25.4 mm.

Create KPs is Active C.S.

<u>KP No.</u>	<u>X in mm</u>	<u>Y in mm</u>	<u>Z in mm</u>
13	13.45	15	94.2
14	13.45	15	157.45
15	13.45	38.11*	157.45 //0.91 D
16	13.45	32.52*	94.2 //0.69 D.

Create Lines 13 ———14 ———15 ——— 16 ———13

Lines Nos. 15 16 17 18

Create area arbitrary by lines no. 15, 16, 17 & 18

Copy this area by X offset = 79.55 mm

Plot lines - Delete area only (the areas just created)

Delete line no. 18 (13 - 16) and line no. 22 (17 - 20)

Create KPs in Active C.S.

<u>KP No.</u>	<u>X in mm</u>	<u>Y in mm</u>	<u>Z in mm</u>
21	40.6	15	44.5 //from Point 12
22	66.0	15	44.5
23	40.6	32.52	69.9
24	66.0	32.52	69.9

Create lines between KPs 13 - 21, 21- 9, 16 – 23 & 23 - 11

Similarly between KPs 17 - 22, 22-10, 20 – 24 & 24 -12.

Create Line Fillet

<u>Between Lines</u>	<u>Fillet Radius in mm</u>	<u>Remarks</u>
17 & 23	$D/2 = 12.7$	Add new lines to a single line with existing lines deleted
15 & 18	12.7	-do-
21 & 27	12.7	-do-
19 & 25	12.7	-do-

Create Line Fillet

<u>Between Lines</u>	<u>Fillet Radius in mm</u>	<u>Remarks</u>
17 & 24	$0.59 D = 15$	Add new lines to a single line with existing lines deleted
21 & 28	15	-do-
15 & 22	$1.32D = 33.52$	-do-
19 & 26	33.52	-do-

Delete KPs No. 13, 16, 17, 20, 21, 22, 23 & 24

Create lines 9 - 11, 10 - 12, 15 - 19, 14 - 18 O.K.

Create area by lines L₇, L₈, L₅, L₆

And divide area A₁ by lines No. 13, 22, 14 and 18

Create area by lines for inner volume and create the inner volume.

Create areas for outer volume and create the outer volume.

Delete, volume and below, inner volume.

4.5.2 Define Element Type

<u>Element Type</u>	<u>Solid 20 node 95</u>
Element option	K ₅ nodal stress

K₆ no extra output

K₁₁ 14point rule

4.5.3 Define Material Property

Material property EX = 2.05×10^3 kg/mm²

NUXY = 0.2

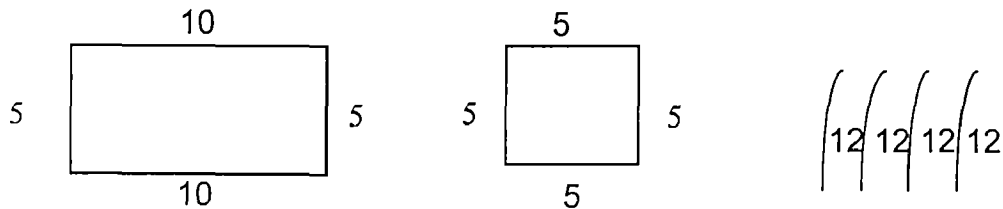
Define default attributes, O.K.

4.5.4 Meshing Of Model

Line division X = 22

Y = 14

Z = 20.



Mesh Volume.

Shape . Tet.

Mesher . Free

4.5.5 Solution Part

New Analysis static O.K.

Apply boundary conditions

Select Nodes Z = 0 (in mm) All DOF

Y = 0 (in mm) All DOF

X = 0 (in mm) All DOF

X = 109 (in mm) All DOF

Apply loads,

i) Load condition 1

Select nodes X = 49.225, 58.267 (in mm)

Y = 69.0 (in mm)

Z = 74.476, 83.973 (in mm)

14 nodes found

Load applied per node is FY = - 12.5 / 14 kg

ii) Load condition 2

Select nodes X = 49.225, 58.267 (in mm)
Y = 69.0 (in mm)
Z = 83.973, 92.476 (in mm)

11 nodes found

Load applied per node is $FY = - 12.5 / 11$ kg

iii) Load condition 3

Select nodes X = 0, 109 (in mm)
Y = 69.0 (in mm)
Z = 69.9, 100.0 (in mm)

Apply pressure on nodes = 0.002 kg/mm²

iv) Load condition 4

Left Side

Select nodes X = 0, 6.35 (in mm)
Y = 69.0 (in mm)
Z = 93.65, 100.0 (in mm)

3 nodes found

Load applied per node is $FY = - 12.5 / 3$ kg

Right Side

Select nodes X = 102.65, 109 (in mm)
Y = 69.0 (in mm)
Z = 93.65, 100.0 (in mm)

3 nodes found

Load applied per node is $FY = - 12.5 / 3$ kg

After application of loads and boundary conditions for each load condition solution was commanded for nodal solution for stress components σ_x (SX), σ_z (SZ) and σ_y (SY) at various Slices, Points and Strips respectively, whose locations are as mentioned in the Tables 4.1, 4.2 and 4.3 and are shown in Fig 4.1 to 4.9. The results are presented in the form of stress contours at respective sections.

TABLE 4.1: LOCATION OF SLICES

Slice No.	Z Co-ord. in mm
0	3.998
1	12.496
2	20.993
3	30.490
4	38.487
5	47.984
6	56.482
7	66.478
8	74.476
9	83.973
10	92.476
11	100.967
12	109.965
13	118.962
14	127.459
15	136.456
16	144.954
17	153.951
18	157.450

TABLE 4.2: LOCATION OF POINTS

Point No.	X Co-ord. in mm
22	2.32
21	7.40
20	12.48
19	17.56
18	22.64
17	27.72
16	32.80
15	37.88
14	42.96
13	48.04
12	53.12
11	58.20
10	63.28
9	68.36
8	73.44
7	78.52
6	83.60
5	88.68
4	93.76
3	98.84
2	103.92
1	109.00

TABLE 4.3: LOCATION OF STRIPS

Strip No.	Y Co-ord. in mm
13	66.04
12	60.96
11	55.88
10	50.80
9	45.72
8	40.64
7	35.56
6	30.48
5	25.40
4	20.32
3	15.24
2	10.16
1	5.08

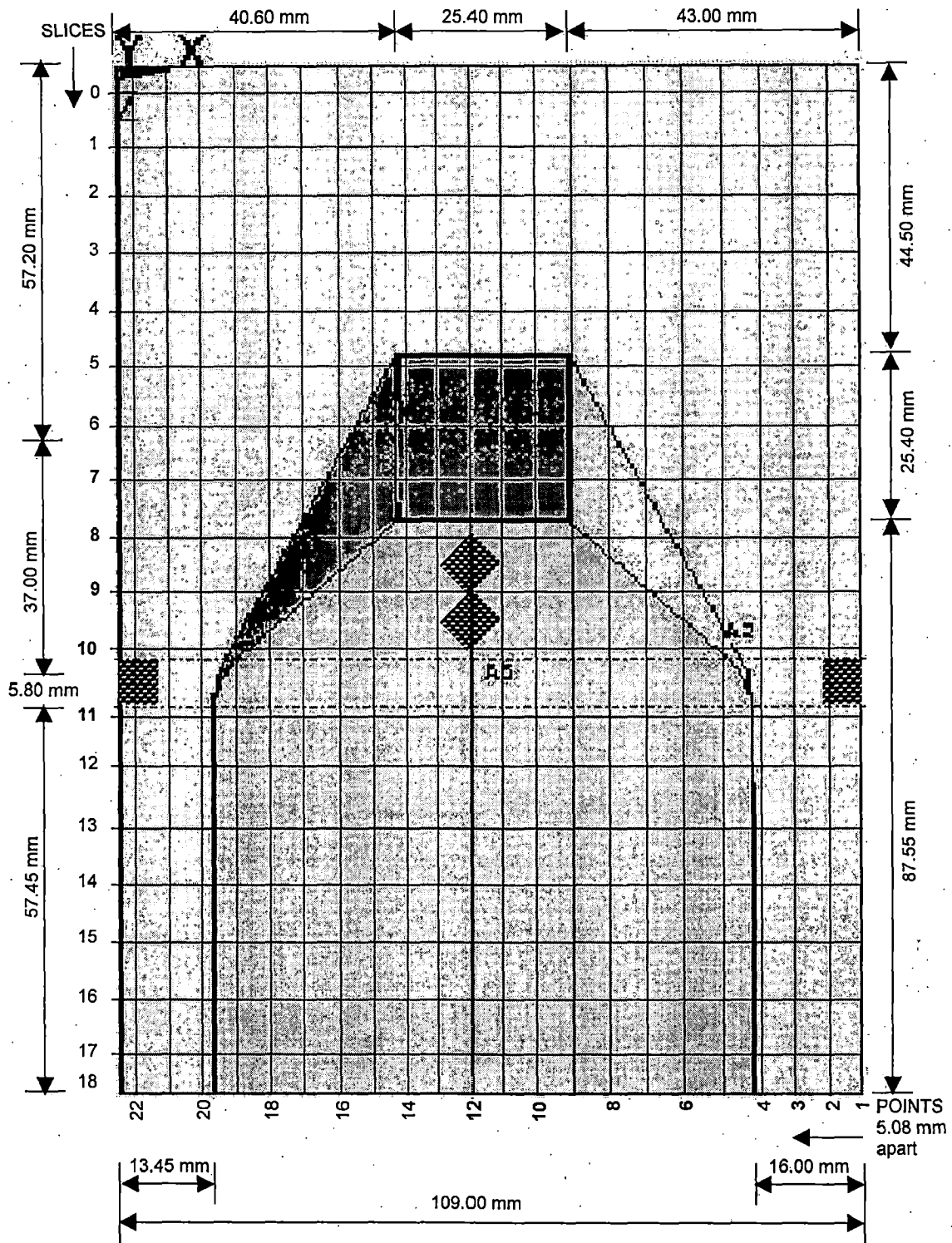


FIG. 4.1: PLAN OF SUBSTRUCTURE SHOWING SLICES AND POINTS
 (Positions of concentrated loads have been shown by hatched bases of loads 6.35 mm x 6.35 mm each)

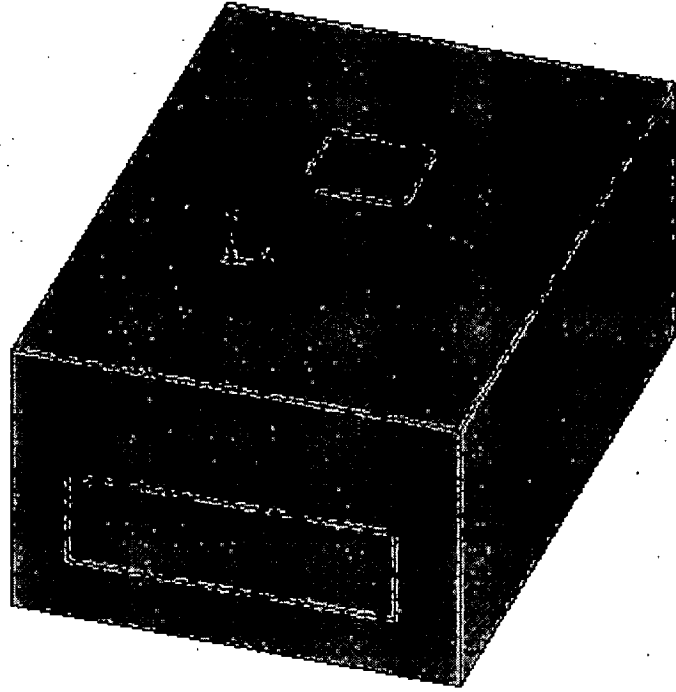


FIG.4.2: SUBSTRUCTURE MODEL

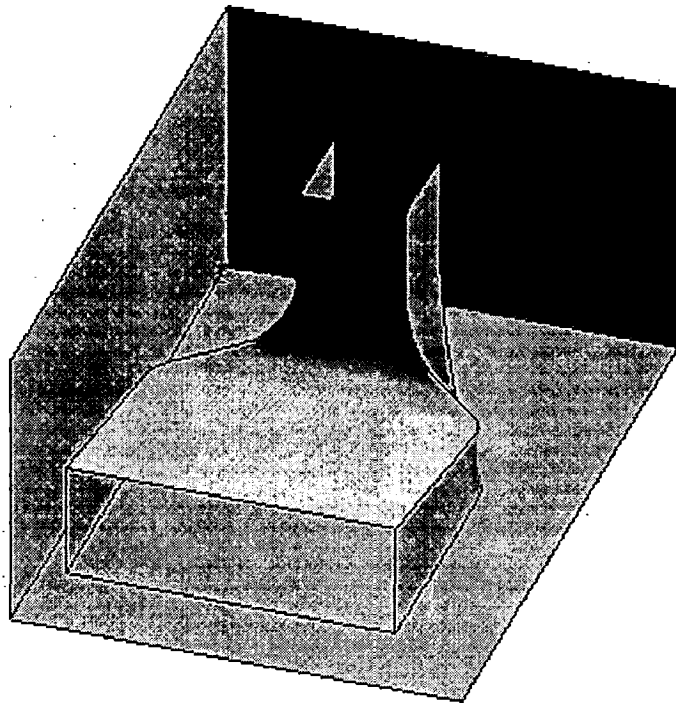


FIG. 4.3: VIEW OF SUBSTRUCTURE MODEL WITH INNER PASSAGE

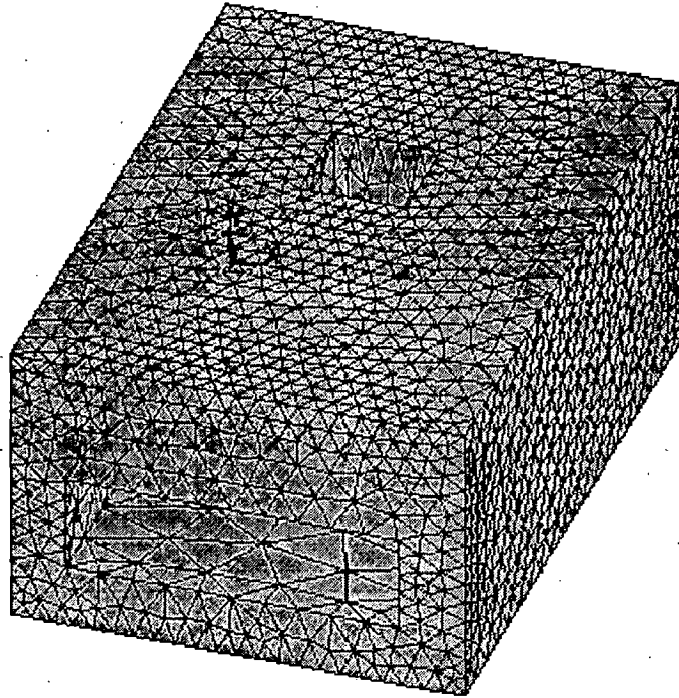


FIG. 4.4: VIEW OF SUBSTRUCTURE MODEL AFTER MESHING

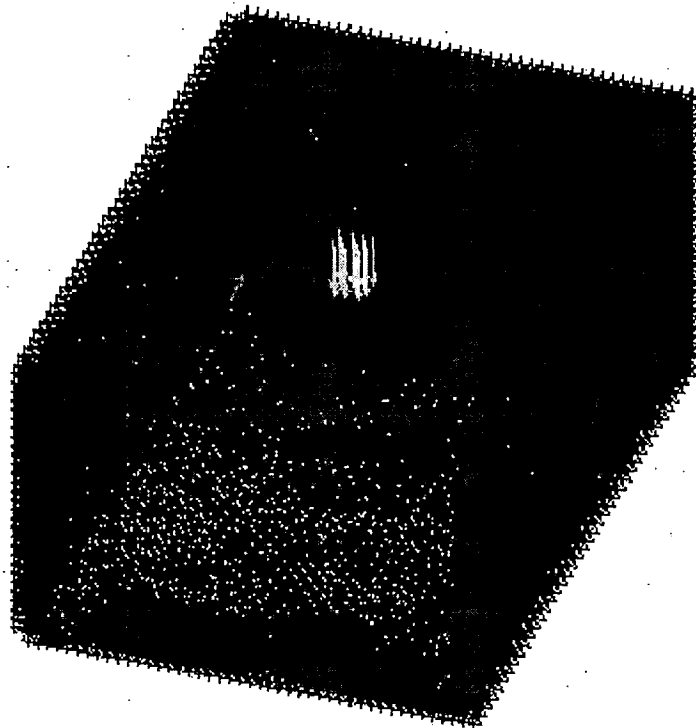


FIG 4.5: SUBSTRUCTURE MODEL

(Loaded with a concentrated load of 12.5 kg over a square base of 6.35 mm x 6.35 mm between Slice 8 & 9 centrally above elbow concrete)

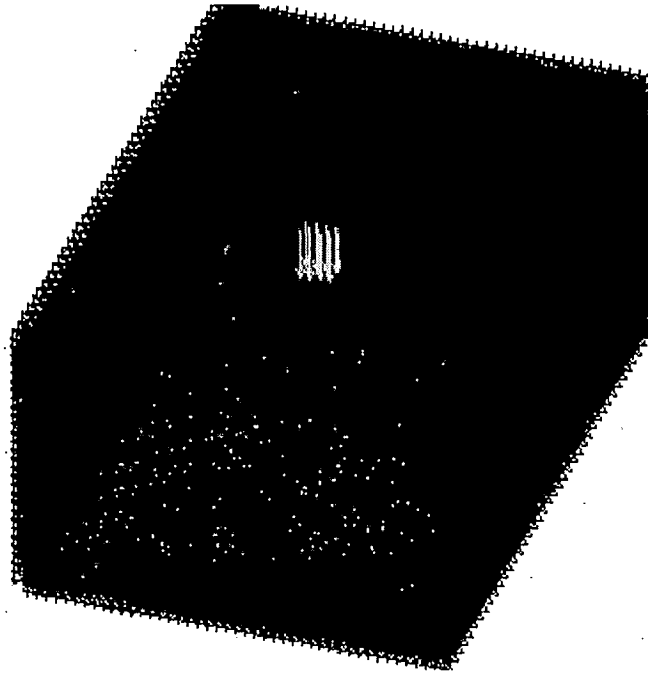


FIG. 4.6: SUBSTRUCTURE MODEL

(Loaded with a concentrated load of 12.5 kg over a square base of 6.35 mm x 6.35 mm between Slice 9 & 10 centrally above elbow concrete)

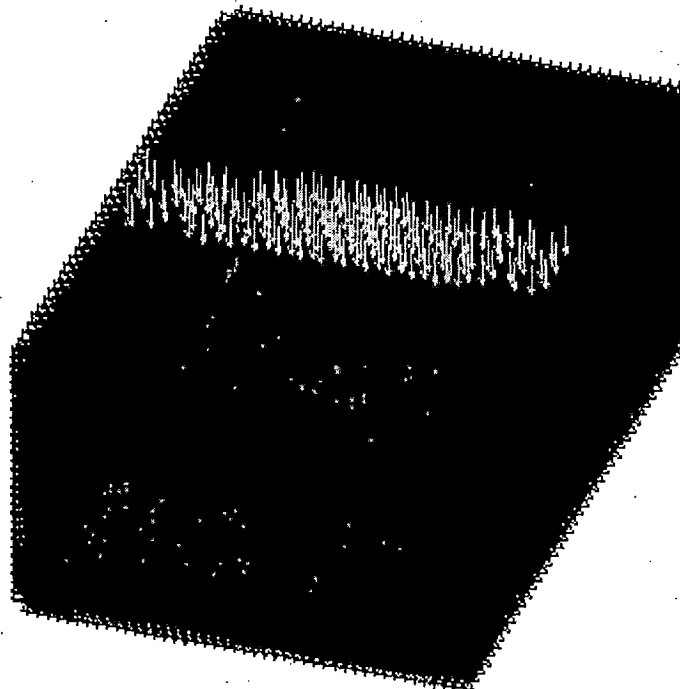


FIG. 4.7: SUBSTRUCTURE MODEL

(Loaded with uniformly distributed load of 0.2 kg/cm² above elbow concrete on top of substructure between Z=69.9 to 100 mm simulating generator barrel load)

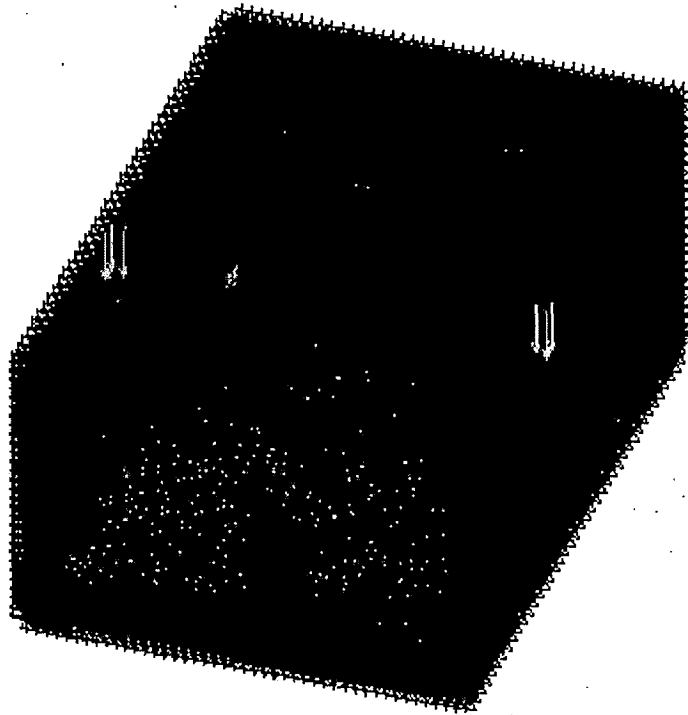


FIG. 4.8: SUBSTRUCTURE MODEL

(Loaded with concentrated loads of 12.5 kg over square bases of 6.35 mm x 6.35 mm each on either supports on the line of downstream power house wall simulating gantry column loads)

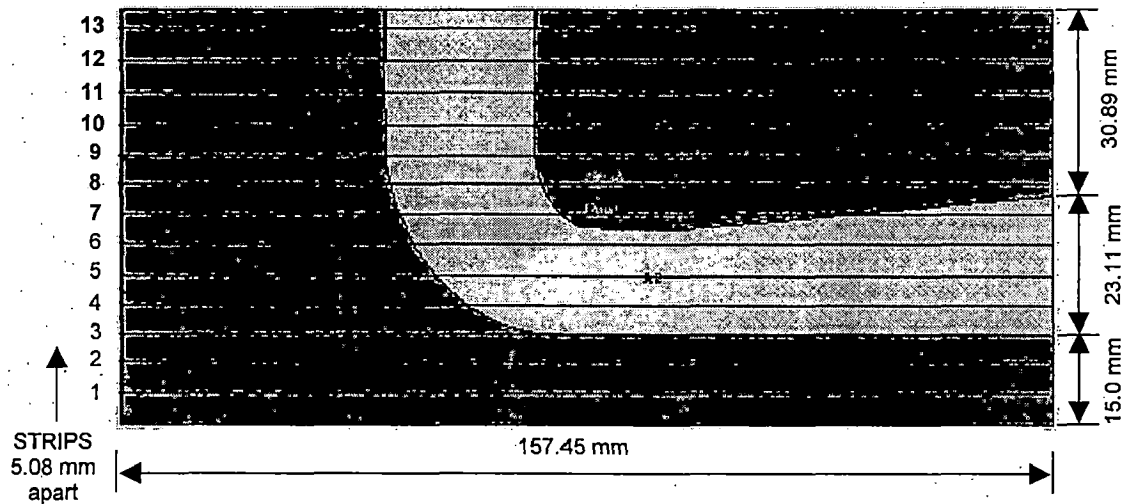


FIG. 4.9: TRANSVERSE SECTION OF THE MODEL AT POINT 12 (X=53.12 mm) SHOWING STRIPS

CHAPTER 5

RESULTS OF ANALYSIS

5.1 NATURE OF STRESS COMPONENT σ_x IN X-DIRECTION

5.1.1 Load Condition 1

A concentrated load of 12.5 kg over a square base of 6.35 mm x 6.35 mm was applied centrally above the elbow concrete between Slice 8 & 9. The component stresses σ_x , σ_y , σ_z have been worked out from the finite element analysis using ANSYS Package and the results are presented in the form of stress contours.

- It is observed that in longitudinal direction i.e. perpendicular to flow direction the draft tube cavity is under tension. The maximum tension occurs at Slice 8 (under the load). As one moves from u/s to d/s it is seen that the effect of tension around the cavity is reduced (Fig. 5.1 to 5.5).
- From Slice 8 (i.e. at $Z = 74.476$ mm) towards upstream the effect of tension is not observed where it is under compression (Fig. 5.1).
- From Slice 8 to towards d/s up to Slice 10 i.e. $Z = 92.476$ mm the draft tube cavity is under tension but this effect is reduced and effect of tension is not found in the concrete beyond Slice 11 ($Z = 100.967$ mm) i.e. in the concrete beyond the power house (Fig. 5.2 to 5.5).
- Depth of tension zone is more in flaring region i.e. from Slice 8 to 9 and maximum concentration of tension is seen above the draft tube opening in the plane of Slice 8 where the magnitude is 1.0313 kg/cm^2 (Fig. 5.2, Tab. 5.2).
- In the longitudinal direction compression zone is marked at top (under the load) and side walls at all sections and at Slice 7 it is under complete compression. At Slice 11 i.e. beyond the power house some tension zone is observed at support (side wall) locations (Fig. 5.1, 5.5).
- At all sections the magnitude of compression is higher than that of tension in the elbow concrete (Tab. 5.1 to 5.5).
- At Slice 8 and 9 there is tension all around the draft tube opening (Fig. 5.2, 5.3).

Results Of Analysis Of Photo Elasticity Study By Nigam⁽¹⁰⁾

- Tension occurs around the draft tube cavity and compression below the loading location towards top of substructure (Fig. 5.69 b, c, d & e) and the effect of tension and compression is of insignificant order at supports.
- Depth of tension zone is more than that of compression (Fig. 5.69 b to e).
- Maximum concentration of tension occurs at Slice 8 and 10 but maximum concentration of compression is at Slice 9 (Fig. 5.69 c) as in case of loading condition 1 (Tab. 5.3).

From the above results of the analyses by two methods it is seen that both show similar stress patterns in elbow concrete. In both the analyses draft tube opening is seen to experience tension around and compression zone develops below loading area only.

5.1.2 Load Condition 2

Concentrated load of 12.5 kg over a base of 6.35 mm x 6.35 mm was applied centrally above elbow concrete between Slice 9 & 10.

- In the longitudinal direction the draft tube cavity around is under tension at flaring portion i.e. at Slice 8 & 9 and towards upstream side it is under complete compression. As one moves from upstream to downstream will find the effect of tension reducing (Fig. 5.7, 5.8).
- At Slice 10 and onwards the concrete over and around the draft tube is under compression and tension has no effect in the concrete beyond the power house wall (Fig. 5.9, 5.10).
- Maximum tension occurs at Slice 8 ($Z = 74.476$ mm) and its magnitude is 0.878 kg/cm^2 (Tab. 5.7).
- At all planes magnitude of compression is higher than that of tension (Fig. 5.6 to 5.10).

Compression zone is observed in the top portion of elbow concrete (maximum under the load) and tension zone is around draft tube cavity (Slice 8, 9) and at support (Slice 10, 11) and complete compression at Slice 7 (Fig. 5.7 to 5.10).

5.1.3 Load Condition 3

Uniformly distributed load of 0.2 kg/cm^2 was applied above the elbow concrete at the top of substructure between $Z=69.9$ to 100.0 mm .

- In the longitudinal direction the concrete around the draft tube cavity is under tension in flaring portion i.e. Slice 8 & Slice 9 (Fig. 5.12, 5.13).
- Towards upstream i.e. Slice 7 and towards downstream Slice 10 and beyond the concrete around the draft tube cavity is under compression (Fig. 5.11, 5.15).
- Maximum tension occurs above top of draft tube at Slice 8 ($Z = 74.476 \text{ mm}$) and magnitude is 0.1069 kg/cm^2 (Fig. 5.12 & Tab. 5.12).
- Compression zone is observed in top zone of elbow concrete under the applied load at Slice 8, 9 and depth of compression zone is more than that of tension (Fig. 5.12, 5.13).
- The concrete above the draft tube is under complete compression at Slice 7, 10 and also at Slice 11 (Fig. 5.11, 5.15).
- Some tension zone is also found towards support beyond Slice 10. (Fig. 5.14, 5.15)

5.1.4 Load Condition 4

Concentrated load of 12.5 kg over square bases of $6.35 \text{ mm} \times 6.35 \text{ mm}$ each were applied at either supports on the line of downstream power house wall simulating gantry column loads between Slice 10 and 11.

- In the longitudinal direction the concrete around the draft tube cavity is under complete compression at all planes (Fig. 5.16 to 5.20).
- Maximum tension occurs at top of elbow portion below load locations on either supports at Slice 9 and its magnitude is 0.1911 kg/cm^2 (Fig. 5.18 and Tab. 5.18).
- Maximum compression occurs at Slice 9 towards supports below the tension zone and its magnitude is 0.1755 kg/cm^2 (Fig. 5.18 and Tab. 5.18).
- Concentration of tension is observed below the point of application of load at support locations (Fig. 5.17 to 5.20).
- Magnitude of compression is lower than that of tension at all planes except in plane of Slice 10 where it is the reverse (Tab. 5.16 to 5.20).

5.2 NATURE OF STRESS COMPONENT σ_z IN Z-DIRECTION

In this series of runs the stress contours are drawn and discussed in half the width of draft tube as the stress in other half will be same (the shape of draft tube being symmetrical about the transverse axis).

5.2.1 Load Condition 1

A concentrated load of 12.5 kg over a square base of 6.35 mm x 6.35 mm was applied centrally above the elbow concrete between Slice 8 & 9.

- In the transverse direction the concrete above the draft tube cavity is under tension at central location at Point 12, 10 & 8 and at Point 6 the concrete above the draft tube cavity is under complete tension. At support (Point 3) it is under complete compression except at restraining edges (Fig. 5.21 to 5.25).
- Compression zone towards central portion occurs below the loading location and at support portions in top zone of concrete (Fig. 5.21, 5.25).
- Tension and compression are maximum at central sections and reduce towards supports (Tab. 5.21 to 5.25).
- Magnitude of compression is lower than tension at support (Point 3, 6) and reverses in central portion (Point 8, 10, 12) (Tab. 5.21 to 5.25).
- Maximum tension occurs at central section above draft tube cavity and its magnitude is 0.7899 kg/cm² (Fig. 5.25 & Tab. 5.25).
- Magnitude of maximum compression is 7.207 kg/cm² at Point 12 under the area of application of load (Tab. 5.25).
- In this direction in central portion the concrete above draft tube is under tension in the entire length both inside and outside of power house wall but the effect gets reduced in the downstream direction (Fig. 5.25).

Results Of Analysis Of Photo Elasticity Study By Nigam⁽¹⁰⁾

- In transverse direction the concrete around draft tube cavity is under tension at all sections (Fig. 5.70 a to e). In load condition 1 in this analysis also it is found under tension at central sections (Fig. 5.21 to 5.25).
- Tension and compression is maximum at central section and reduces towards support sections (Fig. 5.70 a to e). It is similar to the pattern obtained in this analysis.

- Maximum tension and compression occur at central section (Fig. 5.70 e) as has been the case in this analysis (Tab. 5.25).
- In this direction effect of tension gets reduced in the concrete towards the downstream side (Fig. 5.70 a to e) and the same is the case in this analysis (Fig. 5.21 to 5.25).

From the comparison of the results by the two methods it is inferred that the analyses by Photo elasticity and FEM yield similar stress patterns in elbow concrete.

5.2.2 Load Condition 2

Concentrated load of 12.5 kg over a base of 6.35 mm x 6.35 mm was applied centrally above elbow concrete between Slice 9 & 10.

- In the transverse direction the concrete around the draft tube cavity is under tension at central sections i.e. at Point 12, 10, 8 but at support it is under complete compression (Fig. 5.26 to 5.30).
- At support at restraining edges tension zone is observed at the top of elbow concrete (Fig. 5.26) similar to load condition 1.
- Compression zone occurs below the load in the interior or central portion above tension zone and depth of the zones are more or less same (Fig. 5.26 to 5.30).
- The effect of tension in the concrete above draft tube becomes insignificant towards downstream side (Fig. 5.28 to 5.30).
- Magnitude of compression is higher than that of tension at all regions except at support where it is the reverse (Tab. 5.26 to 5.30).
- Maximum tension and compression is observed in central region, Point 12, which gradually reduces towards supports (Tab. 5.26 to 5.30).
- Magnitude of maximum tension is 0.3517 kg/cm^2 and compression is 2.5297 kg/cm^2 (Tab. 5.30). These are less than those obtained under load condition 1 because in this case the point of application of load is away from the axis of draft tube.

5.2.3 Load Condition 3

Uniformly distributed load of 0.2 kg/cm^2 was applied above the elbow concrete at the top of substructure between $Z=69.9$ to 100.0 mm .

- In the transverse direction the concrete around the draft tube cavity inside the power house is completely under tension in the cavity region (Point 12,10, 8) (Fig. 5.33 to 5.35).
- At Point 6 concrete above draft tube cavity is under tension right up to top with lesser intensity at the top as is the case in load condition1 (Fig. 5.32). It is due to restraining effect at the top edge with the support concrete.
- Maximum tension is observed at Point 8 midway between central section and support but maximum compression occurs at central section (Tab. 5.33, 5.35).
- Towards interior, magnitude of compression is higher than that of tension but at support it is the reverse (Tab. 5.31 to 5.35).
- Maximum tension is 0.0331 kg/cm^2 occurring at Point 8 (Tab. 5.33).
- Maximum compression is 0.12550 kg/cm^2 occurring at Point 12(Tab. 5.35).
- The values of maximum tension and compression in this case are less than those in load conditions 1 and 2.

5.2.4 Load Condition 4

Concentrated loads of 12.5 kg over square bases of $6.35 \text{ mm} \times 6.35 \text{ mm}$ each were applied at either supports on the line of downstream power house wall simulating gantry column loads between Slice 10 and 11.

- In the transverse direction the concrete around draft tube cavity is under tension in the cavity region (Point 12, 10, 8) and the effect of tension gets reduced towards upstream and downstream from draft tube cavity (Fig. 5.36 to 5.40).
- At supports i.e. at Point 6 concrete at top and bottom of draft tube is under tension. After a certain depth of tension zone, towards top the concrete is under compression (Fig. 5.37).
- At support i.e. at Point 3 the elbow concrete is in complete compression towards bottom but at top near the point of application of load it is under tension (Fig. 5.36).

- Due to restrain reactions the concrete at upstream top in all locations are in complete tension (Fig. 5.37 to 5.40).
- Maximum tension occurs at support in the top region under the load location and its magnitude is 0.1534 kg/cm² (Tab. 5.36).
- Maximum compression occurs at support but below the tension zone and its magnitude is 0.0654 kg/cm² (Tab. 5.36).

5.3 NATURE OF STRESS COMPONENT σ_y IN Y-DIRECTION

5.3.1 Load Condition 1

A concentrated load of 12.5 kg over a square base of 6.35 mm x 6.35 mm was applied centrally above elbow concrete between Slice 8 & 9.

- In the top-ward direction the concrete over the draft tube cavity is under compression at all levels except at Strip 13 (Y = 66.04 mm) where it is under tension around the cavity and towards upstream side and under compression towards downstream side (Fig. 5.41 to 5.47).
- Concentration of maximum tension and compression occur at u/s and d/s corners of substructure respectively (Fig. 5.41 to 5.47).
- At Strip 10 concentration of tension is observed at u/s and d/s (beyond power house) regions completely and this effect is extended at Strip 11 and 12 where the concentration of tension is observed at support also (Fig. 5.44 to 5.46).
- Magnitude of maximum tension is 0.05490 kg/cm² at Strip 8 at tail end and that of compression is 1.9316 kg/cm² occurring at Strip 11 below loading location (Tab. 5.42, 5.45 & Fig. 5.42, 5.45).

Results Of Analysis Of Photo Elasticity Study By Nigam⁽¹⁰⁾

- In the top ward direction the concrete over the draft tube cavity is under tension at all levels except at strip 13, where it is under tension around draft tube cavity upstream and under compression around cavity downstream (Fig. 5.71 a to g).
- Maximum concentration of tension occurs at Strip 7 (Fig. 5.71 a) but not at Strip 8 as was the case in load condition 1 (Fig. 5.41 to 5.47).
- Maximum concentration of compression occurs at Strip 11 (Fig. 5.71 e) as is the case in load condition 1 (Tab. 5.45).

- Concentration of tension occurs in support regions at all levels (Fig. 5.71 a to g) but in load condition 1 at Strip 11 and Strip 12, tension develops at supports (Fig. 5.45, 5.46).

From the results of two analyses it is observed that the stress patterns in vertical direction differ from each other. However, similarity occurs in development of tension in support regions in Strip 11 and 12 in both analyses. But both analyses yield maximum compression at Strip 11 on the line of loading location.

5.3.2 Load Condition 2

Concentrated load of 12.5 kg over a base of 6.35 mm x 6.35 mm was applied centrally above elbow concrete between Slice 9 & 10.

- In the upward direction concrete above the draft tube cavity is under tension around the cavity at all levels except at Strip 12 and 13 (Fig. 5.48 to 5.54).
- At Strip 10 there is no tension zone u/s of draft tube cavity as is there in case of load condition 1 (Fig. 5.51, 5.44).
- At Strip 12 the cavity is under tension, which was not the case in load condition 1 (Fig. 5.53, 5.46).
- At Strip 11, tension zone is observed at supports and at u/s and d/s (beyond the power house wall) of the cavity (Fig. 5.52), as was the case in load condition 1.
- Tension is maximum at Strip 12 centrally in cavity region and its magnitude is 0.3596 kg/cm^2 whereas maximum compression of 2.6668 kg/cm^2 occurs at Strip 11 (Tab. 5.53, 5.52 & Fig. 5.53, 5.52) on the axis of loading location.
- Magnitude of tension is not so large as compared to that of compression at all levels except at Strip 12 and 13 (Tab. 5.48 to 5.54).
- In this case magnitude of maximum tension and compression is more than those in load condition 1. It may be attributed to the fact that the span of the loaded Slice in this case is more than that of load condition 1.

5.3.3 Load Condition 3

Uniformly distributed load of 0.2 kg/cm^2 was applied above the elbow concrete at the top of substructure between $Z=69.9$ to 100.0 mm .

- In the upward direction the concrete over the draft tube is under compression at all levels except at the Strip 13 where it is under tension as in load condition 1 (Fig. 5.55 to 5.61).
- Strip 10 is also under complete compression as in load condition 2. (Fig. 5.58)
- At Strip 11 the effect in concrete is same as the case in load condition 1 where tension zone is observed at u/s and d/s edges and at support regions (Fig. 5.59).
- At Strip 12 the behaviour in concrete is all the same as in load condition 1. (Fig. 5.60)
- Magnitude of tension is not so high as compression at all levels (Tab. 5.55 to 5.61).
- Maximum tension occurs at Strip 8 at tail end and its magnitude is 0.0111 kg/cm^2 (Tab. 5.56, Fig. 5.56). Maximum compression occurs at Strip 12 in interior region below loading location and its magnitude is 0.17373 kg/cm^2 (Tab. 5.60, Fig. 5.60).

5.3.4 Load Condition 4

Concentrated loads of 12.5 kg over square bases of $6.35 \text{ mm} \times 6.35 \text{ mm}$ each were applied at either supports on the line of downstream power house wall simulating gantry column loads between Slice 10 and 11.

- In upward direction concrete above draft tube cavity is under compression at lower level (Strip 7 & 8) and towards top compression zone is confined to half area from support to central location of draft tube in transverse direction (Fig. 5.62 to 5.68). In other half area it is under tension.
- At Strip 13 compression zone is observed in elbow portion extending towards downstream side whereas towards upstream of elbow it is under tension (Fig. 5.68).
- Maximum tension occurs at Strip 12 in the interior region and its magnitude is 0.00505 kg/cm^2 . Compression is maximum at Strip 11 below

loading location, its magnitude being 0.2999 kg/cm² (Fig. 5.67, 5.66 & Tab. 5.67, 5.66).

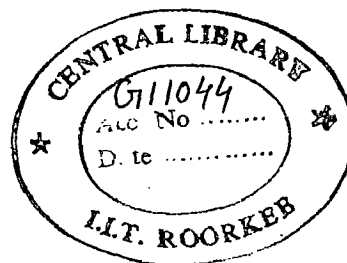
- Magnitude of compression is higher than that of tension at all levels except at Strip 8 where it is more or less the same (Tab. 5.62 to 5.68).

5.4 SUMMARY OF RESULTS

From the above results it can be summarised as:

- In UDL (Load case 3) load condition depth of compression zone is more than that of tension in flaring portion (Fig. 5.12 & 5.13).
- Depth of tension zone is more than that of compression zone above elbow concrete in load condition 1 at Slice 9 ($Z = 83.973$ mm) (Fig. 5.12).
- When the loading condition is changed from load condition 1 to load condition 2 it is observed that in load case 1 we observe tension zone up to top of substructure right from the top of draft tube cavity which is not the case in load case 2 where compression zone extends upto top of substructure at the same location (Fig. 5.22 & 5.27).
- In transverse direction maximum tension and compression zones are not observed at central section when loaded under U.D.L. The concentration of tension occurs at quarter span (Point 8) but compression at central span (Point 12). (Fig. 5.33, Tab. 5.37 & Fig. 5.35, Tab. 5.39).
- Tension occurs in the concrete u/s & d/s of elbow due to restraining reactions in transverse direction (Fig. 5.21 to 5.40).
- The concrete at support reveals the tension zone (at top of substructure) below which compression zone is observed in load case 4 referring component stresses in transverse direction (Fig. 5.36 to 5.40).
- From stress contours for σ_y it is seen in load condition 2 at Strip 10 there is no tension zone u/s of draft tube as is there in load condition 1 (Fig. 5.51 & 5.44).
- If the load is shifted from Slice 8-9 (load condition 1) to Slice 9-10 (load condition 2) the draft tube cavity experiences tension in the concrete surrounding the draft tube in Strip 12, 13 in upward direction (Fig. 5.53, 5.54) & (Fig. 5.46, 5.47).

- The point loads on top of elbow concrete cause large amount of tension and compression in elbow concrete as compared to UDL or Column Loads on draft tube walls.



(a) FEM Analysis

**STRESS CONTOURS PLOTTED FOR SX UNDER LOAD
CONDITION 1**

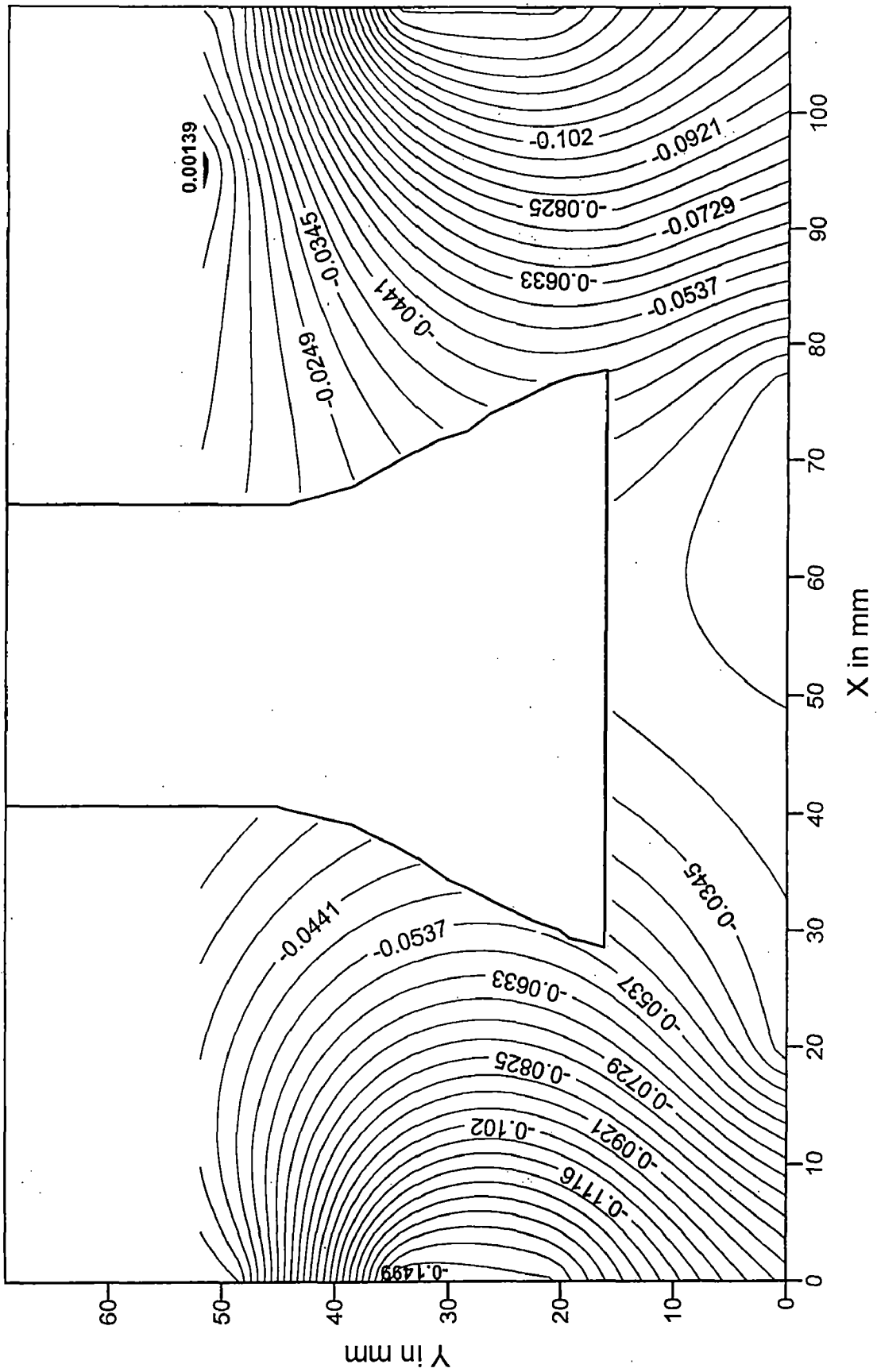


FIG. 5.1: STRESS CONTOURS FOR SX(kg/sq.cm) AT SLICE 7 (Z=66.478 mm) UNDER CONCENTRATED LOAD BETWEEN SLICE 8 & 9.

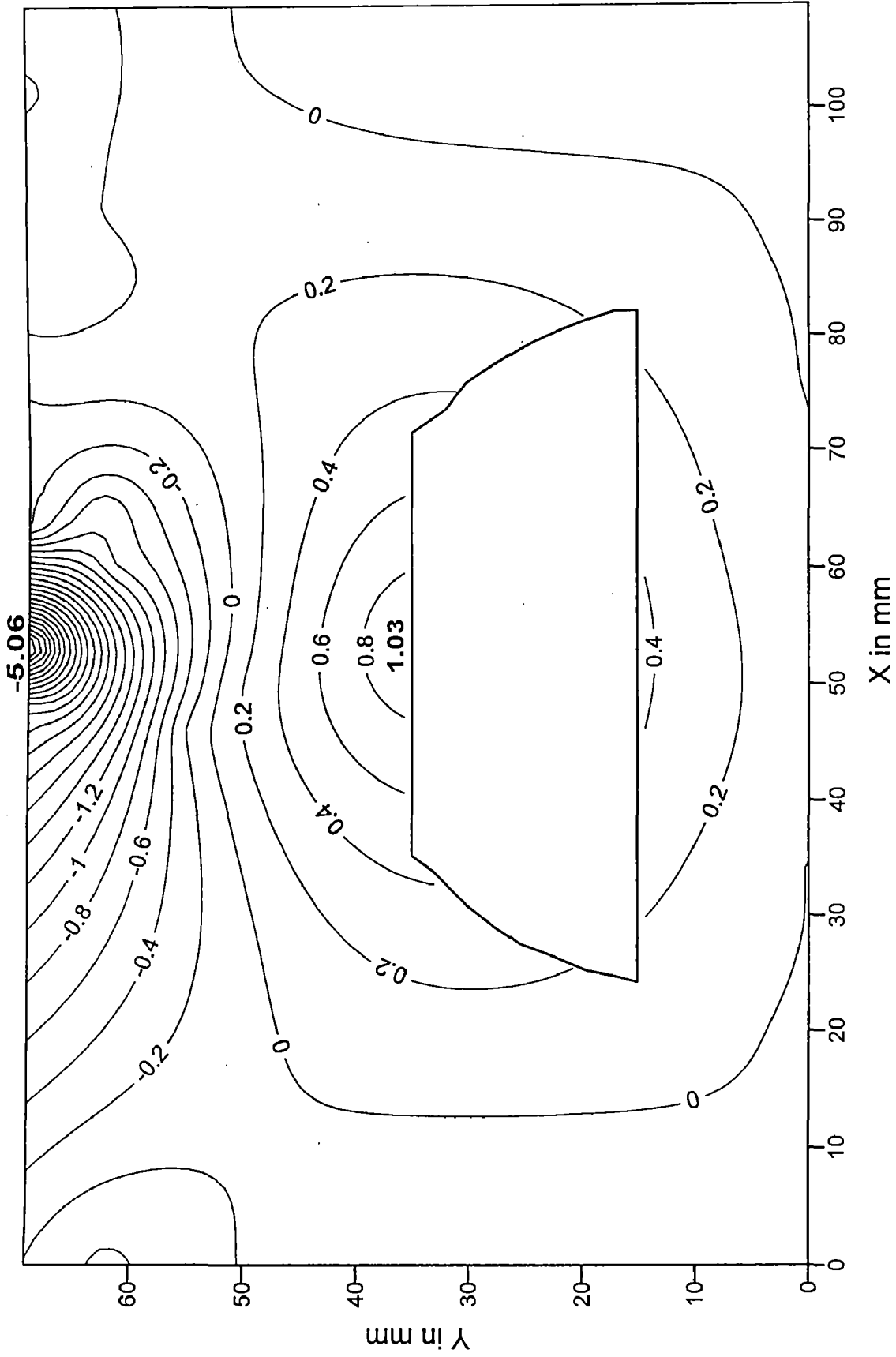


FIG. 5.2: STRESS CONTOURS FOR SX(kg/sq.cm) AT SLICE 8 (Z=74.476 mm) UNDER CONCENTRATED LOAD BETWEEN SLICE 8 & 9.

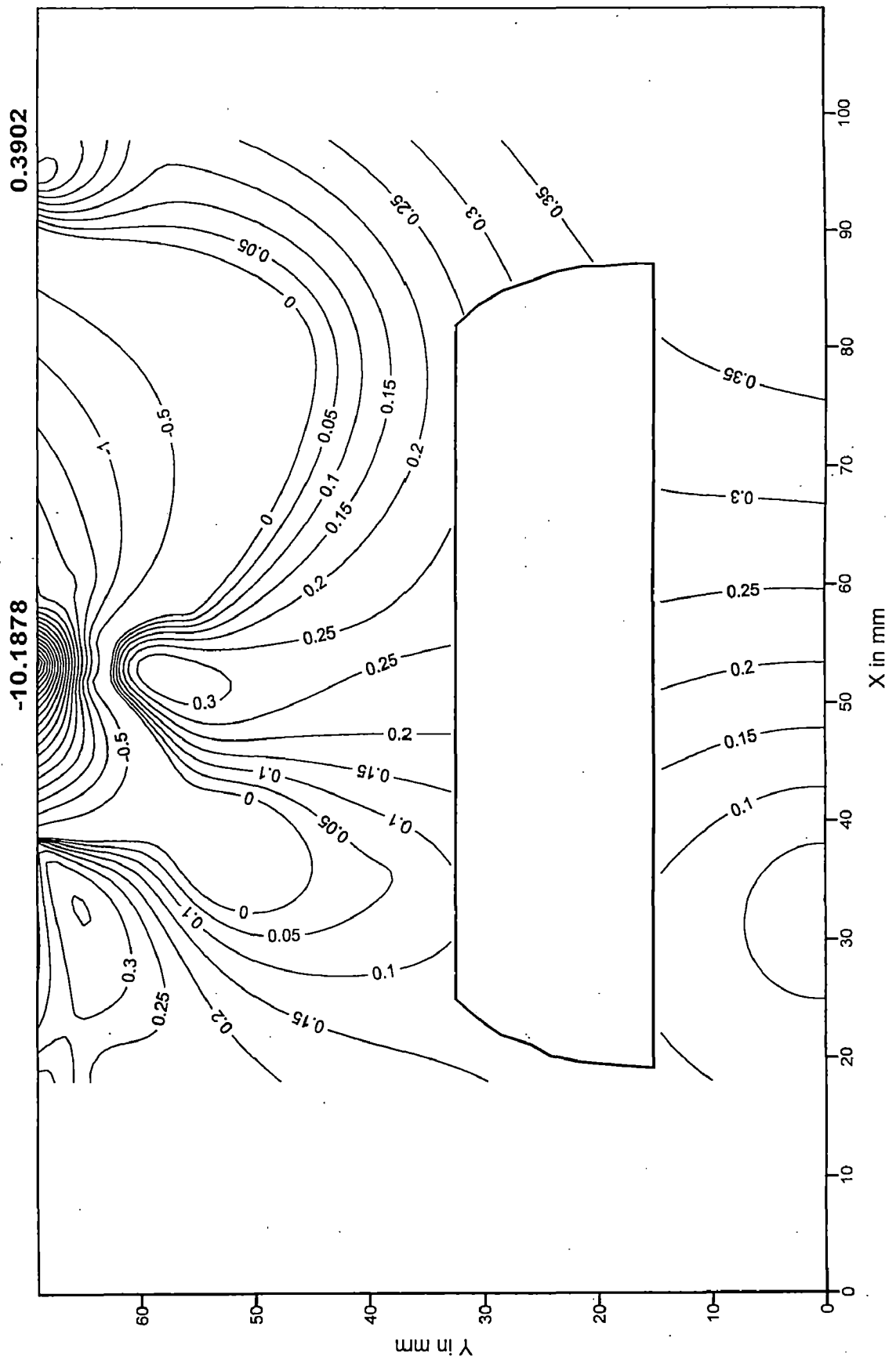


FIG. 5.3: STRESS CONTOURS FOR SX(kg/sq.cm) AT SLICE 9 (Z=83.973 mm) UNDER CONCENTRATED LOAD BETWEEN SLICE 8 & 9.

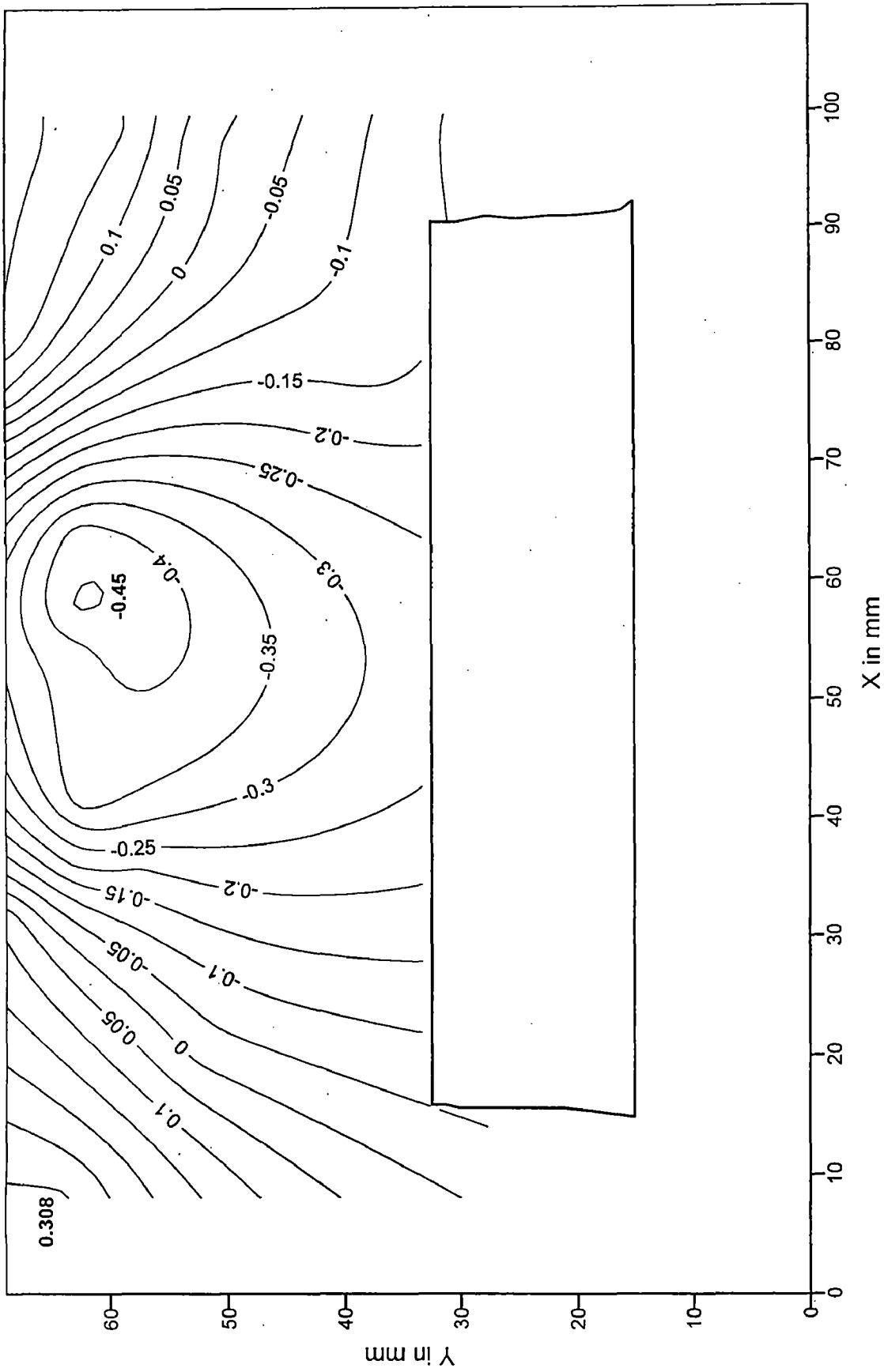


FIG. 5.4: STRESS CONTOURS FOR S_X (kg/sq.cm) AT SLICE 10 ($Z=92.476$ mm) UNDER CONCENTRATED LOAD BETWEEN SLICE 8 & 9.

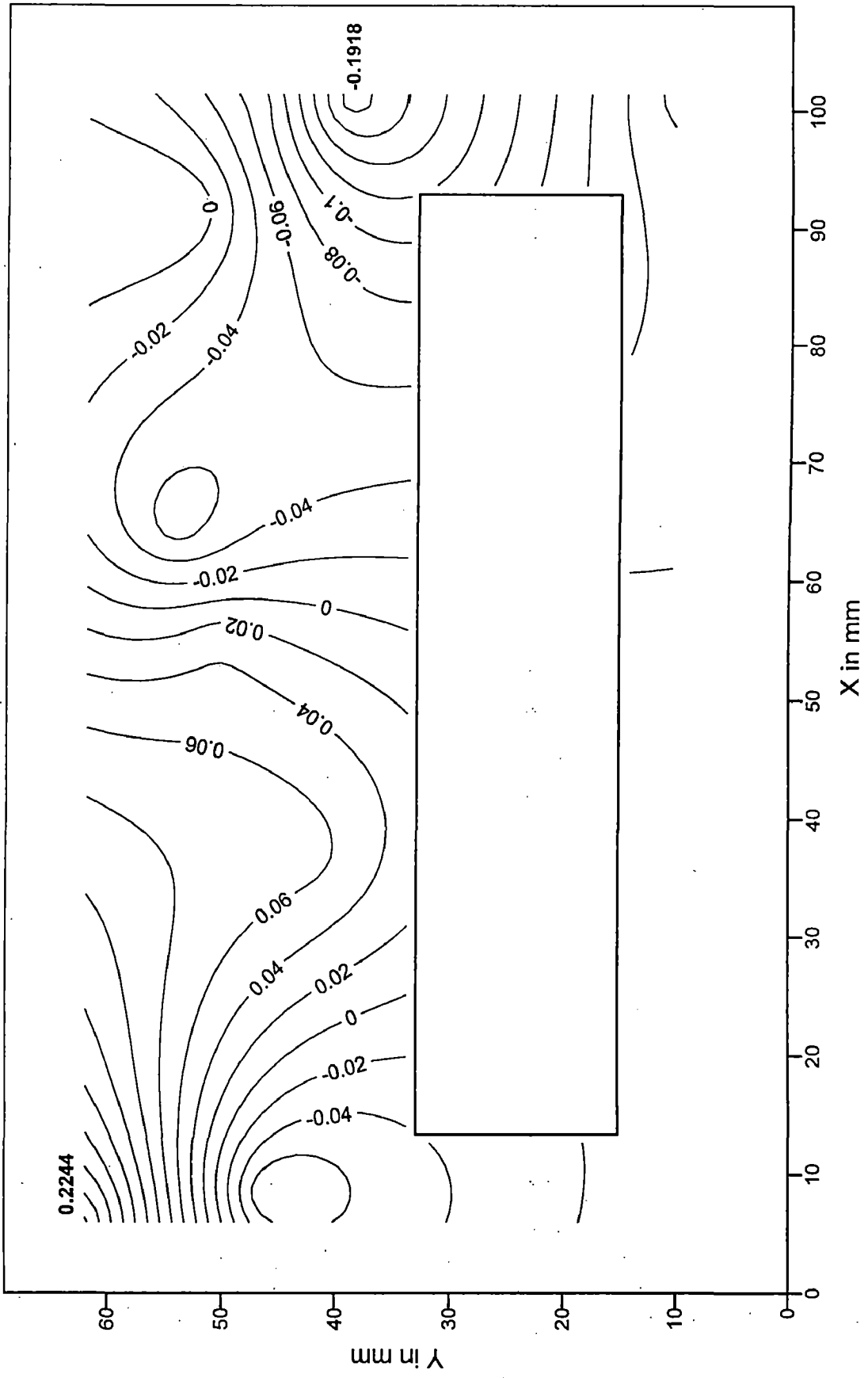


FIG. 5.5: STRESS CONTOURS FOR S_X (kg/sq.cm) AT SLICE 11 ($Z= 100.967$ mm) UNDER CONCENTRATED LOAD BETWEEN SLICE 8 & 9.

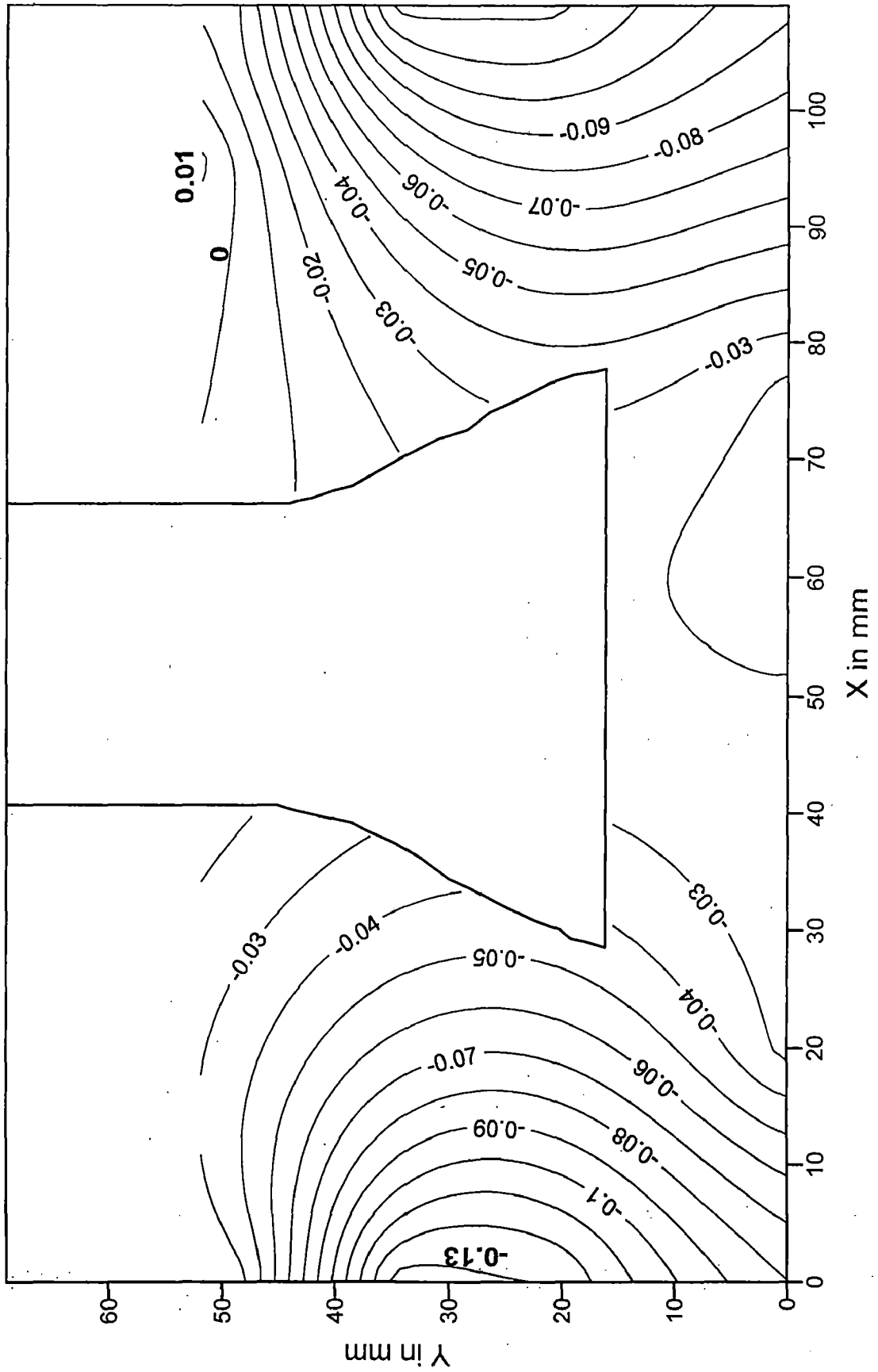


FIG. 5.6: STRESS CONTOURS FOR SX(kg/sq.cm) AT SLICE 7 (Z=66.478 mm) UNDER CONCENTRATED LOAD BETWEEN SLICE 9 & 10.

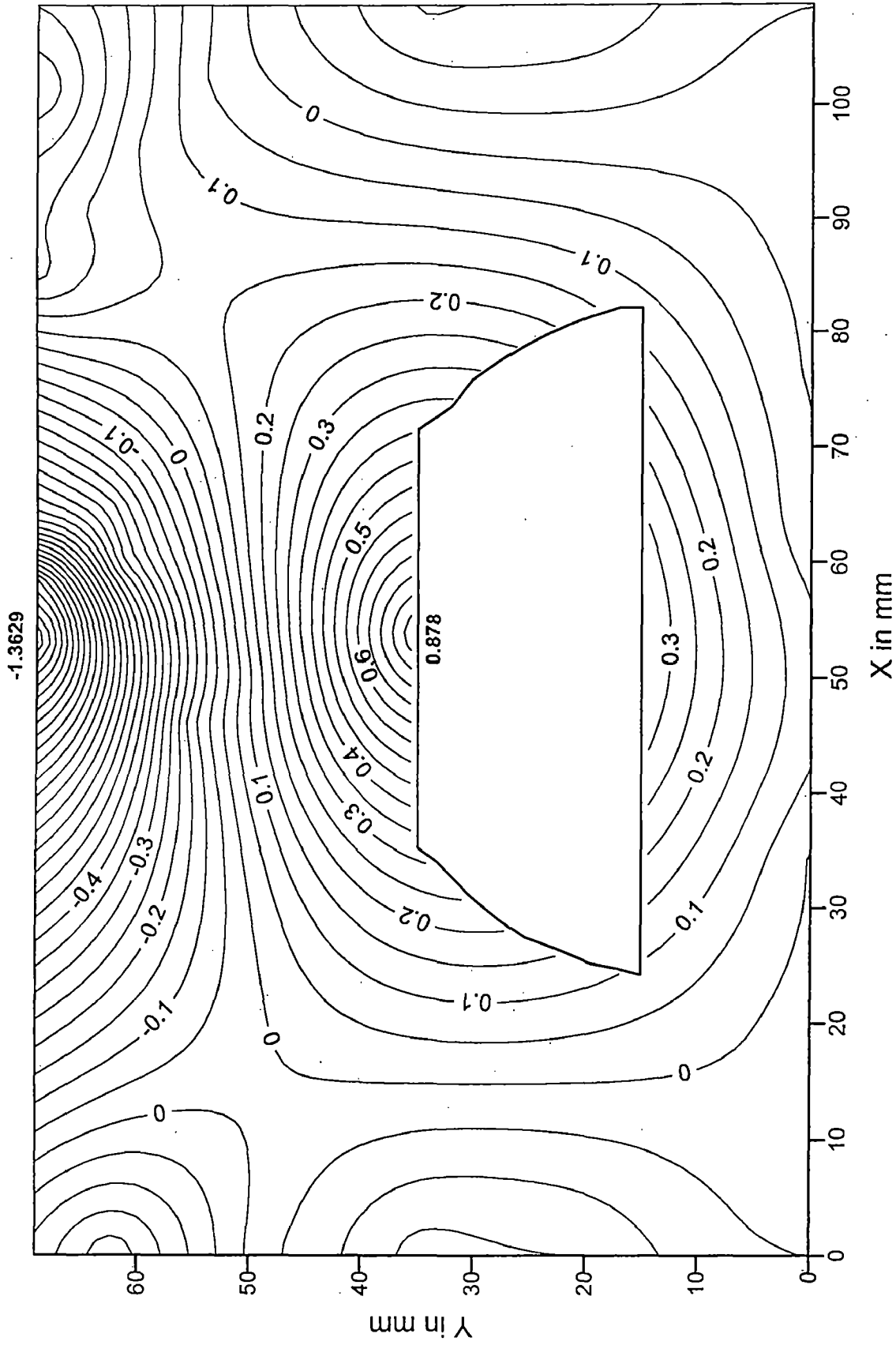


FIG. 5.7: STRESS CONTOURS FOR SX(kg/sq.cm) AT SLICE 8 (Z=74.476 mm) UNDER CONCENTRATED LOAD BETWEEN SLICE 9 & 10.

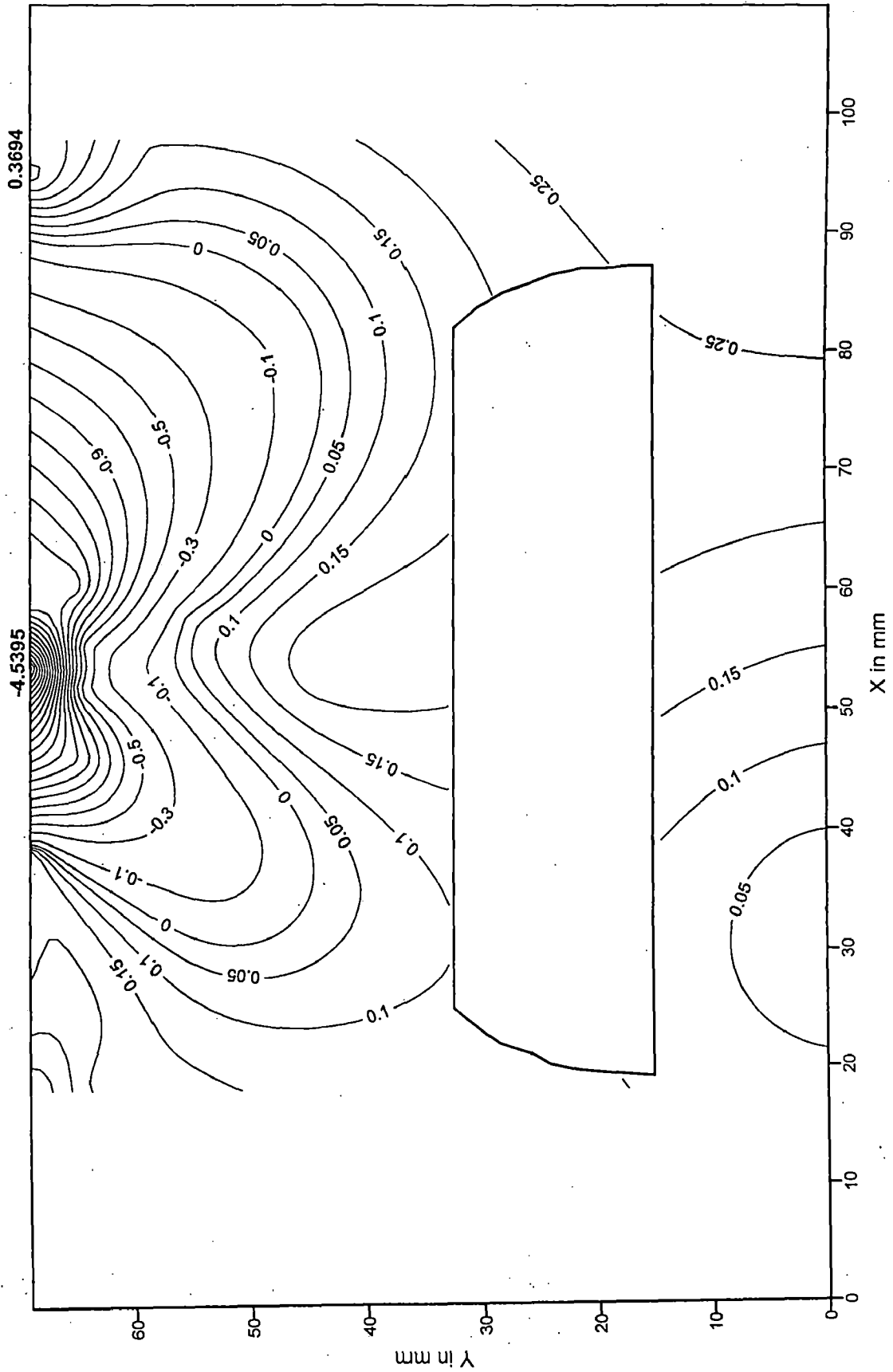


FIG. 5.8: STRESS CONTOURS FOR SX(kg/sq.cm) AT SLICE 9 (Z= 83.973 mm) UNDER CONCENTRATED LOAD BETWEEN SLICE 9 & 10.

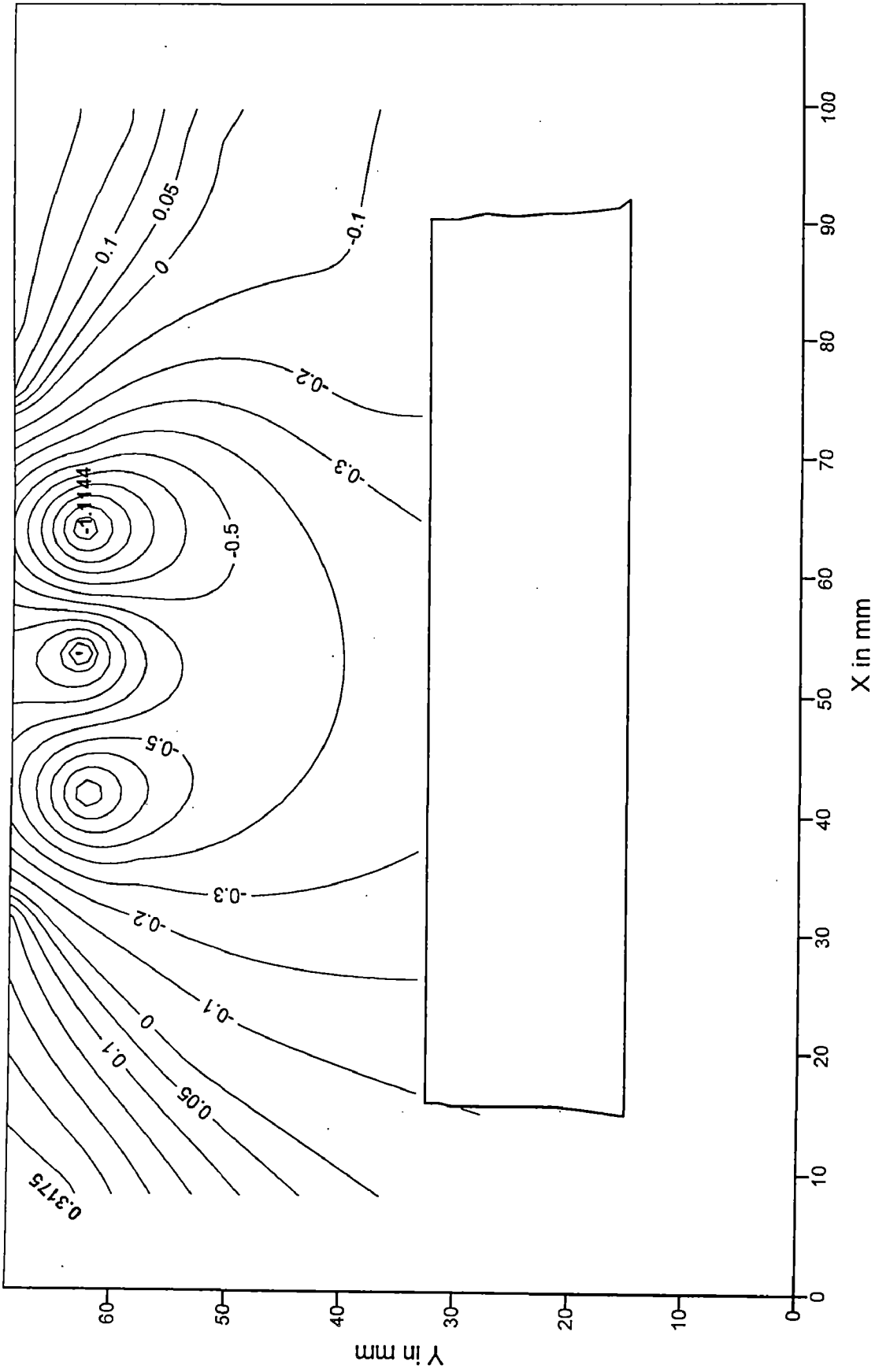


FIG. 5.9: STRESS CONTOURS FOR SX(kg/sq.cm) AT SLICE 10 (Z= 92.476 mm) UNDER CONCENTRATED LOAD BETWEEN SLICE 9 & 10.

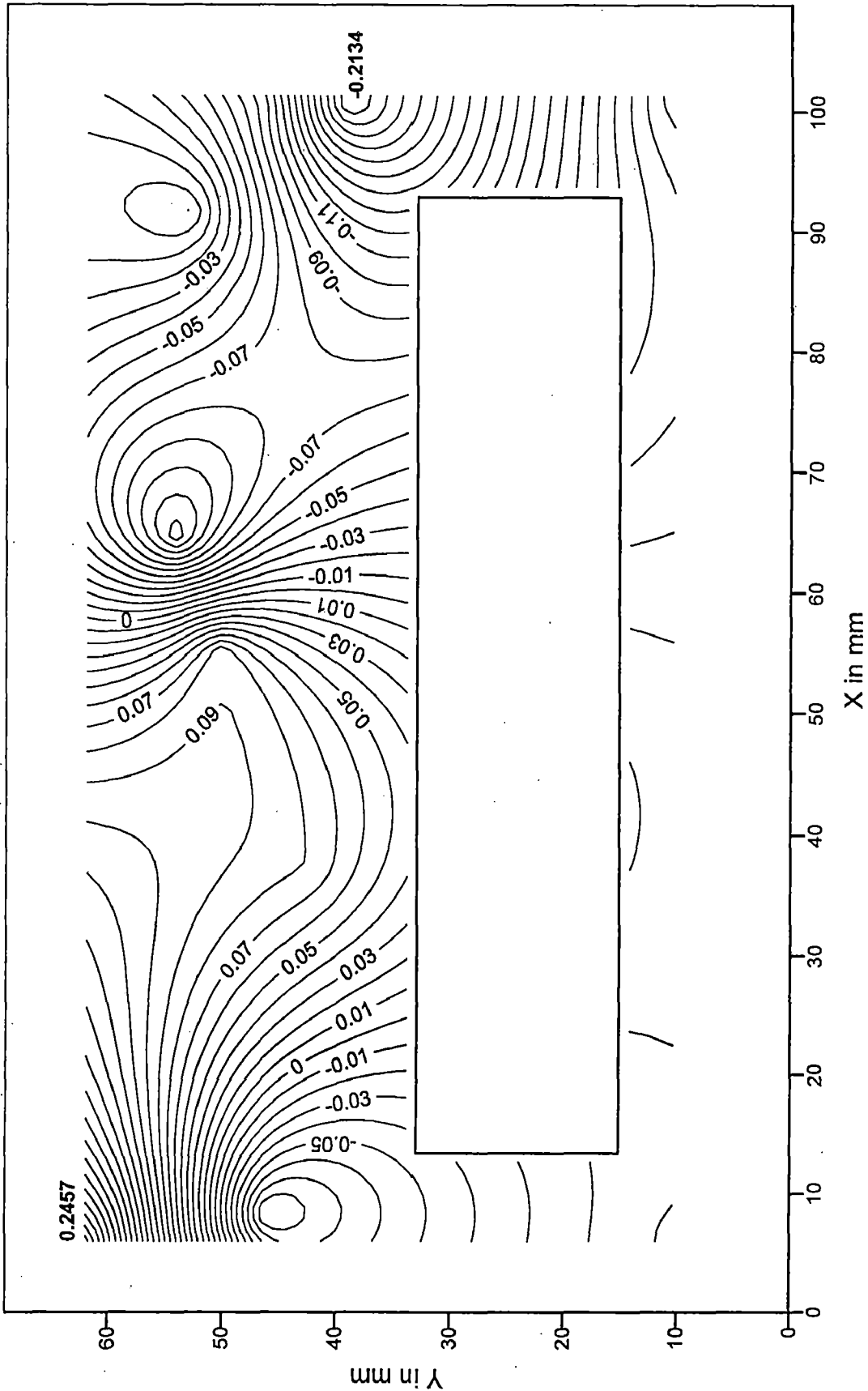


FIG. 5.10: STRESS CONTOURS FOR SX(kg/sq.cm) AT SLICE 11 (Z=100.967 mm) UNDER CONCENTRATED LOAD BETWEEN SLICE 9 & 10.

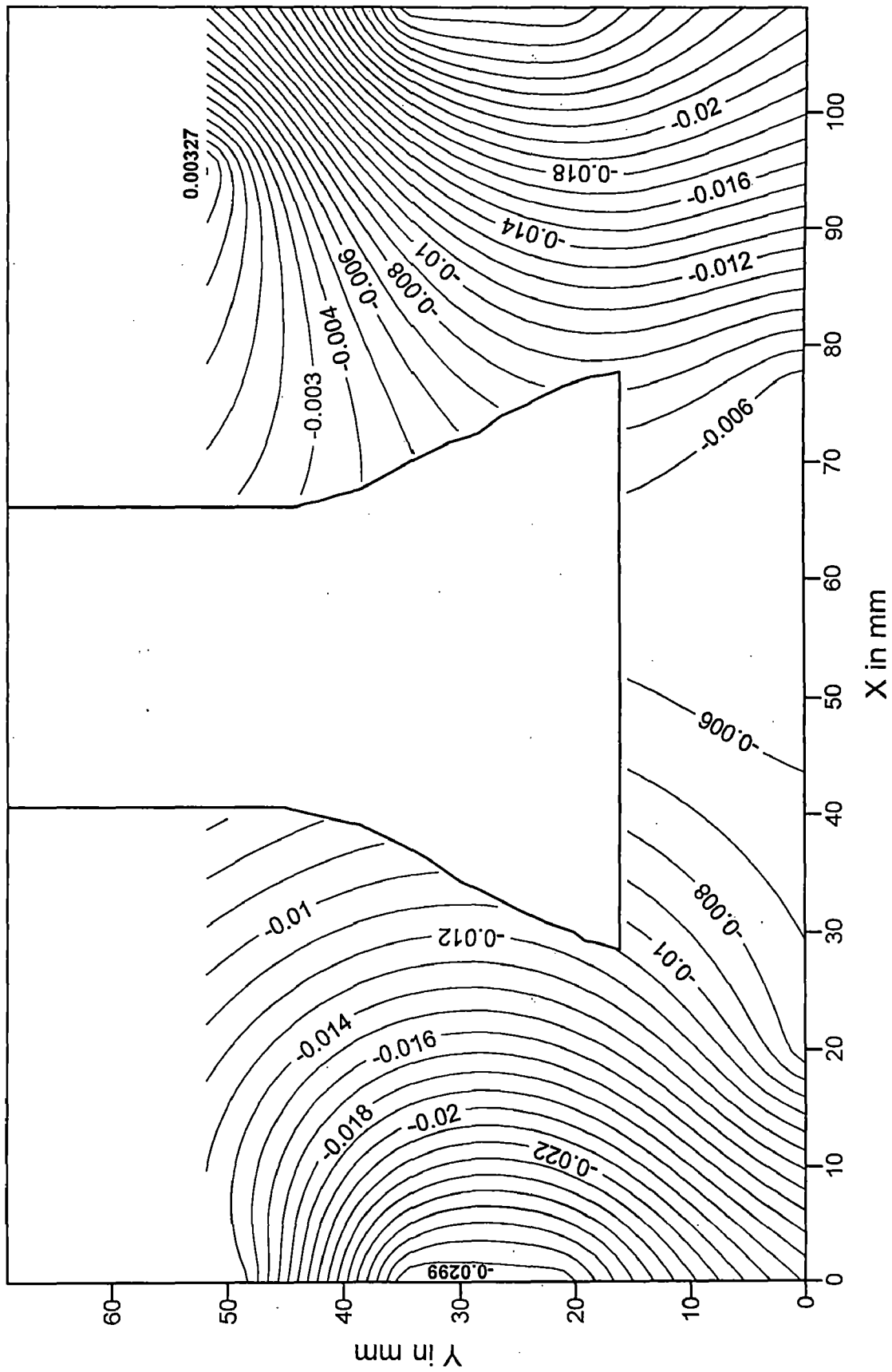


FIG. 5.11: STRESS CONTOURS FOR SX(kg/sq.cm) AT SLICE 7 (Z=66.478 mm) UNDER UDL ABOVE ELBOW CONCRETE.

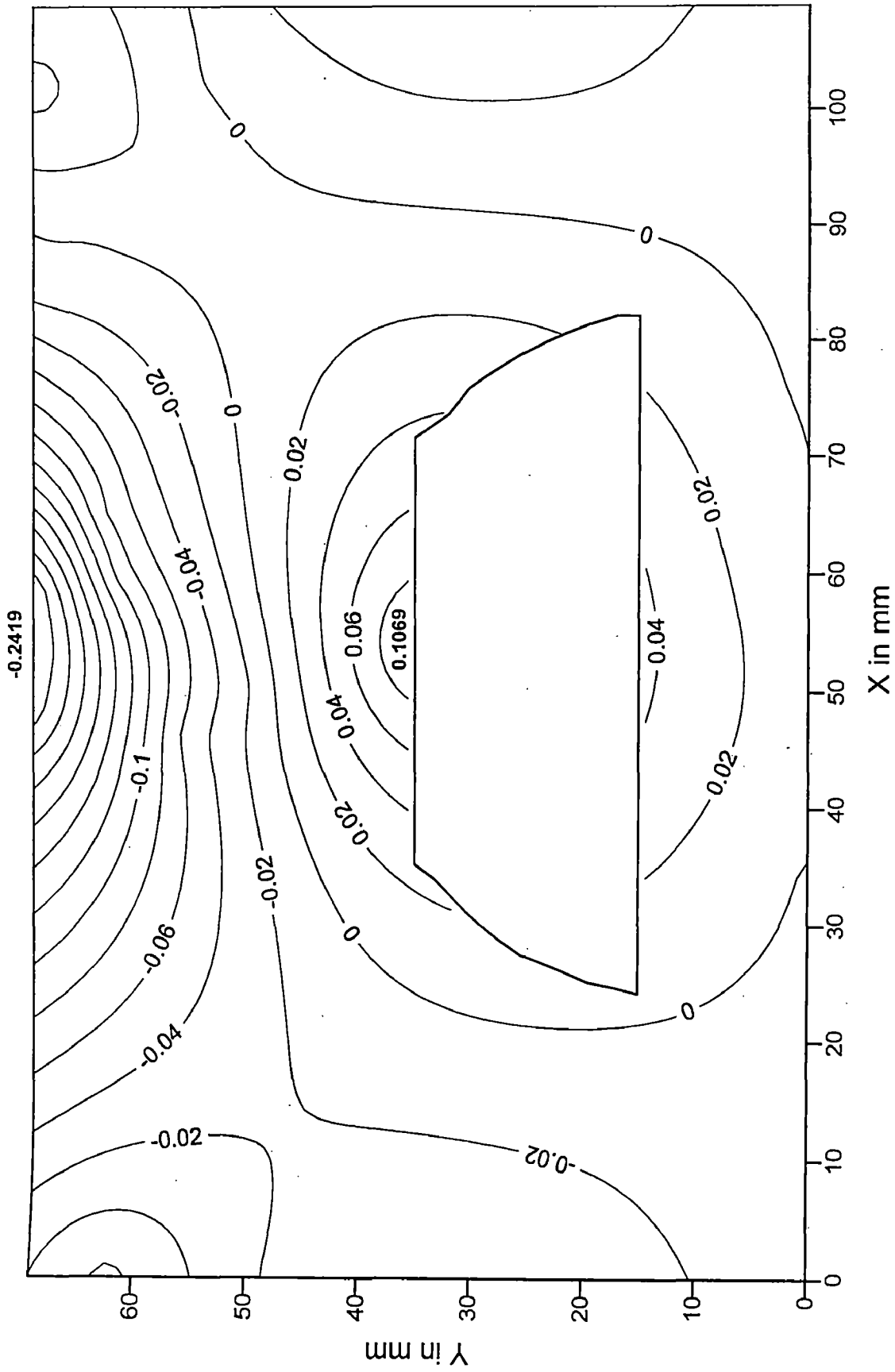


FIG. 5.12: STRESS CONTOURS FOR SX(kg/sq.cm) AT SLICE 8 (Z=74.476 mm) UNDER UDL ABOVE ELBOW CONCRETE.

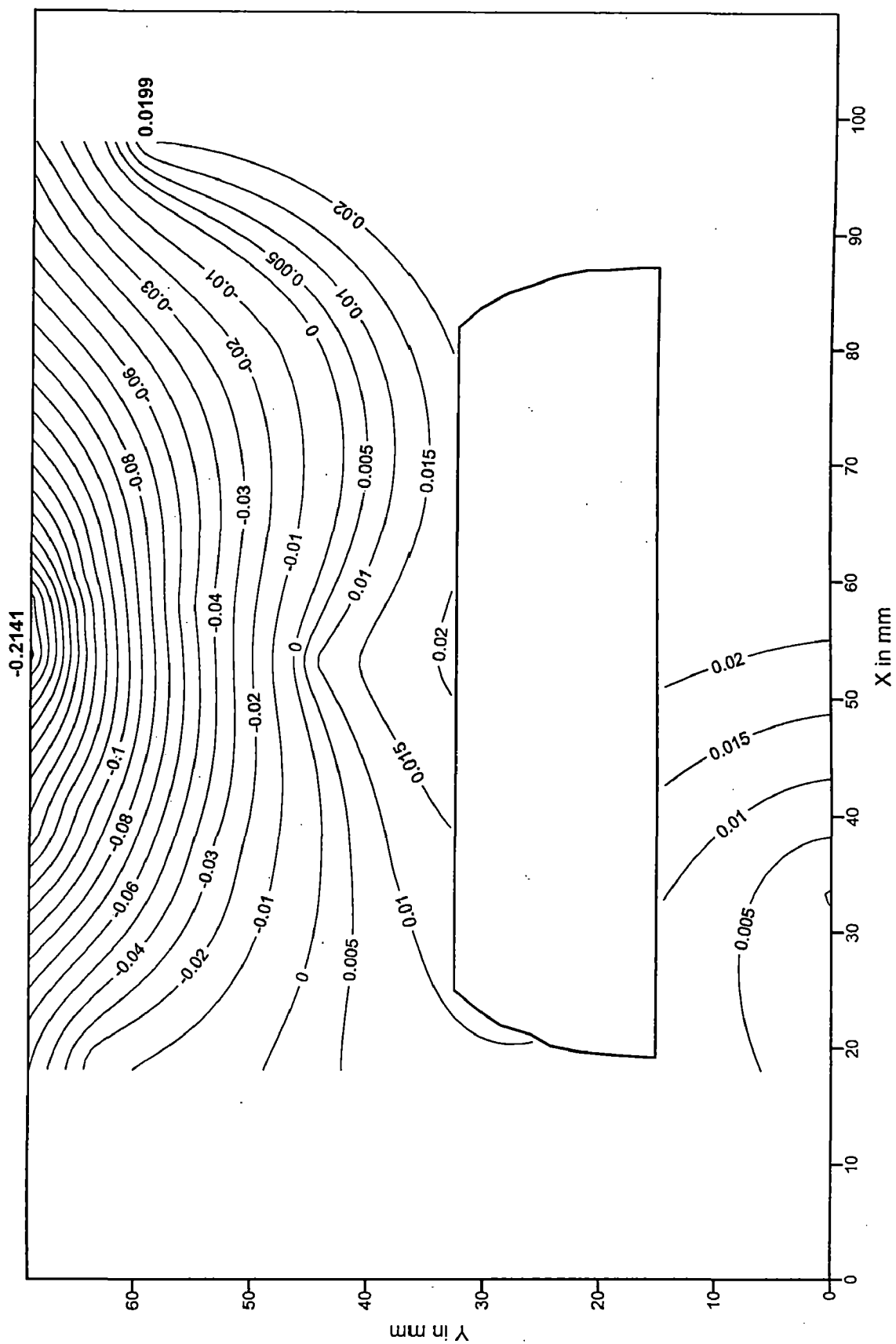


FIG. 5.13: STRESS CONTOURS FOR SX(kg/sq.cm) AT SLICE 9 (Z=83.973 mm) UNDER UDL ABOVE ELBOW CONCRETE.

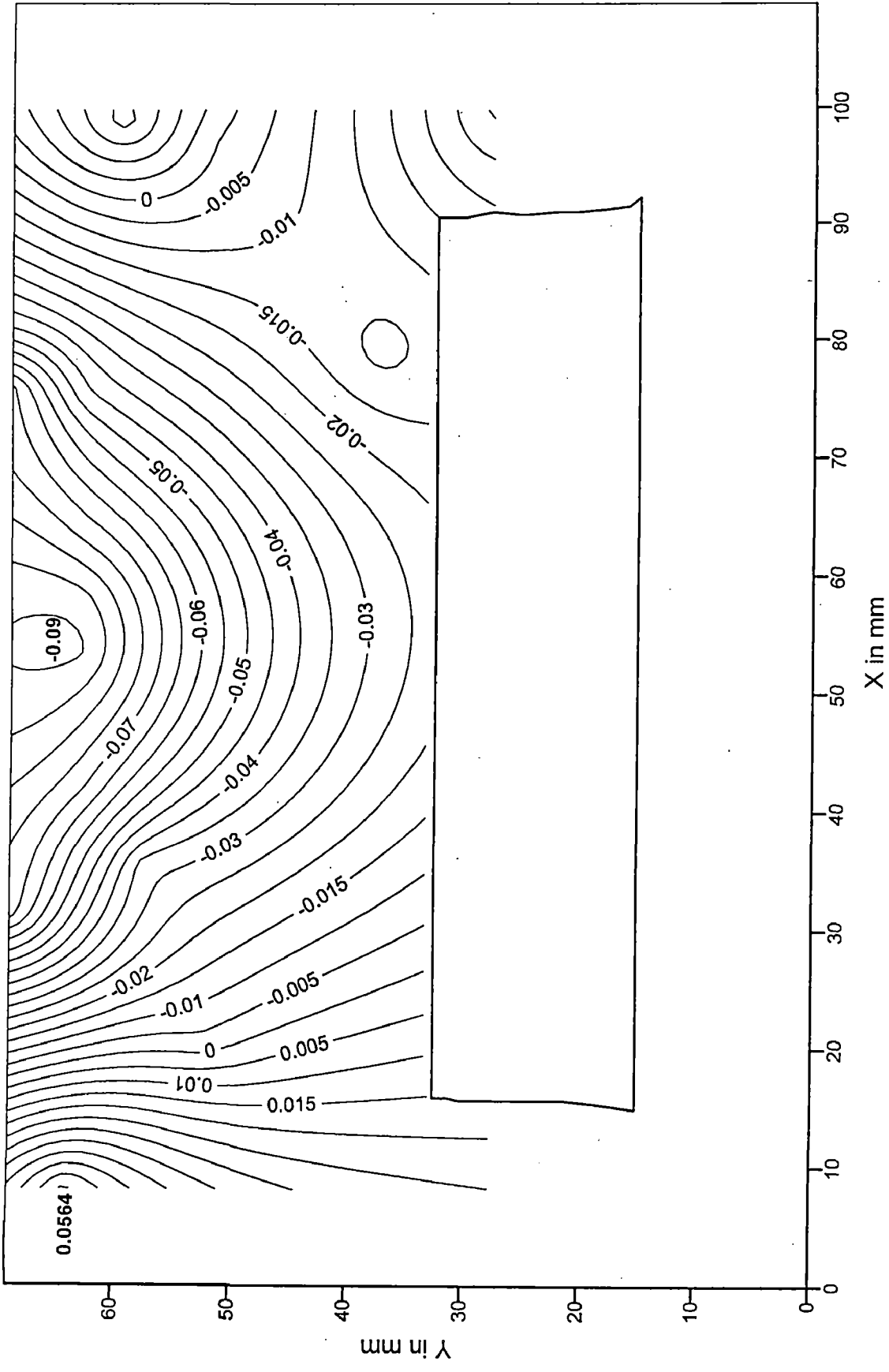


FIG. 5.14: STRESS CONTOURS FOR SX(kg/sq.cm) AT SLICE 10 (Z=92.476 mm) UNDER UDL ABOVE ELBOW CONCRETE.

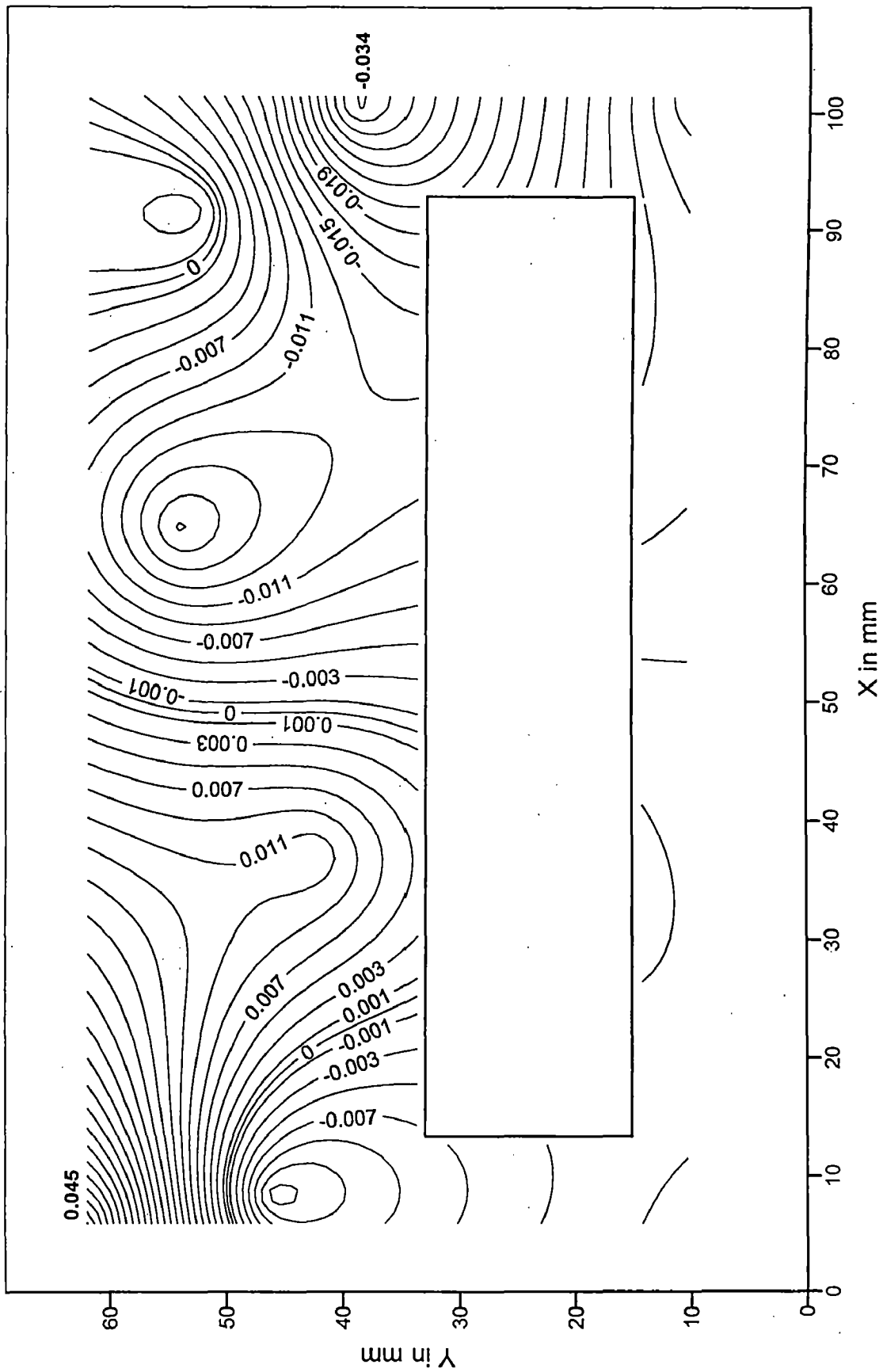


FIG. 5.15: STRESS CONTOURS FOR SX(kg/sq.cm) AT SLICE 11 (Z=100.967 mm) UNDER UDL ABOVE ELBOW CONCRETE.

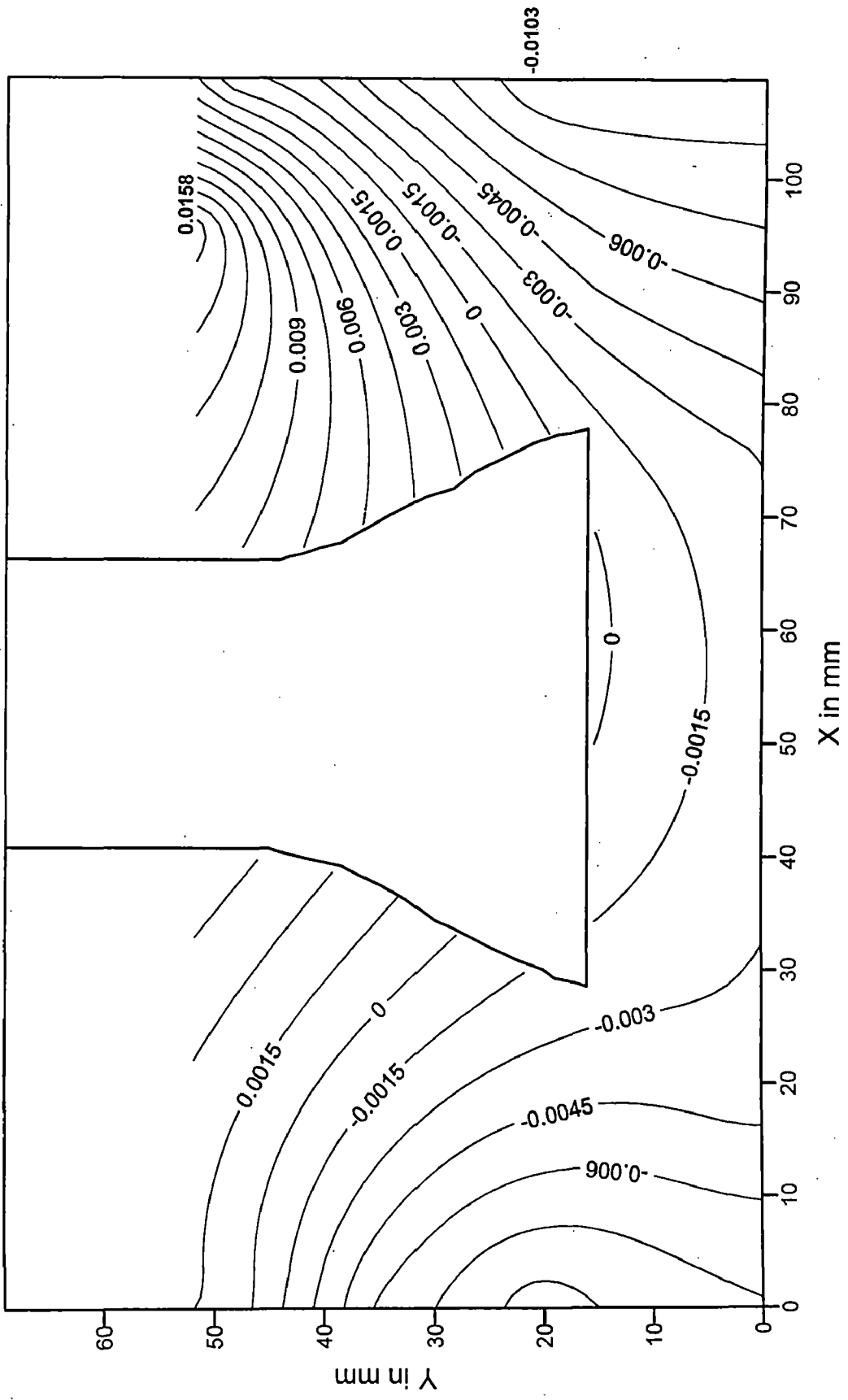


FIG. 5.16: STRESS CONTOURS FOR SX(kg/sq.cm) AT SLICE 7 (Z=66.478 mm) UNDER CONCENTRATED LOAD SIMULATING GANTRY COLUMN LOADS.

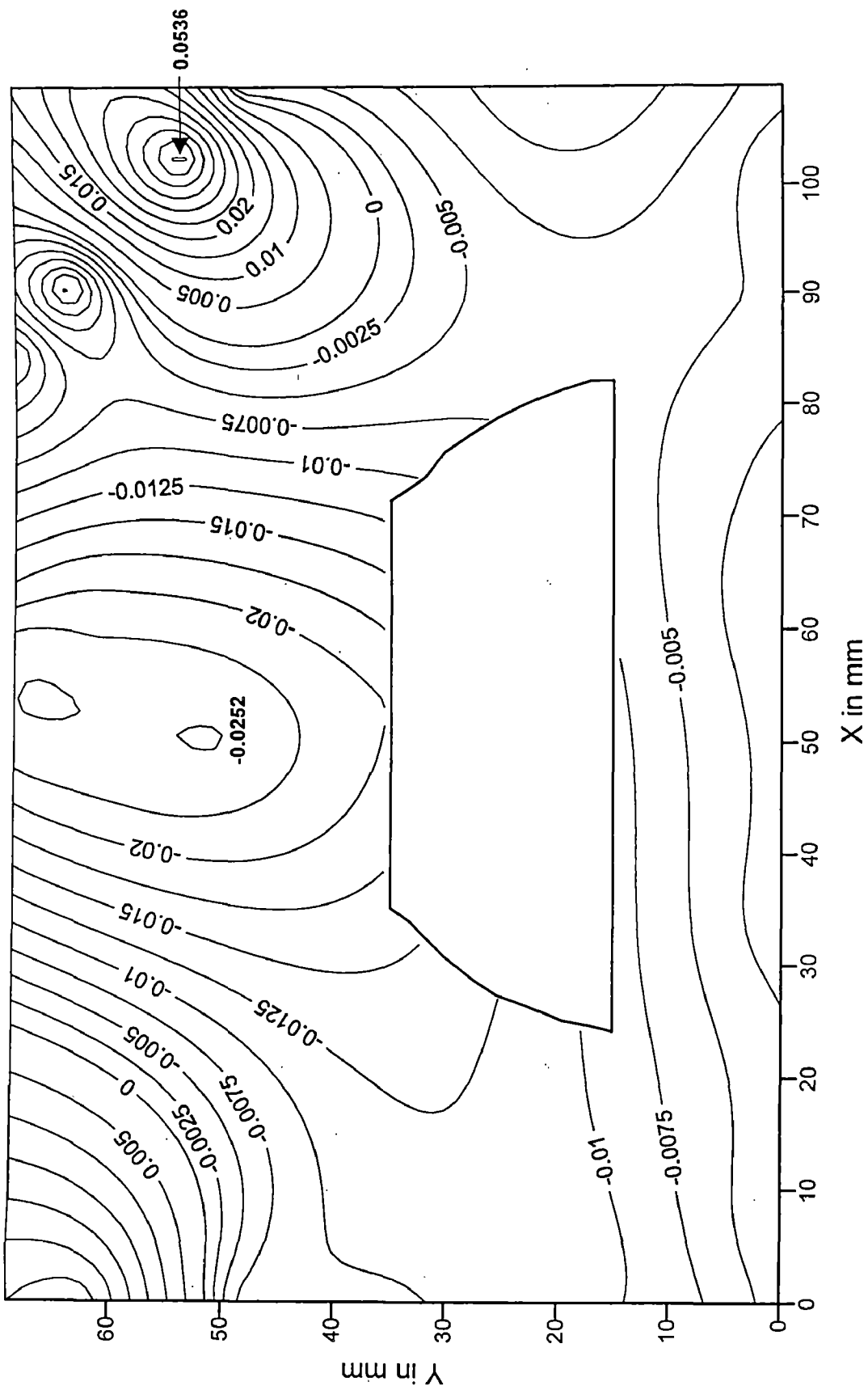


FIG. 5.17: STRESS CONTOURS FOR SX(kg/sq.cm) AT SLICE 8 (Z=74.476 mm) UNDER CONCENTRATED LOAD SIMULATING GANTRY COLUMN LOADS.

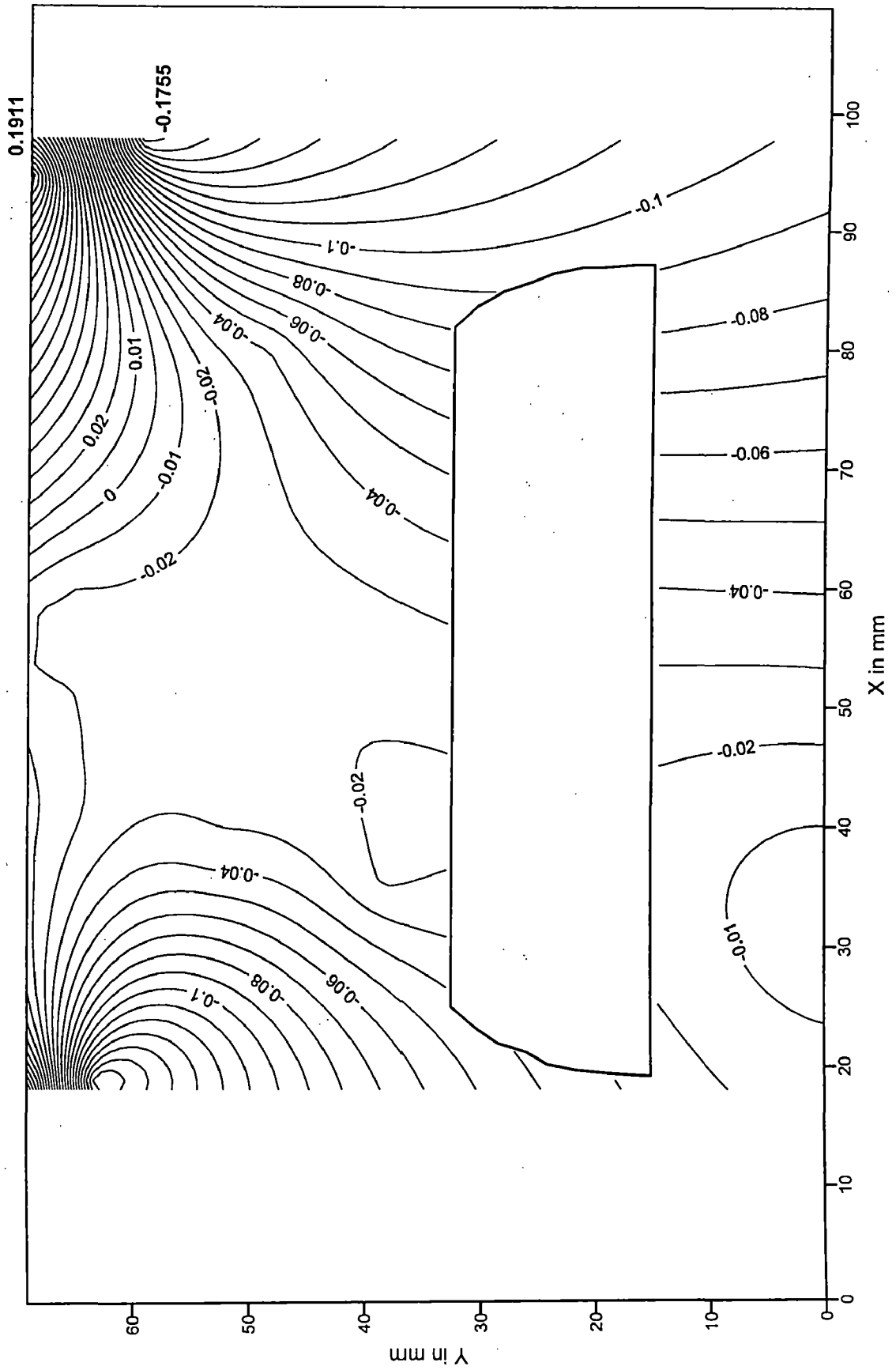


FIG. 5.18: STRESS CONTOURS FOR SX(kg/sq.cm) AT SLICE 9 (Z=83.973 mm) UNDER CONCENTRATED LOAD SIMULATING GANTRY COLUMN LOADS.

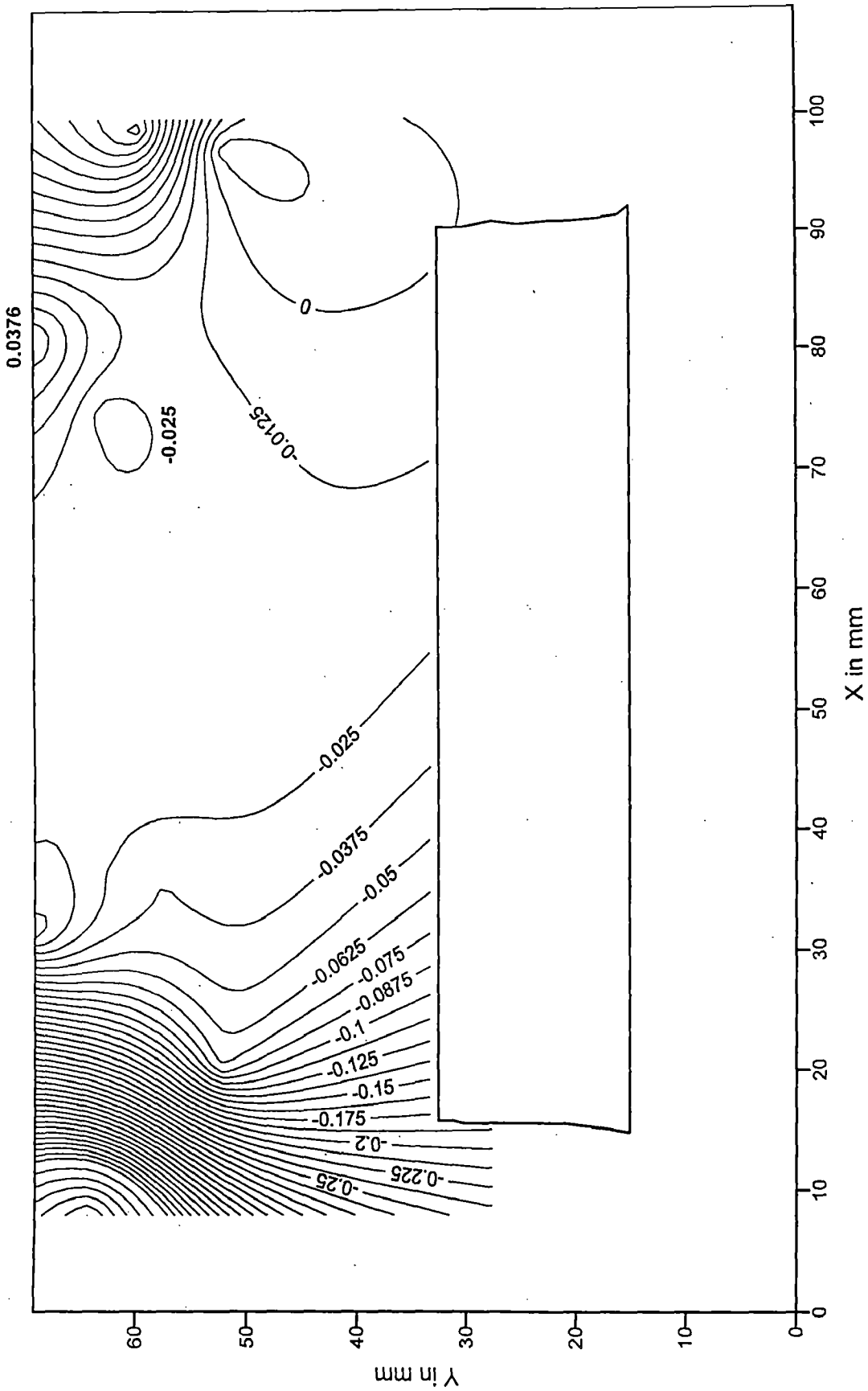


FIG. 5.19: STRESS CONTOURS FOR SX(kg/sq.cm) AT SLICE 10 (Z=92.476 mm) UNDER CONCENTRATED LOAD SIMULATING GANTRY COLUMN LOADS.

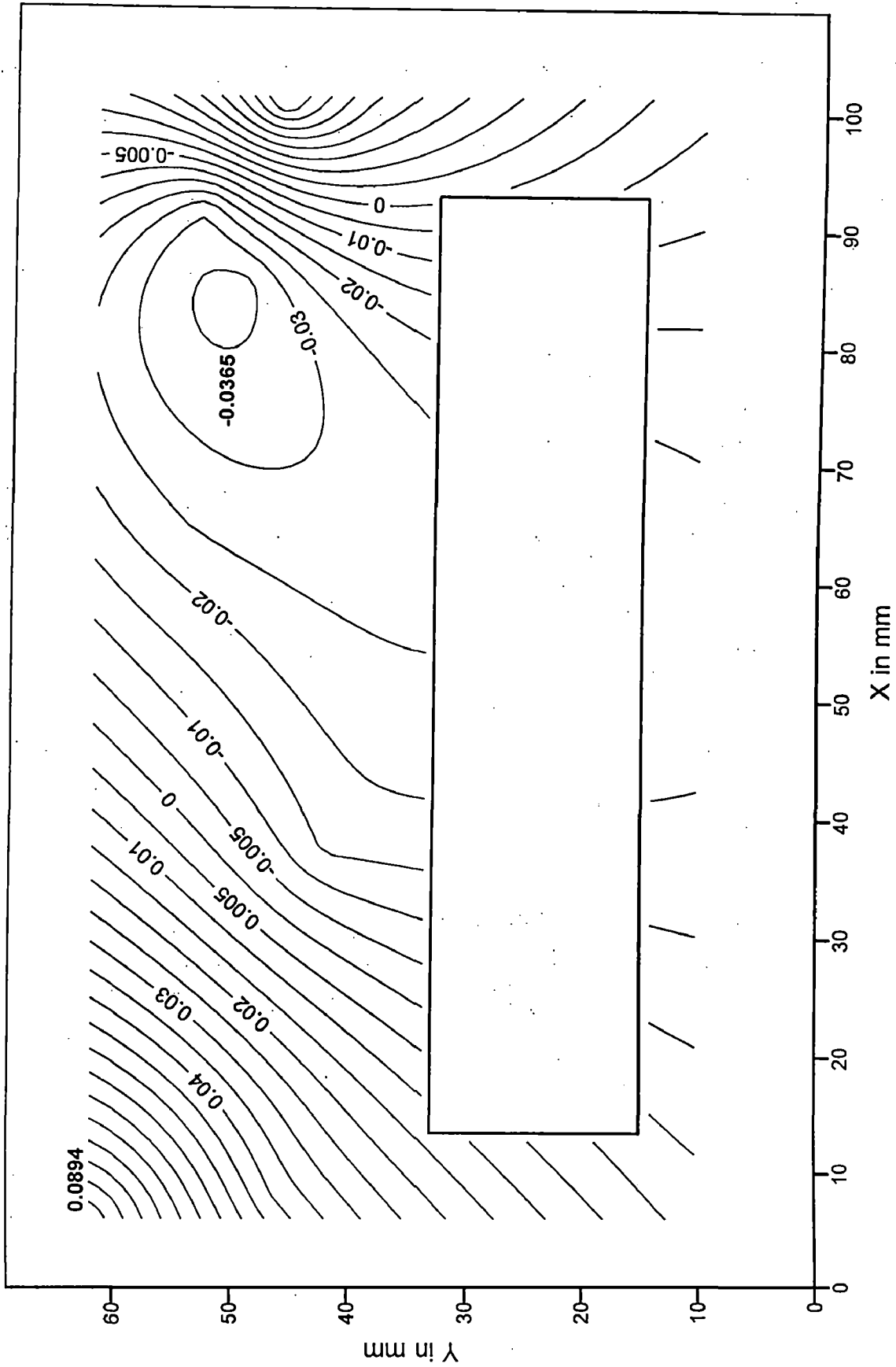


FIG. 5.20: STRESS CONTOURS FOR SX(kg/sq.cm) AT SLICE 11 (Z=100.967 mm) UNDER CONCENTRATED LOAD SIMULATING GANTRY COLUMN LOADS.

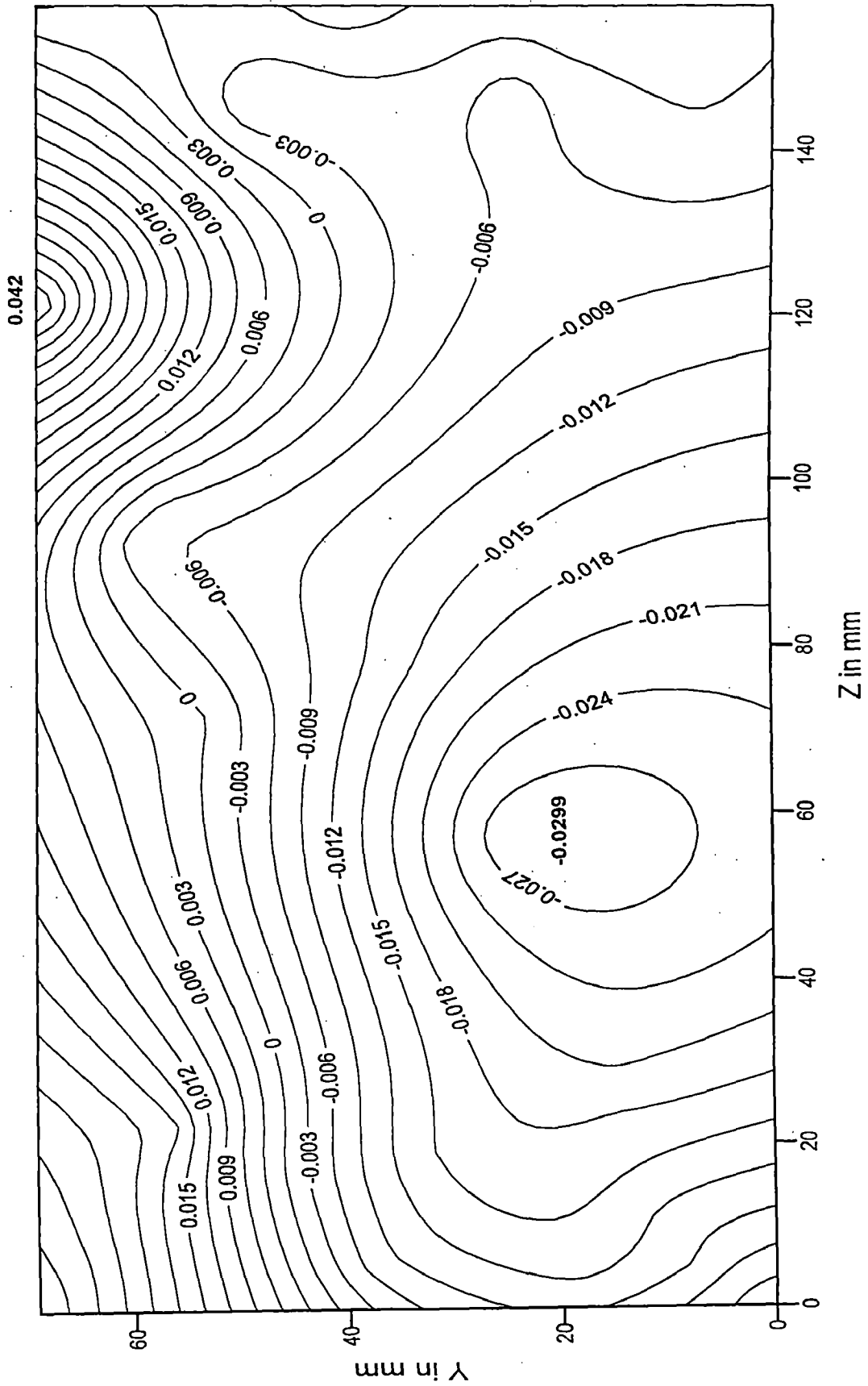


FIG. 5.21: STRESS CONTOURS FOR S_z (kg/sq.cm) AT POINT 3 (X=98.84 mm) UNDER CONCENTRATED LOAD BETWEEN SLICE 8 & 9.

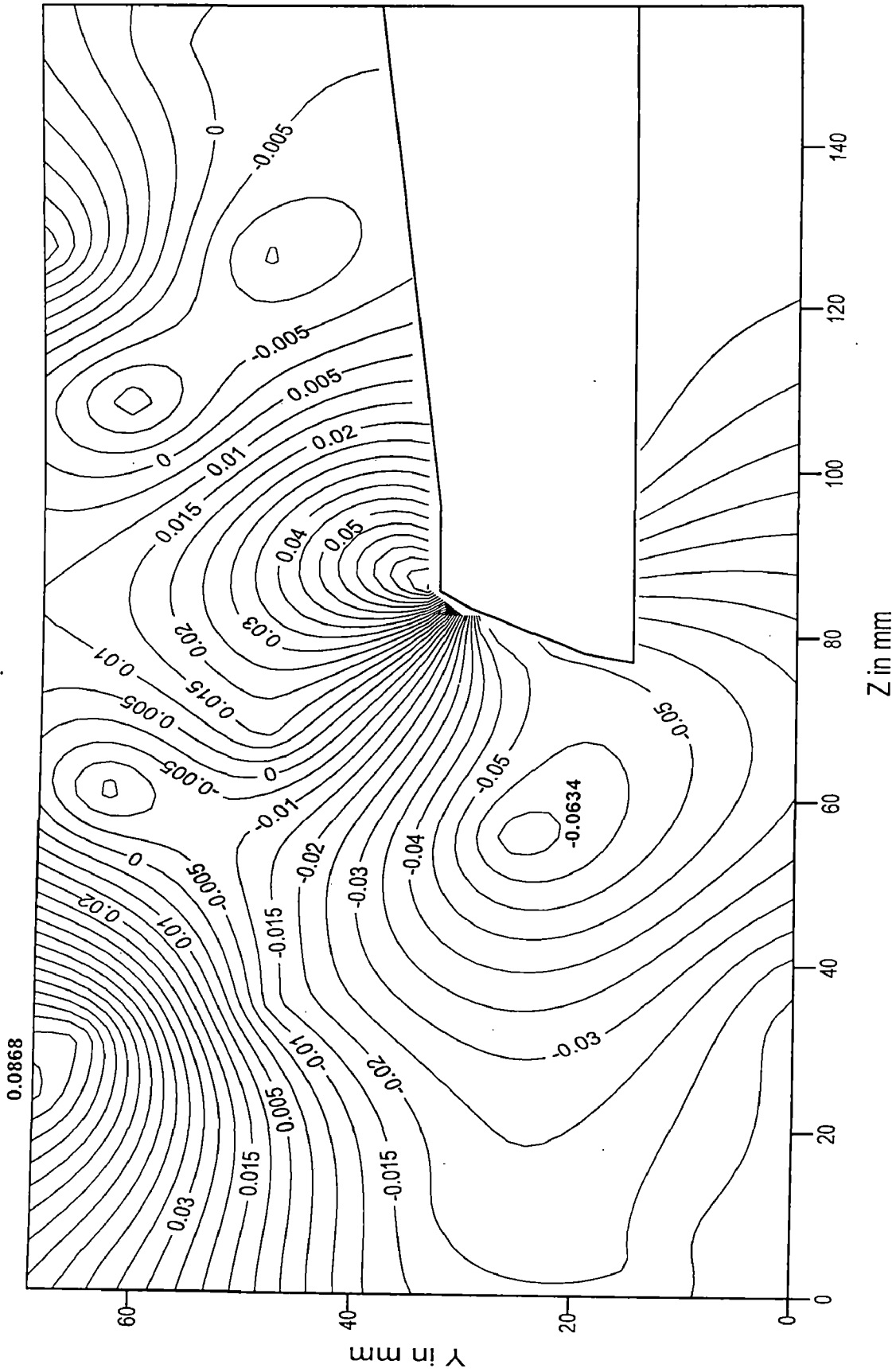


FIG. 5.22: STRESS CONTOURS FOR SZ(kg/sq.cm) AT POINT 6 (X=83.6 mm) UNDER CONCENTRATED LOAD BETWEEN SLICE 8 & 9.

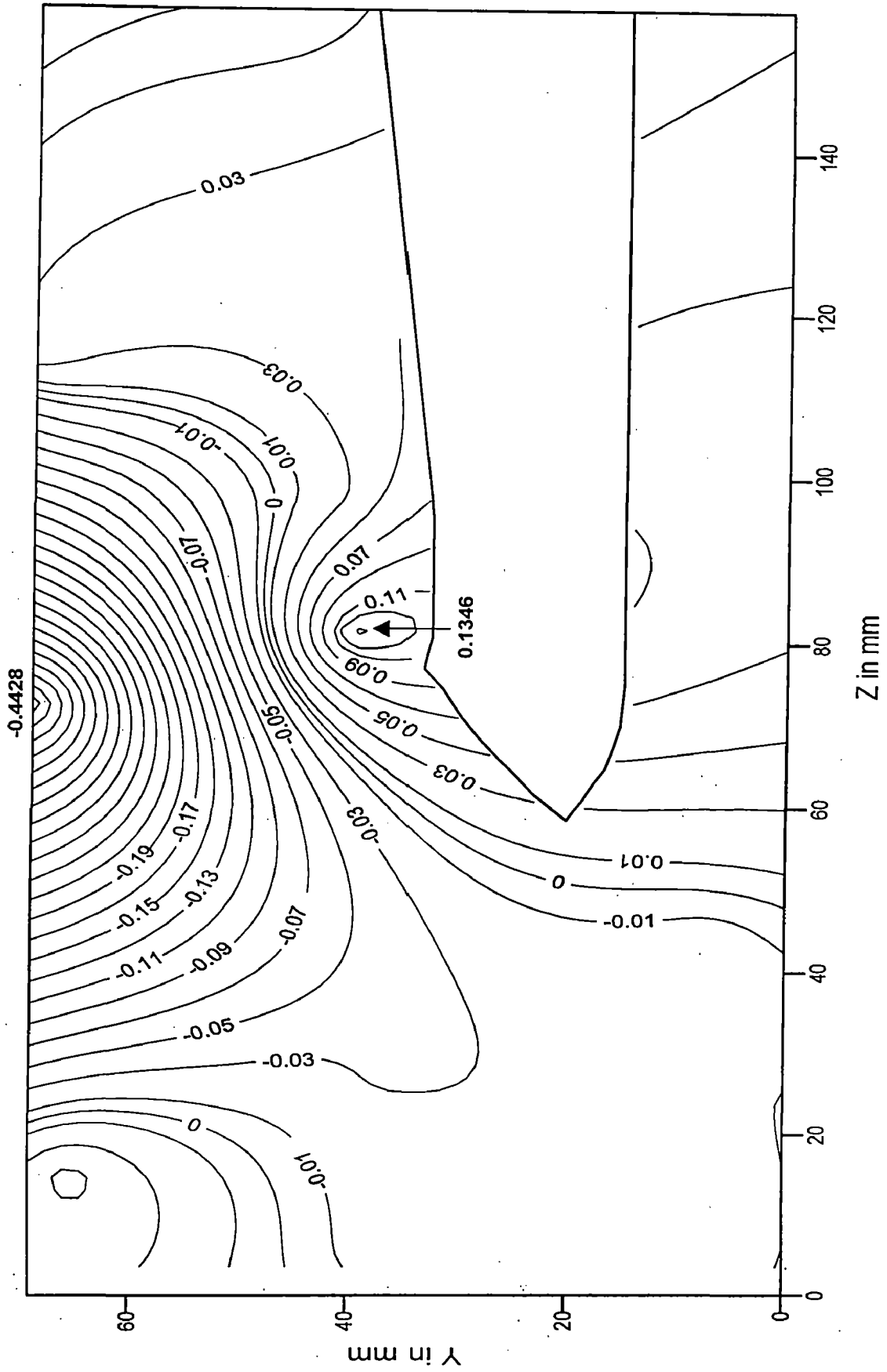


FIG. 5.23: STRESS CONTOURS FOR SZ(kg/sq.cm) AT POINT 8 (X=73.44 mm) UNDER CONCENTRATED LOAD BETWEEN SLICE 8 & 9.

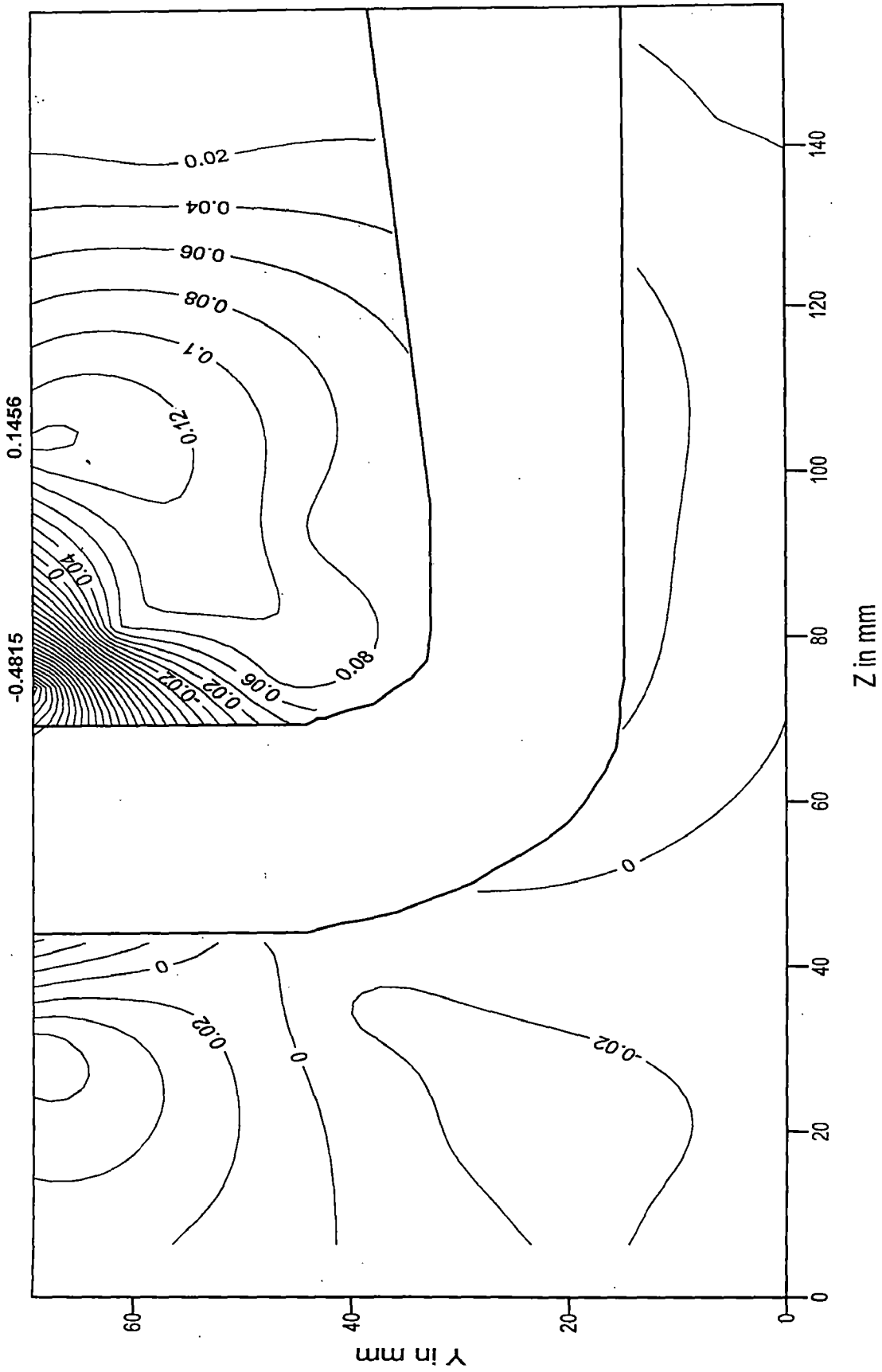


FIG. 5.24: STRESS CONTOURS FOR SZ(kg/sq.cm) AT POINT 10 (X=63.28 mm) UNDER CONCENTRATED LOAD BETWEEN SLICE 8 & 9.

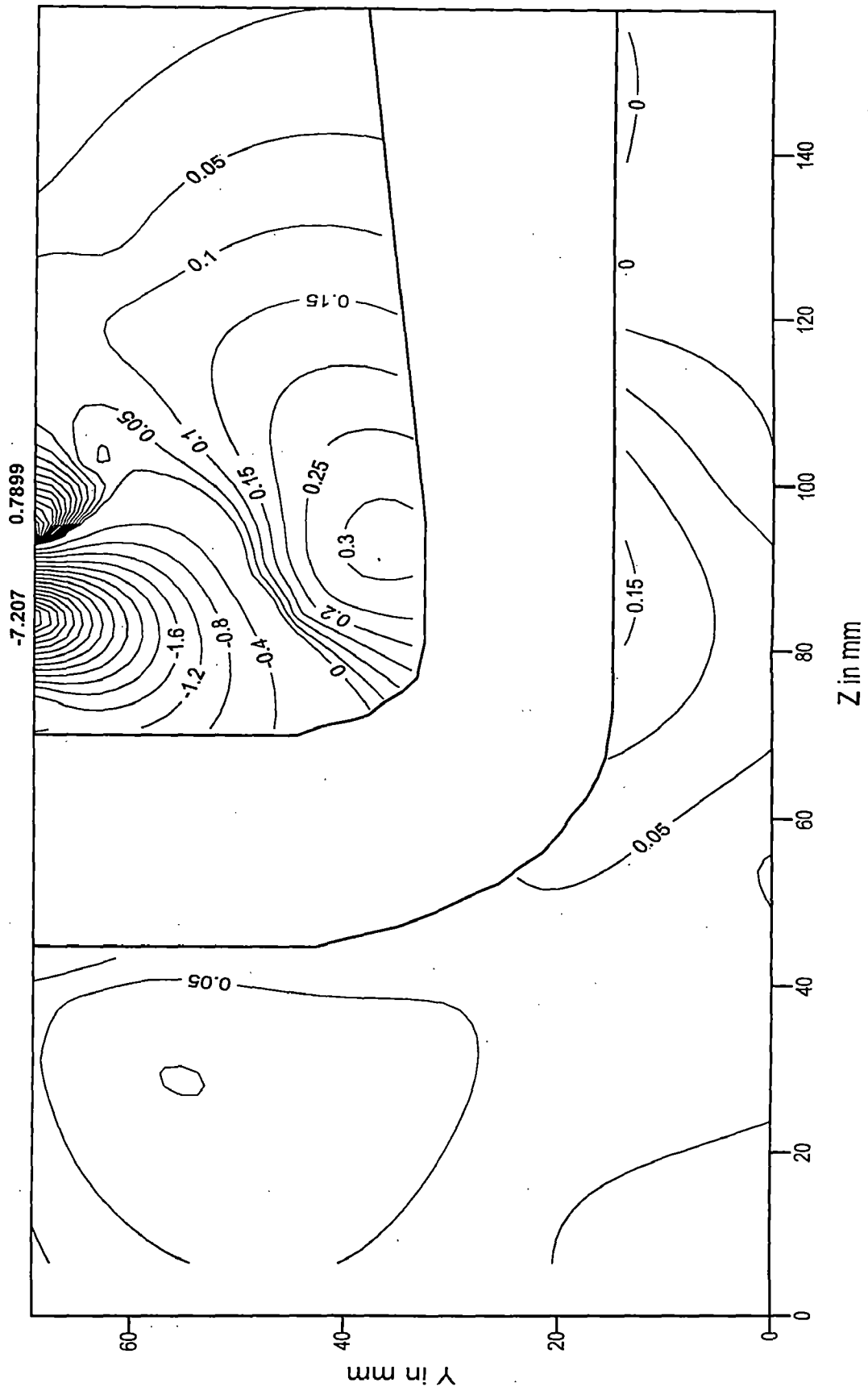


FIG. 5.25: STRESS CONTOURS FOR SZ(kg/sq.cm) AT POINT 12 (X=53.12 mm) UNDER CONCENTRATED LOAD BETWEEN SLICE 8 & 9.

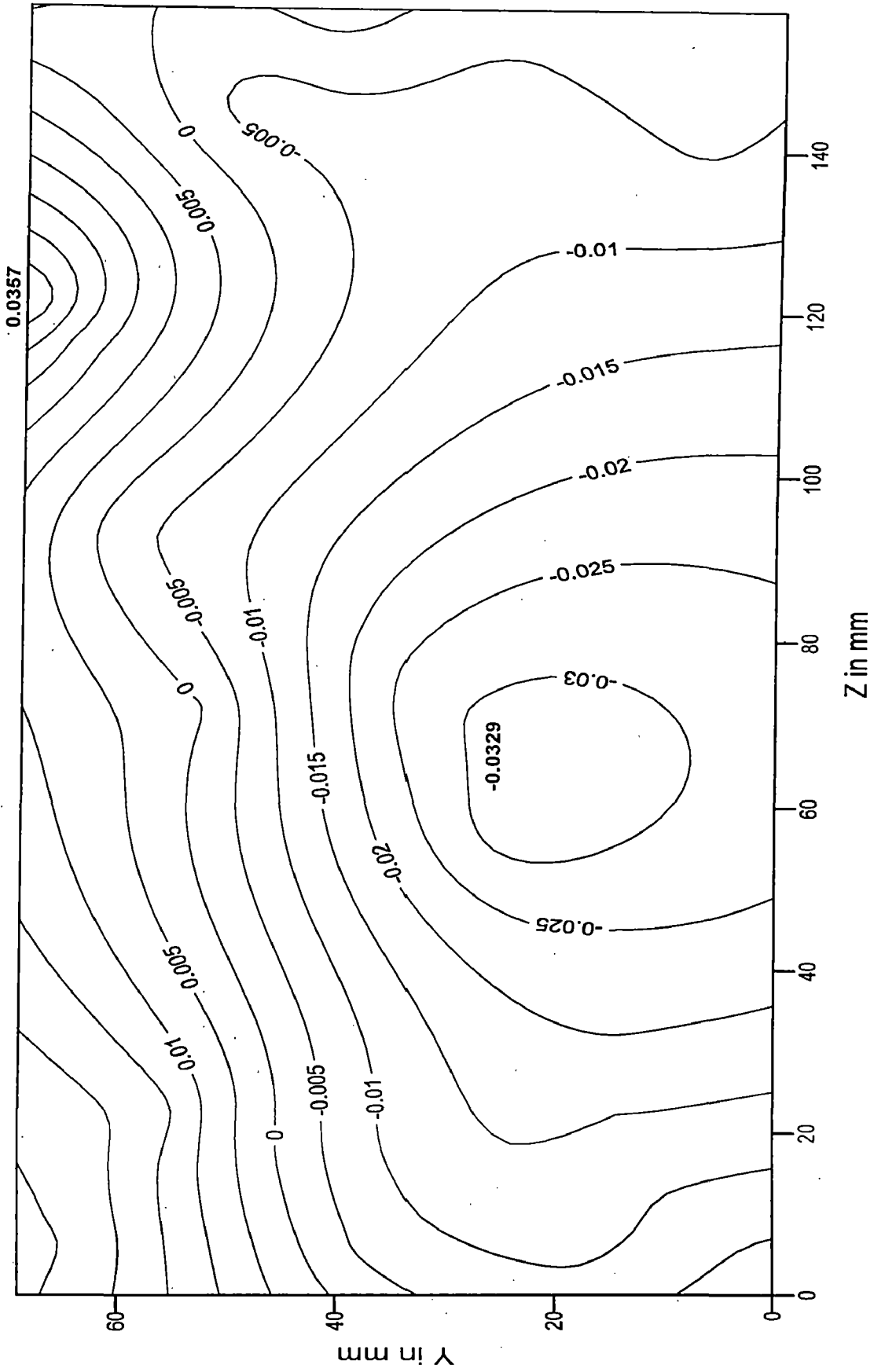


FIG. 5.26: STRESS CONTOURS FOR SZ(kg/sq.cm) AT POINT 3 (X=98.84 mm) UNDER CONCENTRATED LOAD BETWEEN SLICE 9 & 10.

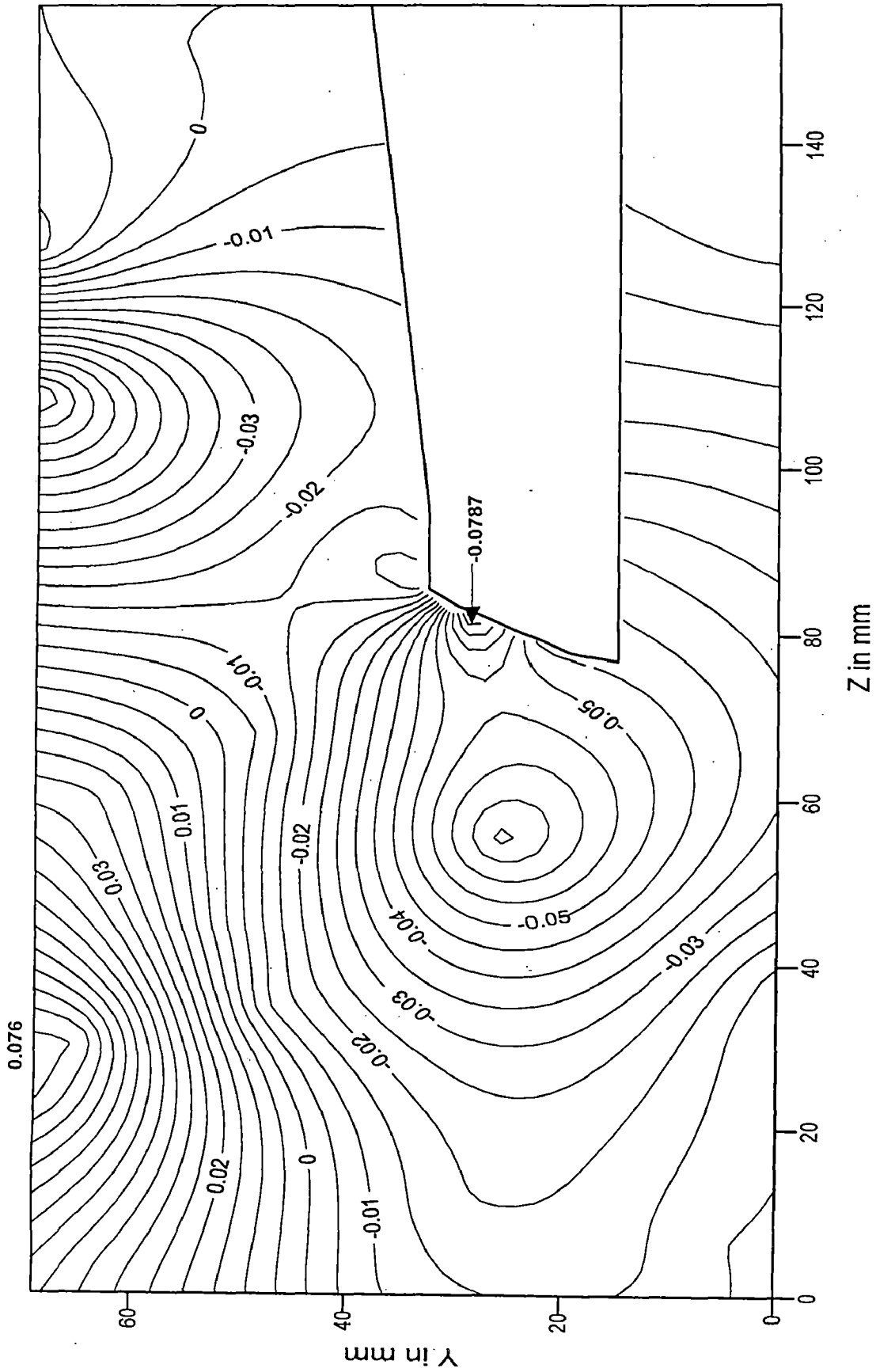


FIG. 5.27: STRESS CONTOURS FOR SZ(kg/sq.cm) AT POINT 6 (X=83.6 mm) UNDER CONCENTRATED LOAD BETWEEN SLICE 9 & 10.

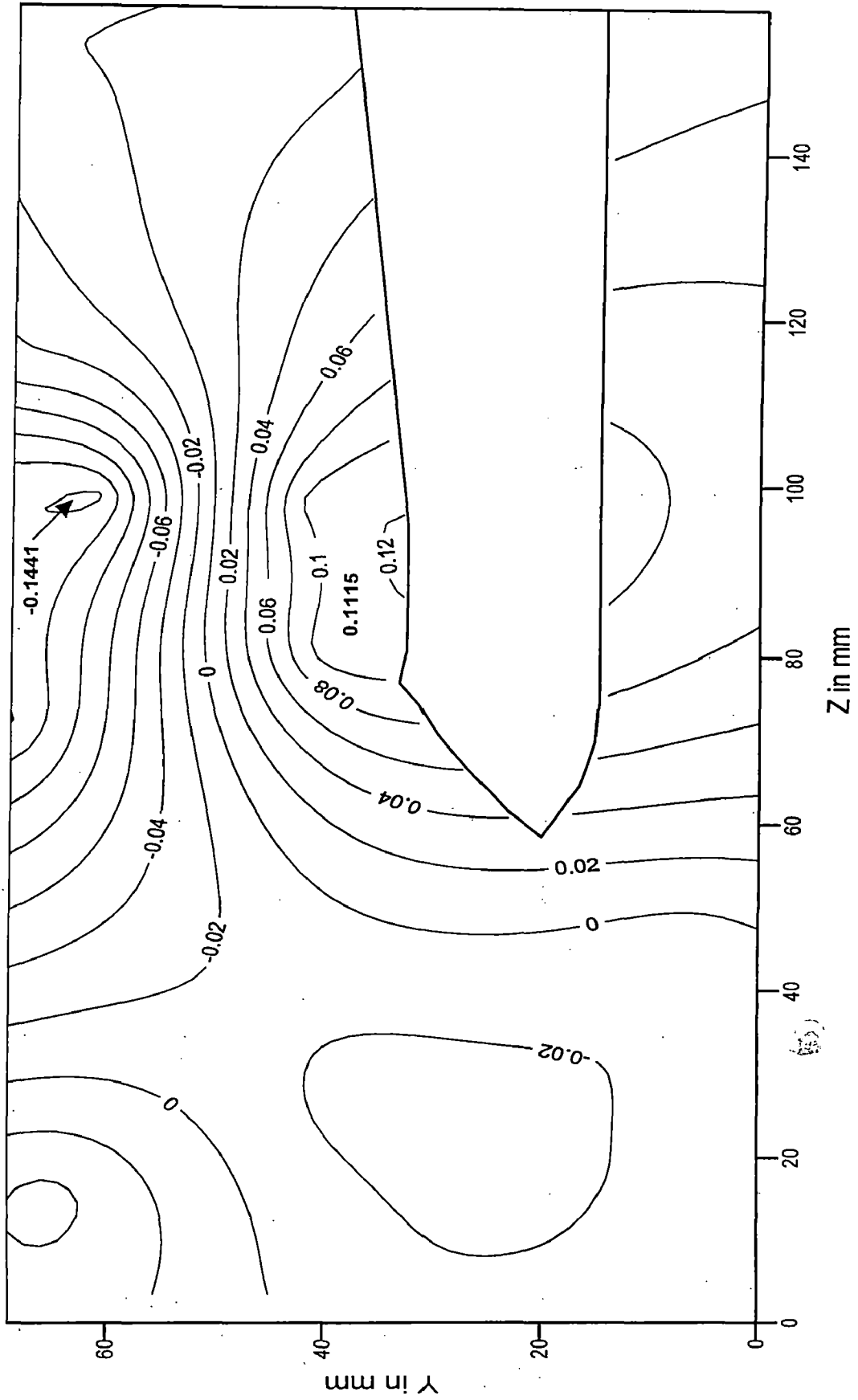


FIG. 5.28: STRESS CONTOURS FOR SZ(kg/sq.cm) AT POINT 8 (X=73.44 mm) UNDER CONCENTRATED LOAD BETWEEN SLICE 9 & 10.

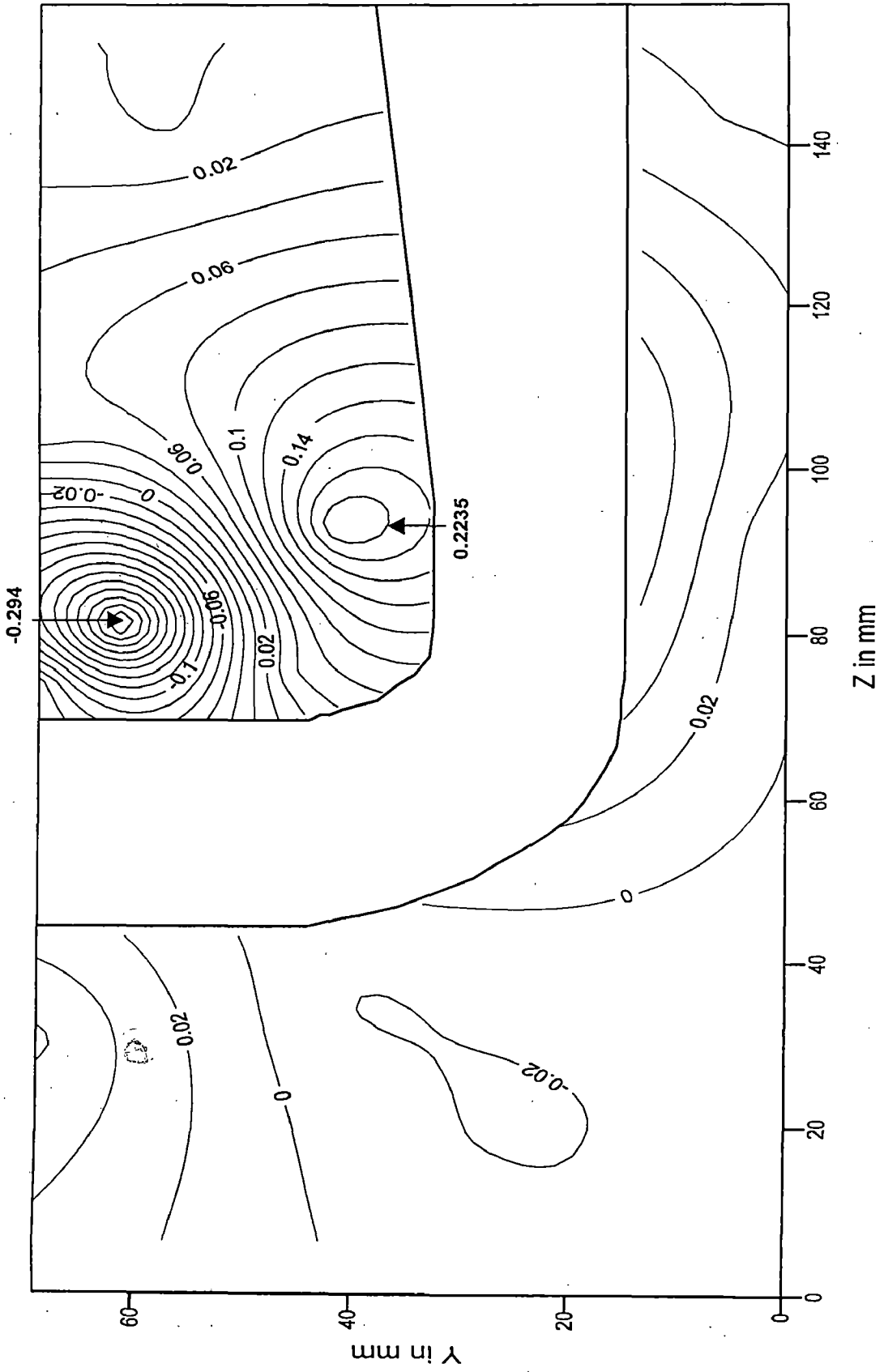


FIG. 5.29: STRESS CONTOURS FOR SZ(kg/sq.cm) AT POINT 10 (X=63.28 mm) UNDER CONCENTRATED LOAD BETWEEN SLICE 9 & 10.

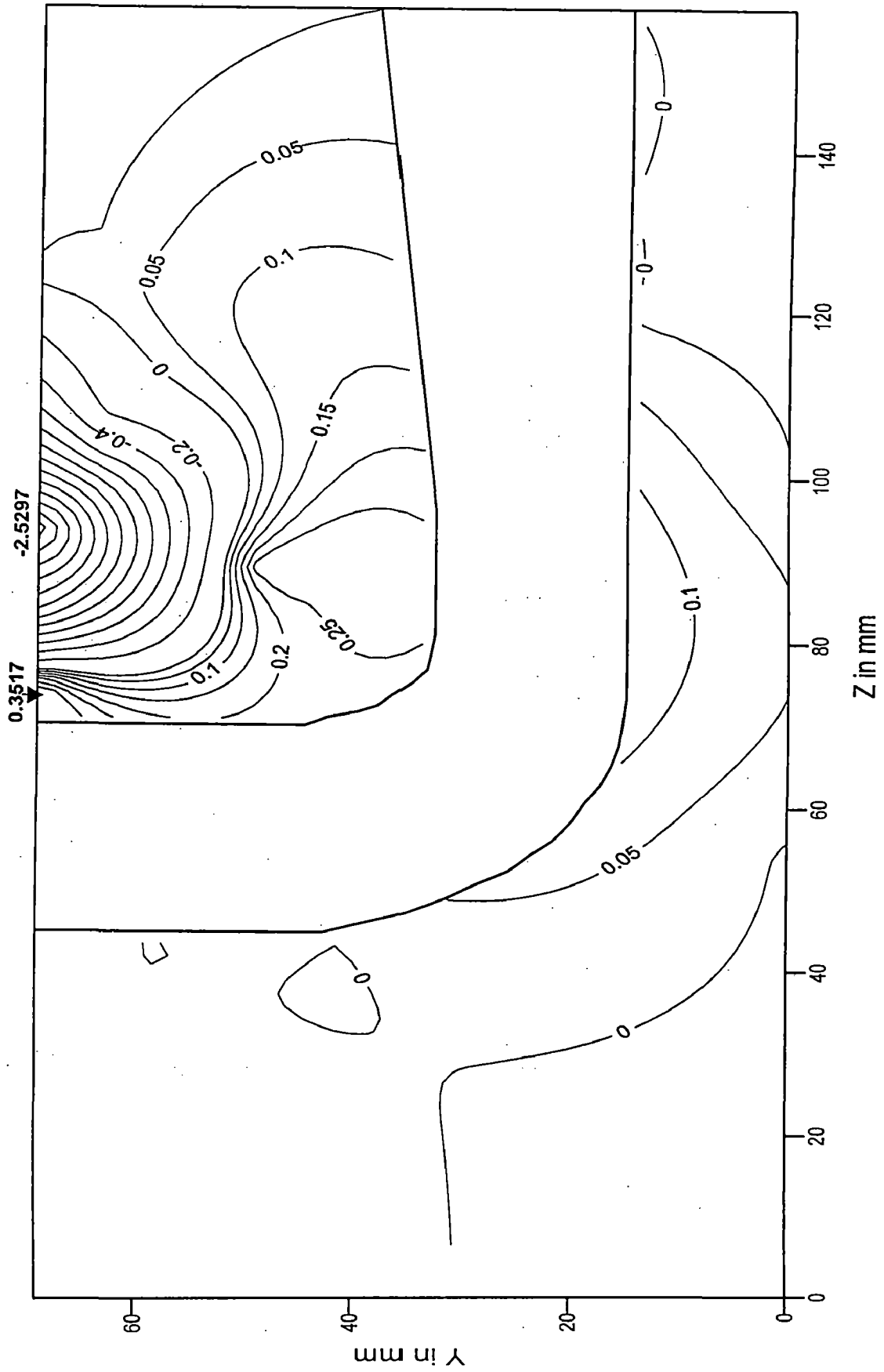


FIG. 5.30: STRESS CONTOURS FOR SZ (kg/sq.cm) AT POINT 12 ($X=53.12$ mm) UNDER CONCENTRATED LOAD BETWEEN SLICE 9 & 10.

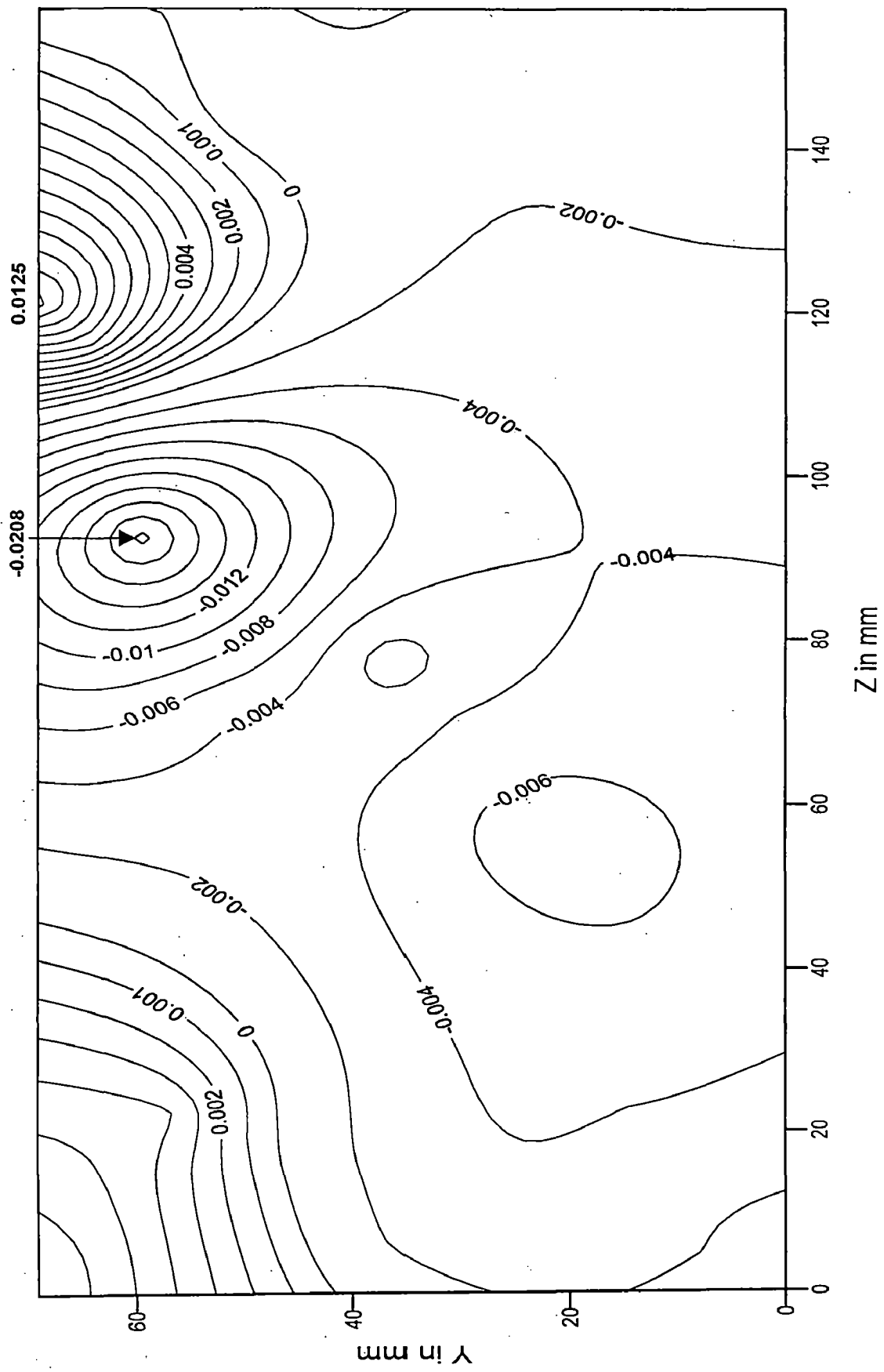


FIG. 5.31: STRESS CONTOURS FOR SZ(kg/sq.cm) AT POINT 3 (X=98.84 mm) UNDER UDL ABOVE ELBOW CONCRETE.

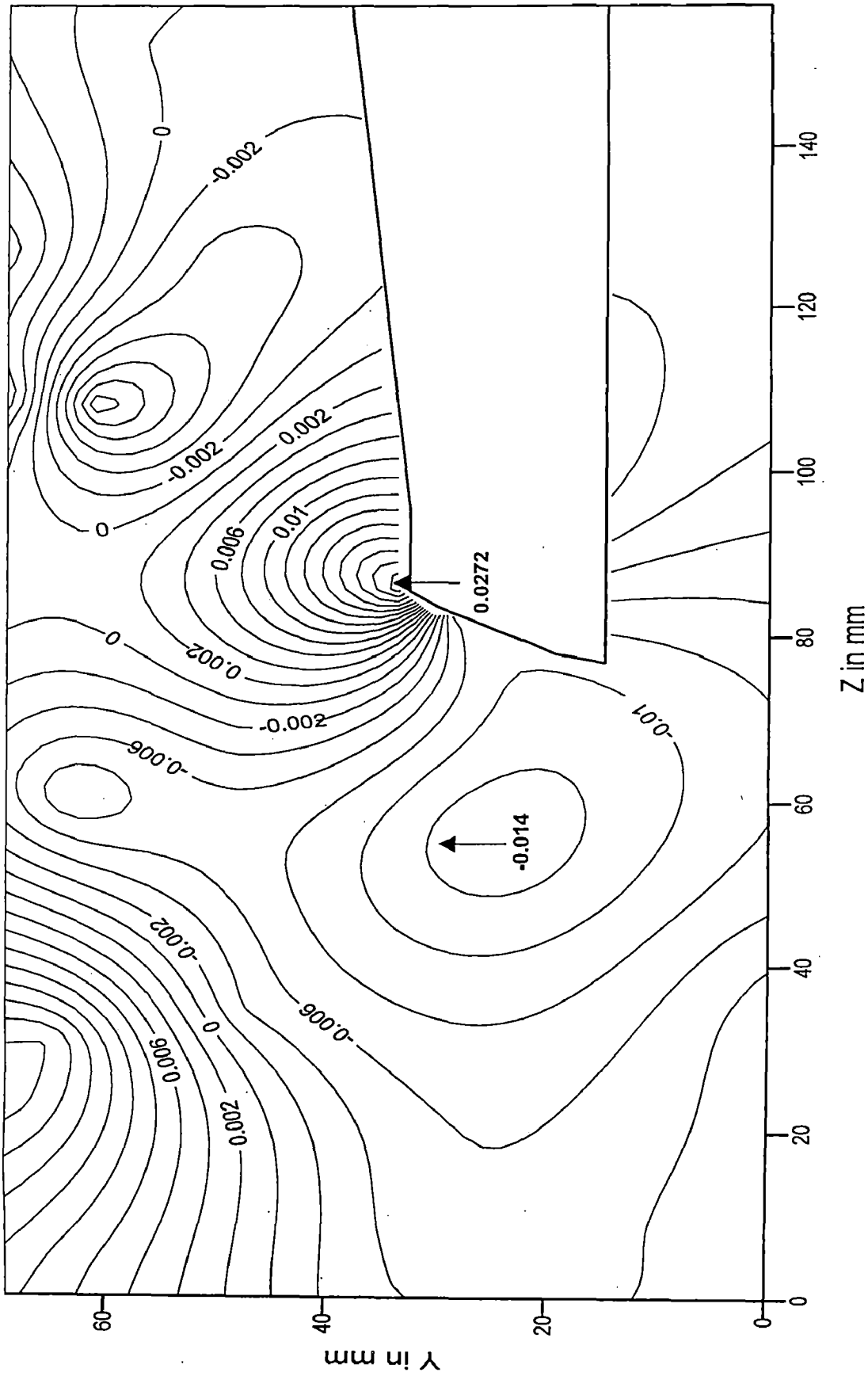


FIG. 5.32: STRESS CONTOURS FOR SZ(kg/sq.cm) AT POINT 6 (X=83.6 mm) UNDER UDL ABOVE ELBOW CONCRETE.

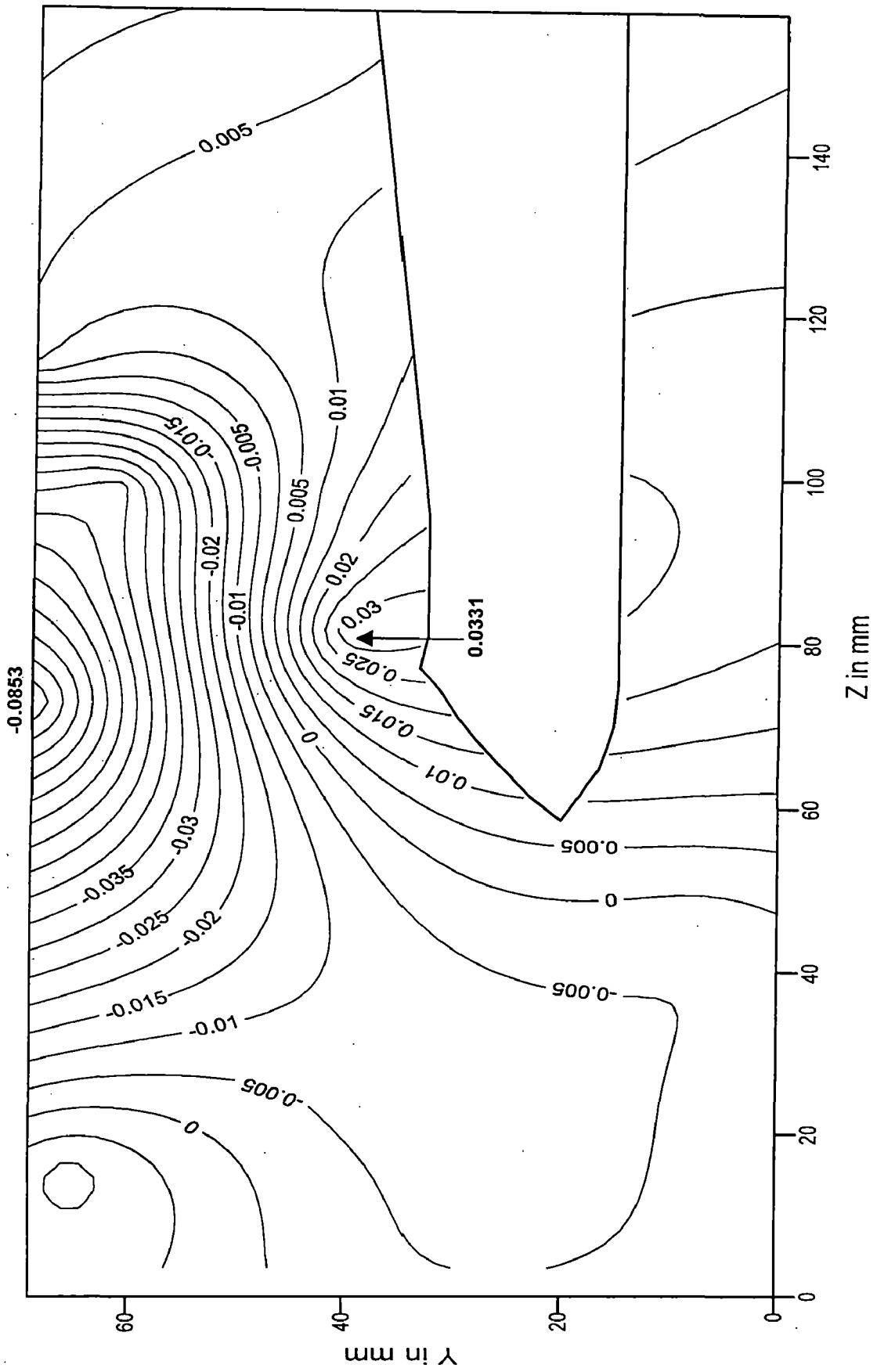


FIG. 5.33: STRESS CONTOURS FOR SZ(kg/sq.cm) AT POINT 8 (X=73.44 mm) UNDER UDL ABOVE ELBOW CONCRETE.

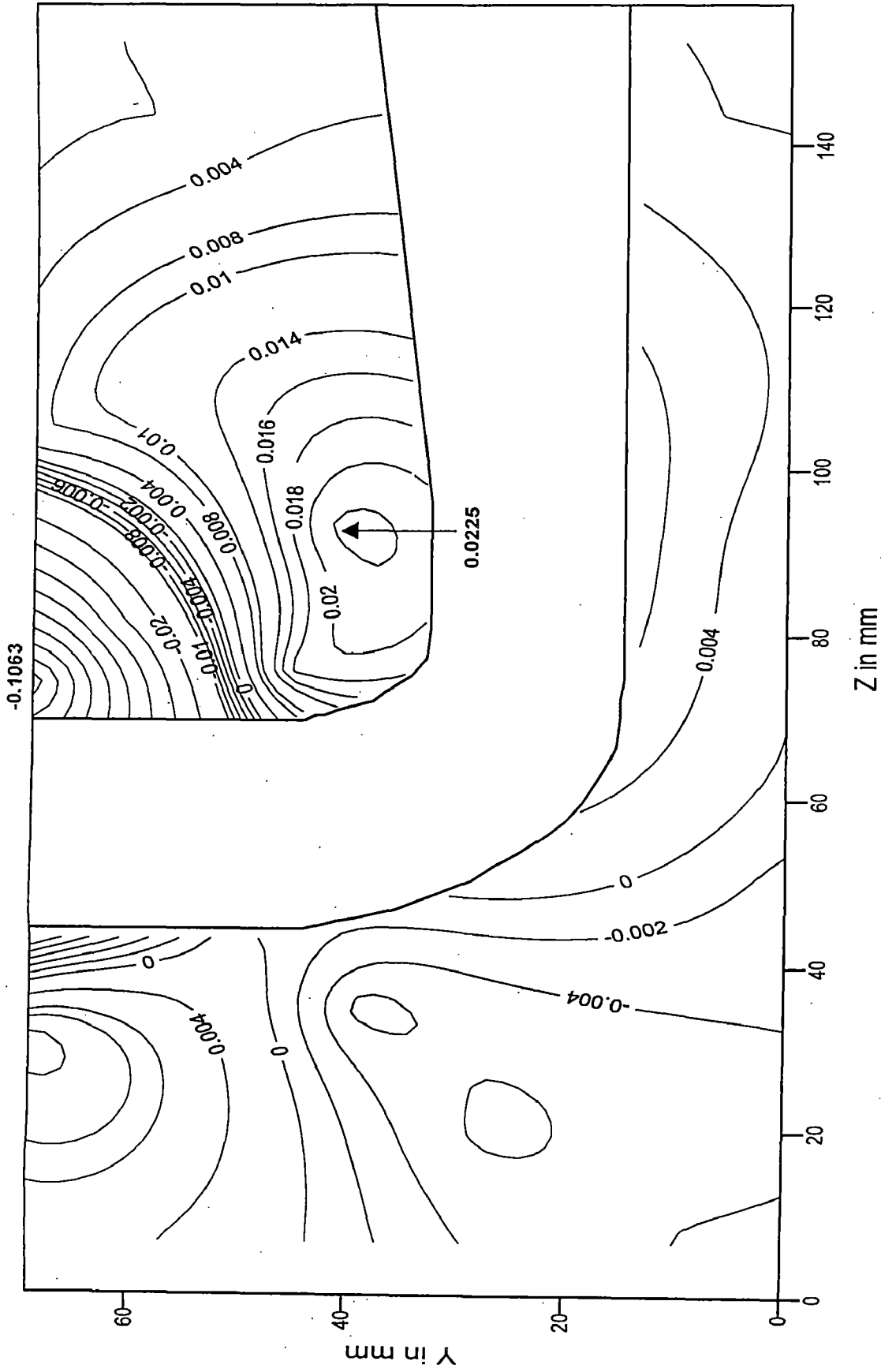


FIG. 5.34: STRESS CONTOURS FOR SZ(kg/sq.cm) AT POINT 10 (X=63.28 mm) UNDER UDL ABOVE ELBOW CONCRETE.

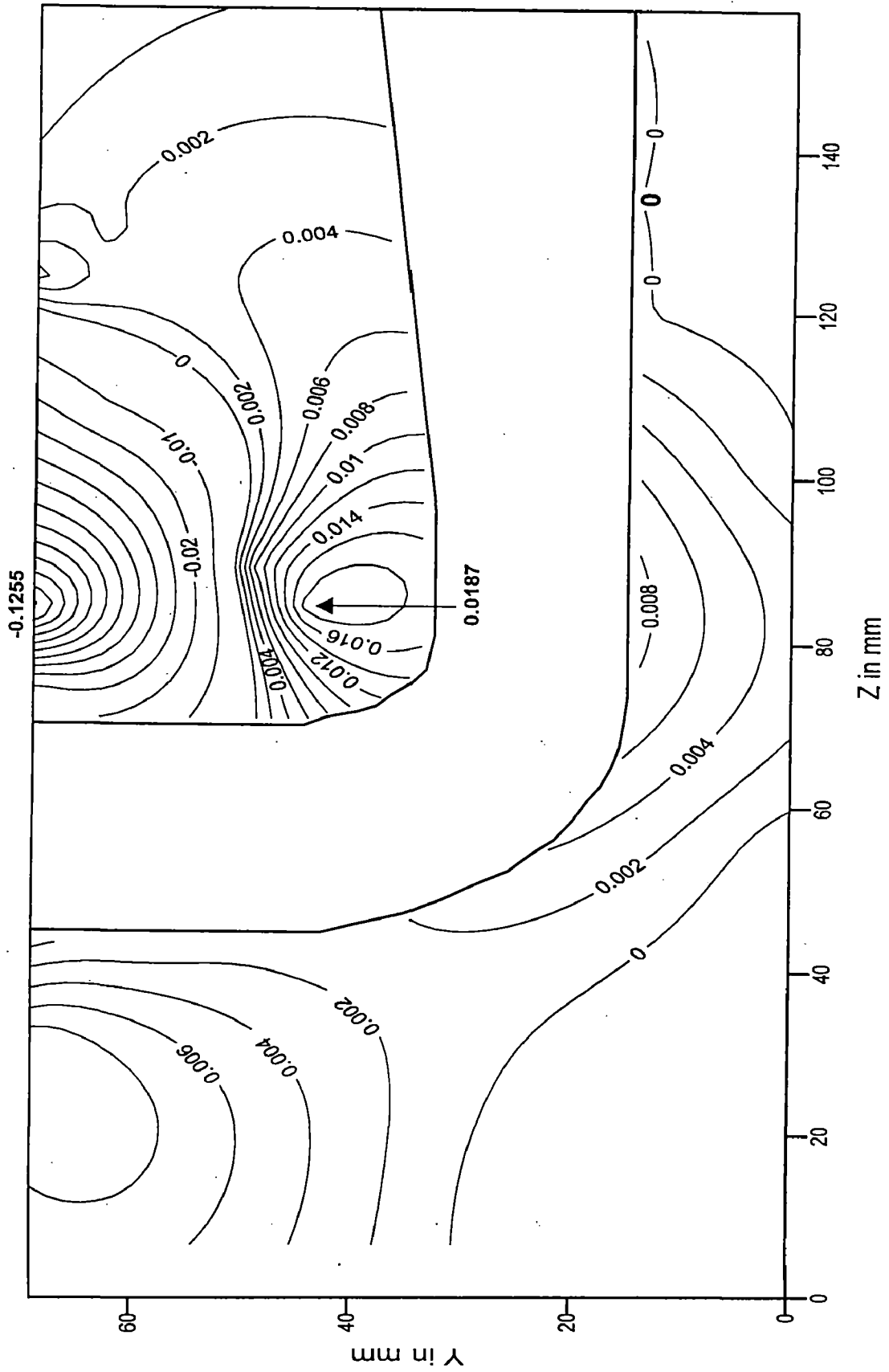


FIG. 5.35: STRESS CONTOURS FOR SZ(kg/sq.cm) AT POINT 12 (X=53.12 mm) UNDER UDL ABOVE ELBOW CONCRETE.

**STRESS CONTOURS PLOTTED FOR SZ UNDER LOAD
CONDITION 4**

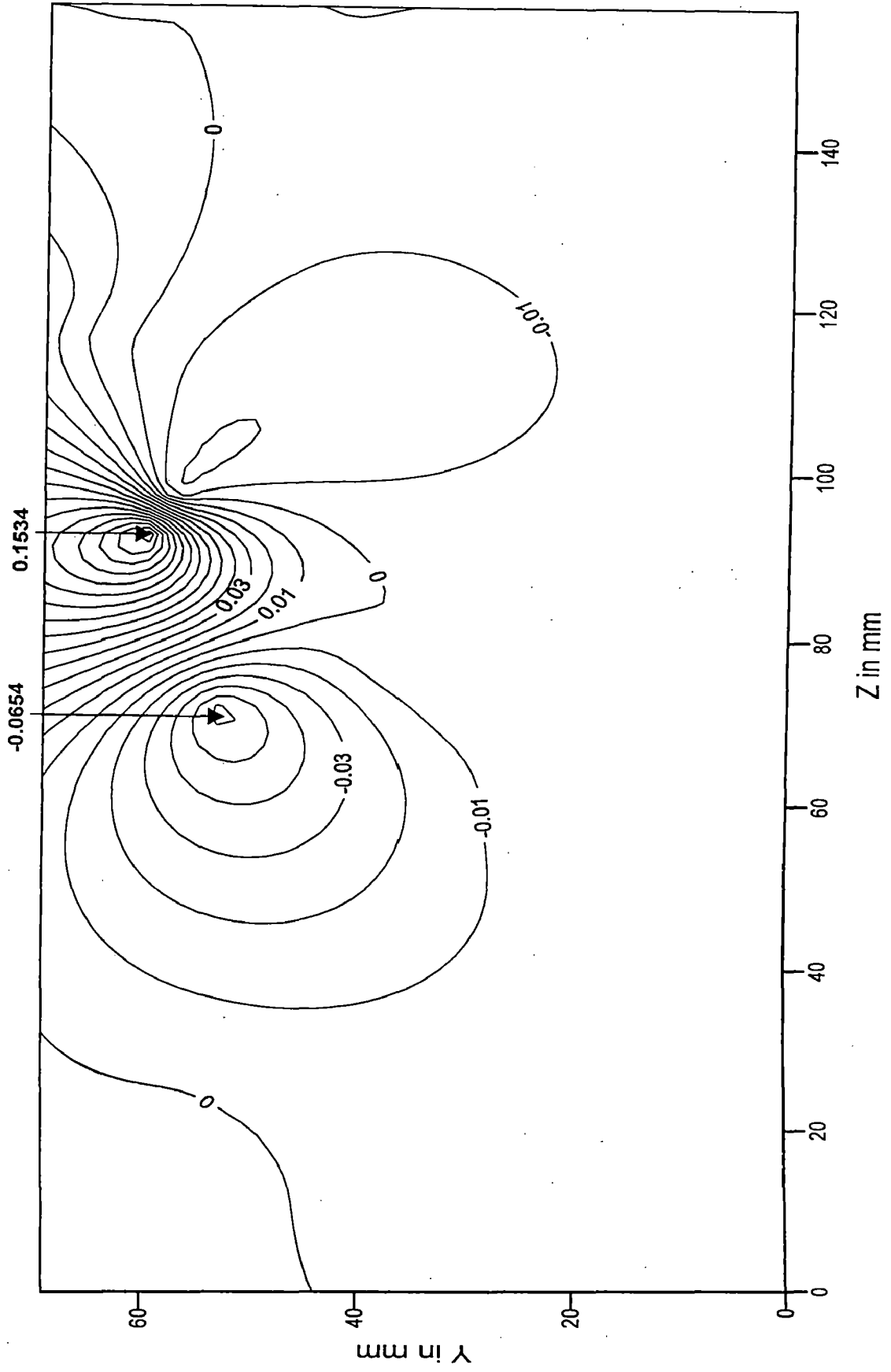


FIG. 5.36: STRESS CONTOURS FOR SZ(kg/sq.cm) AT POINT 3 (X=98.84 mm) UNDER CONCENTRATED LOAD SIMULATING GANTRY COLUMN LOADS.

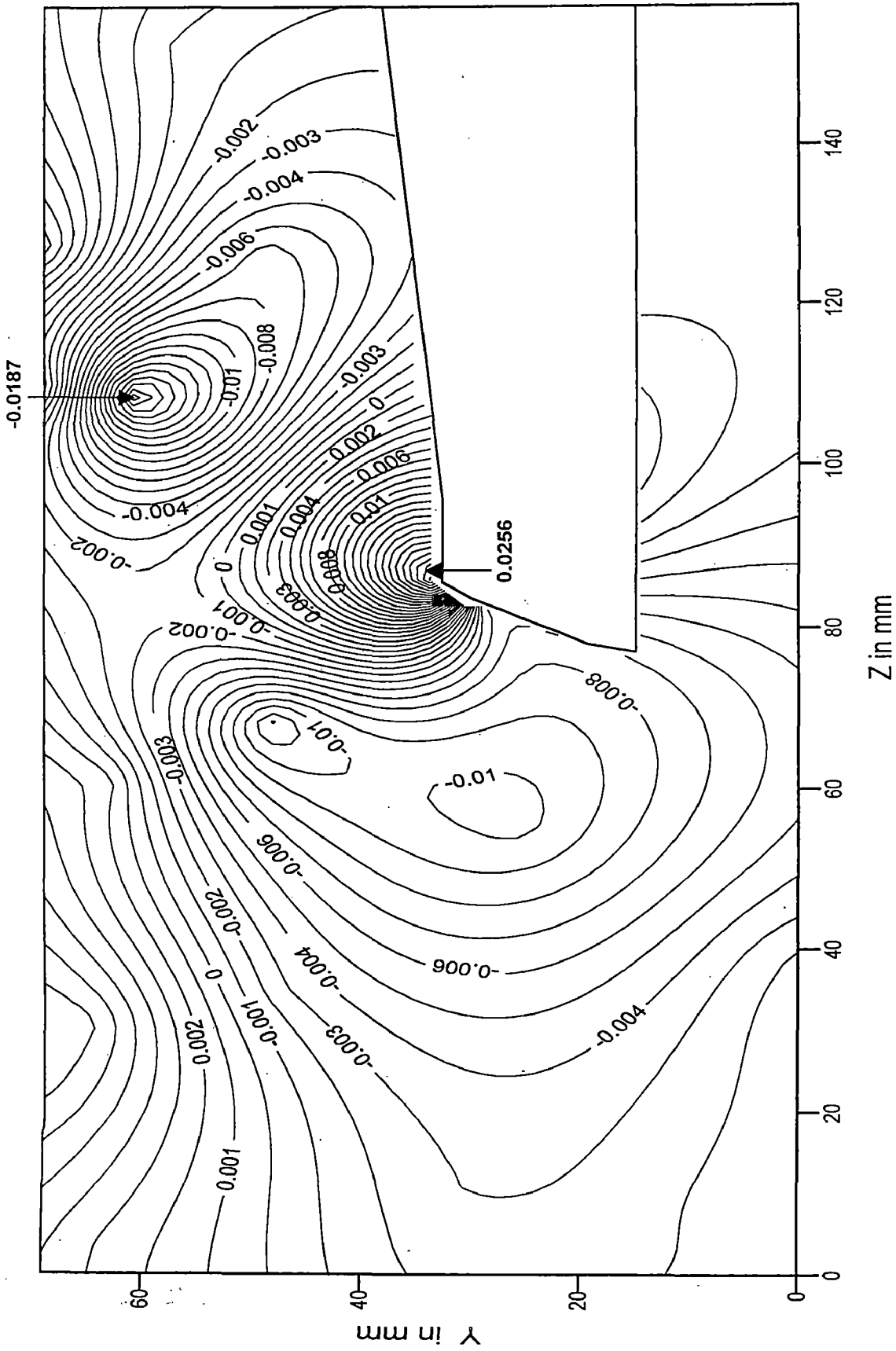


FIG. 5.37: STRESS CONTOURS FOR SZ(kg/sq.cm) AT POINT 6 (X=83.6 mm) UNDER CONCENTRATED LOAD SIMULATING GANTRY COLUMN LOADS.

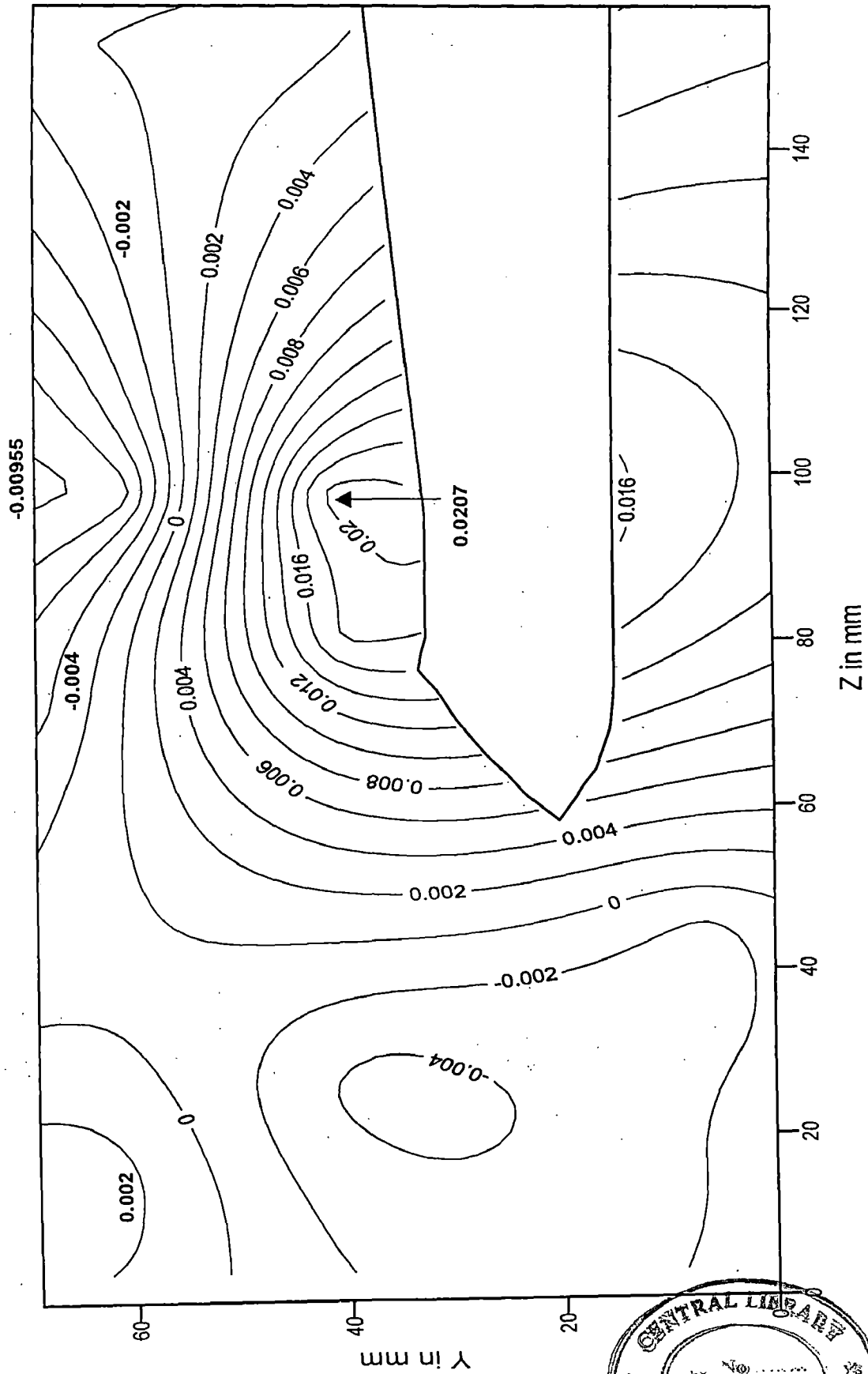
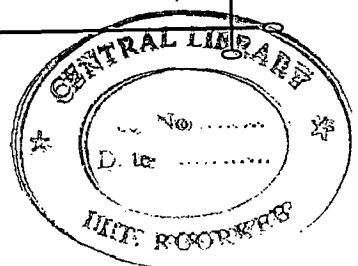


FIG. 5.38: STRESS CONTOURS FOR SZ(kg/sq.cm) AT POINT 8 (X=73.44mm) UNDER CONCENTRATED LOAD SIMULATING GANTRY COLUMN LOADS.



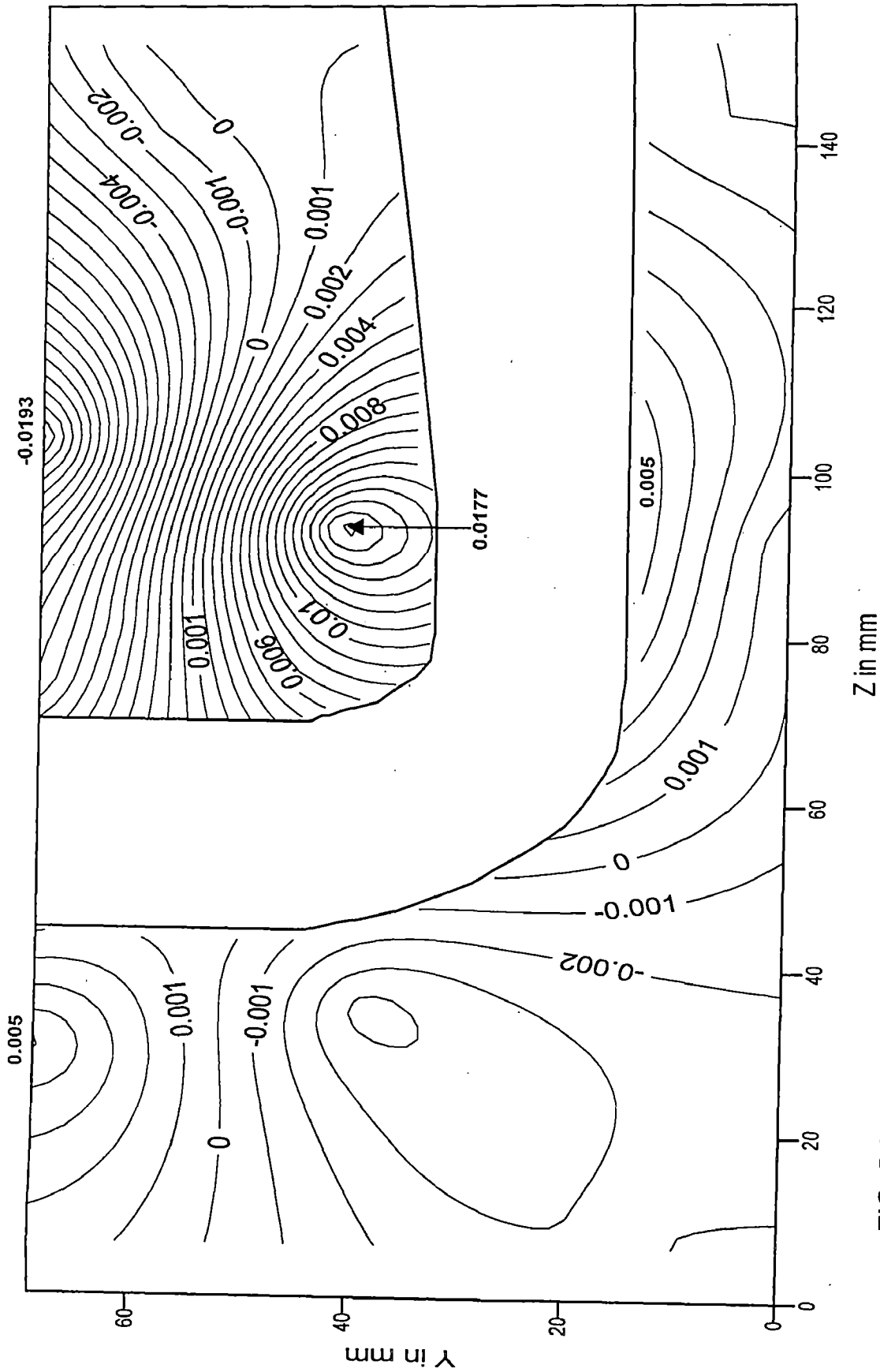


FIG. 5.39: STRESS CONTOURS FOR SZ(kg/sq.cm) AT POINT 10 (X=63.28 mm) UNDER CONCENTRATED LOAD SIMULATING GANTRY COLUMN LOADS.

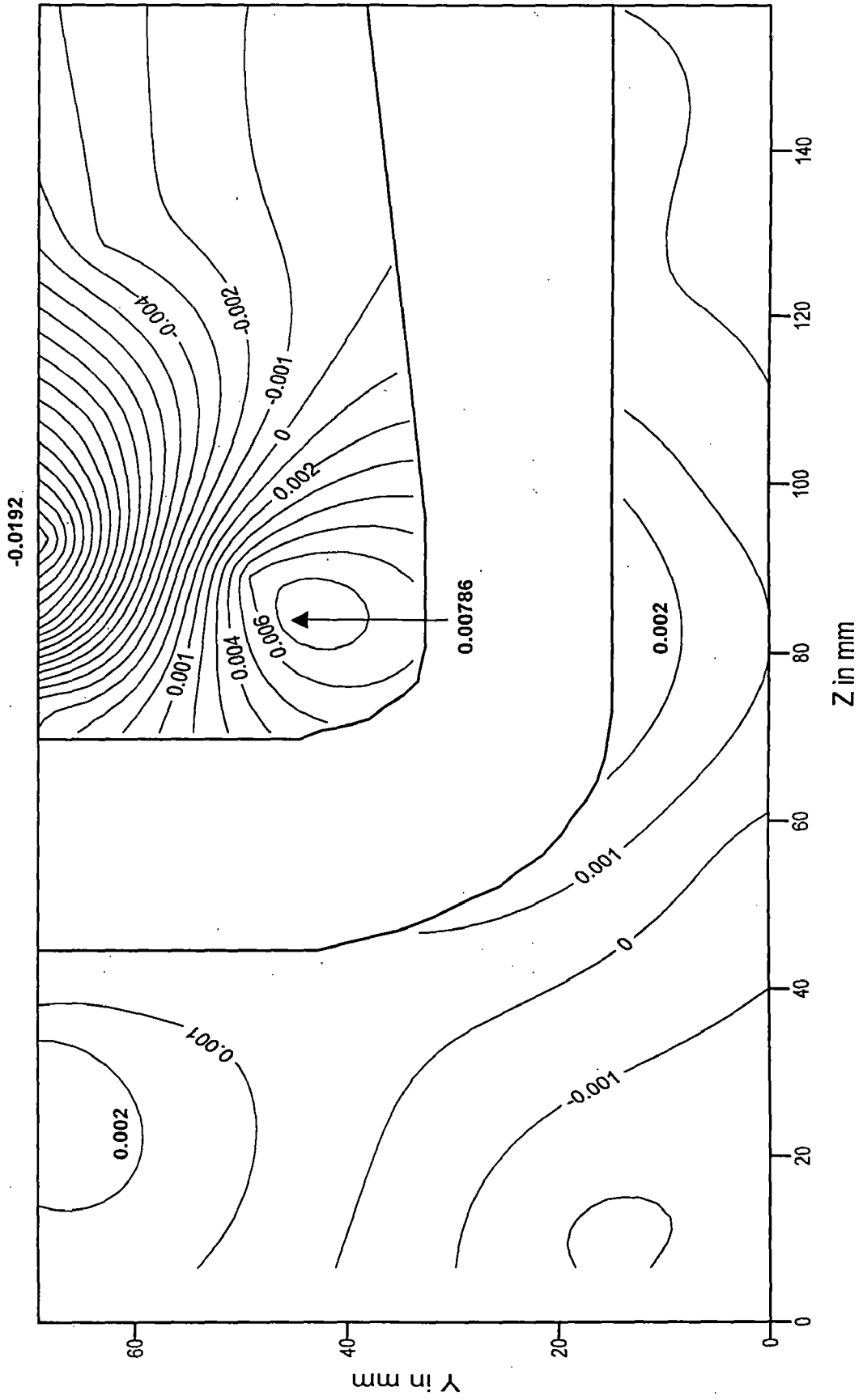


FIG. 5.40: STRESS CONTOURS FOR SZ(kg/sq.cm) AT POINT 12 (X=53.12 mm) UNDER CONCENTRATED LOAD SIMULATING GANTRY COLUMN LOADS.

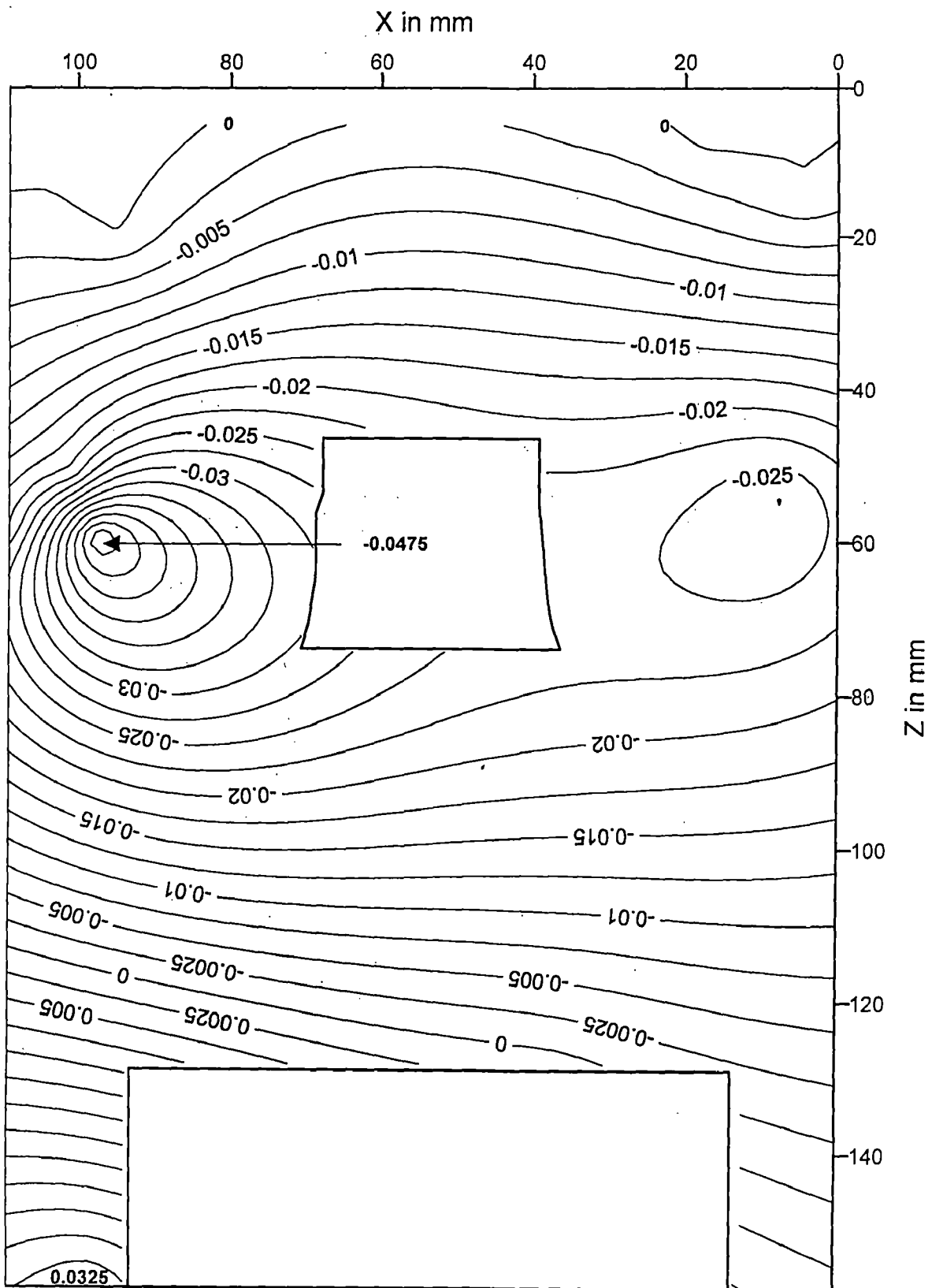


FIG. 5.41: STRESS CONTOURS FOR S_Y (kg/sq.cm) AT STRIP 7 ($Y=35.56$ mm) UNDER CONCENTRATED LOAD BETWEEN SLICE 8 & 9.

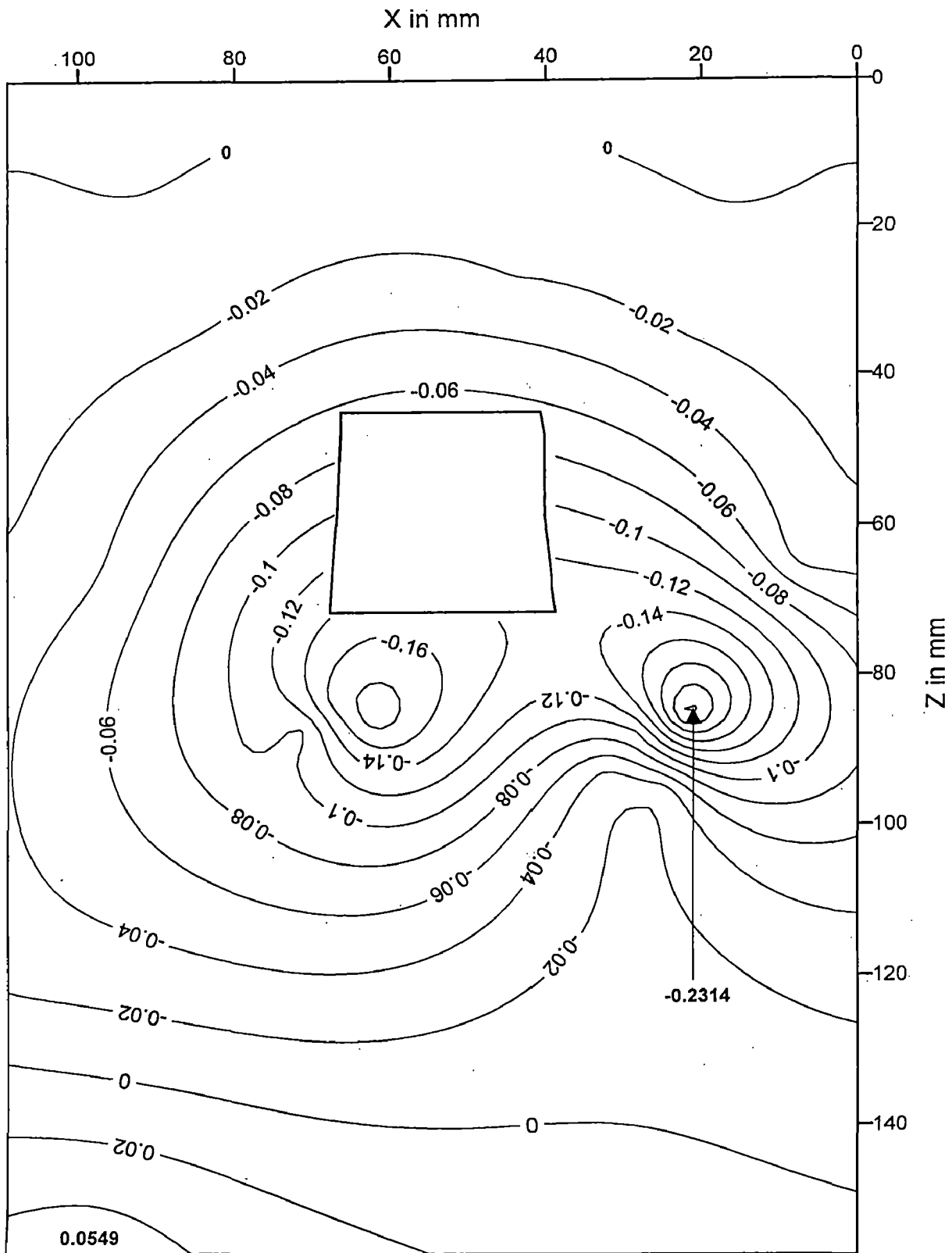


FIG. 5.42: STRESS CONTOURS FOR S_Y (kg/sq.cm) AT STRIP 8 ($Y=40.64$ mm) UNDER CONCENTRATED LOAD BETWEEN SLICE 8 & 9.

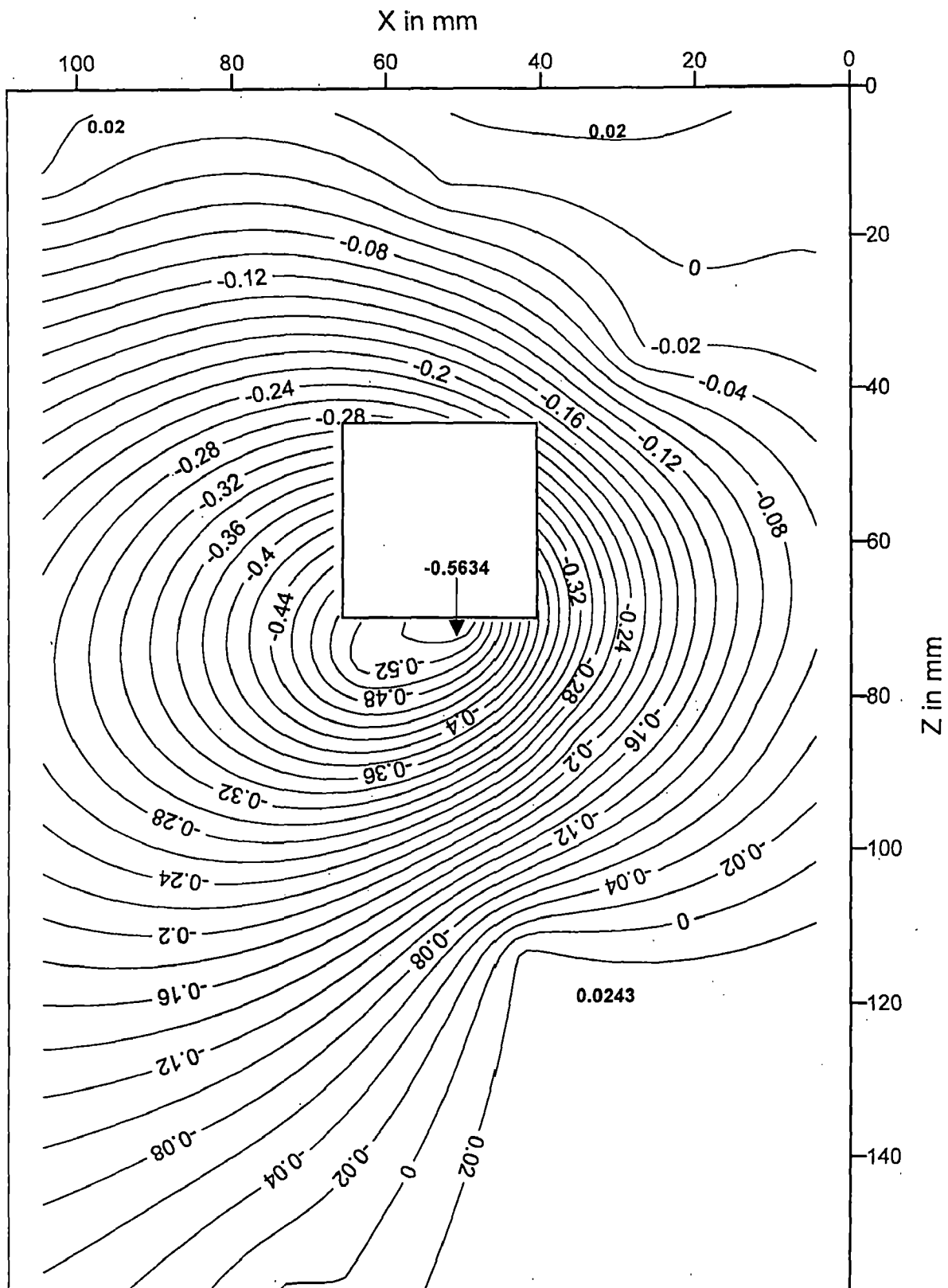


FIG. 5.43: STRESS CONTOURS FOR S_Y (kg/sq.cm) AT STRIP 9 ($Y=45.72$ mm) UNDER CONCENTRATED LOAD BETWEEN SLICE 8 & 9.

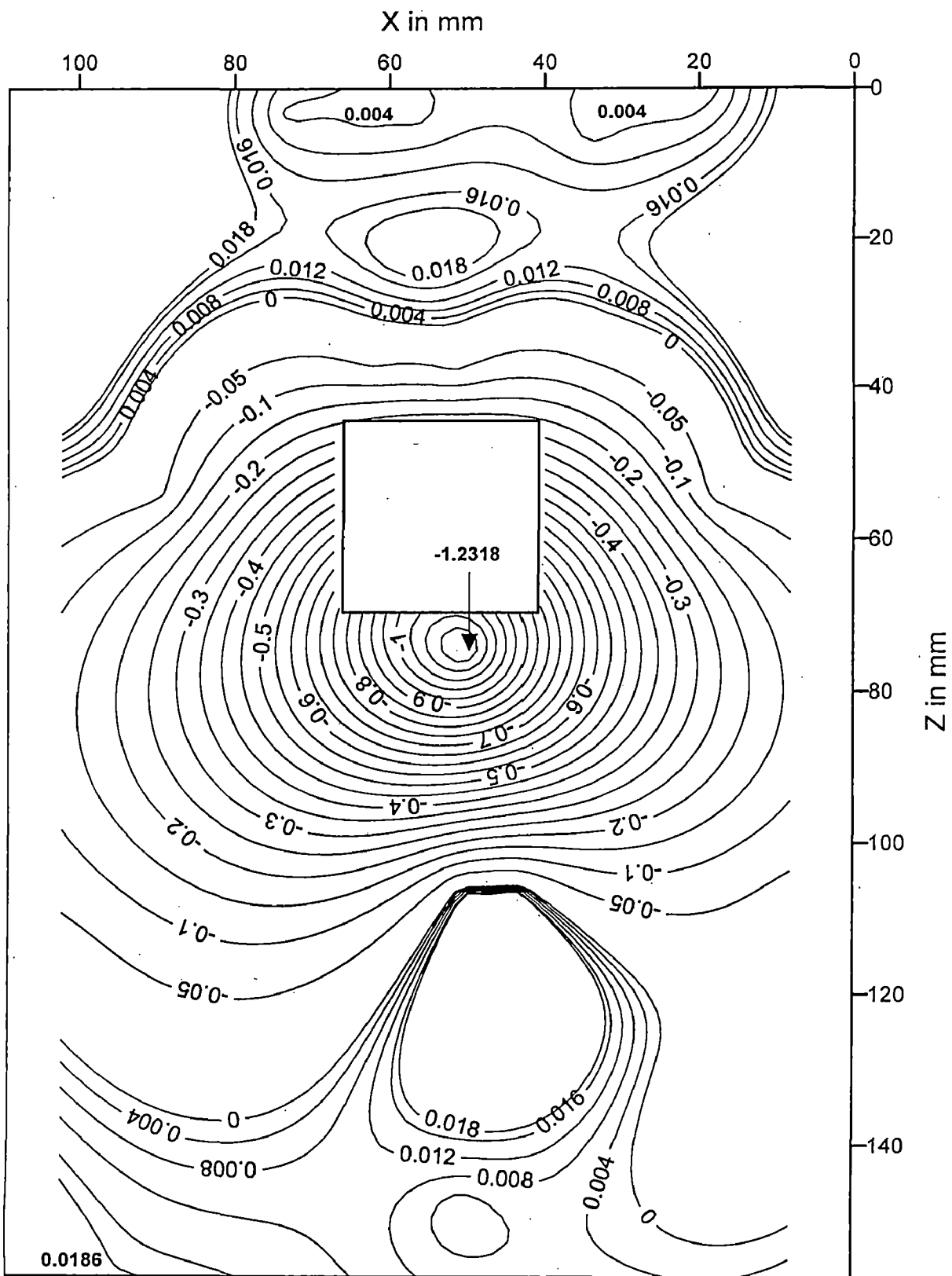


FIG. 5.44: STRESS CONTOURS FOR S_Y (kg/sq.cm) AT STRIP 10 ($Y=50.80$ mm) UNDER CONCENTRATED LOAD BETWEEN SLICE 8 & 9.

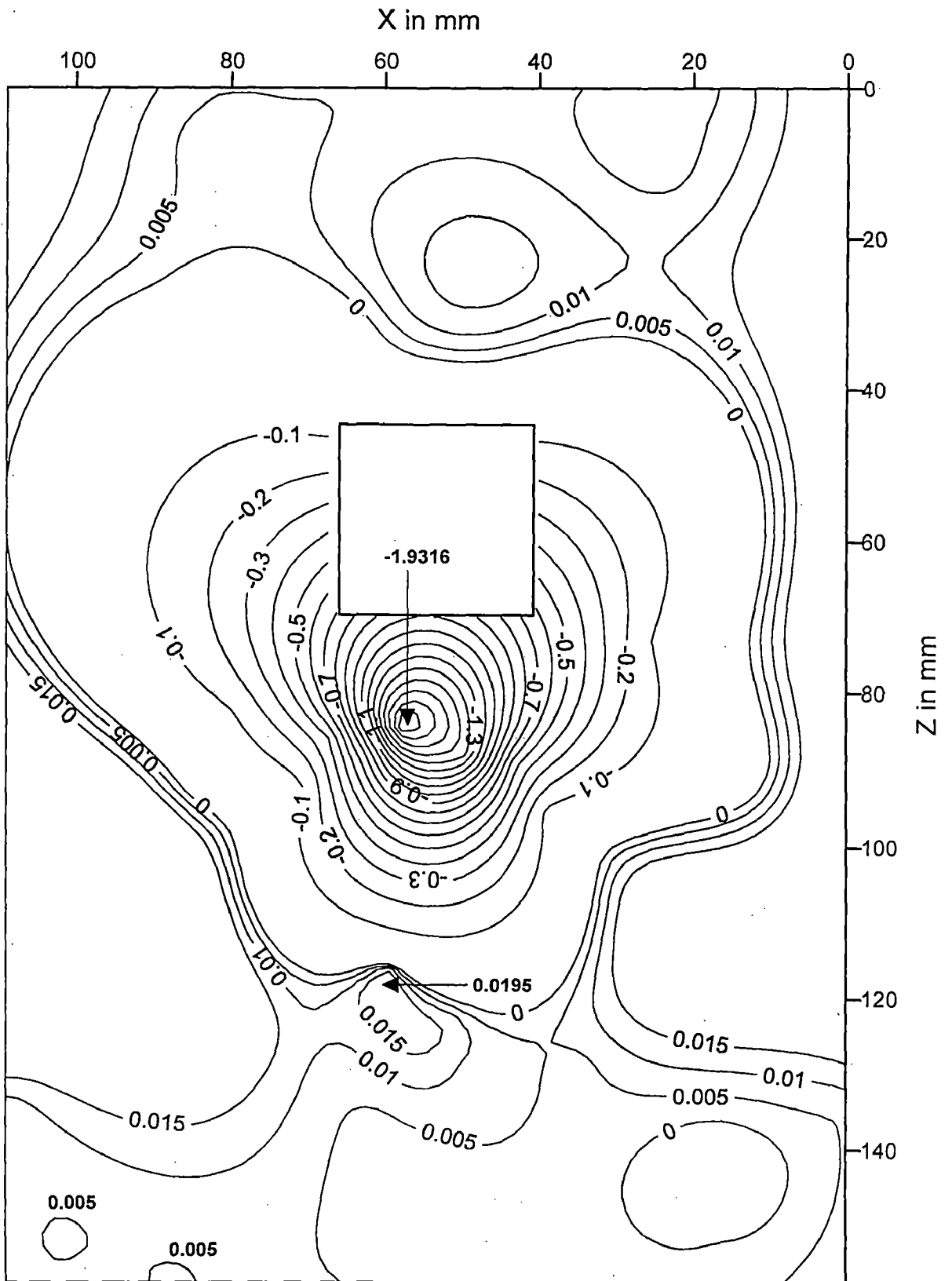


FIG. 5.45: STRESS CONTOURS FOR S_Y (kg/sq.cm) AT STRIP 11 ($Y=55.88 \text{ mm}$) UNDER CONCENTRATED LOAD BETWEEN SLICE 8 & 9.

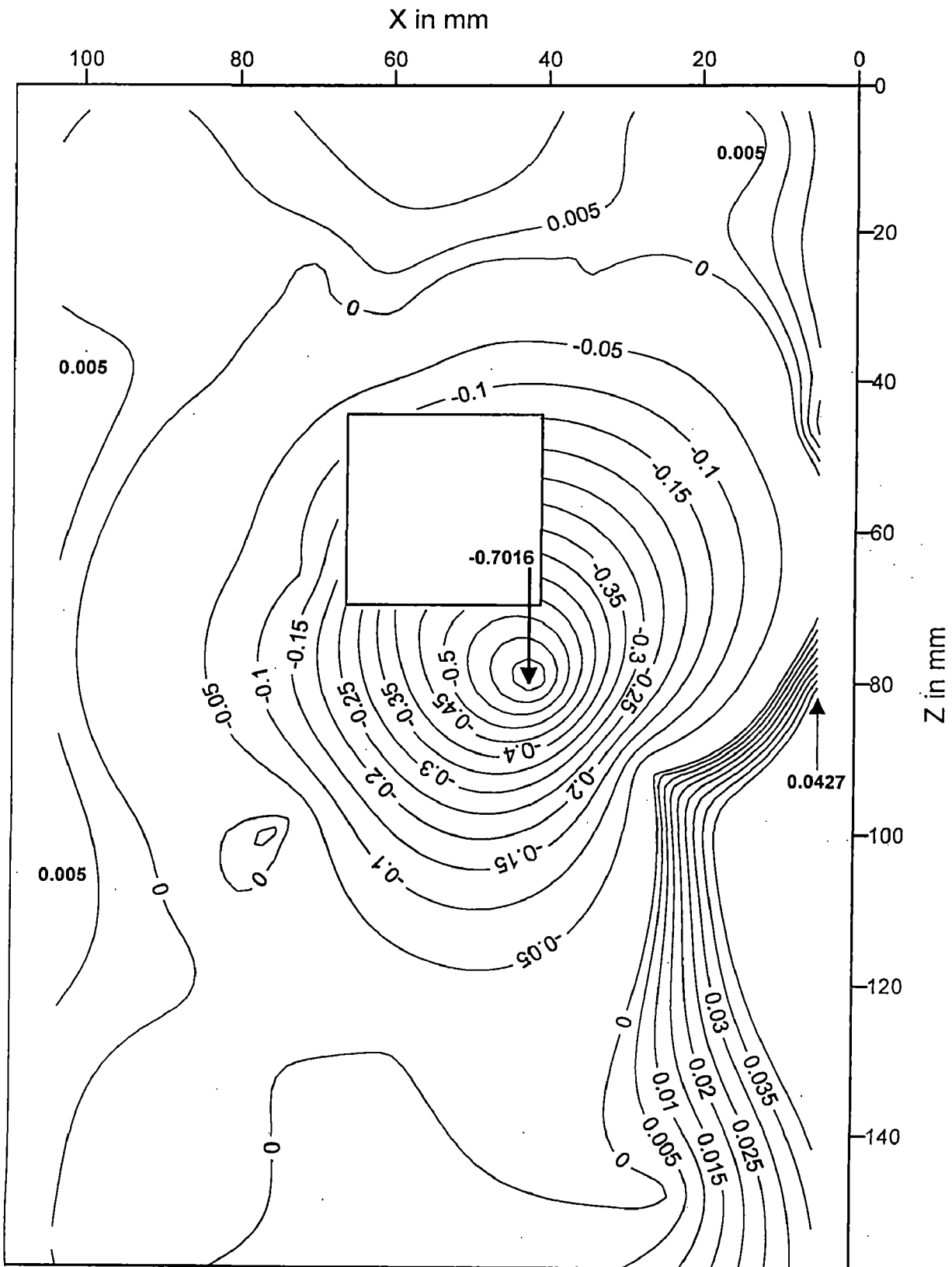


FIG. 5.46: STRESS CONTOURS FOR S_Y (kg/sq.cm) AT STRIP 12 ($Y=60.96 \text{ mm}$) UNDER CONCENTRATED LOAD BETWEEN SLICE 8 & 9.

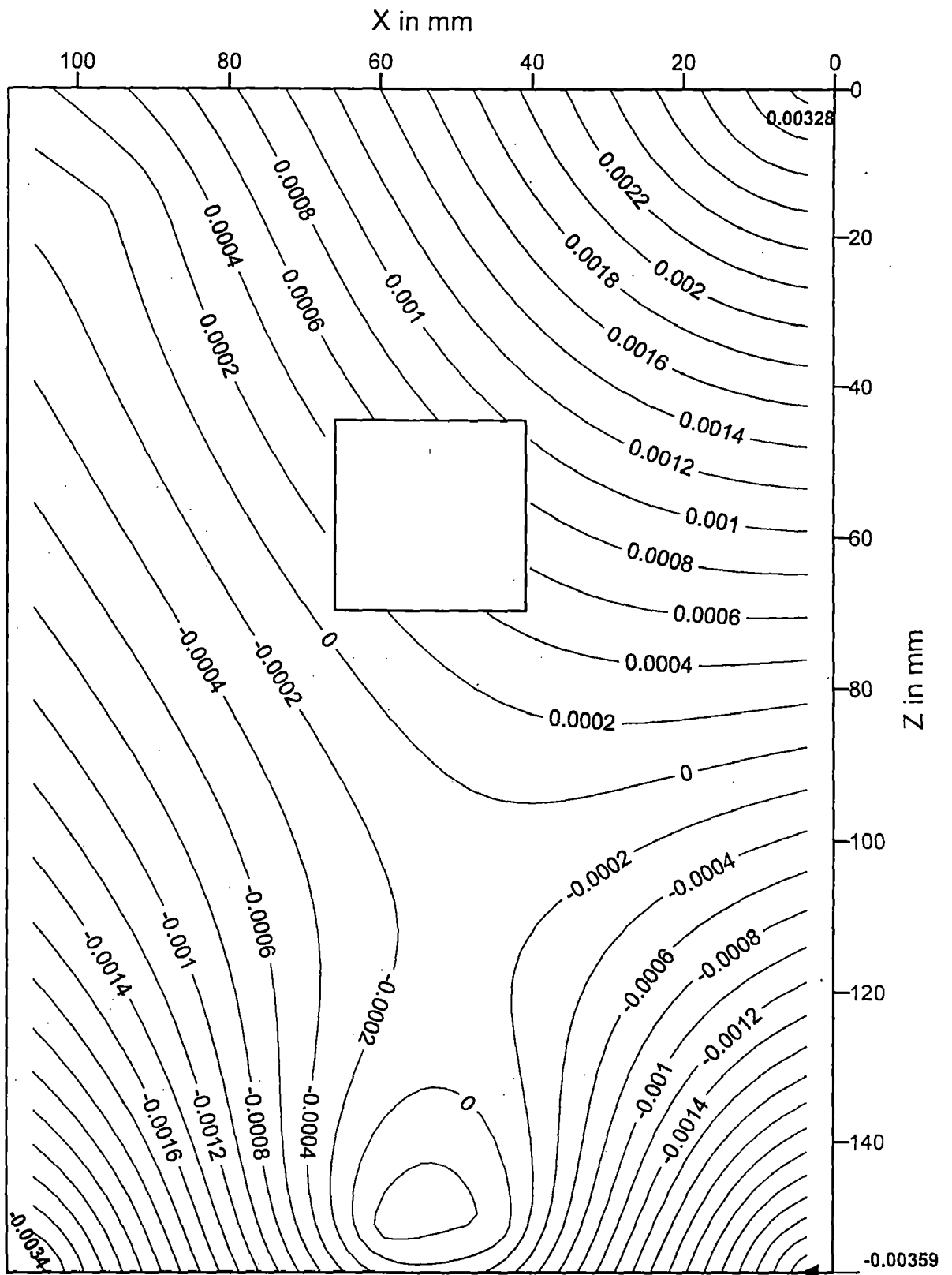


FIG. 5.47: STRESS CONTOURS FOR S_Y (kg/sq.cm) AT STRIP 13 ($Y=66.04$ mm) UNDER CONCENTRATED LOAD BETWEEN SLICE 8 & 9.

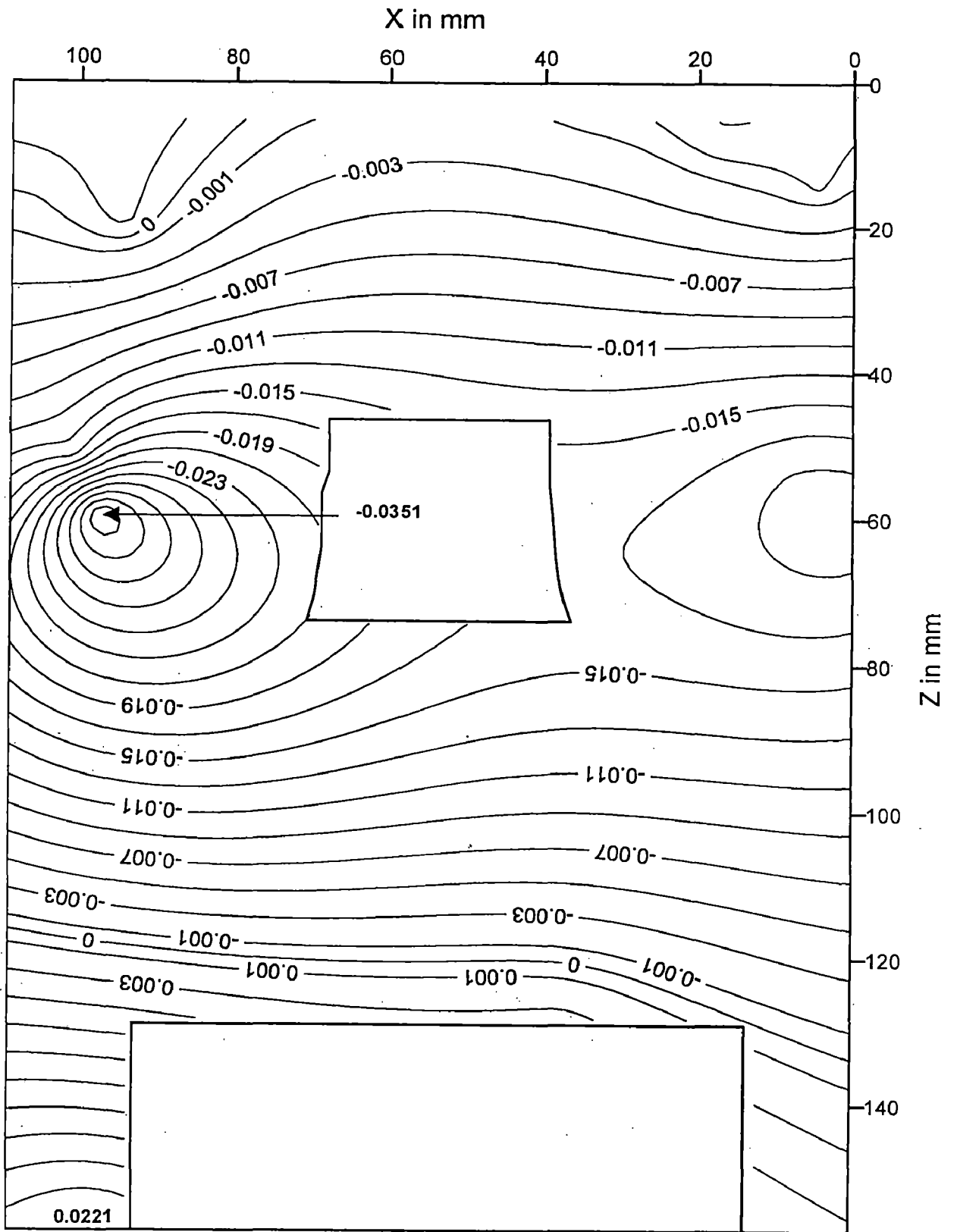


FIG. 5.48: STRESS CONTOURS FOR S_Y (kg/sq.cm) AT STRIP 7 ($Y=35.56$ mm) UNDER CONCENTRATED LOAD BETWEEN SLICE 9 & 10.

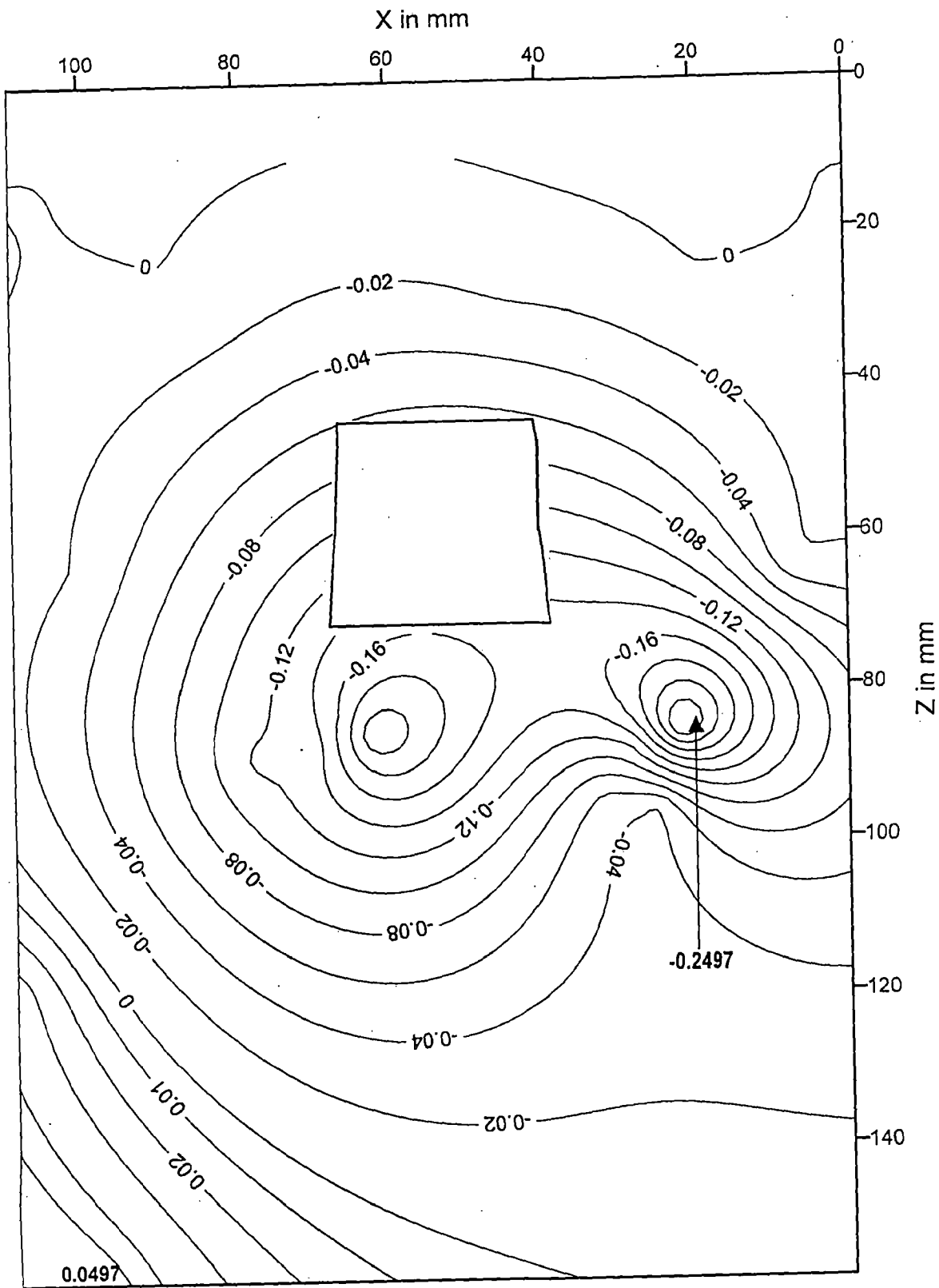


FIG. 5.49: STRESS CONTOURS FOR S_Y (kg/sq.cm) AT STRIP 8 ($Y=40.64$ mm) UNDER CONCENTRATED LOAD BETWEEN SLICE 9 & 10.

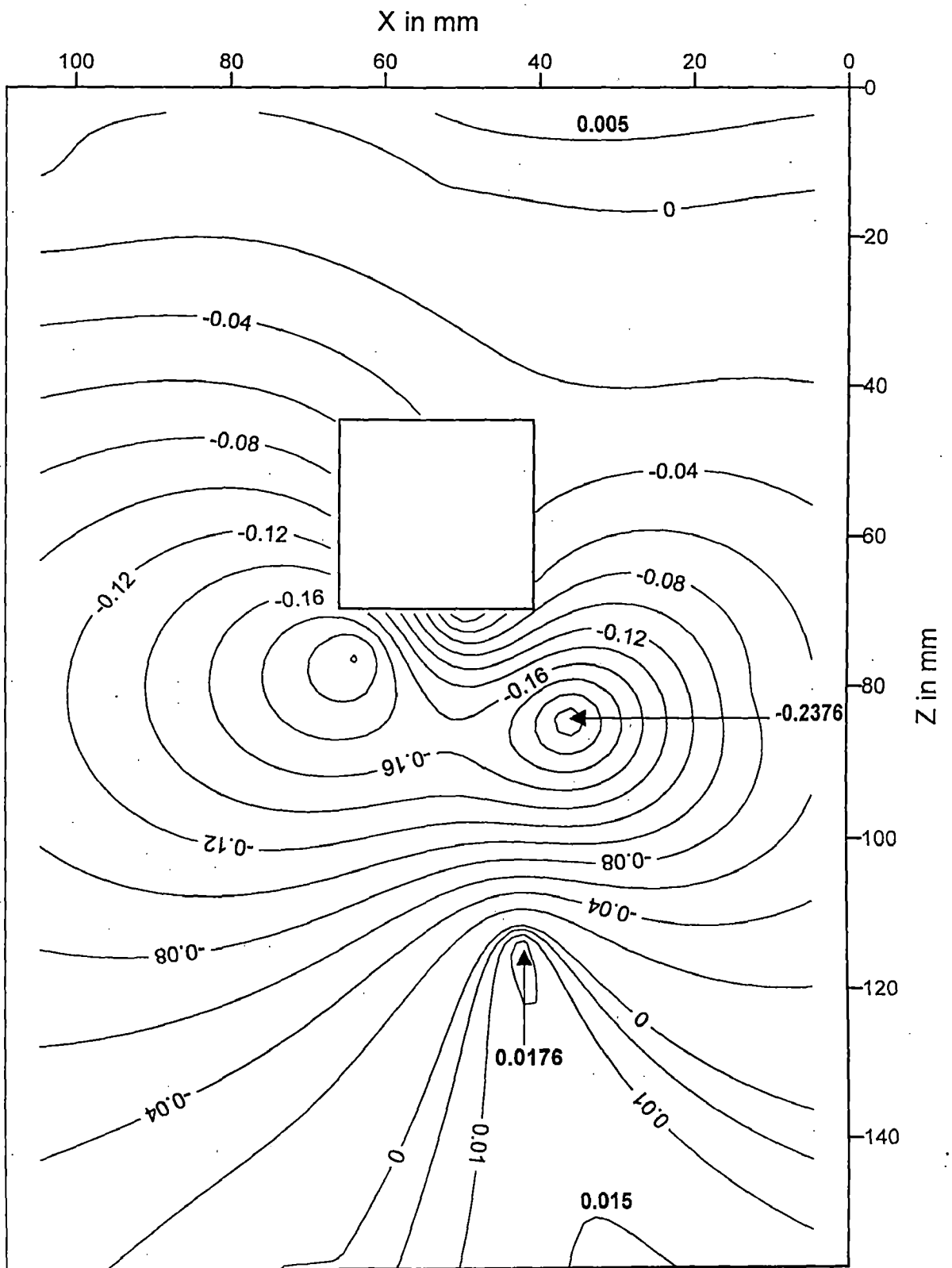


FIG. 5.50: STRESS CONTOURS FOR S_Y (kg/sq.cm) AT STRIP 9 ($Y=45.72$ mm) UNDER CONCENTRATED LOAD BETWEEN SLICE 9 & 10.

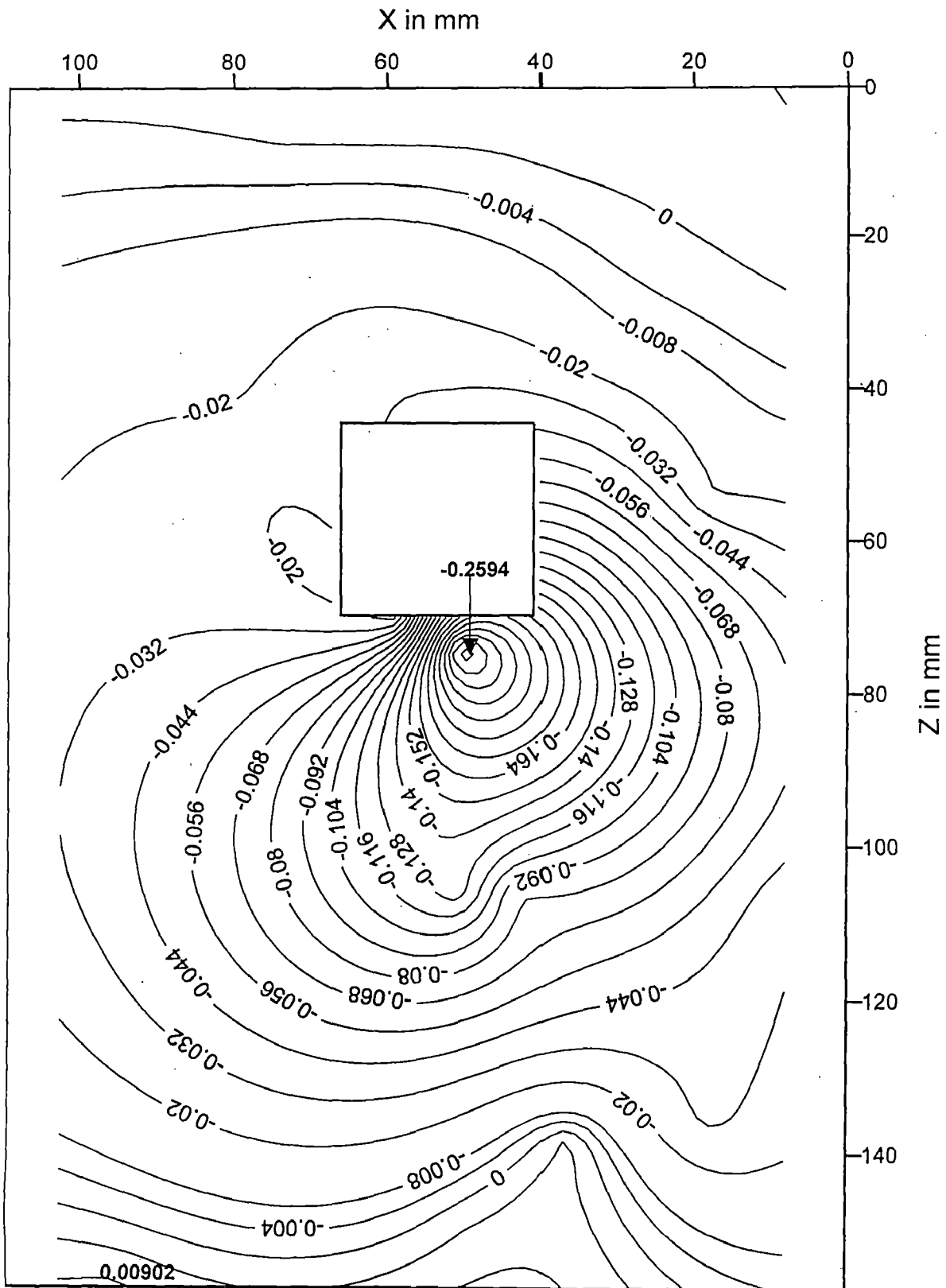


FIG. 5.51: STRESS CONTOURS FOR S_Y (kg/sq.cm) AT STRIP 10 ($Y=50.80$ mm) UNDER CONCENTRATED LOAD BETWEEN SLICE 9 & 10.

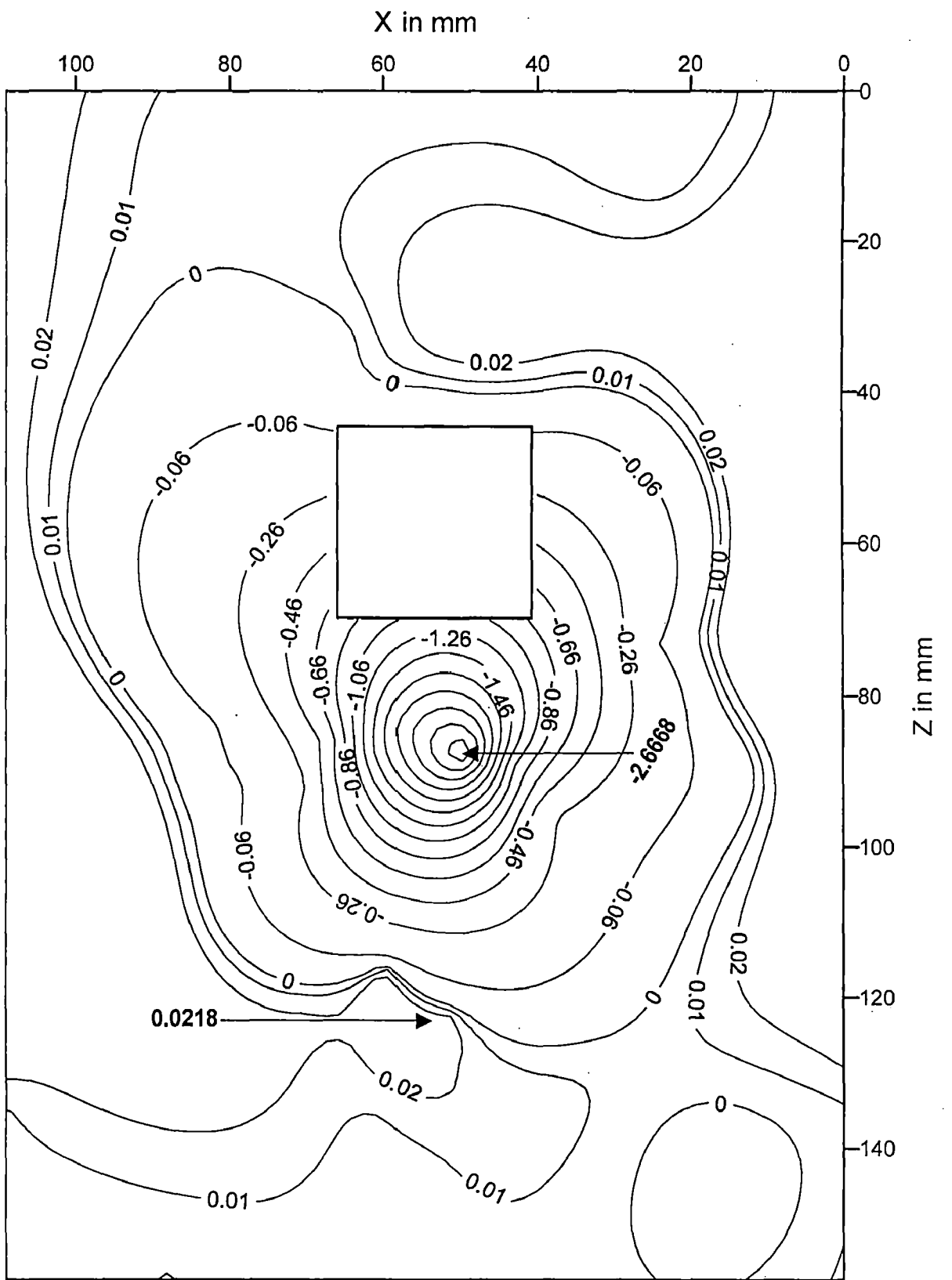


FIG. 5.52: STRESS CONTOURS FOR S_Y (kg/sq.cm) AT STRIP 11 (Y=55.88 mm) UNDER CONCENTRATED LOAD BETWEEN SLICE 9 & 10.

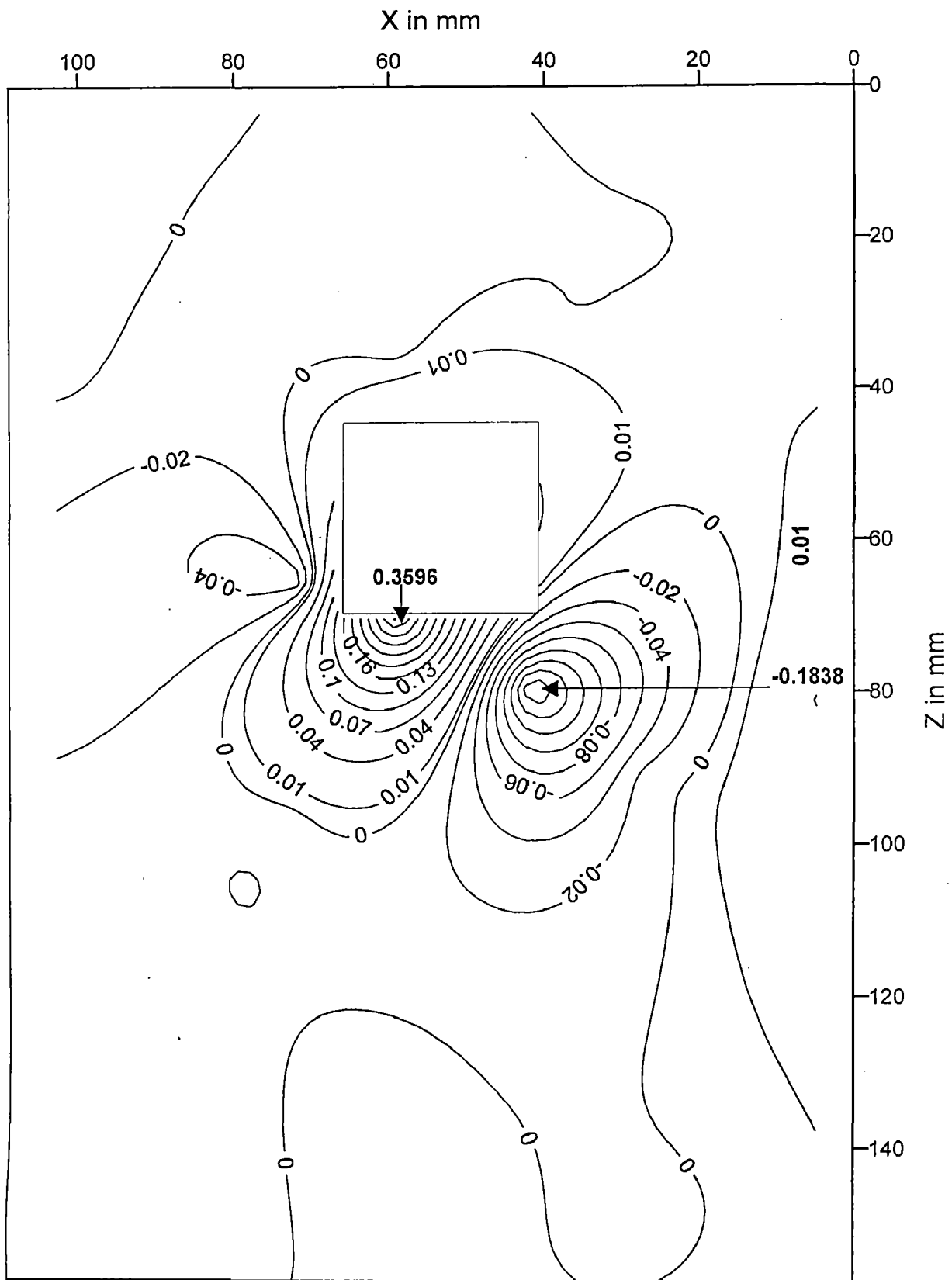


FIG. 5.53: STRESS CONTOURS FOR S_Y (kg/sq.cm) AT STRIP 12 ($Y=60.96$ mm) UNDER CONCENTRATED LOAD BETWEEN SLICE 9 & 10.

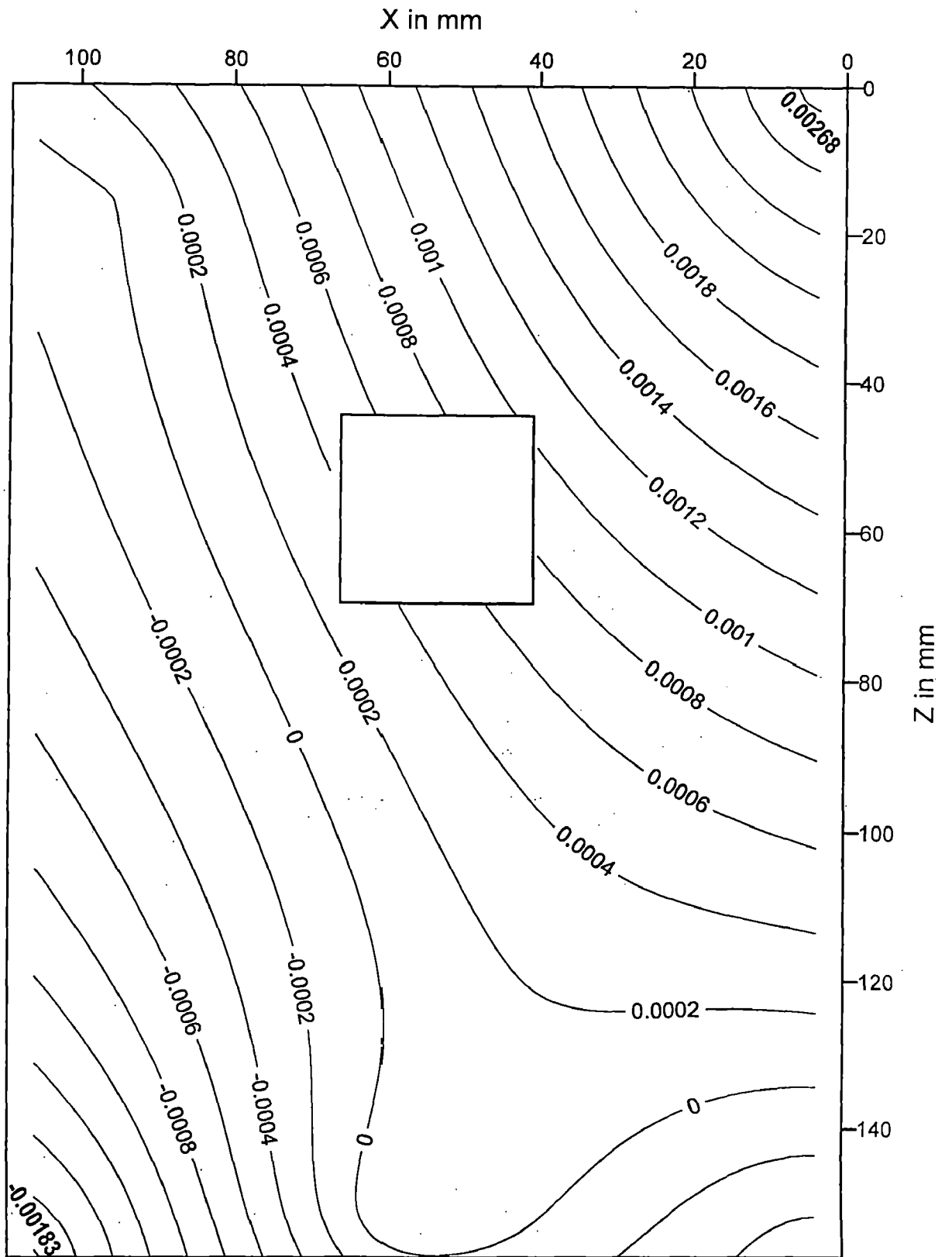


FIG. 5.54: STRESS CONTOURS FOR S_Y (kg/sq.cm) AT STRIP 13 ($Y=66.04$ mm) UNDER CONCENTRATED LOAD BETWEEN SLICE 9 & 10.

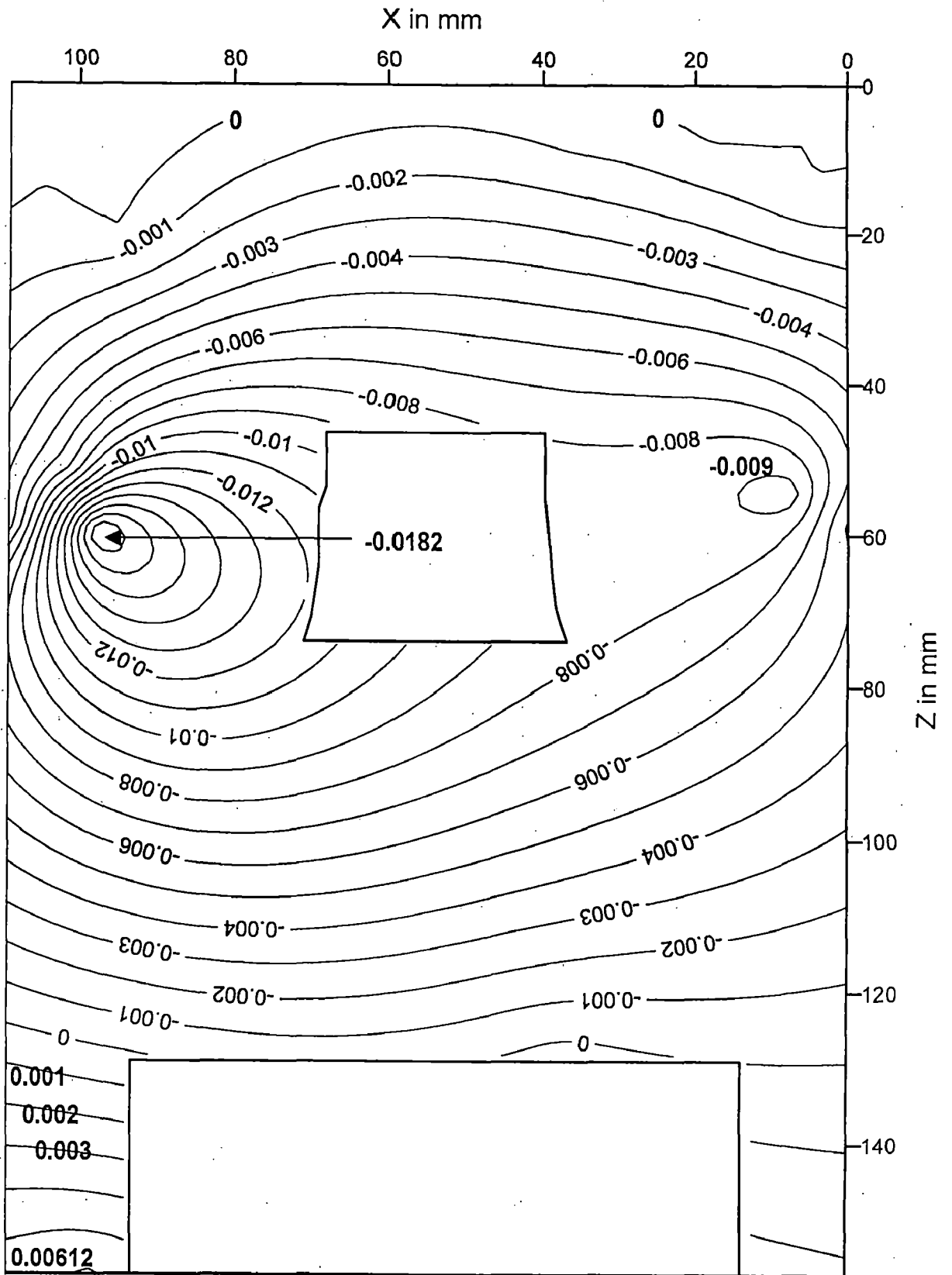


FIG. 5.55: STRESS CONTOURS FOR S_Y (kg/sq.cm) AT STRIP 7 ($Y=35.56$ mm) UNDER UDL ABOVE ELBOW CONCRETE.

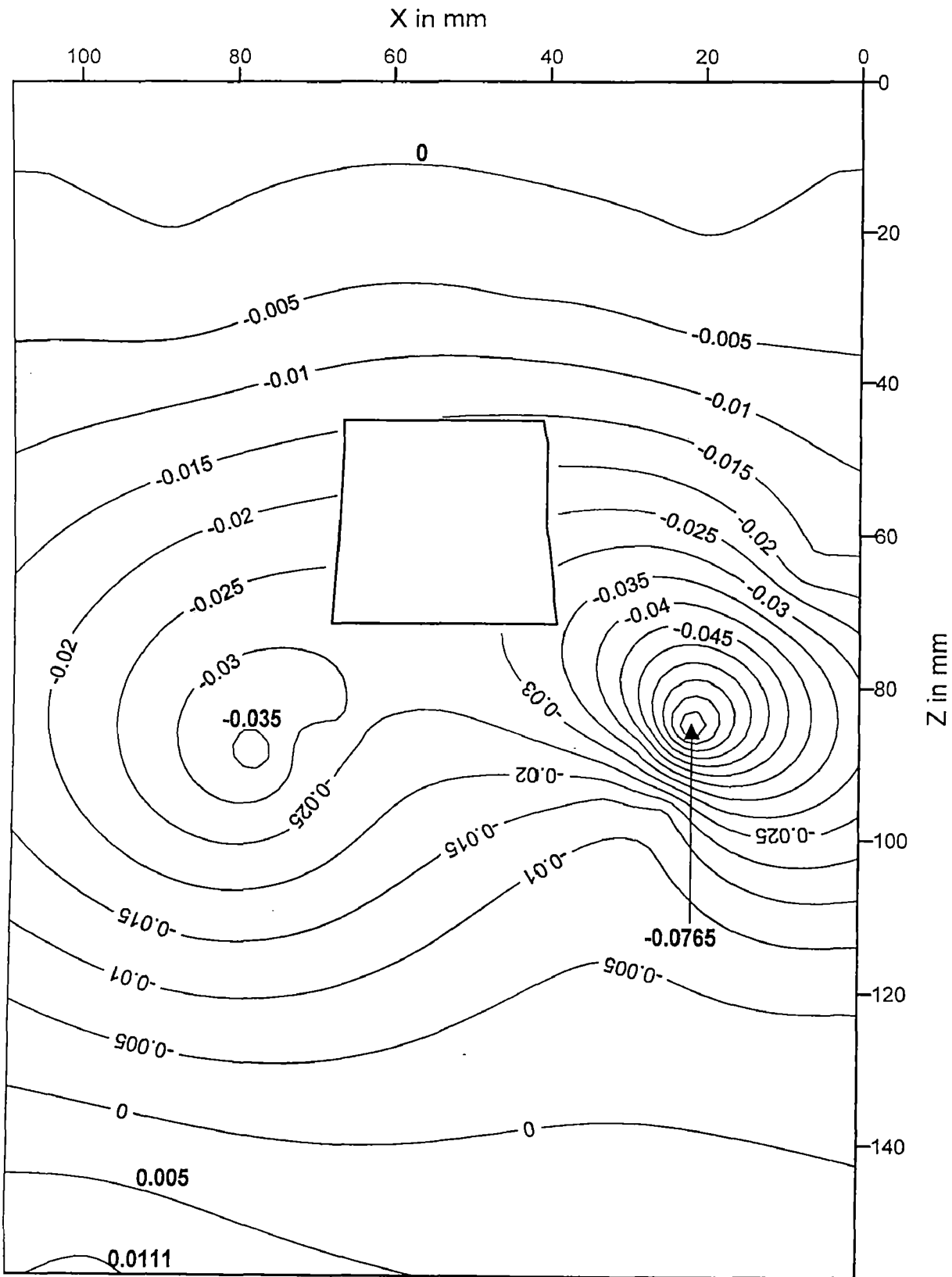


FIG. 5.56: STRESS CONTOURS FOR S_Y (kg/sq.cm) AT STRIP 8 ($Y=40.64$ mm) UNDER UDL ABOVE ELBOW CONCRETE.

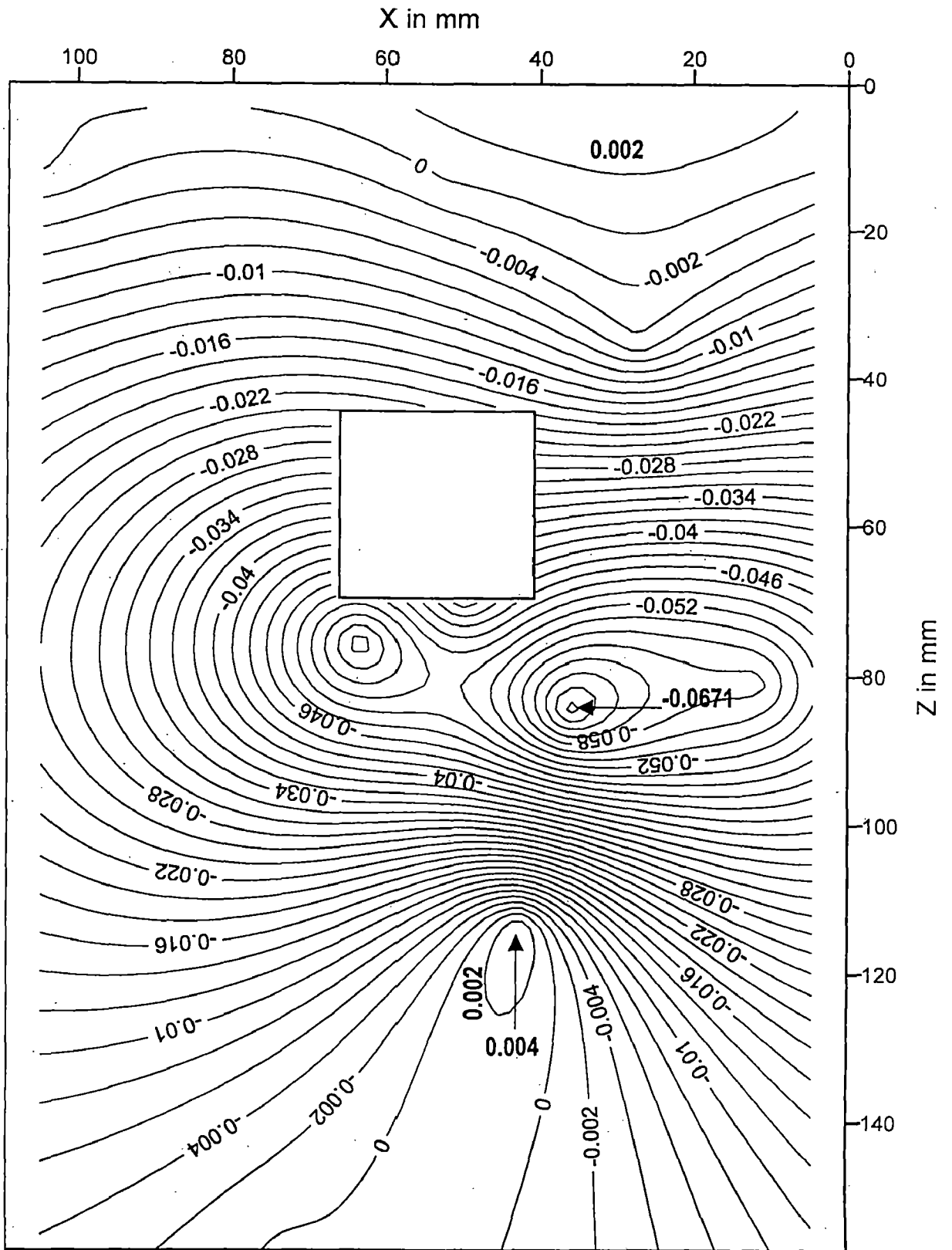


FIG. 5.57: STRESS CONTOURS FOR S_Y (kg/sq.cm) AT STRIP 9 ($Y=45.72$ mm) UNDER UDL ABOVE ELBOW CONCRETE.

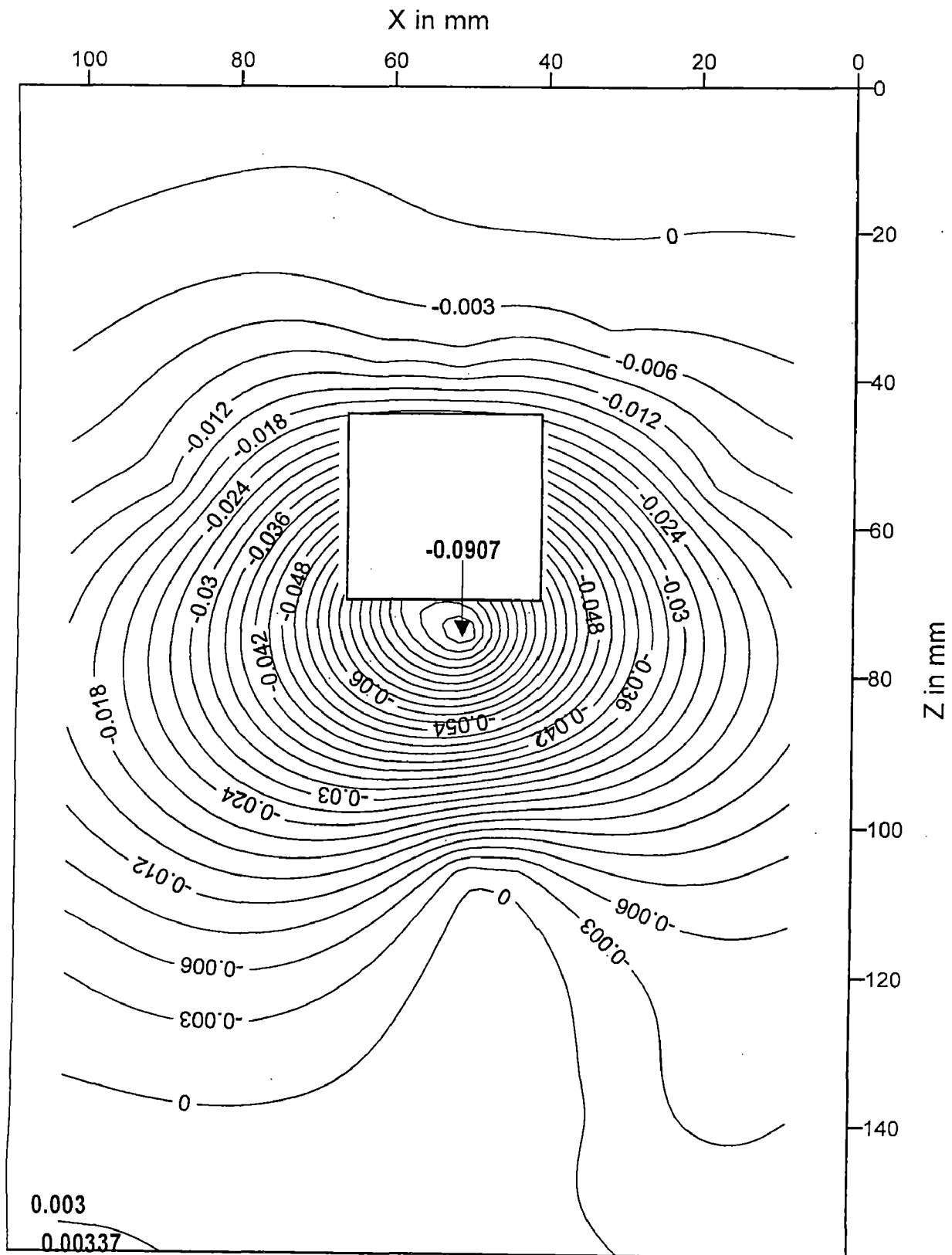


FIG. 5.58: STRESS CONTOURS FOR S_Y (kg/sq.cm.) AT STRIP 10 ($Y=50.80$ mm) UNDER UDL ABOVE ELBOW CONCRETE.

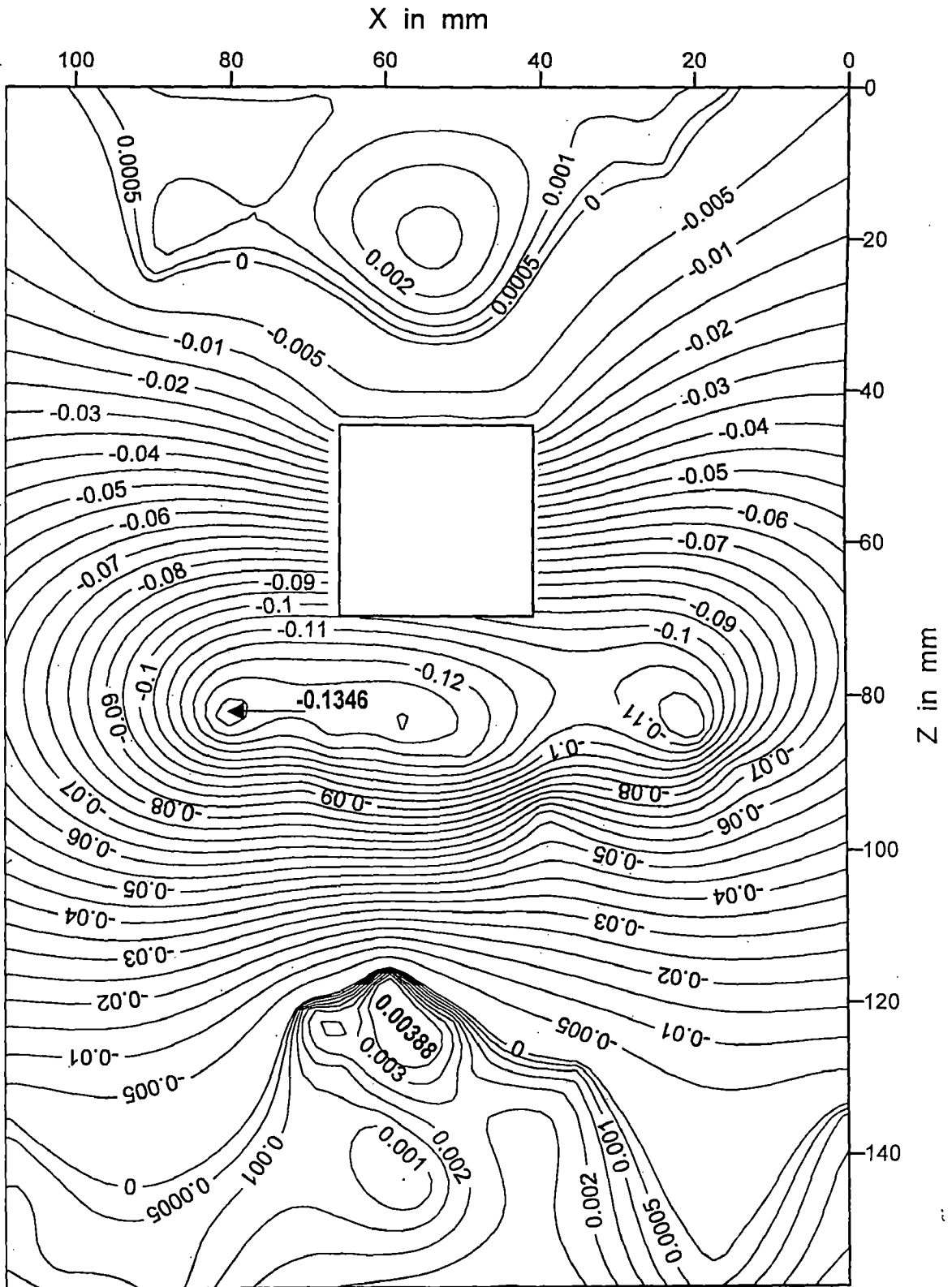


FIG. 5.59: STRESS CONTOURS FOR S_Y (kg/sq.cm AT STRIP 11 ($Y=55.88$ mm) UNDER UDL ABOVE ELBOW CONCRETE.

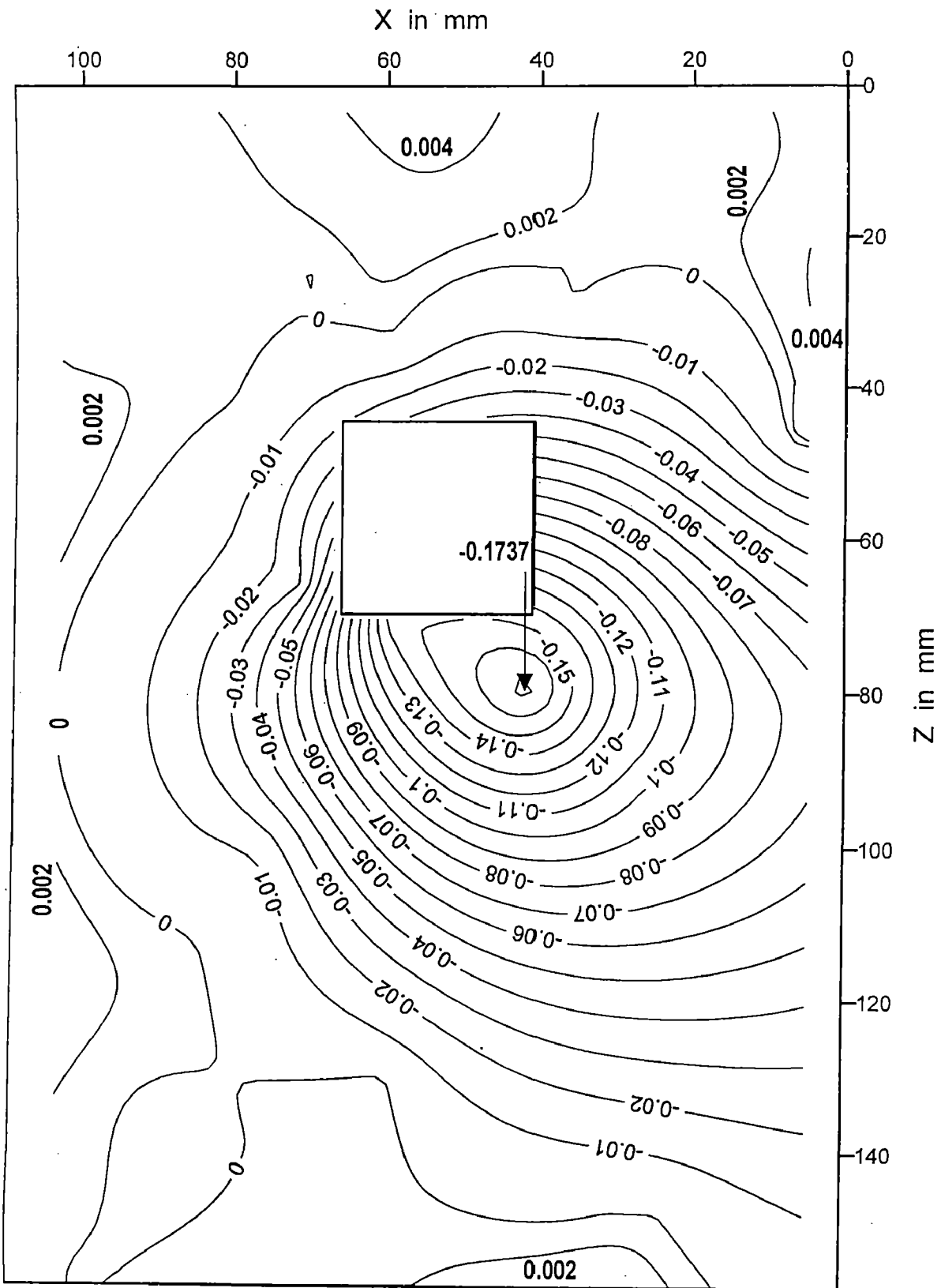


FIG. 5.60: STRESS CONTOURS FOR S_Y (kg/sq.cm) AT STRIP 12 ($Y=60.96$ mm) UNDER UDL ABOVE ELBOW CONCRETE.

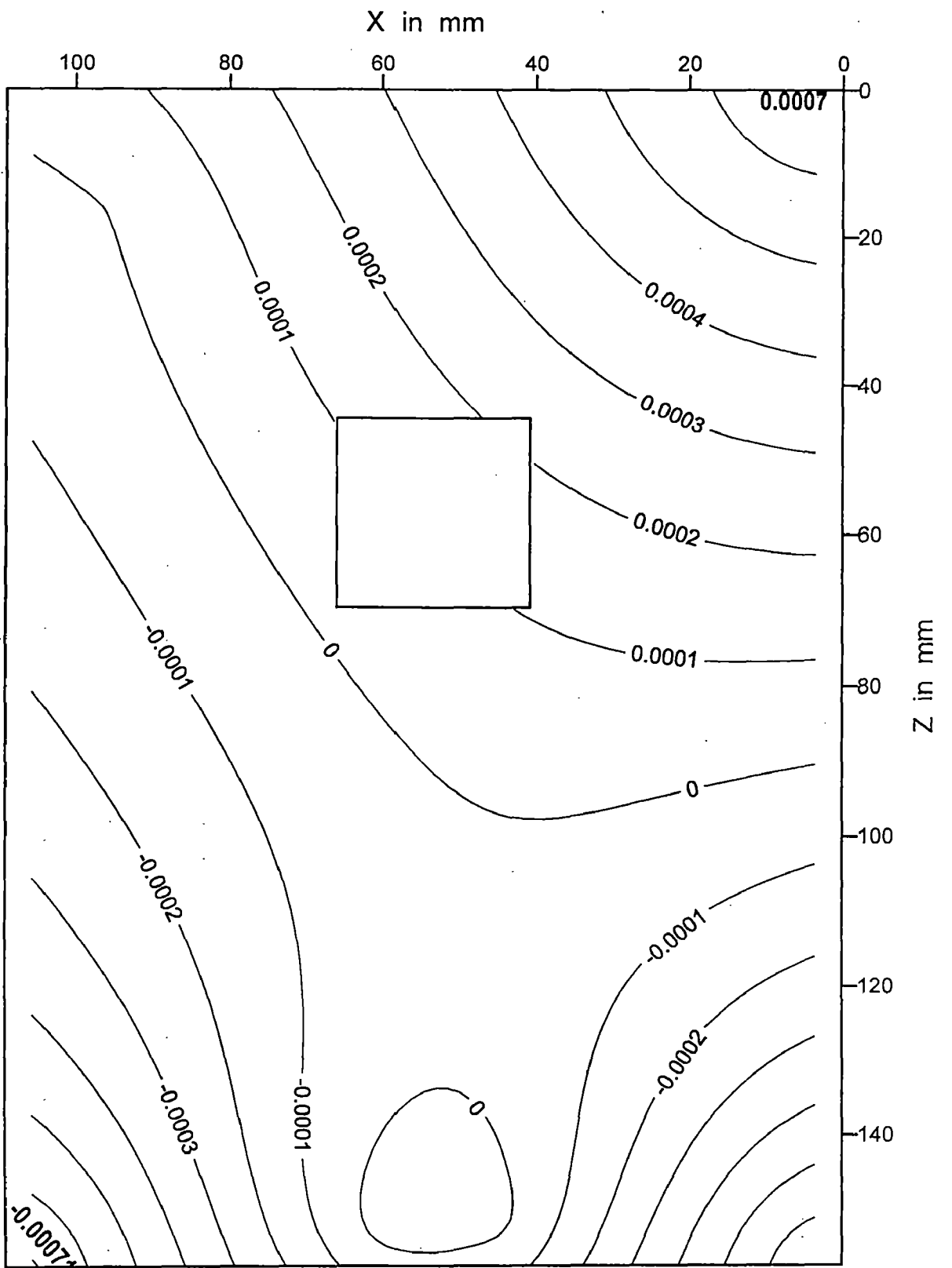


FIG. 5.61: STRESS CONTOURS FOR S_Y (kg/sq.cm) AT STRIP 13 ($Y=66.04$ mm) UNDER UDL ABOVE ELBOW CONCRETE.

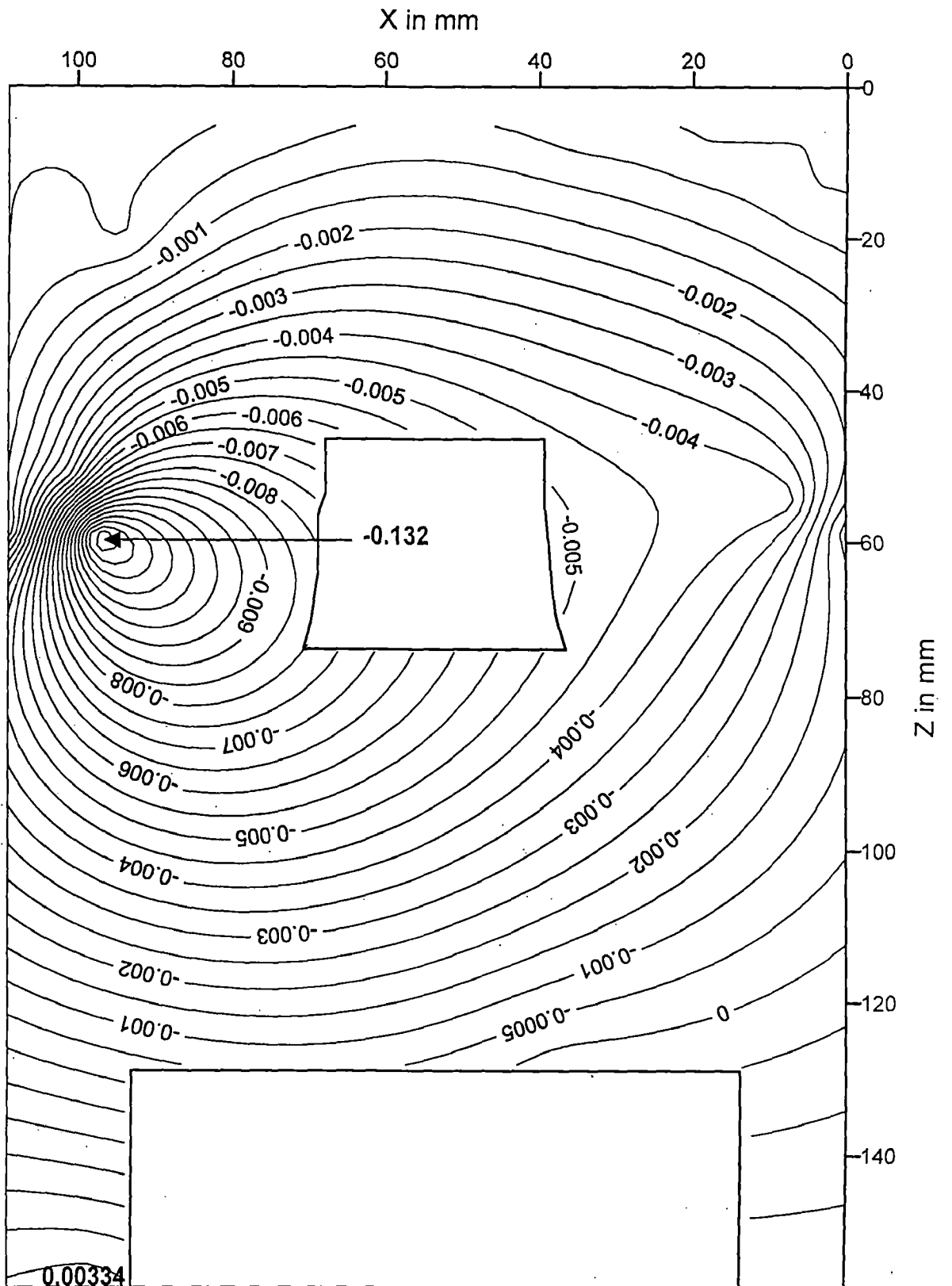


FIG. 5.62: STRESS CONTOURS FOR S_Y (kg/sq.cm) AT STRIP 7 (Y=35.56 mm) UNDER CONCENTRATED LOAD SIMULATING GANTRY COLUMN LOADS.

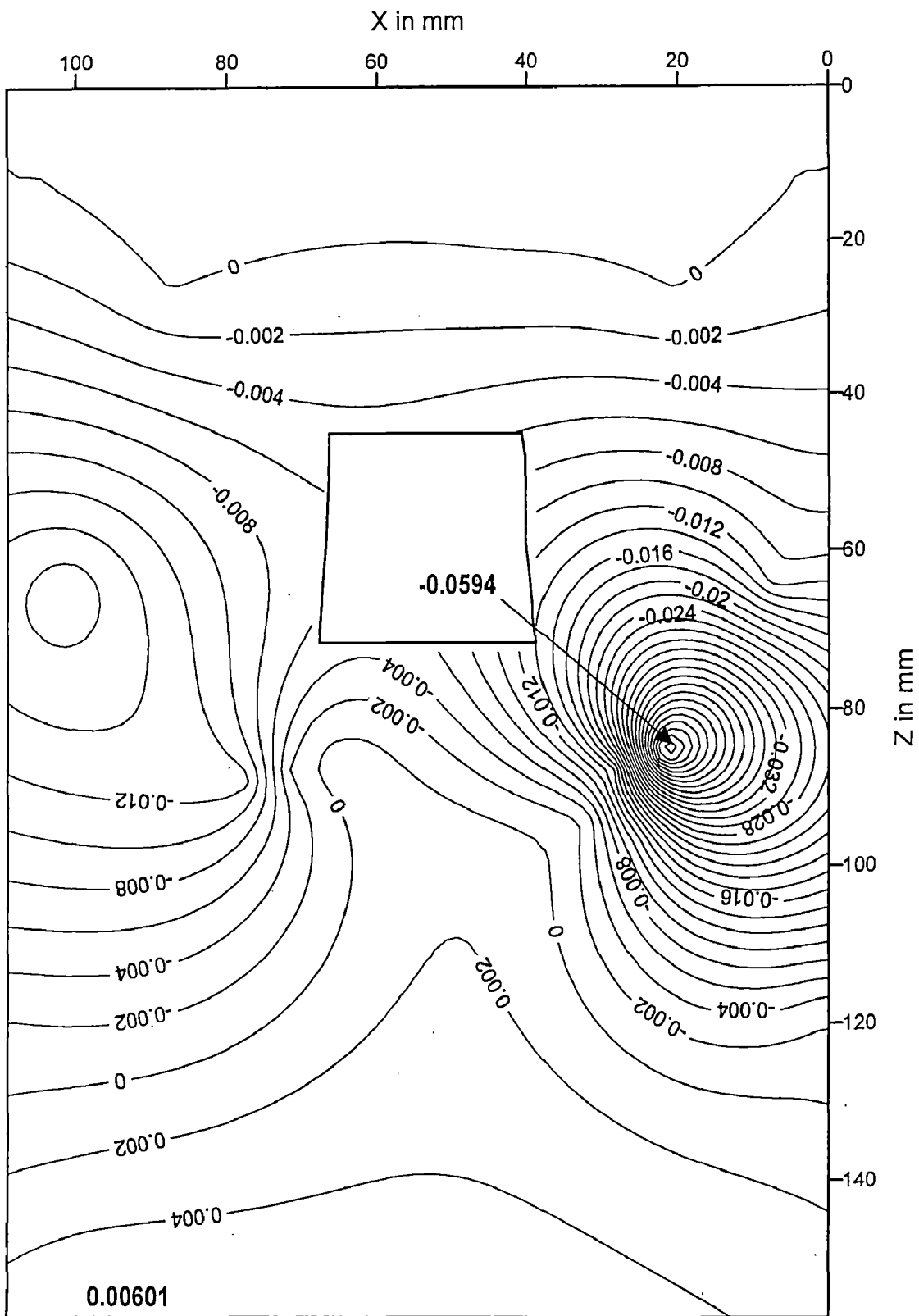


FIG. 5.63: STRESS CONTOURS FOR S_Y (kg/sq.cm) AT STRIP 8 ($Y=40.64$ mm) UNDER CONCENTRATED LOAD SIMULATING GANTRY COLUMN LOADS.

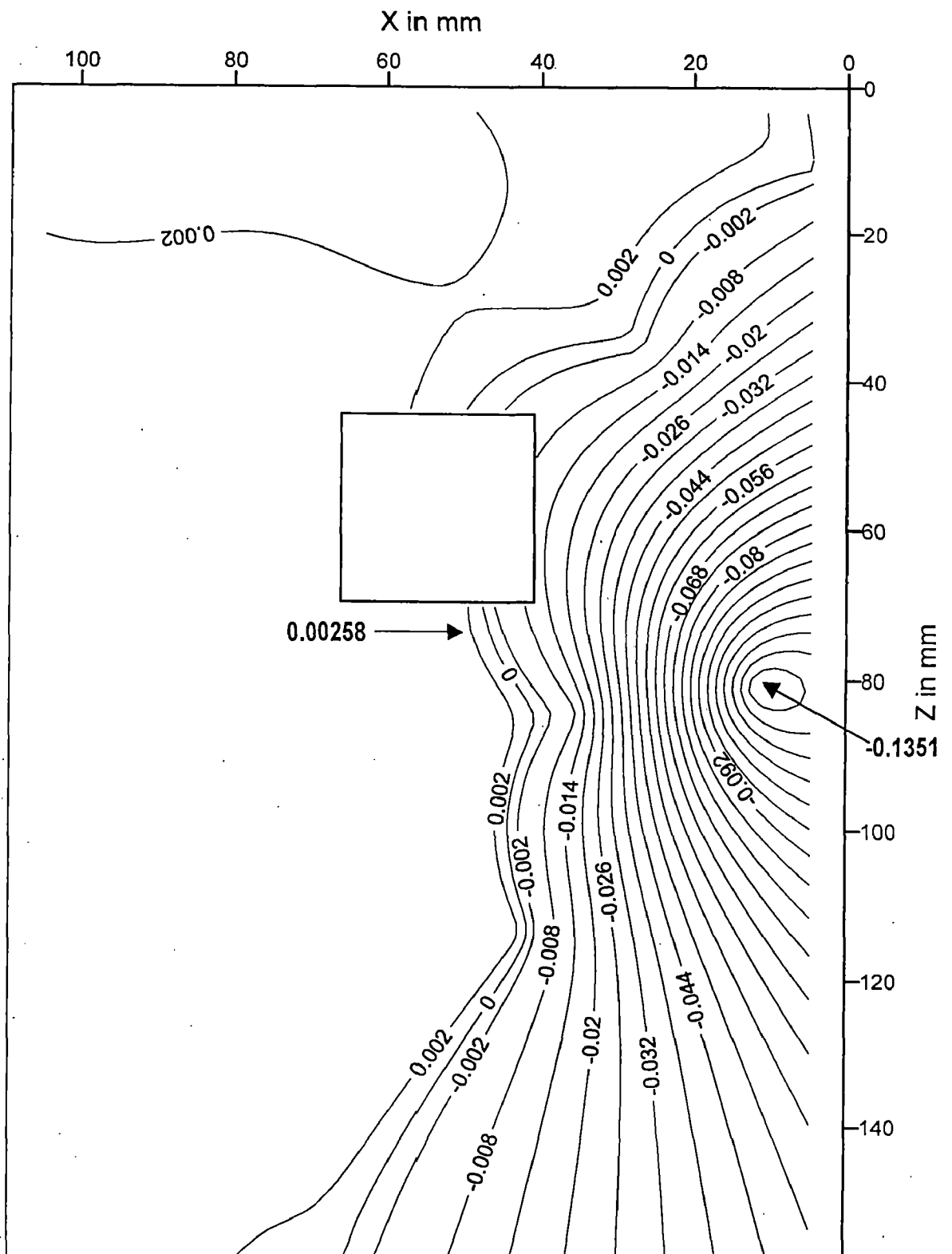


FIG. 5.64: STRESS CONTOURS FOR S_Y (kg/sq.cm) AT STRIP 9 ($Y=45.72$ mm) UNDER CONCENTRATED LOAD SIMULATING GANTRY COLUMN LOADS.

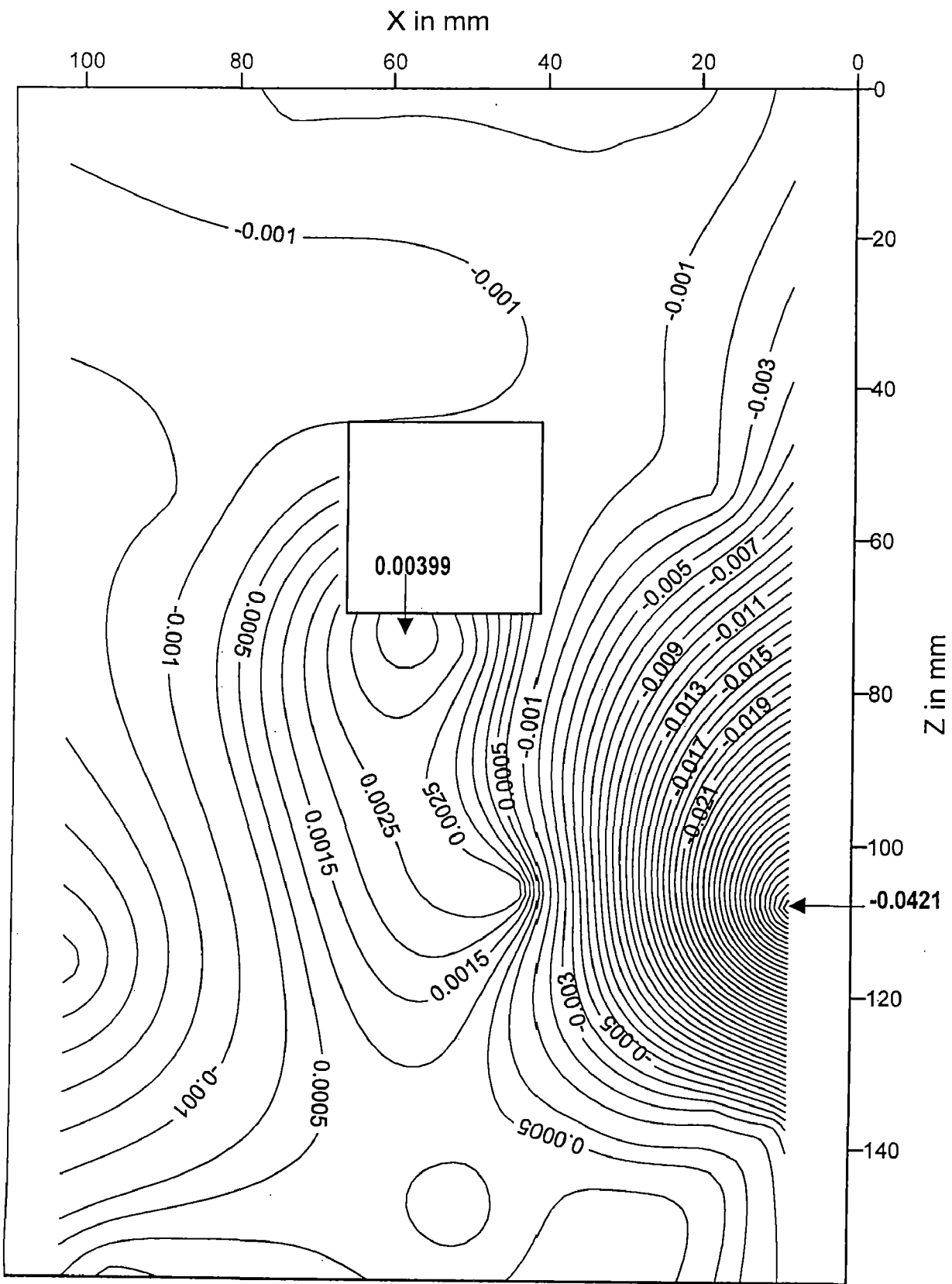


FIG. 5.65: STRESS CONTOURS FOR S_Y (kg/sq.cm) AT STRIP 10 ($Y=50.80$ mm) UNDER CONCENTRATED LOAD SIMULATING GANTRY COLUMN LOADS.

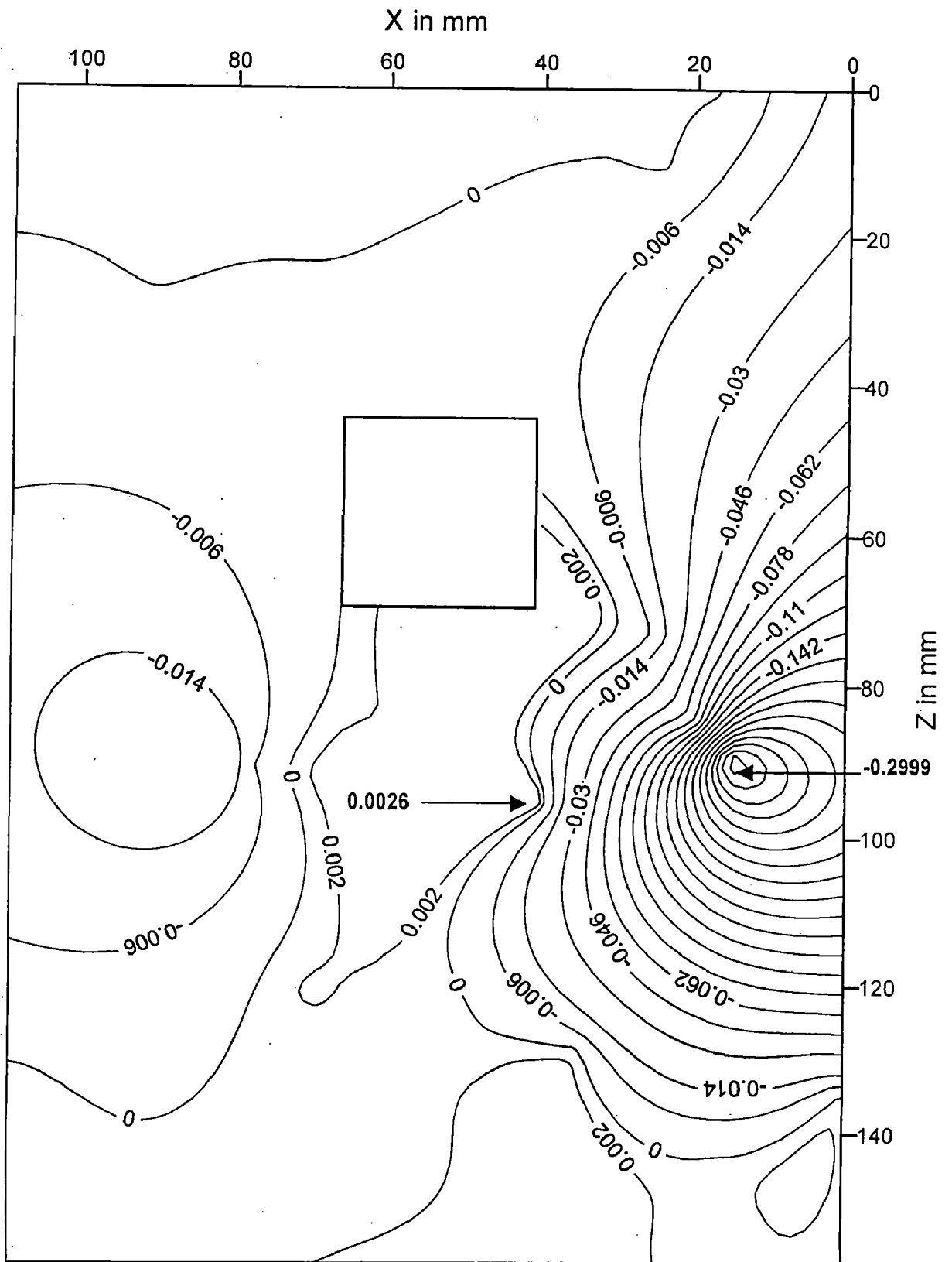


FIG. 5.66: STRESS CONTOURS FOR S_Y (kg/sq.cm) AT STRIP 11 ($Y=55.88$ mm) UNDER CONCENTRATED LOAD SIMULATING GANTRY COLUMN LOADS.

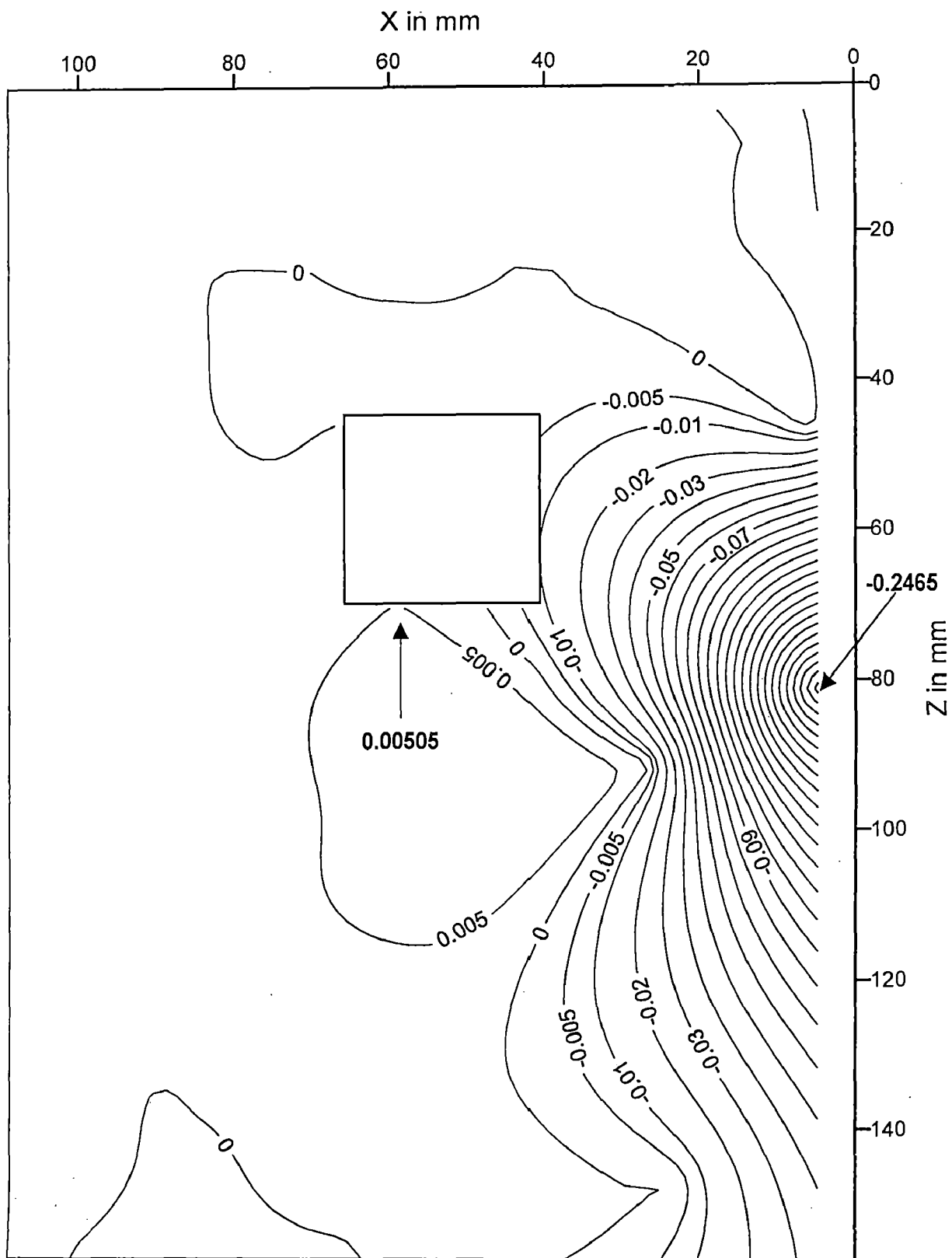


FIG. 5.67: STRESS CONTOURS FOR S_Y (kg/sq.cm) AT STRIP 12 ($Y=60.96$ mm) UNDER CONCENTRATED LOAD SIMULATING GANTRY COLUMN LOADS.

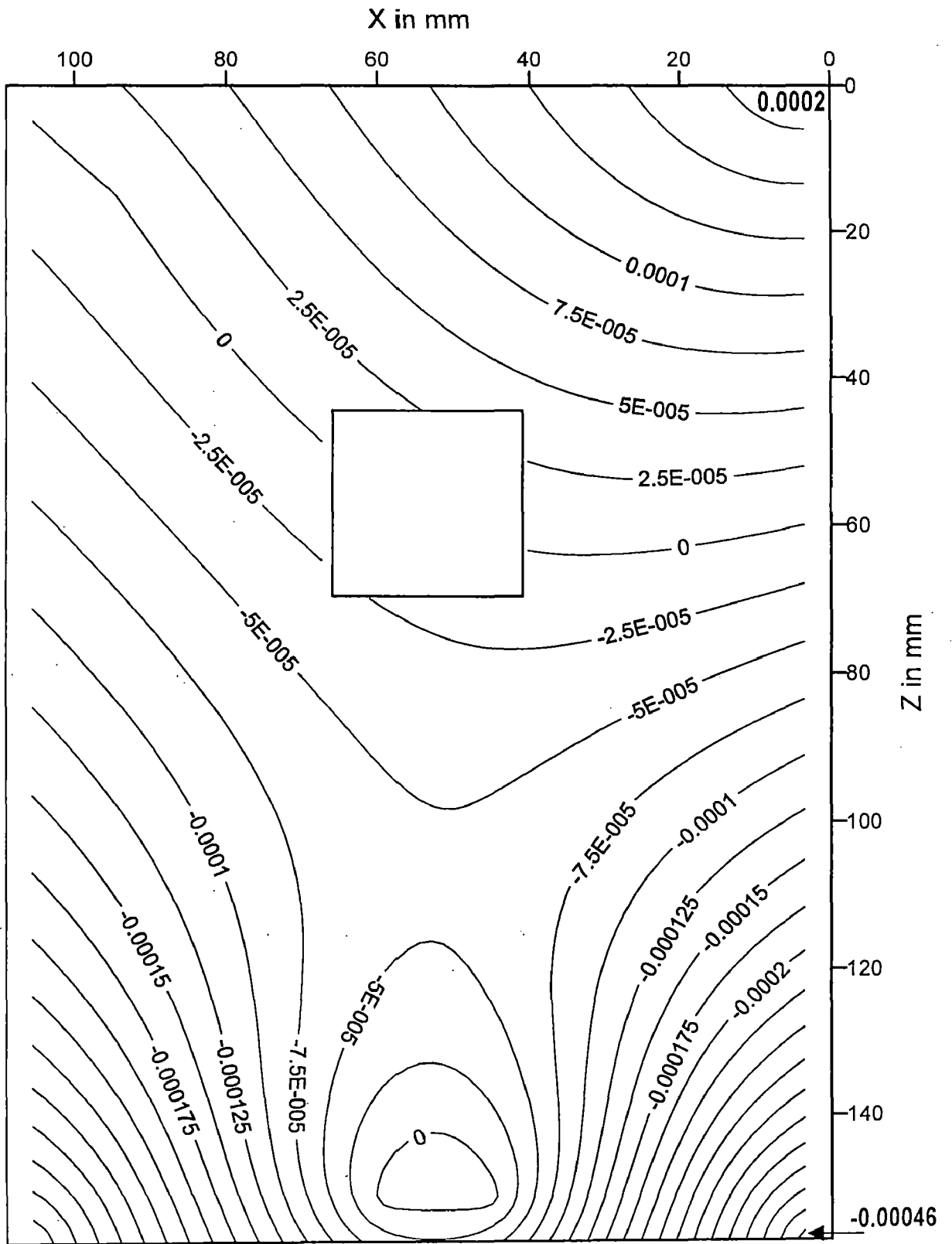
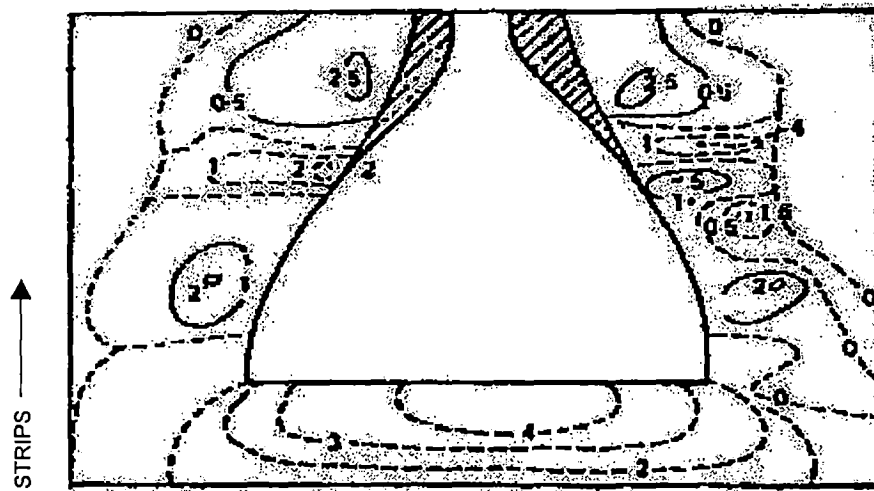
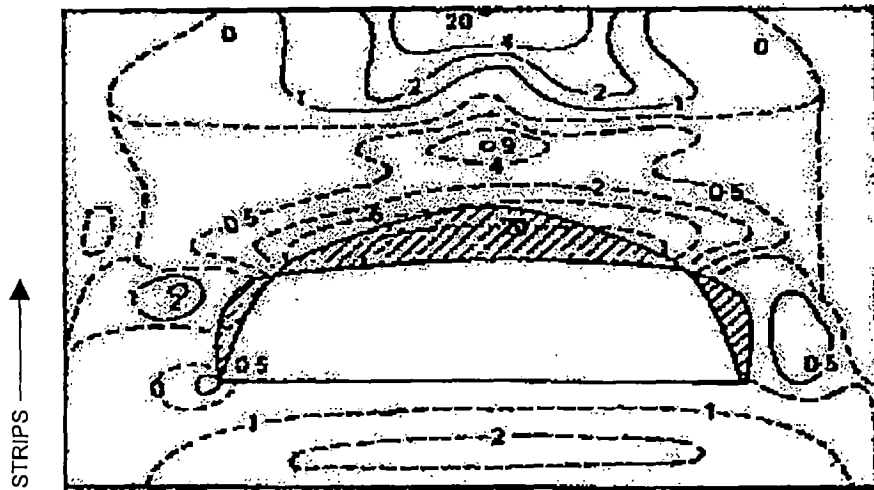


FIG. 5.68: STRESS CONTOURS FOR SY(kg/sq.cm) AT STRIP 13 (Y=66.04 mm) UNDER CONCENTRATED LOAD SIMULATING GANTRY COLUMN LOADS.

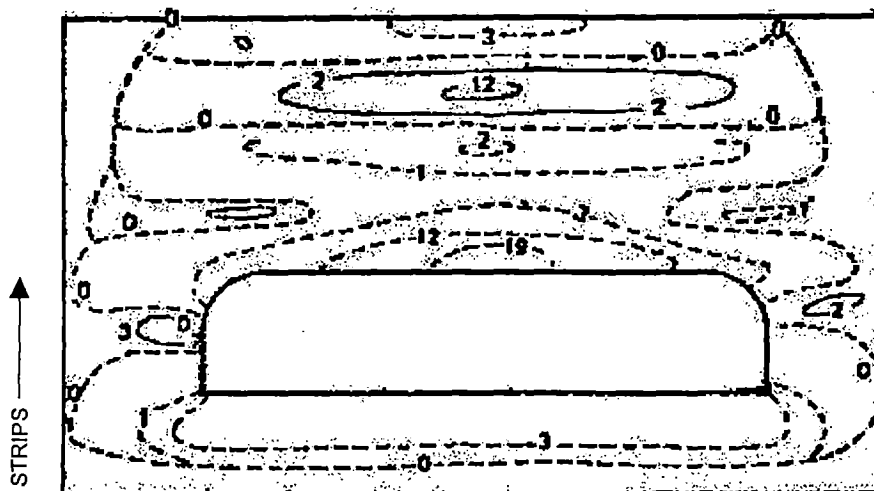
(b) By Photo-elastic Method



(a) SLICE 7

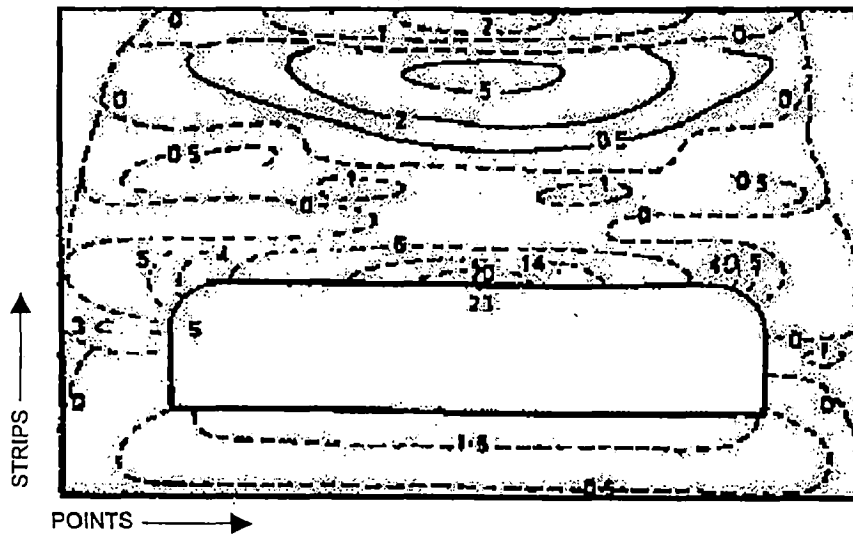


(b) SLICE 8

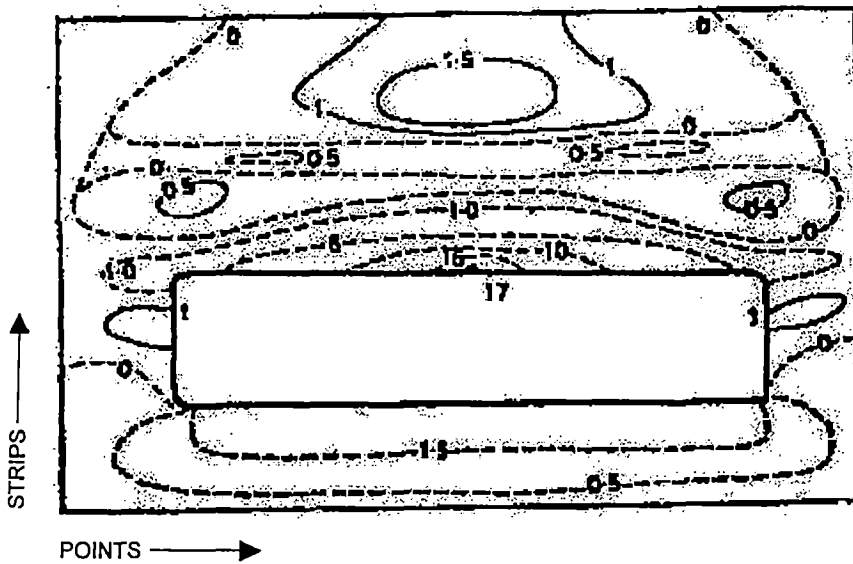


(c) SLICE 9

FIG. 5.69: STRESS CONTOURS PLOTTED FOR $SX^{(10)}$ (Contd.)



(d) SLICE 10

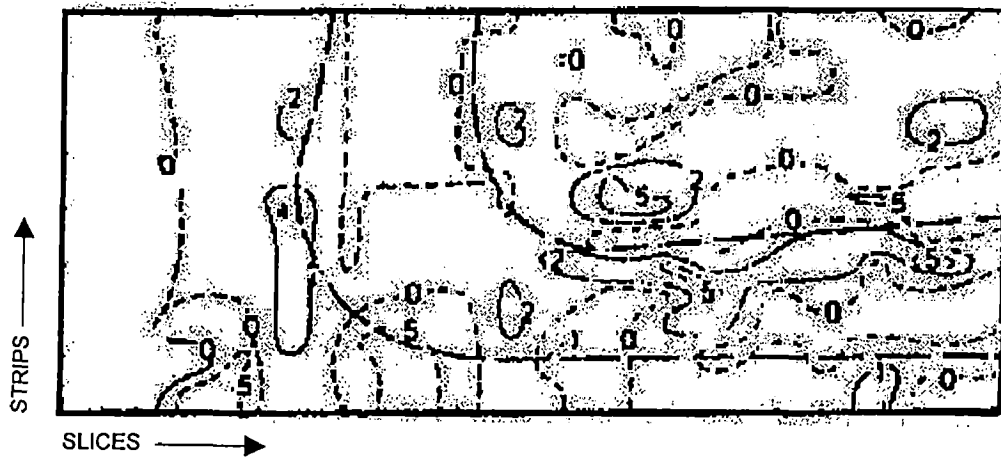


(e) SLICE 11

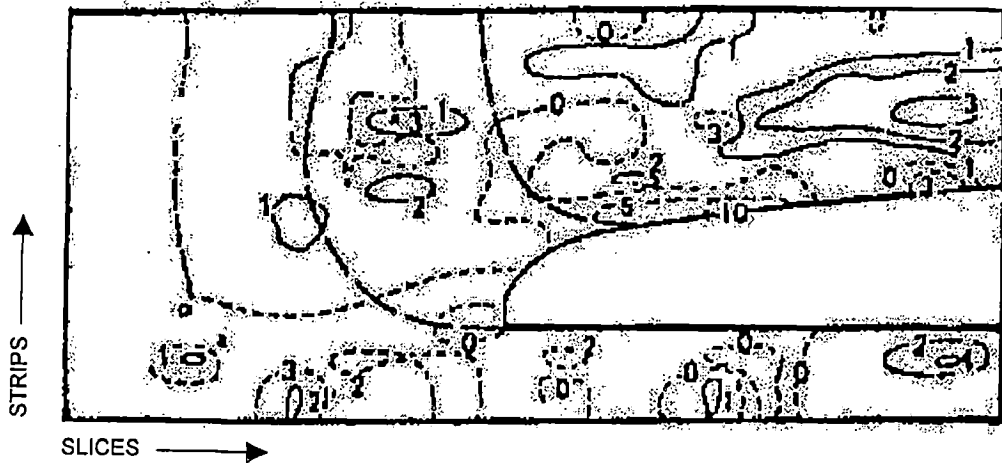
Notes

1. Solid line contour indicates compression and dotted line tension.
2. System of numbering Slices, Points and Strips is same as given in Slicing Plan (Fig. 4.1) & Transverse Section (Fig. 4.9).
3. S.C.F. contours are given on planes of stress denoted by corresponding Slice.

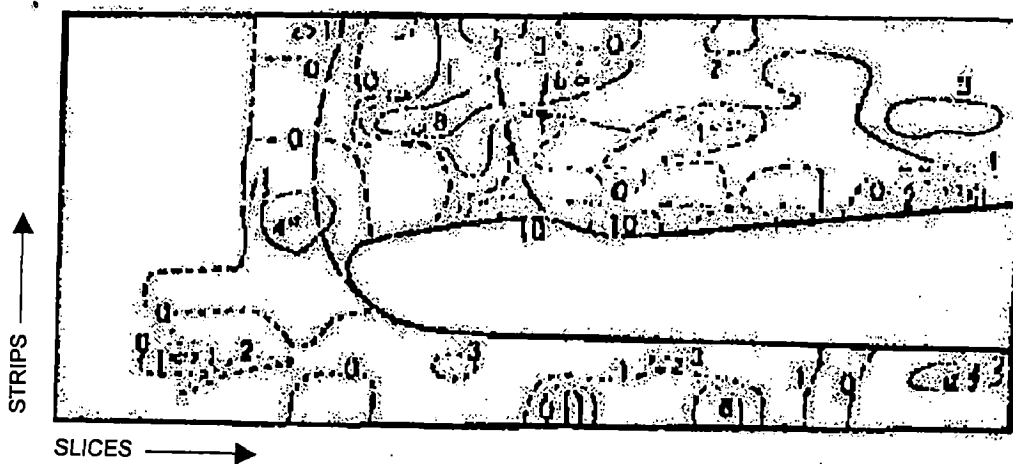
FIG. 5.69: STRESS CONTOURS PLOTTED FOR $SX^{(10)}$



(a) POINT 3

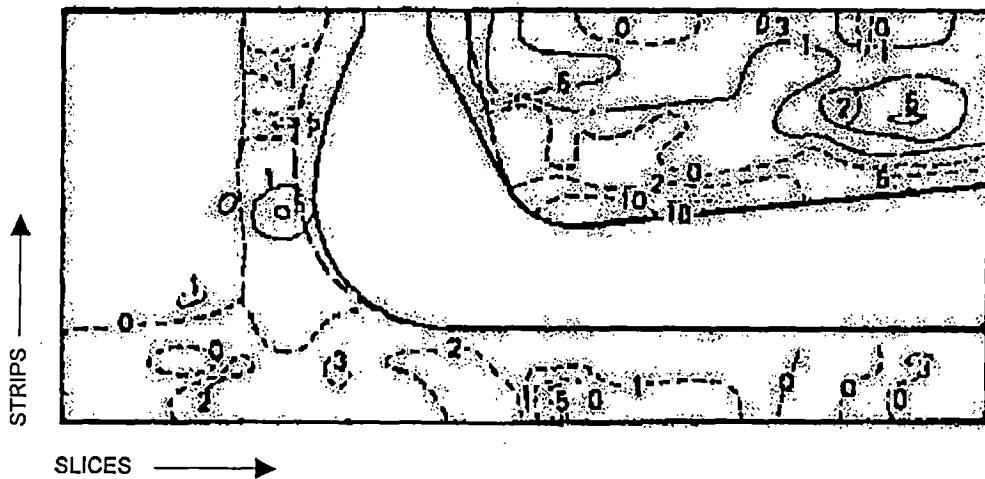


(b) POINT 6

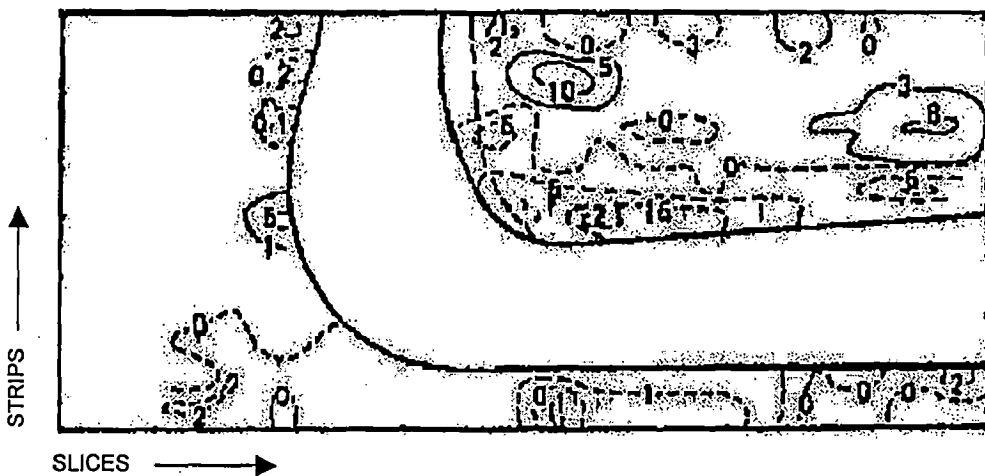


(c) POINT 8

FIG. 5.70: STRESS CONTOURS PLOTTED FOR $SZ^{(10)}$ (Contd.)



(d) POINT 10

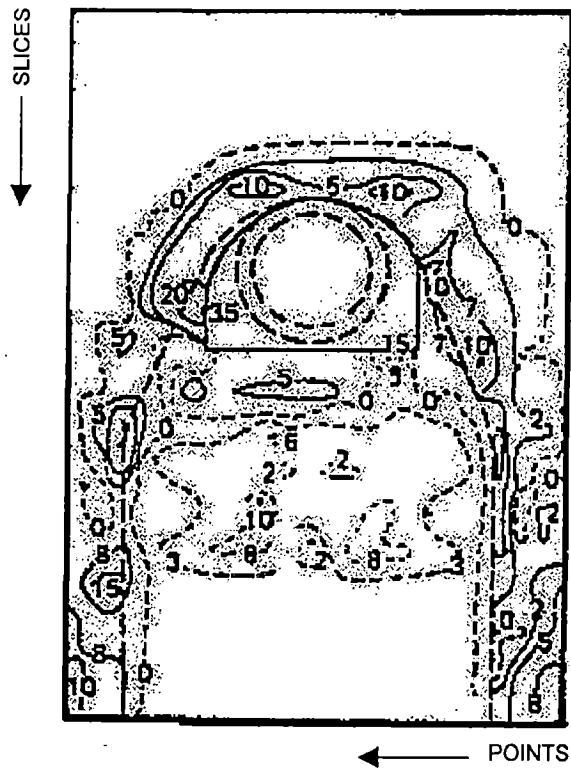


(e) POINT 12

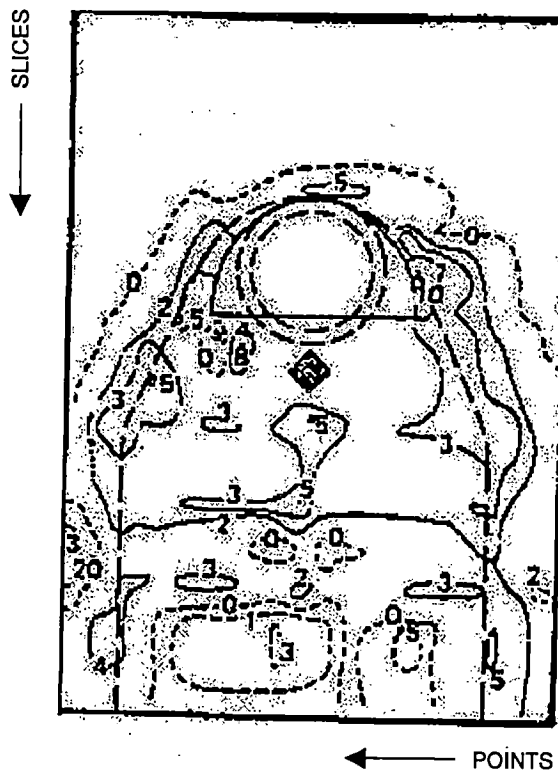
NOTES

1. Solid line contour indicates compression and dotted line tension.
2. System of numbering Slices, Points and Strips is same as given in Slicing Plan (Fig. 4.1) and Transverse Section (Fig. 4.9).
3. S.C.F. contours are given in planes of stress denoted by corresponding Point.

FIG. 5.70: STRESS CONTOURS PLOTTED FOR $SZ^{(10)}$

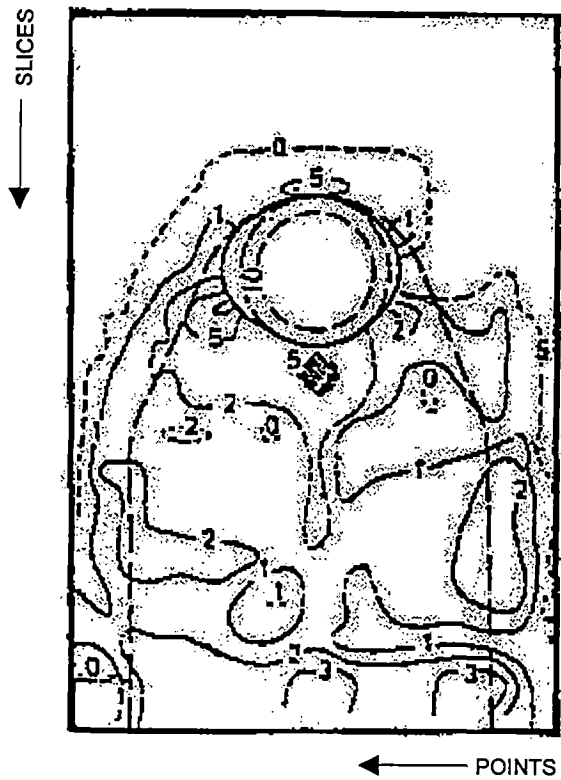


(a) STRIP 7

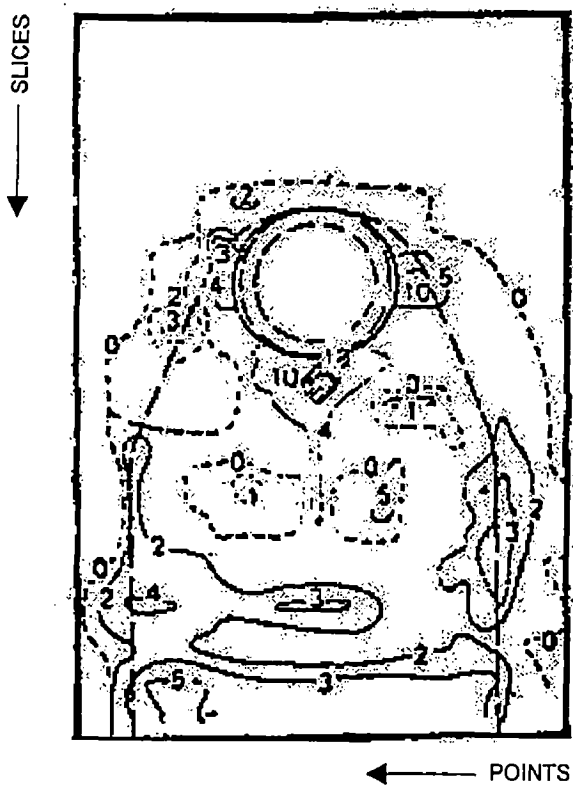


(b) STRIP 8

FIG. 5.71: STRESS CONTOURS PLOTTED FOR $S_y^{(10)}$ (Contd.)

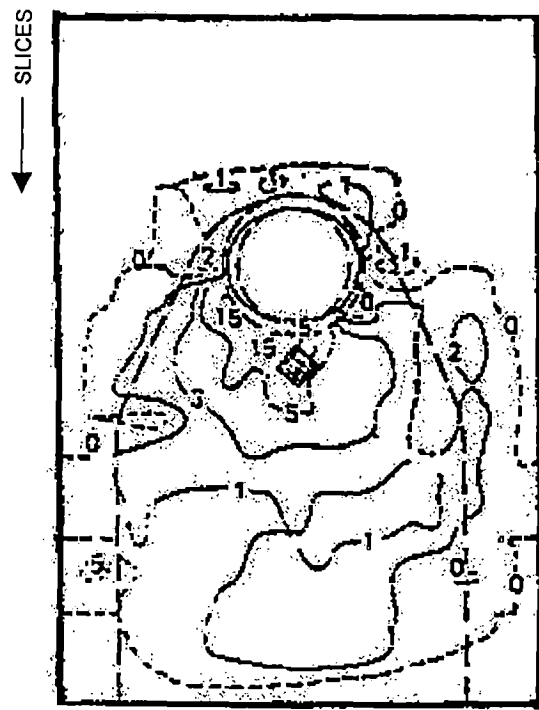


(c) STRIP 9

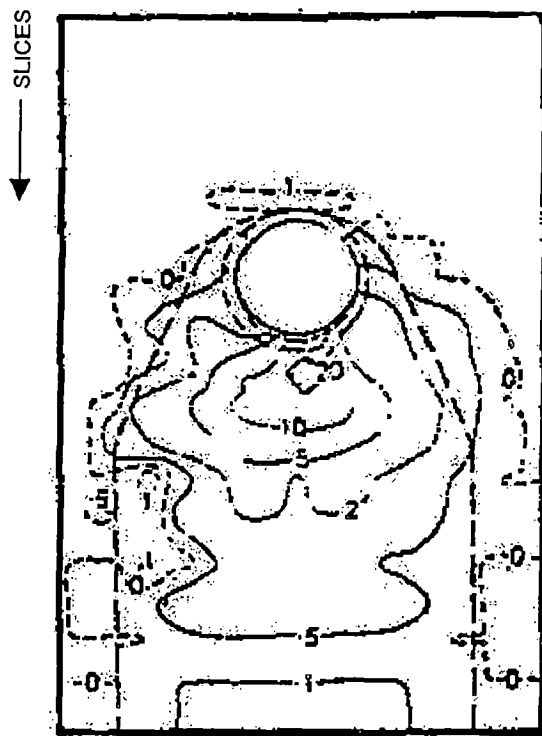


(d) STRIP 10

FIG. 5.71: STRESS CONTOURS PLOTTED FOR $S_{Y^{(10)}}$ (Contd.)

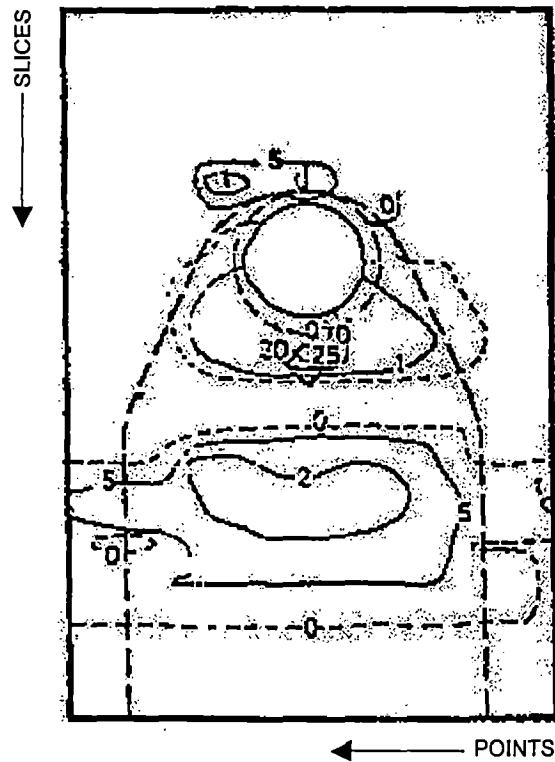


(e) STRIP 11



(f) STRIP 12

FIG. 5.71: STRESS CONTOURS PLOTTED FOR $S_{Y^{(10)}}$ (Contd.)



(g) STRIP 13

NOTES

1. Solid line contour indicates compression and dotted line tension.
2. System of numbering Slices, Points and Strips is same as given in Slicing Plan (Fig. 4.1) and Transverse Section (Fig. 4.9).
3. S.C.F. contours are given in horizontal planes denoted by corresponding Strips.

FIG. 5.71: STRESS CONTOURS PLOTTED FOR $S_Y^{(10)}$

CHAPTER 6

CONCLUSIONS AND SUGGESTIONS

6.1 CONCLUSIONS

- The stress patterns obtained by FEM analysis for a point load on elbow concrete are found generally comparable to the stress patterns obtained by Nigam⁽¹⁰⁾ from Photo Elastic experimental method.
- FEM analysis is a more convenient and less time consuming tool for the analysis of complex structures like elbow concrete in a Power House.
- The stress patterns obtained by FEM analysis for other kind of loading and at different point of application described in Chapter 5 reveal the following.
 1. The elbow concrete around the draft tube cavity within the power house is under tension in both transverse and longitudinal direction for superimposed loads on the cavity.
 2. The zone of tension extends upto about half the depth of concrete over the cavity.
 3. The stresses in elbow concrete around the cavity in vertical direction due to these loads are generally compressive at all levels except at the top.
 4. The stresses in both transverse and longitudinal direction at the top of elbow concrete under these loads are tensile due to fixity with the surrounding mass concrete.
 5. Point loads simulating column loads cause compressive stresses in elbow concrete around the cavity in all directions except at the top where the stresses are tensile.
- The above stress conditions suggest that the behaviour of elbow concrete is in close approximation to that of a deep girder.

6.2 SUGGESTIONS FOR FURTHER STUDY

- The draft tube is having curvature in both the directions and the shape is complex, as in the flaring portion right from the bottom of runner the draft tube diverges from circular to rectangular shape. So attempt can be made in the modeling for attaining the actual shape of draft tube cavity.

- To study the exact behaviour of generator barrel load the substructure should be modeled up to the base of generator foundation containing another cavity for scroll case.
- In the model studied, the presence of construction joint has been omitted which is a deviation from actual construction practice.
- The model considered for analysis in this study has no pier nor galleries and hence study can be extended on a substructure of a specific power house.
- The stress analysis shall be made to study the influence of horizontal forces on the substructure.
- The substructure model shall also be analysed for stresses in dynamic condition.

REFERENCES

1. IS: 456-2000, "Code Of Practice For Plain And Reinforced Concrete", Bureau Of Indian Standards, New Delhi.
2. IS: 4247 (Part III)-1978, "Code Of Practice For Structural Design Of Surface Hydel Power Stations: Part III Substructure", Bureau Of Indian Standards, New Delhi.
3. Cook R.D., Malkus D.S. & Plesha M.S. (1988), "Concepts And Applications Of Finite Element Analysis", John Wiley & Sons, New York.
4. Dally J.W. & Riley W.F. (1965), "Experimental Stress Analysis", Mc. Graw Hill Inc, New York.
5. Dandekar Y.S. (1976), "Design Of Substructure Of Hydro Power Stations", M.E. Dissertation, W.R.D.T.C., I.I.T. Roorkee.
6. Dawe D.J. (1984), "Matrix And Finite Element Displacement Analysis Of Structures", Clarendon Press, Oxford, Birmingham.
7. Desai C.S. & Abel J.F. (1987), "Introduction To The Finite Element Method", C.B.S., Delhi.
8. George W. & Arthur H.N. (1984), "Design Of Concrete Structures", International Students Edition, Mc. Graw Hill Inc, New York.
9. Krishnamoorthy C.S. (1987), "FINITE Element Analysis Theory And Programming", Tata Mc Graw Hill Publishing Company Limited, New Delhi.
10. Nigam P.S. (1985), "Handbook Of Hydro Electric Engineering", Nem Chand And Brothers, Roorkee.
11. Rao S.S. (1998), "The Finite Element Method In Engineering", B. S. Publications, Hyderabad.
12. Reddy J.N. (1993), "An Introduction To The Finite Element Method", Mc. Graw Hill Inc, New York.

APPENDIX

STRESS COMPONENT SX UNDER LOAD CONDITION 1

TABLE 5.1: NODAL STRESSES AT SLICE 7 (Z=66.478 mm)

(Under concentrated load between Slice 8 & 9)

X in mm	Y in mm	SX in kg/cm ²
19.591	0.000	-0.03180
0.000	20.665	-0.14610
0.000	34.690	-0.14990
0.000	48.509	-0.03410
76.288	0.000	-0.02110
90.376	15.297	-0.07900
109.000	20.665	-0.13686
109.000	34.690	-0.13715
95.520	51.826	0.00139
109.000	48.509	-0.02740

TABLE 5.2: NODAL STRESSES AT SLICE 8 (Z=74.476 mm)

(Under concentrated load between Slice 8 & 9)

X in mm	Y in mm	SX in kg/cm ²
0.000	6.812	-0.07240
6.658	0.000	-0.02060
0.000	20.589	-0.16550
19.738	0.000	-0.02710
0.000	34.641	-0.18560
0.000	48.530	-0.04160
34.340	0.000	-0.00491
0.000	62.184	0.25430
53.723	34.607	1.03130
63.219	0.000	0.00126
46.128	55.156	-0.18240
50.274	50.638	0.14800
76.121	0.000	-0.01060
48.081	69.000	-2.44740
59.961	61.488	-0.81750
53.285	69.000	-5.06000
58.377	69.000	-2.35510
64.848	62.477	-0.79770
63.466	69.000	-0.17110
88.959	0.000	-0.02810
109.000	20.589	-0.15530
109.000	34.641	-0.16950
102.250	0.000	-0.01960
84.452	69.000	0.35250
90.732	64.068	0.21290
109.000	6.812	-0.07430
96.432	59.007	0.13190
102.644	53.829	0.04160
109.000	48.530	-0.03580
101.467	69.000	0.43400
109.000	62.184	0.22800

TABLE 5.3: NODAL STRESSES AT SLICE 9 (Z=83.973 mm)

(Under concentrated load between Slice 8 & 9)

X in mm	Y in mm	SX in kg/cm ²
18.624	63.097	0.19570
35.418	38.162	0.04550
37.720	52.753	-0.24140
53.039	44.435	0.25930
40.930	65.469	-0.64600
38.033	69.000	0.25310
45.706	64.613	-1.74450
18.007	69.000	0.38750
57.667	55.724	-0.03230
51.522	64.584	-0.62700
55.286	64.240	-0.59600
53.277	69.000	-10.18780
60.176	65.087	-1.98634
80.143	48.227	-0.10640
58.384	69.000	-2.58570
33.360	0.000	-0.00152
97.705	59.433	0.16170
94.317	69.000	0.39020

TABLE 5.4: NODAL STRESSES AT SLICE 10 (Z=92.476 mm)

(Under concentrated load between Slice 8 & 9)

X in mm	Y in mm	SX in kg/cm ²
20.464	52.248	-0.02190
8.032	64.073	0.30800
35.444	57.572	-0.19020
36.379	63.298	-0.21230
31.442	69.000	0.08710
41.813	62.461	-0.37700
78.899	37.211	-0.12270
53.656	62.900	-0.37700
57.927	62.885	-0.45780
99.781	27.624	-0.18070
69.853	62.737	-0.23840
74.965	62.681	-0.06980
75.663	69.000	0.09360
81.097	69.000	0.19730
98.822	59.567	0.16490
97.339	52.004	0.01420
63.902	62.883	-0.42150

TABLE 5.5: NODAL STRESSES AT SLICE 11(Z=100.967 mm)

(Under concentrated load between Slice 8 & 9)

X in mm	Y in mm	SX in kg/cm ²
6.320	10.651	-0.00868
8.332	46.130	-0.08210
5.922	61.902	0.22440
37.205	42.132	0.06960
55.119	50.215	0.03420
64.581	54.067	-0.07340
101.371	10.311	-0.01320
85.240	49.415	-0.03150
100.825	39.049	-0.19180
91.570	52.947	0.01960
100.851	46.209	-0.07810

TABLE 5.6: NODAL STRESSES AT SLICE 7 (Z=66.478 mm)

(Under concentrated load between Slice 9 & 10)

X in mm	Y in mm	SX in kg/cm ²
19.591	0.000	-0.02750
0.000	20.665	-0.12970
0.000	34.690	-0.13410
0.000	48.509	-0.02490
76.288	0.000	-0.01780
90.376	15.297	-0.06630
109.000	20.665	-0.12230
109.000	34.690	-0.12320
95.520	51.826	0.01190
109.000	48.509	-0.02010

TABLE 5.7: NODAL STRESSES AT SLICE 8 (Z=74.476 mm)

(Under concentrated load between Slice 9 & 10)

X in mm	Y in mm	SX in kg/cm ²
0.000	6.812	-0.06400
6.658	0.000	-0.01840
0.000	20.589	-0.15030
19.738	0.000	-0.02350
0.000	34.641	-0.17340
0.000	48.530	-0.03560
34.340	0.000	-0.00390
0.000	62.184	0.24030
53.723	34.607	0.87800
63.219	0.000	0.00131
46.128	55.156	-0.11090
50.274	50.638	0.06220
76.121	0.000	-0.00901
48.081	69.000	-1.09300
59.961	61.488	-0.36000
53.285	69.000	-1.36290
58.377	69.000	-1.10720
64.848	62.477	-0.31760
63.466	69.000	-0.54250
88.959	0.000	-0.02490
109.000	20.589	-0.14230
109.000	34.641	-0.15890
102.250	0.000	-0.01760
84.452	69.000	0.26070
90.732	64.068	0.18900
109.000	6.812	-0.06660
96.432	59.007	0.12700
102.644	53.829	0.04390
109.000	48.530	-0.03060
101.467	69.000	0.40050
109.000	62.184	0.21700

TABLE 5.8: NODAL STRESSES AT SLICE 9 (Z=83.973 mm)

(Under concentrated load between Slice 9 & 10)

X in mm	Y in mm	SX in kg/cm ²
18.624	63.097	0.17260
35.418	38.162	0.06830
37.720	52.753	-0.22870
53.039	44.435	0.23110
40.930	65.469	-0.64550
38.033	69.000	0.18790
45.706	64.613	-1.49450
18.007	69.000	0.35100
57.667	55.724	-0.00435
51.522	64.584	-0.62630
55.286	64.240	-0.61920
53.277	69.000	-4.53950
60.176	65.087	-1.85250
80.143	48.227	-0.09280
58.384	69.000	-1.81580
33.360	0.000	-0.00119
97.705	59.433	0.15690
94.317	69.000	0.36940

TABLE 5.9: NODAL STRESSES AT SLICE 10 (Z=92.476 mm)

(Under concentrated load between Slice 9 & 10)

X in mm	Y in mm	SX in kg/cm ²
20.464	52.248	-0.03970
8.032	64.073	0.31750
35.444	57.572	-0.34710
36.379	63.298	-0.39110
31.442	69.000	0.16670
41.813	62.461	-0.90070
78.899	37.211	-0.10890
53.656	62.900	0.14940
57.927	62.885	-0.44740
99.781	27.624	-0.18200
69.853	62.737	-0.44570
74.965	62.681	-0.15520
75.663	69.000	0.15460
81.097	69.000	0.21920
98.822	59.567	0.16700
97.339	52.004	0.01140
63.902	62.883	-1.11440

TABLE 5.10: NODAL STRESSES AT SLICE 11 (Z=100.967 mm)

(Under concentrated load between Slice 9 & 10)

X in mm	Y in mm	SX in kg/cm ²
6.320	10.651	-0.00816
8.332	46.130	-0.09260
5.922	61.902	0.24570
37.205	42.132	0.07850
55.119	50.215	0.08770
64.581	54.067	-0.12730
101.371	10.311	-0.01280
85.240	49.415	-0.04940
100.825	39.049	-0.21340
91.570	52.947	0.01090
100.851	46.209	-0.08780

TABLE 5.11: NODAL STRESSES AT SLICE 7 (Z=66.478 mm)
(Under UDL above elbow concrete)

X in mm	Y in mm	SX in kg/cm ²
19.591	0.000	-0.00740
0.000	20.665	-0.02950
0.000	34.690	-0.02990
0.000	48.509	-0.01370
76.288	0.000	-0.00512
90.376	15.297	-0.01540
109.000	20.665	-0.02790
109.000	34.690	-0.02770
95.520	51.826	0.00327
109.000	48.509	-0.01230

TABLE 5.12: NODAL STRESSES AT SLICE 8 (Z=74.476 mm)
(Under UDL above elbow concrete)

X in mm	Y in mm	SX in kg/cm ²
0.000	6.812	-0.01600
6.658	0.000	-0.00475
0.000	20.589	-0.03390
19.738	0.000	-0.00643
0.000	34.641	-0.03730
0.000	48.530	-0.02060
34.340	0.000	-0.00129
0.000	62.184	0.02550
53.723	34.607	0.10690
63.219	0.000	0.00021
46.128	55.156	-0.05090
50.274	50.638	-0.02800
76.121	0.000	-0.00271
48.081	69.000	-0.22910
59.961	61.488	-0.09350
53.285	69.000	-0.24190
58.377	69.000	-0.23800
64.848	62.477	-0.08020
63.466	69.000	-0.18390
88.959	0.000	-0.00683
109.000	20.589	-0.03210
109.000	34.641	-0.03460
102.250	0.000	-0.00460
84.452	69.000	-0.01190
90.732	64.068	0.00394
109.000	6.812	-0.01660
96.432	59.007	0.01840
102.644	53.829	-0.00069
109.000	48.530	-0.01930
101.467	69.000	0.04700
109.000	62.184	0.02010

TABLE 5.13: NODAL STRESSES AT SLICE 9 (Z=83.973 mm)

(Under UDL above elbow concrete)

X in mm	Y in mm	SX in kg/cm ²
18.624	63.097	-0.01280
35.418	38.162	0.00955
37.720	52.753	-0.02830
53.039	44.435	0.01050
40.930	65.469	-0.11510
38.033	69.000	-0.13550
45.706	64.613	-0.12810
18.007	69.000	-0.05050
57.667	55.724	-0.05470
51.522	64.584	-0.14230
55.286	64.240	-0.13780
53.277	69.000	-0.21410
60.176	65.087	-0.13600
80.143	48.227	-0.01080
58.384	69.000	-0.20360
33.360	0.000	-0.00046
97.705	59.433	0.01990
94.317	69.000	-0.04220

TABLE 5.14: NODAL STRESSES AT SLICE 10 (Z=92.476 mm)
(Under UDL above elbow concrete)

X in mm	Y in mm	SX in kg/cm ²
20.464	52.248	-0.00316
8.032	64.073	0.05640
35.444	57.572	-0.03290
36.379	63.298	-0.05850
31.442	69.000	-0.07290
41.813	62.461	-0.06920
78.899	37.211	-0.00805
53.656	62.900	-0.09080
57.927	62.885	-0.08710
99.781	27.624	-0.03610
69.853	62.737	-0.06000
74.965	62.681	-0.04680
75.663	69.000	-0.07140
81.097	69.000	-0.04380
98.822	59.567	0.02240
97.339	52.004	0.00075
63.902	62.883	-0.07260

TABLE 5.15: NODAL STRESSES AT SLICE 11 (Z=100.967 mm)
(Under UDL above elbow concrete)

X in mm	Y in mm	SX in kg/cm ²
6.320	10.651	-0.00233
8.332	46.130	-0.01430
5.922	61.902	0.04530
37.205	42.132	0.01260
55.119	50.215	-0.00736
64.581	54.067	-0.01950
101.371	10.311	-0.00353
85.240	49.415	-0.00367
100.825	39.049	-0.03410
91.570	52.947	0.00425
100.851	46.209	-0.01450

TABLE 5.16: NODAL STRESSES AT SLICE 7 (Z=66.478 mm)
(Under concentrated load simulating gantry column loads)

X in mm	Y in mm	SX in kg/cm ²
19.591	0.000	-0.00367
0.000	20.665	-0.00976
0.000	34.690	-0.00642
0.000	48.509	0.00102
76.288	0.000	-0.00315
90.376	15.297	-0.00462
109.000	20.665	-0.01030
109.000	34.690	-0.00570
95.520	51.826	0.01580
109.000	48.509	-0.00105

TABLE 5.17: NODAL STRESSES AT SLICE 8 (Z=74.476 mm)
(Under concentrated load simulating gantry column loads)

X in mm	Y in mm	SX in kg/cm ²
0.000	6.812	-0.00758
6.658	0.000	-0.00253
0.000	20.589	-0.01240
19.738	0.000	-0.00350
0.000	34.641	-0.00917
0.000	48.530	-0.00818
34.340	0.000	-0.00075
0.000	62.184	0.03340
53.723	34.607	-0.01970
63.219	0.000	0.00004
46.128	55.156	-0.02400
50.274	50.638	-0.02520
76.121	0.000	-0.00197
48.081	69.000	-0.02280
59.961	61.488	-0.02210
53.285	69.000	-0.02500
58.377	69.000	-0.02420
64.848	62.477	-0.01910
63.466	69.000	-0.01820
88.959	0.000	-0.00462
109.000	20.589	-0.01260
109.000	34.641	-0.00748
102.250	0.000	-0.00293
84.452	69.000	0.00340
90.732	64.068	-0.01950
109.000	6.812	-0.00911
96.432	59.007	0.01500
102.644	53.829	0.05360
109.000	48.530	-0.00582
101.467	69.000	0.00373
109.000	62.184	0.02830

TABLE 5.18: NODAL STRESSES AT SLICE 9 (Z=83.973 mm)

(Under concentrated load simulating gantry column loads)

X in mm	Y in mm	SX in kg/cm ²
18.624	63.097	-0.17290
35.418	38.162	-0.01850
37.720	52.753	-0.03350
53.039	44.435	-0.02080
40.930	65.469	-0.01680
38.033	69.000	-0.00754
45.706	64.613	-0.01950
18.007	69.000	0.08560
57.667	55.724	-0.02450
51.522	64.584	-0.02030
55.286	64.240	-0.02070
53.277	69.000	-0.01950
60.176	65.087	-0.01930
80.143	48.227	-0.04160
58.384	69.000	-0.01840
33.360	0.000	-0.00037
97.705	59.433	-0.17550
94.317	69.000	0.19110

TABLE 5.19: NODAL STRESSES AT SLICE 10 (Z=92.476 mm)

(Under concentrated load simulating gantry column loads)

X in mm	Y in mm	SX in kg/cm ²
20.464	52.248	-0.07460
8.032	64.073	-0.60320
35.444	57.572	-0.03800
36.379	63.298	-0.02390
31.442	69.000	0.00496
41.813	62.461	-0.02210
78.899	37.211	-0.00652
53.656	62.900	-0.02000
57.927	62.885	-0.02010
99.781	27.624	-0.00519
69.853	62.737	-0.02370
74.965	62.681	-0.03050
75.663	69.000	0.01110
81.097	69.000	0.03760
98.822	59.567	-0.15570
97.339	52.004	0.01790
63.902	62.883	-0.02110

TABLE 5.20: NODAL STRESSES AT SLICE 11 (Z=100.967 mm)

(Under concentrated load simulating gantry column loads)

X in mm	Y in mm	SX in kg/cm ²
6.320	10.651	-0.00221
8.332	46.130	0.03880
5.922	61.902	0.08940
37.205	42.132	-0.01540
55.119	50.215	-0.01920
64.581	54.067	-0.02480
101.371	10.311	-0.00359
85.240	49.415	-0.03650
100.825	39.049	0.02550
91.570	52.947	-0.02930
100.851	46.209	0.04540

TABLE 5.21: NODAL STRESSES AT POINT 3 (X=98.84 mm)

(Under concentrated load between Slice 8 & 9)

Z in mm	Y in mm	SZ in kg/cm ²
0.000	0.000	0.00000
4.817	8.301	-0.00910
6.933	11.410	-0.01110
10.793	9.229	-0.01050
5.386	18.349	-0.01350
12.105	23.544	-0.01540
22.197	14.376	-0.01710
17.970	24.296	-0.01710
6.876	35.267	-0.00955
5.235	38.279	-0.00653
29.658	14.845	-0.02120
18.930	33.111	-0.01440
15.631	38.578	-0.00885
16.833	44.209	-0.00267
47.200	14.580	-0.02670
14.960	53.927	0.01280
19.506	50.460	0.00682
57.139	24.289	-0.02990
22.109	56.531	0.01920
71.781	31.710	-0.01890
5.878	63.803	0.02650
77.316	36.368	-0.01320
0.000	69.000	0.03280
71.180	52.804	-0.00013
140.802	6.908	-0.00340
92.402	59.567	-0.00489
97.300	57.103	-0.00304
157.450	0.000	-0.00241
157.450	11.681	0.00006
151.190	19.850	-0.00309
147.352	24.569	-0.00717
115.912	64.037	0.02620
151.608	31.664	-0.00234
121.170	69.000	0.04260
145.615	48.783	-0.00571
157.450	40.622	0.00185
157.450	55.955	-0.00016
154.763	63.441	0.00130
157.450	69.000	-0.00034

TABLE 5.22: NODAL STRESSES AT POINT 6 (X=83.6 mm)

(Under concentrated load between Slice 8 & 9)

Z in mm	Y in mm	SZ in kg/cm ²
6.678	6.400	-0.01260
3.533	14.341	-0.02000
32.064	0.000	-0.01240
0.000	34.512	-0.01490
38.641	0.000	-0.01630
0.000	39.463	-0.00896
11.040	30.191	-0.02290
4.058	63.456	0.04260
55.686	25.645	-0.06340
35.203	47.453	-0.01330
24.018	69.000	0.08680
30.912	64.985	0.08100
45.039	51.515	-0.00471
79.681	22.221	-0.04760
82.964	28.778	-0.05640
68.278	48.371	0.01700
85.811	32.520	0.08610
61.139	63.043	-0.01780
131.726	0.000	-0.00053
145.961	4.576	-0.00071
151.058	4.525	-0.00074
108.209	60.987	-0.01870
126.341	48.927	-0.01630
109.089	69.000	-0.00289
126.889	69.000	0.03970
152.582	57.621	0.00086
157.450	53.854	0.00009

TABLE 5.23: NODAL STRESSES AT POINT 8 (X=73.44 mm)

(Under concentrated load between Slice 8 & 9)

Z in mm	Y in mm	SZ in kg/cm ²
5.521	10.411	-0.01820
23.905	0.000	-0.00912
19.113	5.039	-0.01400
18.835	15.584	-0.02490
11.769	26.369	-0.02610
5.388	31.098	-0.02150
36.905	0.000	-0.01510
34.353	8.103	-0.02040
5.127	35.651	-0.01740
5.345	40.104	-0.01170
44.071	6.354	-0.01740
3.396	50.929	0.01040
26.427	37.036	-0.03190
6.703	60.469	0.03780
26.024	43.248	-0.02110
11.703	61.795	0.04330
14.654	65.393	0.05740
80.658	40.182	0.13460
97.912	41.589	0.02180
71.861	69.000	-0.44280
98.278	61.224	-0.08330
114.004	69.000	0.03940
157.450	45.650	0.00000
152.607	62.773	0.00182

TABLE 5.24: NODAL STRESSES AT POINT 10 (X=63.28 mm)

(Under concentrated load between Slice 8 & 9)

Z in mm	Y in mm	SZ in kg/cm ²
50.885	0.000	-0.01050
6.882	8.663	-0.01570
19.781	27.556	-0.02490
35.081	38.728	-0.02480
6.392	18.596	-0.02280
74.218	0.000	0.00065
82.855	0.000	0.00145
44.500	51.253	0.00079
91.320	0.000	0.00130
30.818	69.000	0.07470
7.335	54.782	0.01850
75.675	45.781	0.09300
93.161	41.403	0.06570
81.301	61.484	0.07910
74.203	69.000	-0.48150
143.105	6.355	0.00008
103.791	69.000	0.14560
142.684	57.595	0.00408
152.658	60.821	0.00126

TABLE 5.25: NODAL STRESSES AT POINT 12 (X=53.12 mm)

(Under concentrated load between Slice 8 & 9)

Z in mm	Y in mm	SZ in kg/cm ²
6.826	8.653	-0.01510
9.715	14.682	-0.01970
54.608	0.000	-0.00582
6.484	60.408	0.03410
18.303	65.398	0.04610
45.171	41.405	0.00222
31.135	69.000	0.04280
102.433	0.000	0.00056
44.500	58.587	-0.00225
40.089	69.000	0.00892
83.921	44.436	0.13310
89.104	49.033	0.00068
74.373	69.000	-1.44330
83.571	69.000	-7.20700
93.220	69.000	0.78990
102.693	64.017	-0.01750
107.166	63.818	0.01840
118.336	15.000	0.00124
128.947	63.078	0.03030
124.152	69.000	0.08030
157.450	38.110	0.00002
133.989	15.000	0.00044
157.450	15.000	0.00000

TABLE 5.26: NODAL STRESSES AT POINT 3 (X=98.84 mm)

(Under concentrated load between Slice 9 & 10)

Z in mm	Y in mm	SZ in kg/cm ²
0.000	0.000	0.00000
4.817	8.301	-0.00758
6.933	11.410	-0.00931
10.793	9.229	-0.00896
5.386	18.349	-0.01130
12.105	23.544	-0.01310
22.197	14.376	-0.01500
17.970	24.296	-0.01490
6.876	35.267	-0.00769
5.235	38.279	-0.00503
29.658	14.845	-0.01920
18.930	33.111	-0.01230
15.631	38.578	-0.00718
16.833	44.209	-0.00162
47.200	14.580	-0.02590
14.960	53.927	0.01180
19.506	50.460	0.00686
57.139	24.289	-0.03290
22.109	56.531	0.01780
71.781	31.710	-0.02880
5.878	63.803	0.02440
77.316	36.368	-0.02320
0.000	69.000	0.02610
71.180	52.804	0.00060
140.802	6.908	-0.00419
92.402	59.567	-0.00361
97.300	57.103	-0.00304
157.450	0.000	-0.00365
157.450	11.681	0.00008
151.190	19.850	-0.00375
147.352	24.569	-0.00814
115.912	64.037	0.01800
151.608	31.664	-0.00358
121.170	69.000	0.03570
145.615	48.783	-0.00739
157.450	40.622	0.00249
157.450	55.955	-0.00016
154.763	63.441	0.00148
157.450	69.000	-0.00040

TABLE 5.27: NODAL STRESSES AT POINT 6 (X=83.6 mm)
 (Under concentrated load between Slice 9 & 10)

Z in mm	Y in mm	SZ in kg/cm ²
6.678	6.400	-0.01050
3.533	14.341	-0.01670
32.064	0.000	-0.01010
0.000	34.512	-0.01180
38.641	0.000	-0.01340
0.000	39.463	-0.00662
11.040	30.191	-0.01920
4.058	63.456	0.03580
55.686	25.645	-0.07180
35.203	47.453	-0.00984
24.018	69.000	0.07600
30.912	64.985	0.07480
45.039	51.515	0.00102
79.681	22.221	-0.04290
82.964	28.778	-0.07870
68.278	48.371	-0.00516
85.811	32.520	-0.00622
61.139	63.043	0.02470
131.726	0.000	-0.00071
145.961	4.576	-0.00086
151.058	4.525	-0.00091
108.209	60.987	-0.05200
126.341	48.927	-0.01280
109.089	69.000	-0.07560
126.889	69.000	0.01140
152.582	57.621	0.00033
157.450	53.854	0.00016

TABLE 5.28: NODAL STRESSES AT POINT 8 (X=73.44 mm)

(Under concentrated load between Slice 9 & 10)

Z in mm	Y in mm	SZ in kg/cm ²
5.521	10.411	-0.01510
23.905	0.000	-0.00726
19.113	5.039	-0.01180
18.835	15.584	-0.02160
11.769	26.369	-0.02200
5.388	31.098	-0.01750
36.905	0.000	-0.01220
34.353	8.103	-0.01820
5.127	35.651	-0.01380
5.345	40.104	-0.00886
44.071	6.354	-0.01560
3.396	50.929	0.00986
26.427	37.036	-0.02760
6.703	60.469	0.03210
26.024	43.248	-0.01690
11.703	61.795	0.03720
14.654	65.393	0.04890
80.658	40.182	0.11150
97.912	41.589	0.10880
71.861	69.000	-0.14190
98.278	61.224	-0.14410
114.004	69.000	-0.04610
157.450	45.650	0.00066
152.607	62.773	0.00054

TABLE 5.29: NODAL STRESSES AT POINT 10 (X=63.28 mm)

(Under concentrated load between Slice 9 & 10)

Z in mm	Y in mm	SZ in kg/cm ²
50.885	0.000	-0.00824
6.882	8.663	-0.01290
19.781	27.556	-0.02120
35.081	38.728	-0.02180
6.392	18.596	-0.01880
74.218	0.000	0.00082
82.855	0.000	0.00140
44.500	51.253	0.00021
91.320	0.000	0.00123
30.818	69.000	0.06450
7.335	54.782	0.01630
75.675	45.781	0.05700
93.161	41.403	0.22350
81.301	61.484	-0.29400
74.203	69.000	-0.02760
143.105	6.355	0.00010
103.791	69.000	0.04880
142.684	57.595	-0.00310
152.658	60.821	0.00002

TABLE 5.30: NODAL STRESSES AT POINT 12 (X=53.12 mm)

(Under concentrated load between Slice 9 & 10)

Z in mm	Y in mm	SZ in kg/cm ²
6.826	8.653	-0.01230
9.715	14.682	-0.01630
54.608	0.000	-0.00433
6.484	60.408	0.02830
18.303	65.398	0.03840
45.171	41.405	0.00226
31.135	69.000	0.03550
102.433	0.000	0.00054
44.500	58.587	-0.00206
40.089	69.000	0.00688
83.921	44.436	0.24020
89.104	49.033	0.28490
74.373	69.000	0.35170
83.571	69.000	-1.42230
93.220	69.000	-2.52970
102.693	64.017	-0.60390
107.166	63.818	-0.22650
118.336	15.000	0.00123
128.947	63.078	-0.00072
124.152	69.000	0.03300
157.450	38.110	-0.00062
133.989	15.000	0.00045
157.450	15.000	0.00000

TABLE 5.31: NODAL STRESSES AT POINT 3 (X=98.84 mm)

(Under UDL above elbow concrete)

Z in mm	Y in mm	SZ in kg/cm ²
0.000	0.000	0.00000
4.817	8.301	-0.00209
6.933	11.410	-0.00255
10.793	9.229	-0.00243
5.386	18.349	-0.00314
12.105	23.544	-0.00359
22.197	14.376	-0.00391
17.970	24.296	-0.00397
6.876	35.267	-0.00233
5.235	38.279	-0.00165
29.658	14.845	-0.00485
18.930	33.111	-0.00343
15.631	38.578	-0.00221
16.833	44.209	-0.00085
47.200	14.580	-0.00612
14.960	53.927	0.00266
19.506	50.460	0.00126
57.139	24.289	-0.00700
22.109	56.531	0.00412
71.781	31.710	-0.00371
5.878	63.803	0.00574
77.316	36.368	-0.00079
0.000	69.000	0.00699
71.180	52.804	-0.00443
140.802	6.908	-0.00096
92.402	59.567	-0.02080
97.300	57.103	-0.01510
157.450	0.000	-0.00066
157.450	11.681	0.00002
151.190	19.850	-0.00083
147.352	24.569	-0.00190
115.912	64.037	0.00702
151.608	31.664	-0.00070
121.170	69.000	0.01250
145.615	48.783	-0.00160
157.450	40.622	0.00044
157.450	55.955	-0.00002
154.763	63.441	0.00028
157.450	69.000	-0.00007

TABLE 5.32: NODAL STRESSES AT POINT 6 (X=83.6 mm)

(Under UDL above elbow concrete)

Z in mm	Y in mm	SZ in kg/cm ²
-6.678	6.400	-0.00295
3.533	14.341	-0.00473
32.064	0.000	-0.00284
0.000	34.512	-0.00373
38.641	0.000	-0.00374
0.000	39.463	-0.00242
11.040	30.191	-0.00558
4.058	63.456	0.00902
55.686	25.645	-0.01400
35.203	47.453	-0.00423
24.018	69.000	0.01930
30.912	64.985	0.01810
45.039	51.515	-0.00373
79.681	22.221	-0.00898
82.964	28.778	-0.00860
68.278	48.371	-0.00254
85.811	32.520	0.02720
61.139	63.043	-0.01020
131.726	0.000	-0.00015
145.961	4.576	-0.00020
151.058	4.525	-0.00020
108.209	60.987	-0.01370
126.341	48.927	-0.00518
109.089	69.000	0.00815
126.889	69.000	0.00913
152.582	57.621	0.00012
157.450	53.854	0.00003

TABLE 5.33: NODAL STRESSES AT POINT 8 (X=73.44 mm)
(Under UDL above elbow concrete)

Z in mm	Y in mm	SZ in kg/cm ²
5.521	10.411	-0.00433
23.905	0.000	-0.00210
19.113	5.039	-0.00332
18.835	15.584	-0.00601
11.769	26.369	-0.00641
5.388	31.098	-0.00535
36.905	0.000	-0.00348
34.353	8.103	-0.00491
5.127	35.651	-0.00446
5.345	40.104	-0.00320
44.071	6.354	-0.00425
3.396	50.929	0.00175
26.427	37.036	-0.00814
6.703	60.469	0.00778
26.024	43.248	-0.00572
11.703	61.795	0.00903
14.654	65.393	0.01220
80.658	40.182	0.03310
97.912	41.589	0.01250
71.861	69.000	-0.08530
98.278	61.224	-0.04740
114.004	69.000	0.00593
157.450	45.650	0.00012
152.607	62.773	0.00028

TABLE 5.34: NODAL STRESSES AT POINT 10 (X=63.28 mm)
(Under UDL above elbow concrete)

Z in mm	Y in mm	SZ in kg/cm ²
50.885	0.000	-0.00248
6.882	8.663	-0.00376
19.781	27.556	-0.00632
35.081	38.728	-0.00684
6.392	18.596	-0.00557
74.218	0.000	0.00008
82.855	0.000	0.00030
44.500	51.253	0.00036
91.320	0.000	0.00029
30.818	69.000	0.01620
7.335	54.782	0.00345
75.675	45.781	0.01800
93.161	41.403	0.02250
81.301	61.484	-0.03400
74.203	69.000	-0.10630
143.105	6.355	0.00002
103.791	69.000	0.00699
142.684	57.595	0.00002
152.658	60.821	0.00012

TABLE 5.35: NODAL STRESSES AT POINT 12 (X=53.12 mm)
(Under UDL above elbow concrete)

Z in mm	Y in mm	SZ in kg/cm ²
6.826	8.653	-0.00365
9.715	14.682	-0.00484
54.608	0.000	-0.00141
6.484	60.408	0.00683
18.303	65.398	0.00961
45.171	41.405	0.00080
31.135	69.000	0.00928
102.433	0.000	0.00013
44.500	58.587	-0.00039
40.089	69.000	0.00193
83.921	44.436	0.01870
89.104	49.033	0.00832
74.373	69.000	-0.02740
83.571	69.000	-0.12550
93.220	69.000	-0.07190
102.693	64.017	-0.02660
107.166	63.818	-0.01380
118.336	15.000	0.00027
128.947	63.078	0.00154
124.152	69.000	0.00698
157.450	38.110	0.00000
133.989	15.000	0.00010
157.450	15.000	0.00000

TABLE 5.36: NODAL STRESSES AT POINT 3 (X=98.84 mm)

(Under concentrated load simulating gantry column loads)

Z in mm	Y in mm	SZ in kg/cm ²
0.000	0.000	0.00000
4.817	8.301	-0.00100
6.933	11.410	-0.00124
10.793	9.229	-0.00119
5.386	18.349	-0.00154
12.105	23.544	-0.00181
22.197	14.376	-0.00202
17.970	24.296	-0.00123
6.876	35.267	-0.00202
5.235	38.279	-0.00092
29.658	14.845	-0.00261
18.930	33.111	-0.00177
15.631	38.578	-0.00119
16.833	44.209	-0.00057
47.200	14.580	-0.00395
14.960	53.927	0.00096
19.506	50.460	0.00039
57.139	24.289	-0.00575
22.109	56.531	0.00171
71.781	31.710	-0.00509
5.878	63.803	0.00209
77.316	36.368	-0.00099
0.000	69.000	0.00223
71.180	52.804	-0.06540
140.802	6.908	-0.00118
92.402	59.567	0.15340
97.300	57.103	-0.02150
157.450	0.000	-0.00065
157.450	11.681	0.00002
151.190	19.850	-0.00094
147.352	24.569	-0.00208
115.912	64.037	0.00532
151.608	31.664	-0.00086
121.170	69.000	0.02830
145.615	48.783	-0.00171
157.450	40.622	0.00030
157.450	55.955	0.00000
154.763	63.441	0.00021
157.450	69.000	-0.00004

TABLE 5.37: NODAL STRESSES AT POINT 6 (X=83.6 mm)

(Under concentrated load simulating gantry column loads)

Z in mm	Y in mm	SZ in kg/cm ²
6.678	6.400	-0.00147
3.533	14.341	-0.00239
32.064	0.000	-0.00131
0.000	34.512	-0.00211
38.641	0.000	-0.00176
0.000	39.463	-0.00157
11.040	30.191	-0.00305
4.058	63.456	0.00285
55.686	25.645	-0.01040
35.203	47.453	-0.00277
24.018	69.000	0.00747
30.912	64.985	0.00737
45.039	51.515	-0.00259
79.681	22.221	-0.00678
82.964	28.778	-0.00621
68.278	48.371	-0.01230
85.811	32.520	0.02560
61.139	63.043	0.00235
131.726	0.000	-0.00020
145.961	4.576	-0.00024
151.058	4.525	-0.00022
108.209	60.987	-0.01870
126.341	48.927	-0.00748
109.089	69.000	0.00182
126.889	69.000	0.00768
152.582	57.621	-0.00002
157.450	53.854	0.00005

TABLE 5.38: NODAL STRESSES AT POINT 8 (X=73.44 mm)

(Under concentrated load simulating gantry column loads)

Z in mm	Y in mm	SZ in kg/cm ²
5.521	10.411	-0.00220
23.905	0.000	-0.00095
19.113	5.039	-0.00173
18.835	15.584	-0.00333
11.769	26.369	-0.00353
5.388	31.098	-0.00299
36.905	0.000	-0.00161
34.353	8.103	-0.00298
5.127	35.651	-0.00263
5.345	40.104	-0.00212
44.071	6.354	-0.00275
3.396	50.929	-0.00013
26.427	37.036	-0.00482
6.703	60.469	0.00207
26.024	43.248	-0.00359
11.703	61.795	0.00259
14.654	65.393	0.00382
80.658	40.182	0.01830
97.912	41.589	0.02070
71.861	69.000	-0.00461
98.278	61.224	-0.00955
114.004	69.000	-0.00772
157.450	45.650	0.00014
152.607	62.773	0.00004

TABLE 5.39: NODAL STRESSES AT POINT 10 (X=63.28 mm)
(Under concentrated load simulating gantry column loads)

Z in mm	Y in mm	SZ in kg/cm ²
50.885	0.000	-0.00119
6.882	8.663	-0.00189
19.781	27.556	-0.00367
35.081	38.728	-0.00447
6.392	18.596	-0.00292
74.218	0.000	-0.00002
82.855	0.000	0.00012
44.500	51.253	0.00026
91.320	0.000	0.00016
30.818	69.000	0.00524
7.335	54.782	0.00031
75.675	45.781	0.00672
93.161	41.403	0.01770
81.301	61.484	-0.00509
74.203	69.000	-0.00883
143.105	6.355	0.00001
103.791	69.000	-0.01930
142.684	57.595	-0.00059
152.658	60.821	-0.00007

TABLE 5.40: NODAL STRESSES AT POINT 12 (X=53.12 mm)
(Under concentrated load simulating gantry column loads)

Z in mm	Y in mm	SZ in kg/cm ²
6.826	8.653	-0.00178
9.715	14.682	-0.00246
54.608	0.000	-0.00062
6.484	60.408	0.00133
18.303	65.398	0.00241
45.171	41.405	0.00067
31.135	69.000	0.00266
102.433	0.000	0.00008
44.500	58.587	-0.00002
40.089	69.000	0.00054
83.921	44.436	0.00786
89.104	49.033	0.00617
74.373	69.000	-0.00255
83.571	69.000	-0.01300
93.220	69.000	-0.01920
102.693	64.017	-0.01110
107.166	63.818	-0.00995
118.336	15.000	0.00016
128.947	63.078	-0.00289
124.152	69.000	-0.00597
157.450	38.110	0.00000
133.989	15.000	0.00007
157.450	15.000	0.00000

TABLE 5.39: NODAL STRESSES AT POINT 10 (X=63.28 mm)
(Under concentrated load simulating gantry column loads)

Z in mm	Y in mm	SZ in kg/cm ²
50.885	0.000	-0.00119
6.882	8.663	-0.00189
19.781	27.556	-0.00367
35.081	38.728	-0.00447
6.392	18.596	-0.00292
74.218	0.000	-0.00002
82.855	0.000	0.00012
44.500	51.253	0.00026
91.320	0.000	0.00016
30.818	69.000	0.00524
7.335	54.782	0.00031
75.675	45.781	0.00672
93.161	41.403	0.01770
81.301	61.484	-0.00509
74.203	69.000	-0.00883
143.105	6.355	0.00001
103.791	69.000	-0.01930
142.684	57.595	-0.00059
152.658	60.821	-0.00007

TABLE 5.40: NODAL STRESSES AT POINT 12 (X=53.12 mm)
(Under concentrated load simulating gantry column loads)

Z in mm	Y in mm	SZ in kg/cm ²
6.826	8.653	-0.00178
9.715	14.682	-0.00246
54.608	0.000	-0.00062
6.484	60.408	0.00133
18.303	65.398	0.00241
45.171	41.405	0.00067
31.135	69.000	0.00266
102.433	0.000	0.00008
44.500	58.587	-0.00002
40.089	69.000	0.00054
83.921	44.436	0.00786
89.104	49.033	0.00617
74.373	69.000	-0.00255
83.571	69.000	-0.01300
93.220	69.000	-0.01920
102.693	64.017	-0.01110
107.166	63.818	-0.00995
118.336	15.000	0.00016
128.947	63.078	-0.00289
124.152	69.000	-0.00597
157.450	38.110	0.00000
133.989	15.000	0.00007
157.450	15.000	0.00000

TABLE 5.41: NODAL STRESSES AT STRIP 7 (Y=35.56 mm)

(Under concentrated load between Slice 8 & 9)

X in mm	Z in mm	SY in kg/cm ²
0.000	58.466	-0.02450
7.319	54.468	-0.02770
4.582	14.221	-0.00021
6.279	7.737	0.00011
17.843	7.380	0.00033
27.465	5.363	-0.00099
35.085	5.388	-0.00159
97.456	59.488	-0.04750
37.059	129.066	0.00159
100.718	51.257	-0.02100
109.000	58.467	-0.02010
73.387	5.127	-0.00155
94.542	19.539	0.00004
104.459	14.256	-0.00011
98.256	157.450	0.03250

TABLE 5.42: NODAL STRESSES AT STRIP 8 (Y=40.64 mm)

(Under concentrated load between Slice 8 & 9)

X in mm	Z in mm	SY in kg/cm ²
0.000	118.481	-0.03030
24.774	95.918	-0.02620
21.768	85.317	-0.23140
32.190	93.992	-0.03160
28.199	87.417	-0.10430
98.509	157.450	0.05490
6.978	64.040	-0.03020
61.872	85.924	-0.19200
71.086	87.727	-0.09600
67.137	83.228	-0.16940
0.000	14.104	-0.00100
77.349	88.969	-0.10420
109.000	118.481	-0.02760
20.300	27.232	-0.00474
4.393	10.495	0.00070
43.800	26.294	-0.01870
100.992	64.593	-0.02820
87.803	27.232	-0.00428
104.591	10.485	0.00075
109.000	14.104	-0.00089

TABLE 5.43: NODAL STRESSES AT STRIP 9 (Y=45.72 mm)

(Under concentrated load between Slice 8 & 9)

X in mm	Z in mm	SY in kg/cm ²
42.582	113.257	0.02430
36.007	84.461	-0.23090
11.330	80.812	-0.07560
64.979	157.450	0.00113
73.213	157.450	0.00219
49.865	69.985	-0.56340
63.238	75.675	-0.53140
27.338	35.111	-0.02090
4.536	11.096	0.00155
52.364	13.502	-0.00108
104.520	11.081	0.00161
100.365	3.437	0.00131

TABLE 5.44: NODAL STRESSES AT STRIP 10 (Y=50.80 mm)

(Under concentrated load between Slice 8 & 9)

X in mm	Z in mm	SY in kg/cm ²
17.507	135.034	-0.02210
9.666	137.397	-0.01340
8.099	108.282	-0.02600
43.193	105.897	0.01220
50.267	106.076	0.01110
36.237	138.344	0.01160
17.745	54.080	-0.03090
50.527	148.780	0.00025
50.274	74.260	-1.23180
58.538	69.900	-1.00510
102.142	116.120	-0.01670
32.231	34.265	-0.01880
51.419	37.425	-0.03820
18.347	0.000	0.00231
21.880	3.018	0.00269
62.091	37.017	-0.04110
95.796	157.450	0.01860
31.267	3.773	0.00290
33.928	6.143	0.00271
89.791	54.045	-0.03710
56.251	3.655	0.00277
62.846	3.701	0.00283
73.375	3.396	0.00298

TABLE 5.45: NODAL STRESSES AT STRIP 11 (Y=55.88 mm)

(Under concentrated load between Slice 8 & 9)

X in mm	Z in mm	SY in kg/cm ²
76.504	90.755	-0.04530
70.251	91.622	-0.10270
82.009	90.292	-0.03580
80.622	82.999	-0.07060
66.811	85.832	-0.41737
61.419	87.208	-0.93610
57.668	84.048	-1.93160
49.426	87.580	-1.43692
69.986	120.743	0.00920
42.954	89.084	-0.50070
39.285	95.253	-0.08140
59.569	116.299	0.01950
62.739	122.950	0.01240
65.791	129.346	0.00571
51.399	122.558	0.01290
61.194	136.527	0.00294
66.000	44.500	-0.06370
48.998	129.030	0.00814
14.872	89.670	-0.02470
19.780	84.446	-0.04480
58.676	44.500	-0.05840
56.500	143.861	0.00113
66.177	32.903	-0.01440
24.341	73.259	-0.07150
109.000	134.619	0.00648
34.876	128.949	0.00286
87.943	157.450	0.00432
47.904	44.500	-0.05730
90.607	25.566	0.00162
40.600	44.500	-0.06210
76.198	10.249	0.00214
101.773	152.872	0.00392
98.529	157.450	0.00703
84.659	6.938	0.00286
72.005	0.000	0.00566
68.900	3.304	0.00452
82.329	0.000	0.00553
66.926	0.000	0.00548
61.934	0.000	0.00532
16.851	141.757	-0.00819
56.976	0.000	0.00534
52.021	0.000	0.00528
0.000	134.619	0.00594
16.656	153.550	0.00108
19.314	157.450	0.00210
47.061	0.000	0.00519
42.065	0.000	0.00526
30.630	7.340	0.00289
36.983	0.000	0.00540
23.796	10.796	0.00203
21.792	0.000	0.00494
16.700	0.000	0.00453

TABLE 5.46: NODAL STRESSES AT STRIP 12 (Y=60.96 mm)

(Under concentrated load between Slice 8 & 9)

X in mm	Z in mm	SY in kg/cm ²
23.827	147.490	-0.00107
30.187	147.536	-0.00047
62.978	152.658	0.00061
4.832	80.980	0.04270
60.199	130.455	0.00312
26.676	91.487	-0.00336
79.685	139.045	-0.00201
99.974	157.450	-0.00100
89.504	135.347	-0.00515
5.667	46.446	0.01430
41.504	79.474	-0.70160
6.009	39.219	0.00933
78.812	104.683	0.00366
73.533	98.278	0.00553
83.653	108.209	-0.00340
84.399	102.579	-0.00426
59.088	69.900	-0.40880
19.178	25.143	0.00074
71.569	65.398	-0.10020
14.342	7.692	0.00123
35.549	28.904	-0.00131
36.818	23.823	-0.00069
21.232	7.335	0.00160
17.991	3.655	0.00332
43.887	24.230	-0.00111
27.781	4.068	0.00386
58.865	34.729	-0.00688
67.781	33.210	-0.00403
78.100	43.648	-0.00924
70.236	25.611	-0.00155
102.894	37.879	0.00788
93.619	22.813	0.00106
101.691	27.512	0.00308
92.492	8.446	0.00113
93.090	3.519	0.00337

TABLE 5.47: NODAL STRESSES AT STRIP 13 (Y=66.04 mm)

(Under concentrated load between Slice 8 & 9)

X in mm	Z in mm	SY in kg/cm ²
3.481	157.450	-0.00359
44.827	151.422	0.00016
59.533	151.552	0.00028
105.497	157.450	-0.00353
3.513	0.000	0.00328
93.965	14.557	0.00004

TABLE 5.48: NODAL STRESSES AT STRIP 7 (Y=35.56 mm)

(Under concentrated load between Slice 9 & 10)

X in mm	Z in mm	SY in kg/cm ²
0.000	58.466	-0.02080
7.319	54.468	-0.01940
4.582	14.221	0.00020
6.279	7.737	0.00035
17.843	7.380	0.00080
27.465	5.363	-0.00027
35.085	5.388	-0.00072
97.456	59.488	-0.03510
37.059	129.066	0.00406
100.718	51.257	-0.01410
109.000	58.467	-0.01730
73.387	5.127	-0.00071
94.542	19.539	0.00130
104.459	14.256	0.00027
98.256	157.450	0.02210

TABLE 5.49: NODAL STRESSES AT STRIP 8 (Y=40.64 mm)

(Under concentrated load between Slice 9 & 10)

X in mm	Z in mm	SY in kg/cm ²
0.000	118.481	-0.03850
24.774	95.918	-0.03950
21.768	85.317	-0.24970
32.190	93.992	-0.05970
28.199	87.417	-0.12670
98.509	157.450	0.04970
6.978	64.040	-0.02240
61.872	85.924	-0.22050
71.086	87.727	-0.11950
67.137	83.228	-0.15670
0.000	14.104	-0.00066
77.349	88.969	-0.12540
109.000	118.481	0.03510
20.300	27.232	-0.00134
4.393	10.495	0.00080
43.800	26.294	-0.01250
100.992	64.593	-0.02120
87.803	27.232	-0.00099
104.591	10.485	0.00083
109.000	14.104	-0.00058

TABLE 5.50: NODAL STRESSES AT STRIP 9 (Y=45.72 mm)

(Under concentrated load between Slice 9 & 10)

X in mm	Z in mm	SY in kg/cm ²
42.582	113.257	0.01760
36.007	84.461	-0.23760
11.330	80.812	-0.07530
64.979	157.450	0.00047
73.213	157.450	0.00054
49.865	69.985	-0.01570
63.238	75.675	-0.22530
27.338	35.111	-0.01240
4.536	11.096	0.00144
52.364	13.502	-0.00015
104.520	11.081	0.00149
100.365	3.437	0.00121

TABLE 5.51: NODAL STRESSES AT STRIP 10 (Y=50.80 mm)

(Under concentrated load between Slice 9 & 10)

X in mm	Z in mm	SY in kg/cm ²
17.507	135.034	-0.03530
9.666	137.397	-0.02400
8.099	108.282	-0.03400
43.193	105.897	-0.08200
50.267	106.076	-0.13330
36.237	138.344	0.00487
17.745	54.080	-0.02080
50.527	148.780	0.00266
50.274	74.260	-0.25940
58.538	69.900	-0.01410
102.142	116.120	-0.02380
32.231	34.265	-0.01160
51.419	37.425	-0.02800
18.347	0.000	0.00216
21.880	3.018	0.00238
62.091	37.017	-0.02960
95.796	157.450	0.00902
31.267	3.773	0.00253
33.928	6.143	0.00239
89.791	54.045	-0.02580
56.251	3.655	0.00236
62.846	3.701	0.00244
73.375	3.396	0.00260

TABLE 5.52: NODAL STRESSES AT STRIP 11 (Y=55.88 mm)

(Under concentrated load between Slice 9 & 10)

X in mm	Z in mm	SY in kg/cm ²
76.504	90.755	-0.07890
70.251	91.622	-0.23640
82.009	90.292	-0.04830
80.622	82.999	-0.07570
66.811	85.832	-0.55210
61.419	87.208	-1.42910
57.668	84.048	-1.93640
49.426	87.580	-2.66680
69.986	120.743	0.01680
42.954	89.084	-1.04270
39.285	95.253	-0.32380
59.569	116.299	0.02000
62.739	122.950	0.02060
65.791	129.346	0.01260
51.399	122.558	0.02180
61.194	136.527	0.00756
66.000	44.500	-0.04360
48.998	129.030	0.01630
14.872	89.670	-0.03150
19.780	84.446	-0.04920
58.676	44.500	-0.04360
56.500	143.861	0.00359
66.177	32.903	-0.00984
24.341	73.259	-0.06370
109.000	134.619	0.00942
34.876	128.949	0.00791
87.943	157.450	-0.00071
47.904	44.500	-0.04260
90.607	25.566	0.00185
40.600	44.500	-0.04250
76.198	10.249	0.00182
101.773	152.872	0.00291
98.529	157.450	0.00402
84.659	6.938	0.00234
72.005	0.000	0.00487
68.900	3.304	0.00367
82.329	0.000	0.00483
66.926	0.000	0.00470
61.934	0.000	0.00454
16.851	141.757	-0.01500
56.976	0.000	0.00453
52.021	0.000	0.00448
0.000	134.619	0.00880
16.656	153.550	-0.00465
19.314	157.450	-0.00218
47.061	0.000	0.00441
42.065	0.000	0.00447
30.630	7.340	0.00236
36.983	0.000	0.00465
23.796	10.796	0.00172
21.792	0.000	0.00432
16.700	0.000	0.00396

TABLE 5.53: NODAL STRESSES AT STRIP 12 (Y=60.96 mm)

(Under concentrated load between Slice 9 & 10)

X in mm	Z in mm	SY in kg/cm ²
23.827	147.490	-0.00267
30.187	147.536	-0.00101
62.978	152.658	0.00083
4.832	80.980	0.04130
60.199	130.455	0.00676
26.676	91.487	-0.00860
79.685	139.045	-0.00285
99.974	157.450	-0.00124
89.504	135.347	-0.00807
5.667	46.446	0.01150
41.504	79.474	-0.18380
6.009	39.219	0.00734
78.812	104.683	0.00283
73.533	98.278	-0.01070
83.653	108.209	-0.00365
84.399	102.579	-0.00609
59.088	69.900	0.35960
19.178	25.143	0.00077
71.569	65.398	-0.05130
14.342	7.692	0.00091
35.549	28.904	-0.00058
36.818	23.823	-0.00026
21.232	7.335	0.00120
17.991	3.655	0.00264
43.887	24.230	-0.00058
27.781	4.068	0.00299
58.865	34.729	-0.00486
67.781	33.210	-0.00275
78.100	43.648	-0.00632
70.236	25.611	-0.00084
102.894	37.879	0.00619
93.619	22.813	0.00093
101.691	27.512	0.00227
92.492	8.446	0.00085
93.090	3.519	0.00270

TABLE 5.54: NODAL STRESSES AT STRIP 13 (Y=66.04 mm)

(Under concentrated load between Slice 9 & 10)

X in mm	Z in mm	SY in kg/cm ²
3.481	157.450	-0.00054
44.827	151.422	0.00007
59.533	151.552	0.00015
105.497	157.450	-0.00183
3.513	0.000	0.00268
93.965	14.557	0.00002

TABLE 5.55: NODAL STRESSES AT STRIP 7 (Y=35.56 mm)
(Under UDL above elbow concrete)

X in mm	Z in mm	SY in kg/cm ²
0.000	58.466	-0.00477
7.319	54.468	-0.00955
4.582	14.221	-0.00008
6.279	7.737	-0.00001
17.843	7.380	0.00004
27.465	5.363	-0.00027
35.085	5.388	-0.00040
97.456	59.488	-0.01820
37.059	129.066	0.00053
100.718	51.257	-0.00719
109.000	58.467	-0.00420
73.387	5.127	-0.00038
94.542	19.539	-0.00002
104.459	14.256	-0.00005
98.256	157.450	0.00612

TABLE 5.56: NODAL STRESSES AT STRIP 8 (Y=40.64 mm)
(Under UDL above elbow concrete)

X in mm	Z in mm	SY in kg/cm ²
0.000	118.481	-0.00656
24.774	95.918	-0.01430
21.768	85.317	-0.07650
32.190	93.992	-0.01550
28.199	87.417	-0.03800
98.509	157.450	0.01110
6.978	64.040	-0.01610
61.872	85.924	-0.02360
71.086	87.727	-0.02730
67.137	83.228	-0.03120
0.000	14.104	-0.00026
77.349	88.969	-0.03740
109.000	118.481	-0.00608
20.300	27.232	-0.00103
4.393	10.495	0.00013
43.800	26.294	-0.00365
100.992	64.593	-0.01730
87.803	27.232	-0.00093
104.591	10.485	0.00014
109.000	14.104	-0.00022

TABLE 5.57: NODAL STRESSES AT STRIP 9 (Y=45.72 mm)

(Under UDL above elbow concrete)

X in mm	Z in mm	SY in kg/cm ²
42.582	113.257	0.00400
36.007	84.461	-0.06710
11.330	80.812	-0.05880
64.979	157.450	0.00021
73.213	157.450	0.00039
49.865	69.985	-0.04020
63.238	75.675	-0.05960
27.338	35.111	-0.00434
4.536	11.096	0.00032
52.364	13.502	-0.00010
104.520	11.081	0.00034
100.365	3.437	0.00026

TABLE 5.58: NODAL STRESSES AT STRIP 10 (Y=50.80 mm)

(Under UDL above elbow concrete)

X in mm	Z in mm	SY in kg/cm ²
17.507	135.034	-0.00497
9.666	137.397	-0.00329
8.099	108.282	-0.00702
43.193	105.897	-0.00256
50.267	106.076	-0.00129
36.237	138.344	0.00049
17.745	54.080	-0.01140
50.527	148.780	0.00018
50.274	74.260	-0.09070
58.538	69.900	-0.08190
102.142	116.120	-0.00397
32.231	34.265	-0.00350
51.419	37.425	-0.00748
18.347	0.000	0.00042
21.880	3.018	0.00053
62.091	37.017	-0.00788
95.796	157.450	0.00337
31.267	3.773	0.00056
33.928	6.143	0.00055
89.791	54.045	-0.01120
56.251	3.655	0.00051
62.846	3.701	0.00053
73.375	3.396	0.00057

TABLE 5.59: NODAL STRESSES AT STRIP 11 (Y=55.88 mm)
(Under UDL above elbow concrete)

X in mm	Z in mm	SY in kg/cm ²
76.504	90.755	-0.09730
70.251	91.622	-0.09170
82.009	90.292	-0.10010
80.622	82.999	-0.13460
66.811	85.832	-0.12470
61.419	87.208	-0.11870
57.668	84.048	-0.13080
49.426	87.580	-0.12150
69.986	120.743	0.00253
42.954	89.084	-0.10500
39.285	95.253	-0.05630
59.569	116.299	0.00388
62.739	122.950	0.00276
65.791	129.346	0.00157
51.399	122.558	0.00281
61.194	136.527	0.00082
66.000	44.500	-0.01130
48.998	129.030	0.00191
14.872	89.670	-0.07350
19.780	84.446	-0.12180
58.676	44.500	-0.01140
56.500	143.861	0.00034
66.177	32.903	-0.00257
24.341	73.259	-0.10520
109.000	134.619	0.00014
34.876	128.949	0.00104
87.943	157.450	0.00073
47.904	44.500	-0.01130
90.607	25.566	0.00046
40.600	44.500	-0.01150
76.198	10.249	0.00046
101.773	152.872	0.00065
98.529	157.450	0.00129
84.659	6.938	0.00059
72.005	0.000	0.00112
68.900	3.304	0.00088
82.329	0.000	0.00112
66.926	0.000	0.00106
61.934	0.000	0.00102
16.851	141.757	-0.00195
56.976	0.000	0.00102
52.021	0.000	0.00101
0.000	134.619	0.00125
16.656	153.550	-0.00006
19.314	157.450	0.00028
47.061	0.000	0.00099
42.065	0.000	0.00101
30.630	7.340	0.00059
36.983	0.000	0.00105
23.796	10.796	0.00045
21.792	0.000	0.00100
16.700	0.000	0.00093

TABLE 5.60: NODAL STRESSES AT STRIP 12 (Y=60.96 mm)

(Under UDL above elbow concrete)

X in mm	Z in mm	SY in kg/cm ²
23.827	147.490	-0.00028
30.187	147.536	-0.00010
62.978	152.658	0.00014
4.832	80.980	-0.07530
60.199	130.455	0.00078
26.676	91.487	-0.10210
79.685	139.045	-0.00036
99.974	157.450	-0.00022
89.504	135.347	-0.00110
5.667	46.446	0.00400
41.504	79.474	-0.17370
6.009	39.219	0.00243
78.812	104.683	-0.00147
73.533	98.278	-0.02280
83.653	108.209	-0.00127
84.399	102.579	-0.00615
59.088	69.900	-0.14740
19.178	25.143	0.00023
71.569	65.398	-0.02720
14.342	7.692	0.00026
35.549	28.904	-0.00013
36.818	23.823	-0.00006
21.232	7.335	0.00032
17.991	3.655	0.00068
43.887	24.230	-0.00014
27.781	4.068	0.00077
58.865	34.729	-0.00126
67.781	33.210	-0.00069
78.100	43.648	-0.00154
70.236	25.611	-0.00021
102.894	37.879	0.00207
93.619	22.813	0.00027
101.691	27.512	0.00077
92.492	8.446	0.00023
93.090	3.519	0.00070

TABLE 5.61: NODAL STRESSES AT STRIP 13 (Y=66.04 mm)

(Under UDL above elbow concrete)

X in mm	Z in mm	SY in kg/cm ²
3.481	157.450	-0.00070
44.827	151.422	0.00003
59.533	151.552	0.00004
105.497	157.450	-0.00071
3.513	0.000	0.00070
93.965	14.557	0.00001

TABLE 5.62: NODAL STRESSES AT STRIP 7 (Y=35.56 mm)

(Under concentrated load simulating gantry column loads)

X in mm	Z in mm	SY in kg/cm ²
0.000	58.466	-0.00067
7.319	54.468	-0.00428
4.582	14.221	-0.00004
6.279	7.737	-0.00003
17.843	7.380	0.00000
27.465	5.363	-0.00014
35.085	5.388	-0.00019
97.456	59.488	-0.01320
37.059	129.066	0.00035
100.718	51.257	-0.00395
109.000	58.467	-0.00085
73.387	5.127	-0.00021
94.542	19.539	0.00008
104.459	14.256	-0.00026
98.256	157.450	0.00334

TABLE 5.63: NODAL STRESSES AT STRIP 8 (Y=40.64 mm)

(Under concentrated load simulating gantry column loads)

X in mm	Z in mm	SY in kg/cm ²
0.000	118.481	-0.00259
24.774	95.918	-0.01540
21.768	85.317	-0.05940
32.190	93.992	-0.00263
28.199	87.417	-0.01680
98.509	157.450	0.00601
6.978	64.040	-0.01100
61.872	85.924	0.00064
71.086	87.727	-0.00099
67.137	83.228	-0.00041
0.000	14.104	-0.00012
77.349	88.969	-0.01280
109.000	118.481	-0.00232
20.300	27.232	-0.00008
4.393	10.495	0.00001
43.800	26.294	-0.00077
100.992	64.593	-0.01740
87.803	27.232	-0.00010
104.591	10.485	0.00003
109.000	14.104	-0.00011

TABLE 5.64: NODAL STRESSES AT STRIP 9 (Y=45.72 mm)

(Under concentrated load simulating gantry column loads)

X in mm	Z in mm	SY in kg/cm ²
42.582	113.257	0.00254
36.007	84.461	-0.00433
11.330	80.812	-0.13510
64.979	157.450	0.00008
73.213	157.450	0.00023
49.865	69.985	0.00258
63.238	75.675	0.00171
27.338	35.111	-0.00083
4.536	11.096	0.00007
52.364	13.502	0.00003
104.520	11.081	0.00010
100.365	3.437	0.00005

TABLE 5.65: NODAL STRESSES AT STRIP 10 (Y=50.80 mm)

(Under concentrated load simulating gantry column loads)

X in mm	Z in mm	SY in kg/cm ²
17.507	135.034	-0.00186
9.666	137.397	-0.00158
8.099	108.282	-0.04210
43.193	105.897	0.00310
50.267	106.076	0.00258
36.237	138.344	0.00047
17.745	54.080	-0.00204
50.527	148.780	0.00011
50.274	74.260	0.00299
58.538	69.900	0.00399
102.142	116.120	-0.00660
32.231	34.265	-0.00064
51.419	37.425	-0.00181
18.347	0.000	0.00005
21.880	3.018	0.00008
62.091	37.017	-0.00195
95.796	157.450	0.00170
31.267	3.773	0.00006
33.928	6.143	0.00008
89.791	54.045	-0.00218
56.251	3.655	0.00000
62.846	3.701	0.00002
73.375	3.396	0.00006

TABLE 5.66: NODAL STRESSES AT STRIP 11 (Y=55.88 mm)
 (Under concentrated load simulating gantry column loads)

X in mm	Z in mm	SY in kg/cm ²
76.504	90.755	-0.00387
70.251	91.622	0.00200
82.009	90.292	-0.02630
80.622	82.999	-0.01290
66.811	85.832	0.00174
61.419	87.208	0.00230
57.668	84.048	0.00205
49.426	87.580	0.00192
69.986	120.743	0.00237
42.954	89.084	0.00224
39.285	95.253	0.00260
59.569	116.299	0.00194
62.739	122.950	0.00130
65.791	129.346	0.00103
51.399	122.558	0.00103
61.194	136.527	0.00041
66.000	44.500	-0.00287
48.998	129.030	0.00070
14.872	89.670	-0.29990
19.780	84.446	-0.07160
58.676	44.500	-0.00277
56.500	143.861	0.00014
66.177	32.903	-0.00055
24.341	73.259	-0.00859
109.000	134.619	0.00131
34.876	128.949	0.00120
87.943	157.450	0.00058
47.904	44.500	-0.00264
90.607	25.566	0.00025
40.600	44.500	-0.00276
76.198	10.249	0.00012
101.773	152.872	0.00029
98.529	157.450	0.00070
84.659	6.938	0.00014
72.005	0.000	0.00021
68.900	3.304	0.00014
82.329	0.000	0.00029
66.926	0.000	0.00017
61.934	0.000	0.00014
16.851	141.757	-0.00078
56.976	0.000	0.00012
52.021	0.000	0.00012
0.000	134.619	0.00085
16.656	153.550	-0.00009
19.314	157.450	0.00024
47.061	0.000	0.00011
42.065	0.000	0.00013
30.630	7.340	0.00010
36.983	0.000	0.00016
23.796	10.796	0.00010
21.792	0.000	0.00023
16.700	0.000	0.00023

TABLE 5.67: NODAL STRESSES AT STRIP 12 (Y=60.96 mm)
(Under concentrated load simulating gantry column loads)

X in mm	Z in mm	SY in kg/cm ²
23.827	147.490	-0.00009
30.187	147.536	0.00000
62.978	152.658	0.00006
4.832	80.980	-0.24650
60.199	130.455	0.00032
26.676	91.487	0.00149
79.685	139.045	0.00011
99.974	157.450	-0.00010
89.504	135.347	-0.00010
5.667	46.446	0.00184
41.504	79.474	0.00154
6.009	39.219	0.00096
78.812	104.683	0.00318
73.533	98.278	0.00290
83.653	108.209	0.00241
84.399	102.579	0.00015
59.088	69.900	0.00505
19.178	25.143	0.00009
71.569	65.398	0.00001
14.342	7.692	0.00004
35.549	28.904	0.00002
36.818	23.823	0.00002
21.232	7.335	0.00005
17.991	3.655	0.00014
43.887	24.230	0.00001
27.781	4.068	0.00013
58.865	34.729	-0.00028
67.781	33.210	-0.00016
78.100	43.648	-0.00031
70.236	25.611	-0.00001
102.894	37.879	0.00160
93.619	22.813	0.00011
101.691	27.512	0.00033
92.492	8.446	0.00005
93.090	3.519	0.00019

TABLE 5.68: NODAL STRESSES AT STRIP 13 (Y=66.04 mm)
(Under concentrated load simulating gantry column loads)

X in mm	Z in mm	SY in kg/cm ²
3.481	157.450	-0.00046
44.827	151.422	0.00001
59.533	151.552	0.00001
105.497	157.450	-0.00040
3.513	0.000	0.00020
93.965	14.557	0.00000